
European Association of Remote Sensing Laboratories
Special Interest Group on Forest Fires

Global Observation of Forest and Land Cover Dynamics
(GOFC-GOLD)


# 4th International Workshop on Remote Sensing and GIS Applications to Forest Fire Management:

# Innovative Concepts and Methods in Fire Danger Estimation

Emilio Chuvieco, Pilar Martín and Chris Justice (Editors)

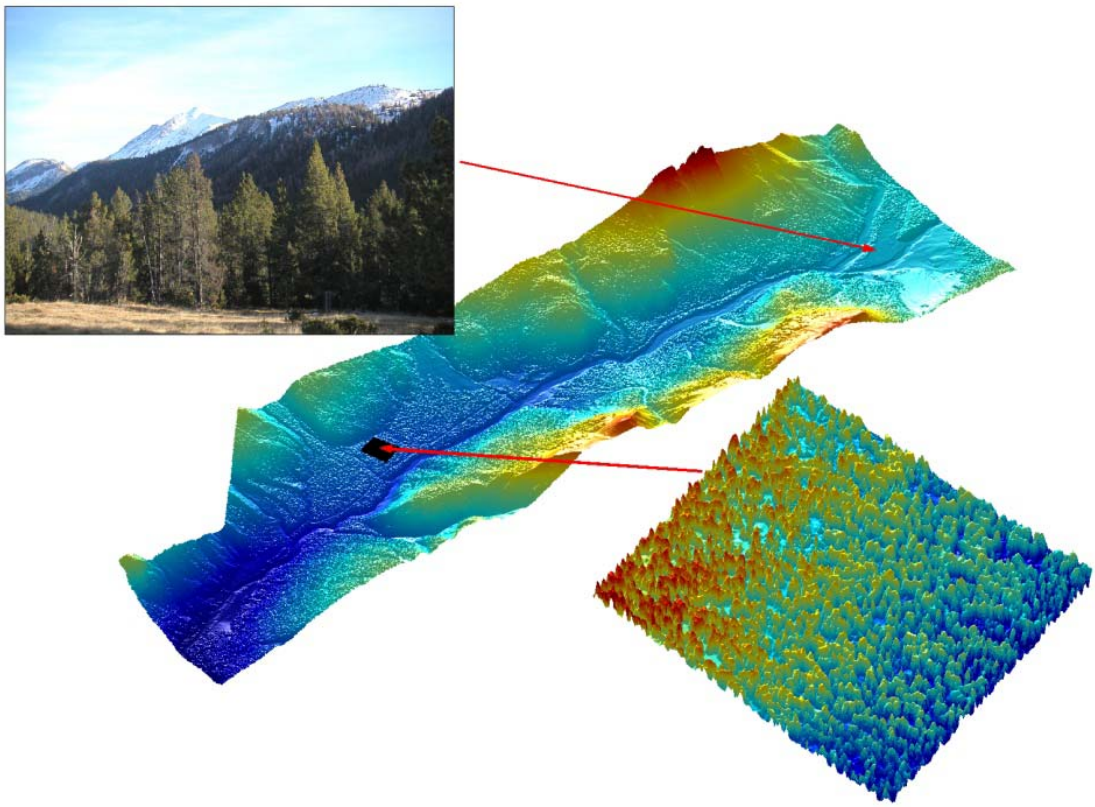

Ghent University
Ghent – Belgium, 5-7 June 2003

Emilio Chuvieco, Pilar Martín and Chris Justice (2003): *Proceedings of the 4th International Workshop on Remote Sensing and GIS applications to Forest Fire Management: Innovative concepts and methods in fire danger estimation*. Ghent University – EARSeL, 233 pages, ISBN: 2-908885-25-5

Front Cover: Shaded representation of DSM (Digital Surface Model) from the test site in a Swiss National Park derived from lidar measurements. From *Morsdorf et al.*, included in this volume.

# CONTENTS

## Session 4. Burned land mapping

## Abstracts presented in parallel
**(For timing reasons, they were not evaluated by the Scientific Committee)**

# Foreword

The growing interest of remote sensing scientists in wildland fires, as well as the expanding use of remote sensing data by fire managers and researchers, explains the notable increase of papers on this topic, published both in peer-review journals, books and technical conferences. The broad relationships between wildland fires and vegetation structure and diversity, land use dynamics, atmospheric emissions and landscape conservation, makes this field of research very attractive for a wide range of professionals.

Much of the fire related remote sensing research conducted over recent years has focused on detecting active fires, especially in Tropical and Boreal ecosystems, since this activity was very relevant for global atmospheric and ecological research as well as fire management. Increasing attention is now being given to automated mapping of burned areas and post-fire monitoring, although for the latter there is a considerable body of research dating back to the late seventies. The user community needs clear documentation of the accuracy of these various satellite-derived products developed using different sensors and different methods. The research community is starting to give priority to developing quantitative assessments of the accuracy of these products.

Fire danger assessment, that is the estimation of those conditions that may lead to fire ignition or facilitate its propagation, has been less covered in remote sensing literature. Different attempts were published in the late eighties, very often without proper consideration to the variables traditionally used by fire managers, and in parallel to operational indices, mainly based on weather data. In recent years, the connection between those operational indices and remote sensing data has expanded, helped by the technical improvements in Earth Observation techniques, on one hand, and a better understanding of the relations between remotely sensed information and fire critical variables. For instance, the estimation of vegetation water condition is now better connected to fuel moisture status, both dead and live components, while the development of lidar and radar processing has made it possible to better parameterize fuel properties.

The EARSeL Special Interest Group on Forest Fires provides a forum for researchers, primarily from Europe to present and discuss recent advances in the discipline and future research directions. The purpose of this international workshop, which continues a series of technical conferences previously held in Alcalá de Henares (Spain), Luso (Portugal), and Paris (France), is to join the expertise of remote sensing and fire scientists in proposing new approaches in Earth Observation in support of operational fire danger estimation. On this occasion, the meeting is co-sponsored by the Global Observation of Forest Cover/Global Observation of Landcover Dynamics (GOFC/GOLD) Fire program, which is providing an international coordination mechanism for improving the availability and use of fire data and securing the long term, operational delivery of fire information in support of global change and natural resource management. GOFC/GOLD provides an enhanced international view to the regular activities of the EARSeL Special Interest Group on Forest Fires. As in previous workshops, we hope this meeting will foster the interaction between the attendants, and promote human and scientific cooperation to better understand fire factors and fire effects, leading to an improved understanding of the role of fire and the improved management of fire in a changing planet.

Emilio Chuvieco, Pilar Martín and Chris Justice

# Session 1. Fuel moisture content estimation

# Application of radiative transfer models to moisture content estimation and burned land mapping

S. Jacquemoud
*Laboratoire Environnement et Développement, Université Paris, Paris, France*
jacquemo@ccr.jussieu.fr

S. L. Ustin
*CSTARS, Department of Land, Air and Water Resources, University of California, Davis, USA*

## 1. INTRODUCTION

Virtually all kinds of vegetation are subject to wildfires. Research programs conducted during the last three decades on fire risk assessment have emphasized the role of vegetation water content to understand biomass burning processes. They nevertheless did not produce satisfying operational methods to determine risk levels. Two different procedures are commonly used to monitor the evolution of fire risk over time (Dauriac et al., 2001):

- The use of meteorological variables averaged over a surface area of 1000 km$^2$ to calculate the water balance of the site;
- The measurement of vegetation water content in a limited number of control plots.

Water balance is the most important factor controlling aboveground primary production, and then fire frequency and intensity. For instance, the arid areas of southern hemisphere Africa burn infrequently because there is rarely enough fuel present to carry a fire across the landscape (a minimum of about 0.5-1 t/ha is needed). Several years of fuel accumulation or an exceptionally wet growing season are required to generate this minimum fuel load in arid areas (FAO, 2001). Where a sufficient amount of fuel accumulates, water content is definitely a key factor in assessing flammability and combustibility. Although there are many measurements of vegetation water content (leaf water potential, stomatal aperture, specific water density, equilibrium moisture content, etc.), Fuel Moisture Content (FMC), Relative Water Content (RWC), and Equivalent Water Thickness (EWT) are commonly used by plant physiologists to determine plant water stress:

$$FMC = \frac{fw - dw}{dw} \qquad RWC = \frac{fw - dw}{tw - dw} \qquad EWT = \frac{fw - dw}{A}$$

where *fw* is fresh weight, *dw* is dry weight, *A* is the leaf area, and *tw* is the turgid weight. FMC defined as the ratio between the quantity of water and either the fresh or dry (formula above) weight is routinely used by forest services to assess fire danger (NPS, 2001). RWC is the ratio of the actual leaf water content to the maximum water content at full turgor. It has been demonstrated to be directly related to leaf water potential, which controls plant response to water stress. However, different species may have the same RWC values with different amounts of water in their leaves because of variance in turgid weight and dry matter weight in nature (Ceccato et al., 2001). In contrast, EWT only depends on the amount of water in the leaf, corresponding to a hypothetical thickness of a single layer

of water averaged over the whole leaf area. Ripple (1984) mentioned that traditional techniques for accurate ground-based evaluation of plant water relations were time consuming, costly, and spatially restrictive, and proposed to combine them with remote sensing techniques for large-area evaluations. Remote sensing is indeed an adapted tool to monitor vegetation moisture, from local to global scale, operationally, and over different ecosystems. As leaves represent the main surfaces of plant canopies, their optical properties are essential to understanding the transport of photons within vegetation, but the "scaling-up" of water estimation methods from leaf- to canopy-level is still a point at issue as seen below, because plant canopies are considerably more complex targets than are leaves.

## 2. REMOTE SENSING OF MOISTURE CONTENT AT THE LEAF LEVEL

Hundreds of papers have detailed variation in spectral properties in relation to leaf biochemical composition and structure, which themselves depend on many factors including the species, developmental or microclimate position of the leaf on the plant, and whether it is stressed or not. One classically divides the optical domain from 400 to 2500 nm in three parts: the visible (400-700 nm) characterized by a strong absorption of light by photosynthetic pigments in a green leaf; the near-infrared plateau (700-1100 nm) where absorption is limited to dry leaf matter but where multiple scattering within the leaf, related to the fraction of air spaces, i.e., to the internal structure, drives the reflectance and transmittance levels; and the middle-infrared (1100-2500 nm) which is also a zone of strong absorption, primarily by water in fresh leaves and secondarily, by dry matter (dry carbon compounds like cellulose and lignin, nitrogen, sugars, and other plant compounds) when the leaf wilts and dries (Figure 1). All of these observations are a prerequisite to extracting biophysical information.

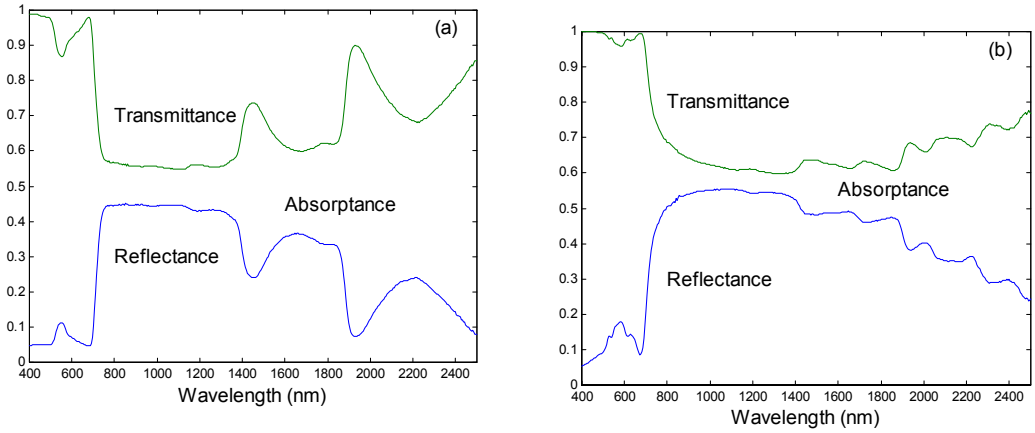


Figure 1. Reflectance and transmittance spectra of (a) fresh and (b) dry poplar (*Populus canadensis*) leaves in the solar domain.

There are two major water absorption features centered near 1450 and 1950 nm that affect the reflectance of healthy leaves, and two minor centered near 970 and 1200 nm. These absorption features result from vibrational transitions involving various overtones and combinations of water's three fundamental vibrational transitions: V1 (H–O–H symmetric stretch mode transition), V2 (H–O–H bending mode transition), and V3 (H–O–H asymmetric stretch mode transition). The absorption feature centered near 970 nm is attributed to a 2V1 + V3 combination, the one near 1200 nm to a V1 + V2 + V3 combination, the one near 1450 nm to a V1 + V3 combination, and the one near 1950 nm to a V2 + V3 combination. Various methods have been developed to extract leaf water content from leaf optical properties.

*2.1 The semi-empirical approach*

The first methods consist of relating spectral indices based on a ratio or some other simple mathematical formula of reflectance, or its derivative, at one or more selected wavelengths – $\rho_{900}/\rho_{970}$, $\rho_{1650}/\rho_{1430}$, $(\rho_{850}-\rho_{2218})/(\rho_{850}-\rho_{1928})$, $(\rho_{850}-\rho_{1788})/(\rho_{850}-\rho_{1928})$, among others – to leaf water content:

$$FMC \text{ or } RWC \text{ or } EWT = f\left(\rho(\lambda_1),\ldots,\rho(\lambda_n)\right)$$

RWC (Hunt et al., 1987, 1989; Bowman, 1989; Inoue et al., 1993; Peñuelas et al., 1993; Peñuelas and Inoue, 1999; Yu et al., 2000; etc.) and EWT (Aoki et al., 1988; Danson et al., 1992; Datt, 1999; Yu et al., 2000; Ceccato et al., 2001; etc.) have been determined this way. Continuum removal, i.e., integration of the area in the absorption below the continuum, has been applied by Tian et al. (2001) to the curve between 1650 and 1850 nm, to estimate RWC. Finally, multiple stepwise regression analysis which establishes a direct regression equation between leaf reflectance (or transmittance) at a few wavelengths, selected by the procedure, and leaf biochemistry has been used by Fourty and Baret (1998) and Gillon et al. (2002) to estimate EWT and FMC, respectively. However, the accuracy of these estimations lack predictability because these relationships do not take into account the partially co-varying anatomical structure and specific leaf area differences between species or leaves.

*2.2 The Modeling approach*

While experimental measurements of leaf optical properties were progressing, deterministic models based on diverse representations of light interactions with plant leaves were also developed. These models are distinguished by the underlying physics and by the complexity of the leaf. The simplest ones consider the blade as a single scattering and absorbing layer. In the most complicated ones, all cells are described in detail (shape, size, position, and biochemical content). Whatever the approach, these models have improved our understanding of the interactions of light with plant leaves. Information about the refractive index and the specific absorption coefficient of leaf constituents is almost always required. Figure 2 presents the latter for chlorophyll, water, and dry matter as a function of the wavelength. One recognizes in the action spectrum of water the three main peaks near 1450, 1950, and 2500 nm, and two minor ones at 970 and 1200 nm. The 970 nm absorption band has very little effect on leaf optical properties so that it sometimes does not occur on leaf spectra.

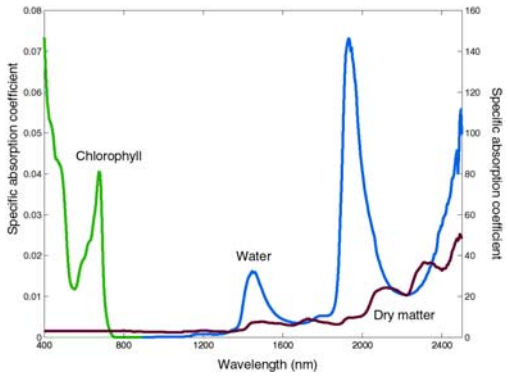


Figure 2. Specific absorption coefficient a) of chlorophyll a+b ($cm^2\ \mu g^{-1}$) on the left scale b) of water ($cm^{-1}$) and dry matter ($cm^2\ g^{-1}$) on the right scale.

Ustin et al. (1999) already extensively reviewed computer-based leaf models from the late sixties to the present. Table 1 categorizes radiative transfer models in three main classes, arranged in increasing order of complexity:

Table 1. Comparison of several leaf optical properties models used in remote sensing.

| Radiative transfer models | Stochastic models | Monte Carlo approaches |
|---|---|---|
| PROSPECT, LIBERTY, LEAFMOD, FRT | SLOP | RAYTRAN, ABM |
| - structure parameter<br>- biochemical contents | - probabilities of scattering and absorption | - description of the leaf internal structure in three dimensions |
| → spectral properties<br>→ chlorophyll fluorescence | → spectral properties<br>→ chlorophyll fluorescence | → spectral properties<br>→ directional properties<br>→ absorption profiles |
| direct + inverse mode | | direct mode |

### *2.2.1 PROSPECT*

Now in widespread use in the remote sensing community, PROSPECT was among the first model to accurately simulate the hemispherical reflectance and transmittance of various plant leaves (monocots or dicots, fresh or senescent leaves) over the solar spectrum. The leaf is represented as a pile of absorbing plates with rough surfaces giving rise to isotropic diffusion (Figure 3). Originally the model used three input parameters (Jacquemoud and Baret, 1990): the structure parameter N (number of compact layers specifying the average number of air / cell walls interfaces within the mesophyll), the chlorophyll a+b concentration $C_{ab}$ (μg cm$^{-2}$), and the equivalent water thickness EWT noted $C_w$ (cm or g cm$^{-2}$).

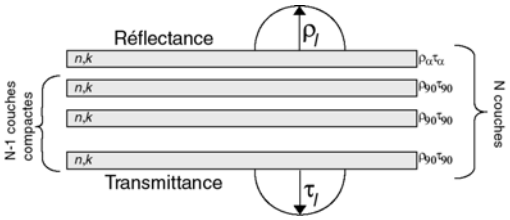


Figure 3. Schematic representation of PROSPECT.

During the summer of 1993 an experiment at the Joint Research Centre (Ispra, Italy) built a database, LOPEX, associating visible / infrared spectra of dry and fresh vegetation elements (leaves, conifer needles, stems, etc.) with physical measurements (thickness, water content, specific leaf area) and biochemical analyses (chlorophyll a+b, proteins, cellulose, lignin, etc.) (Hosgood et al., 1995). LOPEX was used to introduce the full leaf biochemistry into PROSPECT (Jacquemoud et al., 1996). A limit of this process arose however in the inversion of the model when it was discovered that protein content could not be retrieved because of strong water absorption features and cellulose and lignin could not be consistently identified and quantified. As a consequence, the model was simplified to the point that it now considers the dry matter content $C_m$ (g cm$^{-2}$) as a whole instead of treating the leaf biochemical constituents individually (Baret and Fourty, 1997; Jacquemoud et al., 2000). In short, the four input parameters of PROSPECT today are: leaf structure parameter, the chlorophyll a+b concentration, the equivalent water thickness, and the dry matter content. Recent studies based on statistical methods like the Design Of Experiments for Simulation (DOES, Bacour et al., 2002) or the Extended Fourier Amplitude Sensitivity Test (EFAST, Ceccato et al., 2002a) permitted the quantification of the contribution of each of the input parameters to the model outputs, as well as their interactions. Figure 4 shows that variation in transmittance values – it would be similar with reflectance values – are exclusively influenced by N, $C_w$ and $C_m$ in the near and middle infrared. As expected, water has the greatest influence with 80-90% of contribution in the absorption peaks, but N and $C_m$ also significantly affect transmittance values within this range.

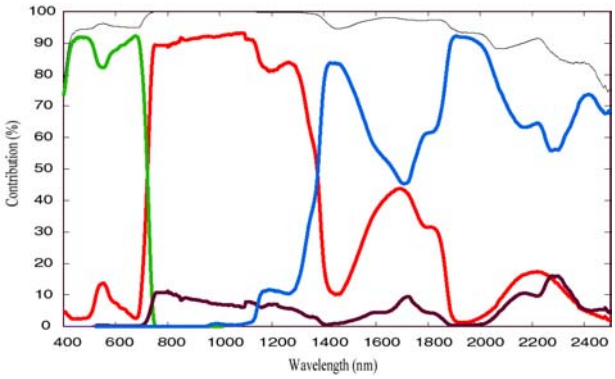


Figure 4. Contribution of chlorophyll concentration $C_{ab}$ (green), equivalent water thickness $C_w$ (blue), dry matter content $C_m$ (brown) and structure parameter N (red) to the leaf transmittance as simulated by PROSPECT. The black curve is the sum of the contributions (Pavan, unpublished).

PROSPECT has been validated by iterative inversion of the model on reflectance and transmittance spectra of about sixty leaves of various species from the LOPEX database, and fourteen leaves of cereal crops (Newnham and Burt, 2001). It generally performs well in terms of spectrum reconstruction. The comparison between measured and estimated values of $C_{ab}$, $C_w$, and $C_m$ also gives satisfactory results on fresh leaves (Table 2).

Table 2. Retrieval of leaf biochemical constituents by inversion of PROSPECT.

| | Constituent | $R^2$ | RMSE |
|---|---|---|---|
| Baret and Fourty (1997) | $C_w$ | × | 0.0025 cm |
| | $C_m$ | × | 0.0016 g cm$^{-2}$ |
| Jacquemoud et al. (2000) | $C_{ab}$ | 0.67 | 9.1 µg cm$^{-2}$ |
| | $C_w$ | 0.95 | 0.0018 cm |
| | $C_m$ | 0.65 | 0.0022 g cm$^{-2}$ |
| Newnham and Burt (2001) | $C_{ab}$ | 0.78 | × |
| | $C_w$ | 0.93 | × |

### *2.2.2 LIBERTY (Leaf Incorporating Biochemistry Exhibiting Reflectance and Transmittance Yields)*

This model was developed specifically to calculate the optical properties of both dried and fresh stacked conifer needles (Dawson et al., 1998a), and to date, it remains the only one designed for this purpose. However, it can also be used for predicting the reflectance and transmittance spectra of a leaf or a stack of leaves in the solar domain. By treating the leaf as an aggregation of cells, with multiple radiation scattering between cells, output spectra are a function of three structural parameters (cell diameter in µm, intercellular air space, leaf thickness) and the combined absorption coefficients of leaf biochemicals (chlorophyll concentration in mg m$^{-2}$, water content in g m$^{-2}$, lignin and cellulose content in g m$^{-2}$, and nitrogen content in g m$^{-2}$). Dawson et al. (1998b) ran LIBERTY to generate reflectance spectra of slash pine needles containing various water, lignin+cellulose, and nitrogen concentrations. This data set was then used for training an artificial neural network which proved to produce more accurate FMC when compared against those generated with spectral indices alone.

### *2.2.3 Other models*

Although PROSPECT and LIBERTY are the most popular leaf optical properties models in remote sensing, other codes have been developed which also take into account leaf water content and are potentially useful in the remote sensing of fire risk assessment: LEAFMOD (*Leaf Experimental*

*Absorptivity Feasibility MODel*, Ganapol et al., 1997) directly based on the radiative transfer equation, SLOP (*Stochastic model for Leaf Optical Propertie*, Maier et al., 1999) where the leaf is partitioned into different tissues and their optical properties simulated by a Markov chain.

## 3. REMOTE SENSING OF MOISTURE CONTENT AT THE CANOPY LEVEL

It would be convenient to be able to estimate the water content of whole canopies in the field using leaf-level methods described above, but extending laboratory results to the field presents some problems (Rollin and Milton, 1998). Besides leaf optical properties, canopy reflectance also depends on plant structure (leaf area index, leaf orientation, leaf size, etc.), background (soil and/or non-photosynthetically active vegetation) optical properties, and viewing geometry (solar and view zenith and azimuth angles). Most of these parameters vary spatially and temporally. For that very reason, it is questionable whether the semi-empirical relationships established at leaf level can be "scaled-up" to whole canopies: How can canopy water content be mapped?

### *3.1 The semi-empirical approach*

There are few studies that have examined the relationships between total canopy water content and spectral reflectance indices. Sims and Gamon (2003) recently proposed the Canopy Structure Index (CSI) that combines the low absorptance water band at 1180 nm with the simple ratio vegetation index to account for the amount of vegetation: CSI produced good correlations with EWT at all canopy thicknesses. Rolin and Milton (1998) defined the Relative Depth Index (RDI) to estimate FMC. Both indices have been tested with reflectance spectra acquired by field portable spectrometers on a limited number of validation points. The Normalized Difference Water Index (NDWI) demonstrated its potential applicability for canopy-level EWT estimation with AVIRIS (Airborne Visible Infrared Imaging Spectrometer) imagery (Gao, 1996; Serrano et al., 2000). More sophisticated techniques like Hierarchical Foreground / Background Analysis (HFBA) introduced by Ustin et al. (1998) also performed well in the retrieval of canopy water content from AVIRIS imagery (Figure 5). The cartography of FMC in urbanized landscapes, such as the chaparral systems of semiarid shrubs in California, is critical to fire assessment. Finally, Ceccato et al. (2002a, 2002b) were innovating in designing a Global Vegetation Moisture Index (GVMI) based on radiative transfer model simulations and adapted to the SPOT-VEGETATION sensor. Field measurements of EWT carried out at canopy level on different formations of West Africa (shrub steppe, shrub savannah, tree savannah, and savannah woodland) validated the new index.

Most of these indices based on spectral variations of the reflectance however pose a problem because water stress is not only manifested in water content change but also in plant architecture change (Jackson, 1986). As wilting progresses, the leaves become more vertical, the cover fraction and consequently, the reflectance, decrease. Radiative transfer models which incorporate the effects of viewing geometry, leaf orientation, and other describers of canopy complexity into reflectance might be better suited to accurately retrieve water content.

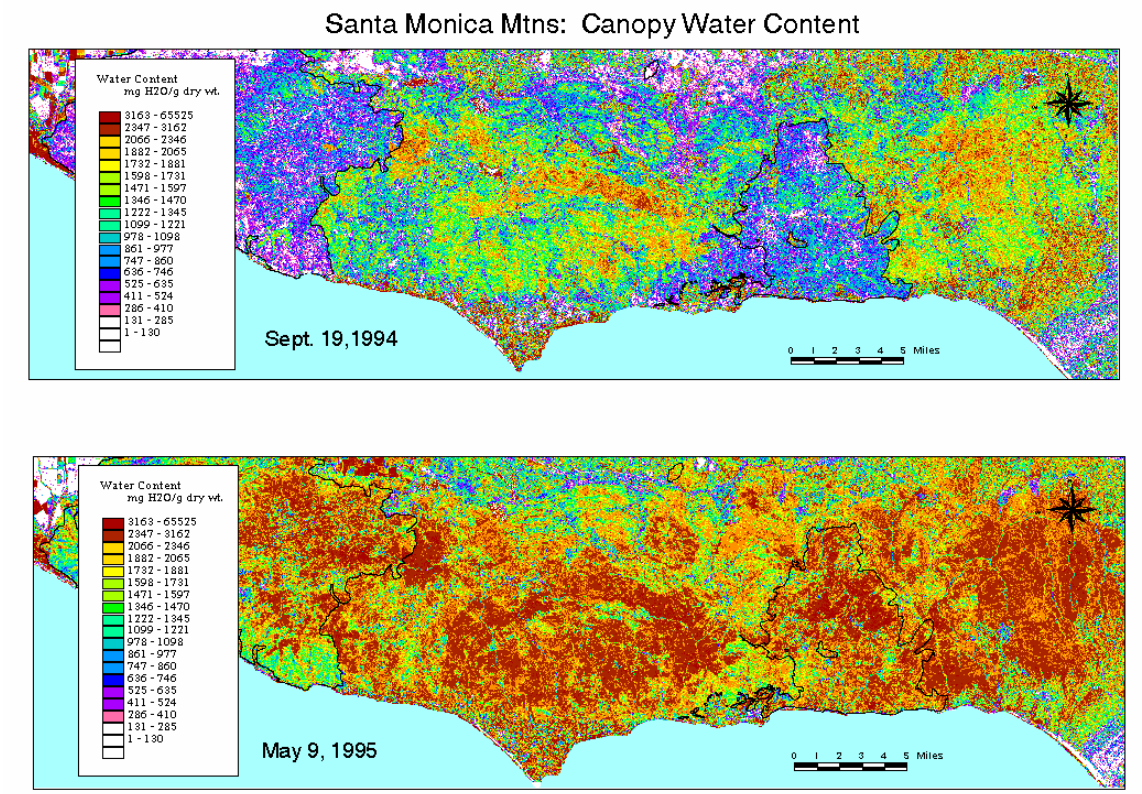


Figure 5. Canopy water content of chaparral communities in the Santa Monica Mountains, bordering Los Angeles and the San Fernando Valley, California, an area subject to frequent catastrophic wildfires in the shrub savanna grasslands. The images were measured in September, at the end of the extended dry season (approximately six months without rain) and in the following spring at the end of the winter rainy season. Data were composited from three AVIRIS flightlines (16 scenes) and atmospherically collected reflectance (after Ustin et al., 1998).

### *3.2 The modeling approach*

Fewer investigations have applied radiative transfer models and inversion techniques for estimating leaf water content from canopy reflectance imagery. The first attempts are quite simple: Schmuck et al. (1993) regarded an AVIRIS spectrum as a linear mixing of soil and vegetation spectra, the latter being modeled with a Kubelka-Munk formula modified to fit an optically thick homogeneous medium. Two spectral windows were use in the fitting: the 500-730 nm region for chlorophyll estimates and the 1500-1650 nm region for water estimates. Compared with the Moisture Stress Index calculated at two dates, the retrieved EWT demonstrated a higher sensitivity. By expressing the reflectance spectrum by modified Beer-Lamber laws, Gao and Goetz (1995) and Roberts et al. (1997) mapped EWT.

Jacquemoud and Baret (1993) were the first to link a leaf optical properties model, PROSPECT, to a canopy reflectance model, SAIL, namely PROSAIL, and to invert it on reflectance spectra (Figure 6). They estimated EWT by iterative inversion of the coupled model on sugar beet (*Beta vulgaris* L.) reflectance spectra acquired at nadir. Such a procedure has been later on successfully extented to AVIRIS and TM equivalent data (Jacquemoud, 1993; Jacquemoud et al., 1995). Danson and Aldakheel (2000) followed the same approach to study diurnal water stress, but nevertheless pointed out the limit of radiative transfer models to represent heterogeneities (clumping effect) in sugar beet crops, and then to simulate a correct reflectance. Finally, Zarco-Tejada et al. (2003) recently showed

that canopy water content could be retrieved by inversion of SAILH from MODIS (MODerate Resolution Imaging Spectroradiometer) reflectance bands, validating that seasonal desiccation of the canopy over the California summer drought can be measured by spectral changes in water absorption for chaparral communities in southern California.

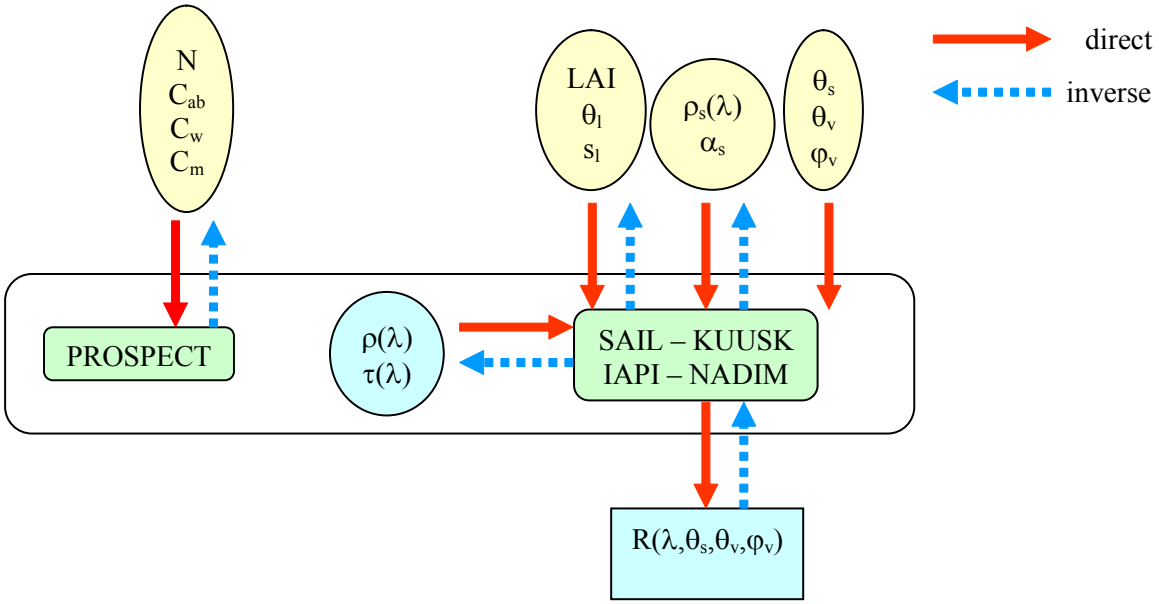


Figure 6. Schematic representation of the PROSPECT + SAIL (or any other canopy reflectance model) model, in direct and inverse modes.

## 4. CONCLUSION

The use of radiative transfer models to estimate moisture content is still in its infancy. Much more work is required before we completely understand the spectral variations of vegetation in relation to changes of water content, both at the leaf and canopy levels. This knowledge is nevertheless crucial to developing more accurate retrieval methods: models can be use in direct mode to build new indices optimized for the wavebands / view angles of actual sensors, but also in inversion. Although iterative inversions are still time consuming and not operational to date, artificial neural networks or look-up table techniques can be set up and tested on VEGETATION data on SPOT4, or MODIS data on TERRA satellites. Of course, emphasis must be placed on supporting field measurements to validate them.

The mapping of burned areas with models has not been evaluated in this review because of the small numbers of studies: Roy et al. (2002) proposed to detect variations in observed MODIS reflectance by inverting a parametric BRDF model. Finally, the spectral and bidirectional radiative properties of burnt scenes surprisingly have not given rise to any extensive study despite obvious usefulness.

## 5. REFERENCES

Bacour, C., Jacquemoud, S., Tourbier, Y., Dechambre, M. & Frangi, J.P. 2002. Design and analysis of numerical experiments to compare four canopy reflectance models. *Remote Sensing of Environment*, 79(1):72-83.

Baret, F. & Fourty, T. 1997. Estimation of leaf water content and specific leaf weight from reflectance and transmittance measurements. *Agronomie*, 17(9-10):455-464.

Bowman, W.D. 1989. The relationships between leaf waterstatus, gas exchange, and spectral reflectance in cotton leaves. *Remote Sensing of Environment*, 30:249-255.

Ceccato, P., Flasse, S., Tarantola, S., Jacquemoud, S. & Grégoire, J.M. 2001. Detecting vegetation water content using reflectance in the optical domain. *Remote Sensing of Environment*, 77(1):22-33.

Ceccato, P., Gobron, N., Flasse, S., Pinty, B. & Tarantola, S. 2002a. Designing a spectral index to estimate vegetation water content from remote sensing data: Part 1. Theoretical approach. *Remote Sensing of Environment*, 82:188-197.

Ceccato, P., Flasse, S. & Grégoire, J.M. 2002b. Designing a spectral index to estimate vegetation water content from remote sensing data: Part 2. Validation and applications. *Remote Sensing of Environment*, 82:198-207.

Danson, F.M., Steven, M.D., Malthus, T.J. & Clark, J.A. 1992. High-spectral resolution data for determining leaf water content. *International Journal of Remote Sensing*, 13(3):461-470.

Datt, B. 1999. Remote sensing of water content in Eucalyptus leaves. *Australian Journal of Botany*, 47(6):909-923.

Danson, F.M. & Aldakheel, Y.Y. 2000. Diurnal water stress in sugar beet: spectral reflectance measurements and modelling. *Agronomie*, 20(1):31-39.

Dauriac, F., Deshayes, M., Gillon, D. & Roger, J.M. 2001. Suivi de la teneur en eau de la végétation méditerranéenne par télédétection. Application au risque de feu de forêt. In *Colloque SIRNAT "Systèmes d'Information et Risques Naturels"*, 6-7 décembre 2001, Sophia-Antipolis (France), 10 p.

Dawson, T.P., Curran, P.J. & Plummer, S.E. 1998. LIBERTY - Modelling the effects of leaf biochemical concentration on reflectance spectra. *Remote Sensing of Environment*, 65:50-60.

Dawson, T.P., Curran, P.J. & Plummer, S.E. 1998. The biochemical decomposition of slash pine needles from reflectance spectra using neural networks. *International Journal of Remote Sensing*, 19(7):1433-1438.

Food and Agriculture Organization. 2001. *Global Forest Fire Assessment 1990-2000*. Forest Resources Assessment Programme, Working Paper 55, 495 p.

Fourty, T. & Baret, F. 1998. On spectral estimates of fresh leaf biochemistry. *International Journal of Remote Sensing*, 19(7):1283-1297.

Ganapol, B., Johnson, L., Hammer, P., Hlavka, C. & Peterson, D. 1998. LEAFMOD: a new within-leaf radiative transfer model. *Remote Sensing of Environment*, 6:182-193.

Gao, B.C. & Goetz, A.F.H. 1995. Retrieval of equivalent water thickness and information related to biochemical components of vegetation canopies from AVIRIS data. *Remote Sensing of Environment*, 52:155-162.

Gao, B.C. 1996. NDWI – A normalized difference water index for remote sensing of vegetation liquid water from space. *Remote Sensing of Environment*, 58:257-266.

Gillon, D., Dauriac, F., Deshayes, M., Valette, J.C. & Moro, C. 2002. Foliage moisture content and spectral characteristics using near infrared reflectance spectroscopy (NIRS), in *Proc. IV International Conference on Forest Research*, Luso (Portugal), 18-23 November 2002, 13 p.

Hosgood, B., Jacquemoud, S., Andreoli, G., Verdebout, J., Pedrini, G. & Schmuck, G. 1995. *Leaf Optical Properties EXperiment 93 (LOPEX93)*. European Commission, Joint Research Centre, Institute for Remote Sensing Applications, Report EUR 16095 EN.

Hunt, E.R., Rock, B.N. & Nobel, P.S. 1987. Measurement of leaf relative water content by infrared reflectance. *Remote Sensing of Environment*, 22:429-435.

Hunt, E.R. & Rock, B.N. 1989. Detection of changes in leaf water content using near and middle-infrared reflectances. *Remote Sensing of Environment*, 30(1):43-54.

Inoue, Y., Morinaga, S. & Shibayama, M. 1993. Non-destructive estimation of water status of intact crop leaves based on spectral reflectance measurements. *Japanese Journal of Crop Science*, 62(3):462-469.

Jackson, R.D. 1986. Remote sensing of biotic and abiotic plant stress. *Annual Review of Phytopathology*, 24:265-287.

Jacquemoud, S. & Baret, F. 1990. PROSPECT: a model of leaf optical properties spectra. *Remote Sensing of Environment*, 34:75-91.

Jacquemoud, S. & Baret, F. 1992. Estimating vegetation biophysical parameters by inversion of a reflectance model on high spectral resolution data. In *Crop Structure and Ligth Microclimate: Characterization and Applications* (C. Varlet-Grancher, R. Bonhomme and H. Sinoquet, eds), Editions de l'INRA (Versailles), pp. 339-350.

Jacquemoud, S. 1993. Inversion of the PROSPECT+SAIL canopy reflectance model from AVIRIS equivalent spectra: theoretical study. *Remote Sensing of Environment*, 44:281-292.

Jacquemoud, S., Baret, F., Andrieu, B., Danson, F.M. & Jaggard, K. 1995. Extraction of vegetation biophysical parameters by inversion of the PROSPECT+SAIL models on sugar beet canopy reflectance data. Application to TM and AVIRIS sensors. *Remote Sensing of Environment*, 52:163-172.

Jacquemoud, S., Ustin, S.L., Verdebout, J., Schmuck, G., Andreoli, G. & Hosgood, B. 1996. Estimating leaf biochemistry using the PROSPECT leaf optical properties model. *Remote Sensing of Environment*, 56:194-202.

Jacquemoud, S., Bacour, C., Poilve, H. & Frangi, J.P. 2000. Comparison of four radiative transfer models to simulate plant canopies reflectance – Direct and inverse mode. *Remote Sensing of Environmnent*, 74:471-481.

Maier, S.W., Lüdeker, W. & Günther, K.P. 1999. SLOP: A revised version of the stochastic model for leaf optical properties. *Remote Sensing of Environment*, 68(3):273-280.

National Park Service. 2001. *Fire Monitoring Handbook*. National Inter-agency Fire Center, Boise (ID), 288 p.

Newnham, G.J. & Burt, T. 2001. Validation of a leaf reflectance and transmittance model for three agricultural crop species. In *IEEE Geoscience and Remote Sensing Symposium (IGARSS'01)*. Vol. 7, pp. 2976 -2978.

Peñuelas, J., Filella, I., Biel, C., Serrano, L. & Savé, R. 1993. The reflectance at the 950-970 nm region as an indicator of plant water status. *International Journal of Remote Sensing*, 14(10):1887-1905.

Peñuelas, J. & Inoue, Y. 1999. Reflectance indices indicative of changes in water and pigment contents of peanut and weat leaves. *Photosynthetica*, 36(3):355-360.

Ripple, W.J. 1986. Spectral reflectance relationships to leaf water stress. *Photogrammetric Engineering & Remote Sensing*, 52(10):1669-1675.

Roberts, D.A., Green, R.O. & Adams, J.B. 1997. Temporal and spatial patterns in vegetation and atmospheric properties form AVIRIS. *Remote Sensing of Environment*, 62:223-240.

Rollin, E.M. & Milton, E.J. 1998. Processing of high spectral resolution reflectance data for the retrieval of canopy water content information. *Remote Sensing of Environment*, 65:86-92.

Roy, D.P., Lewis, P.E., Justice, C.O. 2002. Burned are mapping using multi-temporal moderate spatial resolution data – a bidirectional reflectance model-based expectation approach. *Remote Sensing of Environment*, 83:263-286.

Schmuck, G., Verdebout, J., Ustin, S.L., Sieber, A. & Jacquemoud, S. 1993. Vegetation and biochemical indices retrieved from a multispectral AVIRIS data set. In *Proc. 25th International Symposium on Remote Sensing and Global Environmental Change*, Graz (Austria), 4-8 April 1993, pp. 273-281.

Serrano, L., Ustin, S.L., Roberts, D.A., Gamon, J.A. & Peñuelas, J. 2000. Deriving water content of chaparral vegetation from AVIRIS data. *Remote Sensing of Environment*, 74(3):570-581.

Sims, D.A. & Gammon, J.A. 2003. Estimation of vegetation water content and photosynthetic tissue area from spectral reflectance: a comparison of indices based on liquid water and chlorophyll absorption features. *Remote Sensing of Environment*, 84(4):526-537.

Tian, Q., Tong, Q., Pu, R., Guo, X. & Zhao, C. 2001. Spectroscopic determination of wheat water status using 1650-1850 nm spectral absorption features. *International Journal of Remote Sensing*, 22(12):2329-2338.

Ustin, S.L., Roberts, D.A., Jacquemoud, S., Pinzon, J., Gardner, M., Scheer, G.J., Castaneda, C.M. & Palacios, A. 1998. Estimating canopy water content of chaparral shrubs using optical methods. *Remote Sensing of Environment*, 65:280-291.

Ustin, S.L., Smith, M.O., Jacquemoud, S., Verstraete, M.M. & Govaerts Y.M. 1999. Geobotany: vegetation mapping for Earth sciences. In *Remote Sensing of the Earth Sciences: Manual of Remote Sensing* (A.N. Rencz, ed). John Wiley & Sons (New York), Vol. 3, pp. 189-248.

Yu, G.R., Miwa, T., Nakayama, K., Matsuoka, N. & Kon, H. 2000. A proposal for universal formulas for estimating leaf water status of herbaceous and woody plants based on spectral reflectance properties. *Plant Soil*, 227(1-2):47-58.

Zarco-Tejada, P.J., Rueda, C.A. & Ustin, S.L. 2003. Water content estimation in vegetation with MODIS reflectance data and model inversion methods. *Remote Sensing of Environment*, 85:109-124.

# Combining NDVI and Surface Temperature for the estimation of fuel moisture content in forest fire danger assessment

E. Chuvieco & D. Cocero
*Department of Geography, University of Alcalá, Madrid, Spain*
emilio.chuvieco@uah.es

P. Martín & J. Martínez
*Institute of Economy and Geography, CSIC, Madrid, Spain*

J. de la Riva & F. Pérez
*Department of Geography, University of Zaragoza, Zaragoza, Spain*

Keywords: Fuel Moisture Content, NOAA-AVHRR, NDVI, Surface Temperature

ABSTRACT: This paper is presents an empirical method for deriving FMC for Mediterranean grasslands and shrub species based on multitemporal analysis of NOAA-AVHRR data. The method is based on long-term field measurements of FMC, and it is based on multitemporal composites of NDVI and surface temperatures. It was tested on several regions with similar species, providing a robust estimation, which makes it possible to be applied in operational management.

## 1. BACKGROUND

Reduction of the severe environmental impacts caused by forest fires requires better means to estimate fire danger conditions. Most research in the use of remote sensing techniques to forest fire applications have focused on detecting active fires, mainly using mid-infrared images (Ahern et al. 2001; Martín et al. 1999). More recently, burned land mapping is also widely extended, both at local and global scales (Barbosa et al. 1999; Koutsias et al. 1999). However, fewer activities have been reported in the pre-fire phase, which is critical to better manage fire suppression resources to reduce fire ignitions and mitigate fire propagation rates. Within this approach, remote sensing tools may greatly help the characterization of the fuel bed, both with respect to biomass loads and structural properties (commonly referred as fuel types: Deeming 1975; Riaño et al. 2002), on one hand, and water status, on the other. The latter will be the basis for this paper.

Several authors have proven that the amount of water contained in vegetation tissues is a critical variable in fire ignition and fire propagation modelling (Van Wagner 1967; Viney 1991). In forest fire danger literature, water content of plants is commonly expressed as Fuel Moisture Content (FMC), defined as the percentage of water weight over sample dry weight:

$$FMC = \left( \frac{W_w - W_d}{W_d} \right) * 100 \qquad (1)$$

where $W_w$ is the wet weight and $W_d$ the dry weight of the same sample. This variable is mostly obtained through field sampling using gravimetric methods (wet samples are weighted, then oven-dried at 60 or 100º C: Viegas et al. 1992 and weighted again to find out the water weight). FMC can be referred to both live and dead species. The latter are the most related to fire ignition, since dead fuels are generally much drier than live fuels. However, FMC of live plants is also critical in fire propagation modelling (Renkin & Despain 1992). In this paper, we will just focus on the estimation of

FMC for live species, since vegetation canopy most commonly hinders dead materials lying on the forest floor.

The estimation of FMC from remote sensing images have been successfully reported for herbaceous species using NDVI multitemporal series of NOAA-AVHRR data, but problems were found for shrubs and trees (Chuvieco et al. 1999; Leblon 2001; Paltridge & Barber 1988]). Laboratory spectral measurements have also been undertaken, showing divergence results in the visible and near infrared, although short wave infrared bands (SWIR) were proven the most sensitive to water content variations (Bowman 1989; Cohen 1991). Simulation studies based on physical models have recently proven that NDVI is not a good indicator of FMC, since it is severely influenced by other variables that are not related to water content (Ceccato et al. 2001; Ceccato et al. 2002). Additionally, these studies have shown that FMC can not be directly retrieved from reflectance measurements, but rather it should be used the equivalent water thickness (EWT: water content / leaf surface), which is directly related to water absorption in the SWIR wavelengths. However, since EWT is not used in forest fire literature, it is less useful for fire danger estimation. Assuming a constant relation between leaf area and leaf weight within each species, FMC may be considered a function of EWT (Chuvieco et al. 2003). Therefore, it can be estimated from reflectance measurements when the estimation is restricted to a single species. Application to several species would require a correction factor that takes into account the differences in leaf area-leaf weight from the reference species.

## 2. METHODS

Field measurements of FMC have been performed from early April to the end of September between 1996 and 2002 in the Cabañeros National Park (Central Spain) to derive the model (1996 to 1999 data) and testing it (2000 to 2001). Additionally, field samplings with the same protocol were performed in other regions within Spain. The plots are quite distant from the original study site (Fig. 1), and have different elevations. However, they have similar species, being part of the Mediterranean ecosystem. In this paper, results will be reported for grasslands and Cistus ladanifer, a widely extended shrub across the Mediterranean basin.

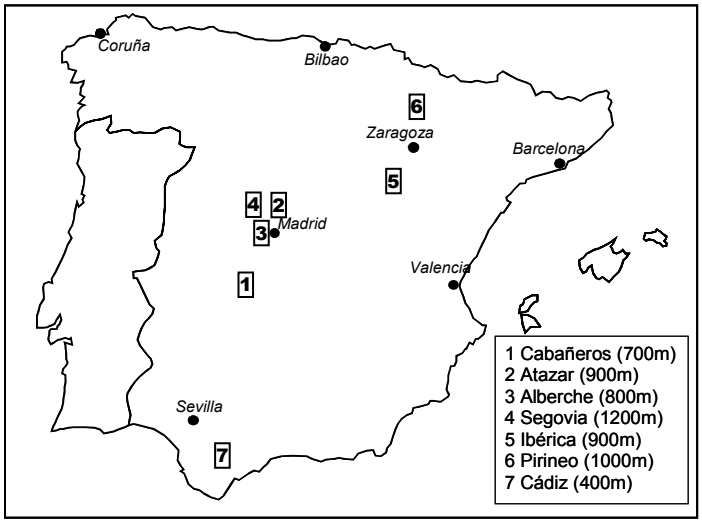


Field samples were composed of terminal leaves for shrubs, whereas the whole plant was extracted for herbaceous species. Three samples per species and plot were collected every 8 days between 12 and 16 hours GMT, and average values were computed for each day and plot.

AVHRR images were acquired by University of Alcala's HRPT receiving station. Raw digital to reflectance conversion was based on NOAA coefficients (including degradation rates), and surface temperature (ST) was based on methods proposed by Coll and Caselles (1997). Geometrical correction was based on orbital models and multitemporal matching was improved by manual control points and automatic correlation. Daily data was synthetised in 8-day composites using maximum NDVI values. The median value of a 3x3 pixels window was extracted from each composite to correlate with field measurements.

Empirical fittings were based on linear regression analysis. The model was based on 88 observations for each species, grasslands and *C. ladanifer*, acquired during four years (1996 to 1999),

covering spring and summer conditions. Independent variables considered were NDVI (since water content decrease also influences chlorophyll activity in herbaceous plants) and ST (based on proven relations between evapotranspiration rates and plant temperature). Additionally, a temporal variable based on Julian day (from 1 to 365) was included, to take into account seasonal trends in FMC.

Empirical fittings were based on linear regression analysis. The model was based on 88 observations for each species, grasslands and *C. ladanifer*, acquired during four years (1996 to 1999), covering spring and summer conditions. Independent variables considered were NDVI (since water content decrease also influences chlorophyll activity in herbaceous plants) and ST (based on proven relations between evapotranspiration rates and plant temperature). Additionally, a temporal variable based on Julian day (from 1 to 365) was included, to take into account seasonal trends in FMC.

## 3. RESULTS

The very diverse physiological conditions and FMC values of grasslands and the shrub species advised to derive two different empirical equations, as follows:

$$FMCg = 155.439 + 452.43 * NDVI - 1.627 * ST - 0.747 * JD \quad (2)$$

for grasslands, with a determination coefficient ( $r^2$) of 0.652 ($p<0.001$), and

$$FMCc = 188.553 + 74.168 * NDVI - 2.011 * ST - 0.221 * JD \quad (3)$$

for *C.ladanifer*, with $r^2= 0.623$ ($p<0.001$). In both cases, NDVI is the Normalized Difference Vegetation Index, ST the surface temperature and JD the Julian day. Significance values were 2.81776E-05 for NDVI, 0.082696741 for ST and 0.028254138 for JD in the case of grasslands, and 3.08017E-07 for NDVI, 0.000820745 for ST and 0.000880976 for JD in the case of *C.ladanifer*.

The assessment of these equations was undertaken with other periods (years 2000-2001) in the same study site (Cabañeros), and in other study sites, with good results in all cases. Figures 2 and 3 show observed and predicted values for both vegetation types in the different regions sampled. When mixing data from 3 different regions, determination coefficients are 0.85 for grasslands and 0.74 for *C.ladanifer*. Data from Alberche-Atazar, Segovia and Cabañeros were included in the case of grasslands and from Cabañeros, Sevilla and Alberche for *C.ladanifer*. In spite of being quite far from each other (several hundred kilometres) and with different elevation ranges, the model shows similar prediction ability in the different study sites.

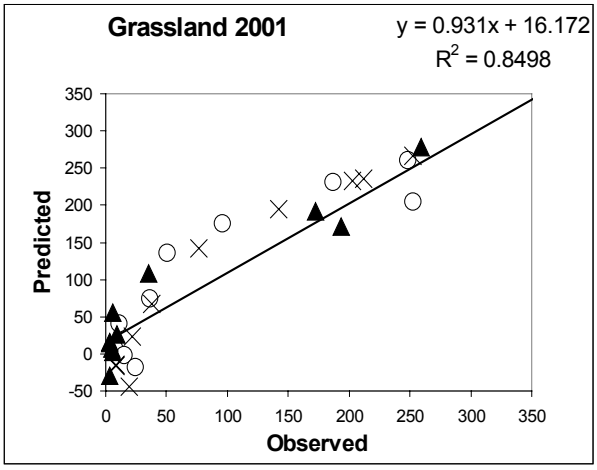


Figure 2: Observed and predicted FMC values of grassland: ▲Cabañeros plots; ○ Alberche-Atazar plots; x Segovia plots.

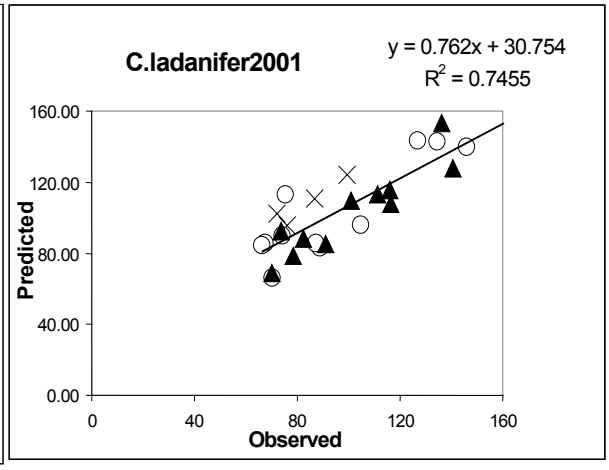


Figure 3: Observed and predicted FMC values of *C.ladanifer*: ▲Cabañeros plots; ○ Alberche-Atazar plots; x Sevilla plots.

## 4. DISCUSSION

The empirical model generated from NDVI, ST and Julian Day shows consistent predictive power to estimate FMC of grasslands and *C.ladanifer*, a typical Mediterranean shrub species. The model was tested in plots located several hundred kilometres apart, and with different elevation ranges. Therefore, it might serve as a basis for testing it in operational scenarios. The extension to other shrub species may be based on coefficients based on the specific leaf area of *C.ladanifer* and other species, but this hypothesis should be tested in future studies.

## 5. REFERENCES


Ahern, F. J., Goldammer, J. G., & Justice, C. O. (Eds.). 2001. *Global and Regional Vegetation Fire Monitoring from Space: Planning a coordinated international effort*. The Haghe, The Netherlands: SPB Academic Publishing.

Barbosa, P. M., Grégoire, J. M., & Pereira, J. M. C. 1999. An algorithm for extracting burned areas from time series of AVHRR GAC data applied at a continental scale. *Remote Sensing of Environment*, Vol. 69: 253-263.

Bowman, W. D. 1989. The relationship between leaf water status, gas exchange, and spectral reflectance in cotton leaves. *Remote Sensing of Environment*, Vol. 30: 249-255.

Ceccato, P., Flasse, S., Tarantola, S., Jacquemoud, S., & Grégoire, J. M. 2001. Detecting vegetation leaf water content using reflectance in the optical domain. *Remote Sensing of Environment*, Vol. 77: 22-33.

Ceccato, P., Gobron, N., Flasse, S., Pinty, B., & Tarantola, S. 2002. Designing a spectral index to estimate vegetation water content from remote sensing data: Part 1 Theoretical approach. *Remote Sensing of Environment*, Vol. 82: 188–197.

Chuvieco, E., Deshayes, M., Stach, N., Cocero, D., & Riaño, D. 1999. Short-term fire risk: foliage moisture content estimation from satellite data. In E. Chuvieco (Ed.), *Remote Sensing of Large Wildfires in the European Mediterranean Basin*: 17-38. Berlin: Springer-Verlag.

Chuvieco, E., Aguado, I., Cocero, D., & Riaño, D. 2003. Design of an Empirical Index to Estimate Fuel Moisture Content from NOAA-AVHRR Analysis In Forest Fire Danger Studies. *International Journal of Remote Sensing*, Vol. (in press).

Cohen, W. B. 1991. Temporal versus spatial variation in leaf reflectance under changing water stress conditions. *International Journal of Remote Sensing*, Vol. 12: 1865-1876.

Coll, C. & Caselles, V. 1997. A global split-window algorithm for land surface temperature from AVHRR data: validation and algorithm comparison. *Journal of Geophysical Research*, Vol. 102B14: 16697-16713.

Deeming, J. E. 1975. Fuel models in the national fire danger rating system. *Journal of Forestry*, Vol. 73 (No6): 347-350.

Koutsias, N., Karteris, M., Fernández, A., Navarro, C., Jurado, J., Navarro, R., & Lobo, A. 1999. Burnt land mapping at local scale. In E. Chuvieco (Ed.), *Remote Sensing of Large Wildfires in the European Mediterranean Basin*: 123-138. Berlin: Springer-Verlag.

Leblon, B. 2001. Forest Wildfire Hazard Monitoring Using Remote Sensing: A Review. *Remote Sensing Reviews*, Vol. 20 (No1): 1-57.

Martín, M. P., Ceccato, P., Flasse, S., & Downey, I. 1999. Fire detection and fire growth monitoring using satellite data. In E. Chuvieco (Ed.), *Remote Sensing of Large Wildfires in the European Mediterranean Basin*: 101-122. Berlin: Springer-Verlag.

Paltridge, G. W. & Barber, J. 1988. Monitoring grassland dryness and fire potential in Australia with NOAA/AVHRR data. *Remote Sensing of Environment*, Vol. 25: 381-394.

Renkin, R. A. & Despain, D. G. 1992. Fuel moisture, forest type, and lightning-caused fire in Yellowstone National Park. *Canadian Journal of Forest Research*, Vol. 22: 37-45.

Riaño, D., Chuvieco, E., Salas, J., Palacios-Orueta, A., & Bastarrica, A. 2002. Generation of fuel type maps from Landsat TM images and ancillary data in Mediterranean ecosystems. *Canadian Journal of Forest Research*, Vol. 32: 1301-1315.

Van Wagner, C. E. 1967. Seasonal variation in moisture content of Eastern Canadian tree foliage and the possible effect on crown fires: 15: Forestry Branch, Canada.

Viegas, D. X., Viegas, T. P., & Ferreira, A. D. 1992. Moisture content of fine forest fuels and fire occurrence in central Portugal. *The International Journal of Wildland Fire*, Vol. 2 (No2): 69-85.

Viney, N. R. 1991. A review of fine fuel moisture modelling. *International Journal of Wildland Fire*, Vol. 1 (No4): 215-234.

# Sensitivity of remotely sensed spectral reflectance to variation in fuel moisture content

F.M. Danson & P. Bowyer
*Telford Institute of Environmental Systems, School of Environment and Life Sciences, University of Salford, Mancheste, UK*
f.m.danson@salford.ac.uk

Keywords: fuel moisture content, spectral reflectance, sensitivity modeling

ABSTRACT: Fuel moisture content (FMC) is computed from leaf fresh and dry weight and is a relative measure of vegetation water content used extensively in fire risk modelling. FMC is a dimensionless variable that is related to both leaf water content and to leaf dry matter content. This paper uses a vegetation canopy model to examine the sensitivity of remotely sensed data to variation in the FMC. The research employs a global sensitivity analysis technique that provides insights into the key factors driving canopy reflectance at different wavelengths and evaluates the potential for estimating FMC by canopy reflectance model inversion.

## 1. INTRODUCTION

Fuel moisture content (FMC) is a key parameter in forest fire risk modelling because it is closely related to the probability of ignition within the vegetation canopy. However, collection of FMC data from field measurements is labour-intensive and does not provide the spatial and temporal data dimensions that are required to drive spatially explicit fire-risk models. Airborne and satellite remote sensing do provide data with the appropriate spatial and temporal dimension and there is now good evidence that FMC may be mapped using vegetation indices (VI) derived from such data (Hardy and Burgan 1999, Chuvieco *et al*. 2002). There are a number of limitations to the VI approach however, including the site- and time-specific nature of the calibration equations derived, the influence of 'external' variables like viewing and illumination geometry, and the failure to incorporate *a priori* information (Danson, Rowland and Baret, 2003). Some of these limitations may be overcome by the application of radiative transfer model inversion to estimate FMC from satellite remote sensing data. This paper is the first stage in the evaluation of this approach.

A requirement of a well-posed remote sensing inversion problem is that relationships exist between the model outputs and the model inputs that correspond to the biophysical variables of interest (Jacquemoud *et al*.1995). In the case of FMC this is problematic however, because it is a dimensionless combination of two independent biophysical properties of the leaves: the water content and the dry matter content (Ceccato *et al*. 2001). Hence, at the leaf level there is no unique relationship between reflectance and FMC. At the canopy level this problem is confounded by spatial variation in leaf area index and other variables like canopy structure which influence canopy reflectance. A possible way forward is to constrain the model inversion by incorporating *a priori* information in the inversion procedure. To pursue this approach it is important to quantify the contribution of the biophysical and environmental variables to the variation in remotely sensed reflectance. The results of Ceccato *et al*. (2002) indicated that, at the canopy level, leaf reflectance is the most important variable determining canopy reflectance. In this paper the relative contribution of leaf water content and leaf dry matter content to canopy reflectance are evaluated separately since they contribute independently to variation in FMC. In addition, a geometric-optical model is used to examine the influence of

variation in canopy structure, which is likely to affect remotely sensed reflectance in areas with incomplete vegetation cover. Since there are no measured data sets that allow this to be done over a wide range of conditions, an approach was adopted where radiative transfer model simulations provide inputs to a sensitivity analysis (SA).

## 2. METHODOLOGY

Simulations were performed in three stages: first, at leaf level using the Prospect model (Jacquemoud and Baret 1990), second, at canopy level using the combined Prospect and SAIL model (PROSAIL) and third, at canopy level using the Prospect and a geometric optical model GeoSAIL (PROGOSAIL) (Huemmrich 2001). This approach allowed a step-wise introduction of the effect of canopy structure and the identification of the variance induced in the remotely sensed data.

Two different approaches to SA have been implemented in the terrestrial remote sensing literature, *local* and *global*. Local SA concentrates on the impact of individual factors in the model by allowing a single model parameter to vary, while the others remain fixed. The sum-squared difference from a base case is then used as a measure of the relative importance of each parameter in driving variation in reflectance. A local SA provides information on how variation in each parameter produce variation in the model output, known here as the first-order effects.

A global SA differs to the local SA method significantly in that the full range of the model parameter variability is explored (rather than variability around a mean value) and the model parameters are varied simultaneously in model runs, rather than varying one parameter at a time. The results of a global SA therefore provide information on the interactions of the model parameters in driving model output variance. The global SA method used in this research was the Extended Fourier Amplitude Sensitivity Test (EFAST) (Saltelli *et al*. 1999), which is an extension of the classical Fourier Amplitude Sensitivity Test (FAST) and first applied to optical remote sensing data by Ceccato *et al*. (2001). FAST allows calculation of the first-order effects (additive) of variation in the model parameters, while the EFAST allows calculation of both the first- and total-order effects resulting from the interactions of all the model parameters.

In the work described in this paper the model variables were set to predefined ranges and a uniform statistical distribution representing a global range of all variables (table 1). 5000 randomly selected sets of model data were drawn from the ranges specified and input to the three models. This resulted in 5000 simulated reflectance spectra (400-2500nm) for each model. These data were then input into the EFAST analysis and sensitivity data computed.

## 3. RESULTS

The results of the analysis were visualised by plotting the first order and total order sensitivity indices for the outputs from each of the model simulations. At the leaf level the results confirmed those of Ceccato *et al*. (2001) with sensitivity to leaf chlorophyll in the visible region, to leaf dry matter in the near infrared (NIR) and leaf water content in the short-wave infrared (SWIR). Since FMC is a combination of both leaf water content and leaf dry matter content, the estimation of FMC from remotely sensed data is likely to require reflectance data in both the NIR and at SWIR wavelengths.

At the canopy level the results from the turbid medium PROSAIL model complement those of Ceccato *et al*. (2002) as they show sensitivity to leaf water and dry matter content at high spectral resolution (Figure 1a). Leaf dry matter (or specific leaf weight, SLW) is the dominant variable in the NIR and is therefore likely to confound attempts to estimate FMC using VI that include a NIR waveband. At wavelengths beyond 1100nm LAI becomes dominant and this will also confound variation caused by differences in leaf water and dry matter content, and therefore FMC. The results for the geometric-optical model (PROGOSAIL, figure 1b) highlight the critical effect of variation in

canopy fractional cover that is dominant in the SWIR. The effects of variation in solar zenith angle are also significant compared with the turbid medium case.

Table 1. Radiative transfer model variable ranges

| Model Parameter | PROSPECT | PROSAIL | PROGOSAIL |
|---|---|---|---|
| Illumination and Viewing Geometry | | | |
| Solar zenith angle (SZA) | | 17 - 70 | 17 - 70 |
| Leaf Level | | | |
| Leaf chlorophyll content (Cab) (µg m-2) | 1 – 75 | 1 - 75 | 1 – 75 |
| Leaf water content (EWT) (g cm-2) (cm) | 0.0001 - 0.085 | 0.0001 - 0.085 | 0.0001 - 0.085 |
| Leaf dry matter (SLW) (g cm-2) | 0.0014 - 0.05 | 0.0014 - 0.05 | 0.0014 - 0.05 |
| N (Leaf structure parameter) | 1 - 6.65 | 1 – 6.65 | 1 - 6.65 |
| Canopy Level | | | |
| Leaf area index (LAI) | | 0.001 - 6 | 0.001 - 6 |
| Fraction of vegetation cover | | | 0 - 1 |

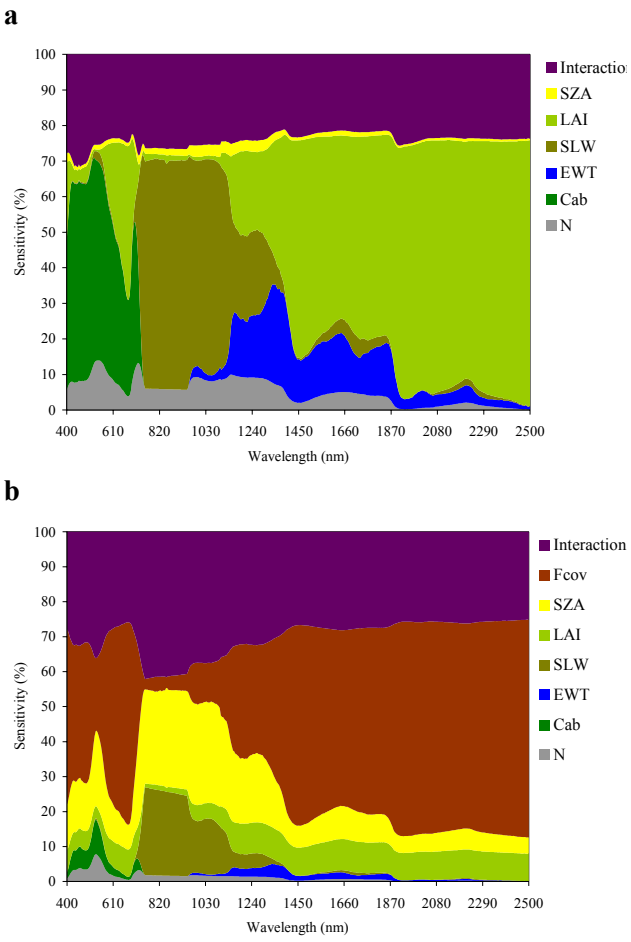


Figure 2. First order sensitivity and interactions for a) turbid medium PROSAIL model and b) geometric optical PROGOSAIL model

These results suggest that successful estimation of FMC using VI is likely to be possible where there is limited spatial and temporal variation in fractional cover, LAI and leaf dry matter content. Under these conditions, the variation in spectral response of the canopy is controlled primarily by leaf water content. Simulations were performed with the model variable ranges set to those found at field sites in central Spain and southern France and the results confirm that under local conditions the sensitivity of canopy reflectance to variation in leaf water content, and FMC, is significantly increased.

## 4. CONCLUSIONS

This research has highlighted the nature of the problem of estimating FMC from remotely sensed data. It has confirmed that VI approaches should combine data in the NIR with data at a longer wavelength in the SWIR. It has also highlighted that in 'real' vegetation canopies where the canopy is clumped in individual tree or shrub crowns, the spatial variation in LAI and fractional cover are likely to confound attempts to estimate FMC from remotely sensed data. The application of VI to estimate FMC at local scale may be feasible if spatial and temporal variation in LAI and leaf dry matter content is low. An alternative approach is to use radiative transfer model inversion where data on canopy geometry, canopy LAI and solar zenith angle can be incorporated into a model inversion strategy. These variables can then be fixed in the inversion and their effect on reflectance removed. In the next stage of this research further sensitivity analyses will be performed to examine the effect of incorporating such information and the use radiative transfer model inversion techniques to estimate FMC will be evaluated.

## 5. REFERENCES


Ceccato, P., Flasse, S., Tarantola, S., Jacquemoud, S. & Grégoire, J.M. 2001. Detecting Vegetation Leaf Water Content Using Reflectance in the Optical Domain. *Remote Sensing of Environment* 77, 22-33.

Ceccato, P., Gobron, N., Flasse, S., Pinty, B. & Tarantola, S. 2002. Designing a Spectral Index to Estimate Vegetation Water Content from Remote Sensing Data. Part 1: Theoretical Approach. *Remote Sensing of Environment* 82, 188-197.

Chuvieco, E., Riaño, D., Aguado, I., & Cocero, D. 2002. Estimation of Fuel Moisture Content From Multitemporal Analysis of Landsat Thematic Mapper Reflectance Data: Applications In Fire Danger Assessment. *International Journal of Remote Sensing* 23, 2145-2162.

Danson, F.M., Rowland, C.S. & Baret, F. 2003. Training a Neural Network to Estimate Crop Leaf Area Index, *International Journal of Remote Sensing* (in press).

Hardy, C.C., & Burgan, R.E. 1999. Evaluation of NDVI for Monitoring Live Moisture in Three Vegetation Types of the Western U.S. *Photogrammetric Engineering and Remote Sensing* 65, 603-610.

Huemmrich, K.F. 2001. The Geosail Model: a Simple Addition to the SAIL Model to Describe Discontinuous Canopy Reflectance. *Remote Sensing of Environment* 75, 423-431.

Jacquemoud, S., & Baret, F.1990. PROSPECT: A Model of Leaf Optical Properties Spectra. *Remote Sensing of Environment* 34, 75-91.

Jacquemoud, S., Baret, F., Andrieu, B., Danson, F.M., & Jaggard, K. 1995. Extraction of Vegetation Biophysical Parameters by Inversion of the PROSPECT + SAIL Models on Sugar Beet Canopy Reflectance Data. Application to TM and AVIRIS Sensors. *Remote Sensing of Environment* 52, 163-172.

Saltelli, A., Tarantola, S. & Chan, K. P-S. 1999. A Quantitative Model-Independent Method for Global Sensitivity Analysis of Model Output, *Technometrics* 41, 39-56.

# Fuel Moisture Content Estimation using Terra Modis sensor: a first approach in South-Eastern France

F. Dauriac, M. Deshayes & P. Coing
*Cemagref-Engref, Montpellier, France*
dauriac@teledetection.fr

Keywords: remote sensing, Terra MODIS, FMC, SWIR, BRDF effects, Mediterranean area

ABSTRACT: Vegetation indices derived from satellite data are often applied to assess physiological variables of plants, including fuel moisture content (FMC). This study is focused on the use of Terra MODIS data, including its improved short-wave infrared bands, to estimate the FMC of the Mediterranean vegetation in South-Eastern France. Daily surface temperature (ST), daily reflectance and 16-day reflectance products are compared to field FMCs. This first approach illustrates atmospheric and bi-directional reflectance distribution function (BRDF) effects on daily data. First improvements to select field samples and to process Modis data are suggested.

## 1. INTRODUCTION AND STATE-OF-THE-ART

Fuel moisture content (FMC) is one of the critical factors affecting forest fire danger. It is taken into account in most fire danger and fire behavior modeling systems (Rothermel *et al*., 1986; Andrews *et al.*, 1990; Hartford *et al*., 1991). Both fire ignition and propagation are closely linked to FMC. At present time FMC is currently obtained from field campaigns but this method limits its temporal and spatial application.

Remote sensing techniques could represent a very convenient way of data acquisition for detecting vegetation water content on a large scale and several times during the season. Until now, studies have generally relied on establishing an empirical relationship between FMC and reflectance in one or more wavebands, sometimes combined in an index.

Fourty and Baret (1998) have demonstrated that water content and dry matter content of the leaves are robustly accessible by reflectance measurements. Leaves are the most appropriate vegetation components to correlate their water content with the information obtained from Earth Observation (EO) data. The moisture index used is the Fuel Moisture Content noted FMC, defined as the proportion of the amount of water versus the dry weight of the sample. This index is the most commonly used to measure plant water stress (Blackmarr and Flanner, 1968; Simard, 1968; Viney, 1991; Viegas *et al.*, 1992). It is easy to obtain and very sensitive to changes of fresh weight (Chuvieco *et al*., 2002).

New Earth observation satellites explore the environment with better spatial, spectral and temporal accuracy. Plant physiological parameters are studied in the visible and infrared part of the electromagnetic spectrum. Several studies have shown the interest of the thermal bands of NOAA-AVHRR (Deshayes *et al.*, 1998; Chuvieco *et al.*, 1999) but the results remained heterogeneous. Ceccato *et al*. (2002a, 2002b) have recently develop a new index using both near infrared (NIR) and SWIR bands of Spot Vegetation to predict the water stress of savannas in western Africa. At local scale Chuvieco *et al*. (2002) have showed good FMC estimation with Landsat Thematic Mapper data.

## 2. OBJECTIVES

In this study Terra Modis data are used with an improved spectral coverage including three SWIR bands. The main work consists in examining indices and maps to estimate FMC from EO-data.

The following innovations can be highlighted: (1) The use of spatially and spectrally improved satellite data sources, since they should provide a clearer discrimination of water absorption bands; (2) an extended and improved field protocol to collect FMC.

## 3. METHODOLOGY

### *3.1 Field data collection: spatial variability of FMC and production of pixel-wise FMC*

The experimental part of the project consists in collecting spatial and temporal evolutions of FMC. The study was carried out on summer 2001, from June to October. The FMC field collection was made twice a week on 37 different sites distributed over the French Mediterranean zone (total area of 80,000 km²) where the major disturbance is wildfires (0.5% of fire sensitive areas is burnt every year). Two sampling protocols are distinguished:

- a first protocol comprises 29 sites, 20 to 80km apart from one another, sampled by the French National Forest Service (ONF) through its FMC survey network. For each site, the FMC sampled represents roughly an area of 20 by 20m (decametric scale).
- a second protocol comprises 8 sites, controlled by two research institutes (Cemagref and Inra), with a FMC collection at two different scales: a decametric scale inside each site (20 by 20m and 40 by 40m, with collection of nine samples) and an hectometric scale between sites (300 to 400m apart from one another). To facilitate the use of EO data, these sites were selected on areas known a priori as having both a flat relief (to avoid influence of illumination effects) and a uniform monospecific vegetation cover, with a height below 4 to 5 meters (to enable a quicker field collection). The FMC sampling at hectometric scale provides a pixel-wise FMC, linked to the size of one MODIS pixel.

Totally on all sites, twenty different Mediterranean species (trees and shrubs) are collected. On all sites, the climate is Mediterranean with a marked summer drought and an annual rainfall varying from 500 to 900 mm.

FMC missing values (for days without sampling) are linearly interpolated. No estimation is made if the time between two samples exceeds five days or if the day is rainy. During summer 2001, for each ONF site two species were collected. But information on coverage of each species were not available. As tests have showed a better correlation with the average FMC of the two monitored species than with the FMC of one species alone, the average FMC seems to better represent the FMC at canopy scale and of course at Terra Modis scale. The use of low-resolution satellite data does not permit analysis at species level in most ecosystems because one pixel usually contains a mixture of several species (Ceccato *et al*., 2001).

### *3.2 Terra MODIS data collection and processing*

The field measurements of FMC are then put in relation with daily reflectance, surface temperature and derived indices obtained from Terra MODIS data. Three different types of Terra Modis data were used: (1) daily reflectance data: *MOD09 GHK, surface reflectance daily L2G*; (2) 16-day reflectance data: *MOD43 B4, nadir BRDF-adjusted reflectance 16-day L3*; (3) daily surface temperature data: *MOD11 A1, land surface temperature/emissivity daily L3*. Both *MOD09* and *MOD11* are provisional products, i.e. products only partially validated. These data are viewed as early science validated products and useful for exploratory scientific studies. Quality may not be optimal since validation and quality assurance are ongoing. At the opposite, *MOD43* is a validated product at stage 1, i.e. its product accuracy has been estimated using a small number of independent measurements obtained from selected locations and time periods and ground-truth/field program efforts. These validated data are high quality products suitable for longer term or systematic scientific studies and publication.

For reflectance data, the best product proposed by NASA (National Aeronautics and Spatial Administration) is the validated 16-day surface reflectance (*MOD43*). Reflectance values in each band can be used without further corrections. In order to be put in relation with this 16-day reflectance a FMC value had to be proposed, as the original FMC values were collected with a twice a week periodicity. The average FMC on the corresponding 16-day periods was chosen. However by having a look at the data, it has been noted that FMC values vary at a 5- to 10-day temporal scale for most sites. Therefore the 16-day average removes a part of the initial FMC variability.

At the opposite, the provisional daily reflectance data (MOD09) need some calibration to remove the biggest errors (i.e. reflectance over 1, negative value below –0.05). However, after this preprocessing numerous data still remain with high reflectance values (over 0.7), because of BRDF effects.

Another preprocessing was needed to take care of a too important soil influence on some of our sites. As mentioned above, we have poor information for most of the sites and particularly on the canopy *vs.* soil cover ratio. Ancillary field experiences with field radiometer carried out in a few sites near Montpellier has showed the interest of a simple NIR/R ratio, also called Ratio Vegetation Index (RVI) (Pearson *et al*., 1972). Data with a value of this index below 4 were rejected as a below 4 value appeared as a serious expression of a not sufficiently vegetated soil. 45% of the original data were eliminated with this filter.

Concerning surface temperature data (*MOD11*) no corrections are needed. Days with temperatures below 15°C (unusual for the sites and period studied) are removed automatically by the previous RVI>4 filter.

After all these preprocessing steps, the eight initial bands (seven reflectances and ST) and a variety of twelve indices, combining two to four bands (such as NDVI, GVMI, SLAVI, GRARI, NDVI/ST…) were tested.

At the end of this presentation of data and methods used, a short summary can be made. The different phases of processing have left us with 55% of the initial EO-data, after the use of a RVI>4 soil adjusting filter which improves both daily *MOD09* and *MOD11* data. The daily products delivered by NASA are still provisional and subject to BRDF effects. We have noted that the available field data are heterogeneous and not entirely adapted to this preliminary study.

## 4. RESULTS

First results are presented hereafter, concerning on the one hand the correlation between FMC and EO data on the different sites with field measurements, and on the other hand the interest of maps of indices generally used for FMC assessment.

### *4.1 Site-wise temporal variability of FMC*

A remark should be made first on the spatial variability of FMC and the production of pixel-wise FMC. On the sites of the second protocol, using the nested decametric and hectometric scales, a strong correlation is always noted between the different samples of the same decametric site, the correlation is reduced when one compares sites situated at 300 to 400 meters. This means that –in these sites at least- the use of the FMC of only one local site to represent the whole pixel-wise FMC would produce a certain error. On these sites, the production of the pixel-wise FMC by averaging different measurements collected 300 to 400 meters apart is justified.

As most of our sites do not benefit from this improved protocol, the processing has been organised in two groups: one group with test sites benefiting from pixel-wise FMC sampling and one with all the data mixed without distinction. In the following tests, field FMC and Modis data are compared, for the two groups of sites, for each Modis product used and during different periods including limited humid or arid ones. In Table 1, the first results are presented, with the best coefficient of determination ($r^2$) of linear regression between FMC and the best derived index.

In both cases (sites with extended protocol or all sites mixed) results are not radically different. For the 2001 period, sites sampled at hectometric scale have not given correlation as good as expected. Both for daily and 16-day data, two reasons can be given: (a) on the *Q. ilex* site, the FMC varies only from 65 to 88%, denoting a species well adapted to important drought conditions; (b) for the sites with small scrubs of *Quercus coccifera*, the biomass may be too low and the soil influence too big. For daily data, as temporal profiles of daily surface temperature and reflectance appear quite noisy, one important reason can be added with the strong influence of BRDF effects, not corrected up to now (but this will be the next step). For 16-day data, another reason, already mentioned, may lie with the length of the averaging period, not fully in phase with the evolution of FMC of the vegetation.

Generally speaking, no significant relation is identified between FMC and bands or FMC and indices. However it can be noted that the use of indices combining SWIR bands (such as NIR/SWIR, GVMI, NDII) improves the relation, but there is no important improvement when using indices combining ST.

Besides, the use of multiple regression or non-linear regression raises the determination coefficient ($r^2$) to 0.4 for all sites and bands, to 0.9 in some selected sites (accounting for less than 10% of initial data).

Tests on two limited periods, humid (high FMC) and arid (low FMC), show better FMC estimation for humid ones (i.e. 5-14 July, Table 1), but not the arid one. No plausible explanation has been found.

Table 1. First results with Modis data (daily reflectance, daily surface temperature, 16-day reflectance)

| | Series | | Only 8 sites controlled | | | All 37 sites | | |
|---|---|---|---|---|---|---|---|---|
| | Characteristics | Scale | $r^2$ max | Best index | Size | $R^2$ max | Best index | Size |
| daily | 7 bands (reflectance) | 463m | 0.13 | $NIR/SWIR_2$ | 212 | 0.30 | $NIR/SWIR_2$ | 1325 |
| | 8 bands (reflectance & ST) | 927m | 0.13 | $NDII_2/ST$ | 199 | 0.24 | $NDII_m/ST$ | 1268 |
| | humid period: 5-14 July | 463m | 0.81 | $GVMI_1$ | 26 | 0.53 | $NIR/SWIR_m$ | 156 |
| | arid period: 8-17 Septemb. | 463m | 0.02 | $GVMI_1$ | 17 | 0.15 | $NIR/SWIR_m$ | 137 |
| 16 d. | 7 bands (16-day reflect.) | 927m | 0.21 | $NIR/SWIR_2$ | 30 | 0.29 | SARVI2 | 162 |

$_1$: first SWIR band centred at 1240nm $_2$: second SWIR band centred at 1640nm $_m$: average of the 3 SWIR bands

### *4.2 A priori scene-wise spatial variability of FMC*

As the sites selected for the improved protocol may not have been optimally selected, another approach was undertaken using maps of indices generally used for FMC assessment. The idea was to determine classes of behaviour check the spatial organisation of these classes and analyse the behaviour of the selected sites in comparison with the obtained classes. This approach was done using high and low resolution data.

For high resolution data, seven Spot 4 HRVIR images (spatial resolution of 20m) covering the sites near Montpellier were used. The NDII index (Hunt and Rock 1989) was selected and a map of the NDII spatial variation was made (Roldan *et al*., 2003). 5 classes of NDII behaviour were made using unsupervised classification. On the map, these classes have shown a spatial coherence, with areas of higher and lower NDII variation. Furthermore test sites chosen in 2001 correspond to areas on the map showing a low variation of the index.

Similar tests were performed with Modis data using eight *MOD43* 16-day images. At the MODIS pixel scale, a similar spatial coherence is observed with homogeneous groups of pixels. These pixels with a common behaviour correspond to real objects in the field such as evergreen forest, pines, chaparrals, etc.

These maps will be used to provide new locations for 2003 test sites, in order to collect FMC in areas with a higher variation of the index.

## 5. DISCUSSION AND CONCLUSION

The general conclusions of this preliminary study are that daily or 16-day correlation between field FMC and MODIS derived indices have not shown the expected significance. This is due to several reasons: (a) daily reflectance products do show high BRDF effects that need to be corrected; (b) field sites with a too high soil exposure or a vegetation cover showing little FMC variation may not be adapted to the monitoring of their FMC using EO data; (c) a field protocol implying leaf collection at a few hectometres apart has proved useful to produce a pixel-wise FMC.

On the other side this preliminary study has produced maps highlighting different classes of NDII variations using high (SPOT HRVIR) and low (MODIS) resolution data. The maps have shown a spatial coherence, and pointed out areas where a higher FMC variation can be expected. The next step of the project will be to select sites in such areas and monitor them during summer 2003.

## 6. REFERENCES


Andrews, P.L. & Chase, C.H. 1990. The BEHAVE fire behavior prediction system. The Compiler, Vol. 8: 4-9.

Blackmarr, W.H. & Flanner, W.B. 1968. Seasonal and diurnal variation in moisture content of six species of Pocosin shrubs. SE-33, Southeastern Forest Experiment Station, U.S. Forest Service, Asheville.

Ceccato, P., Flasse, S. & Gregoire, J.M. 2002b. Designing a spectral index to estimate vegetation water content from remote sensing data Part 2. Validation and applications, Remote Sensing of Environment, Vol. 82, Elsevier Science Inc., New-York, USA: 198-207.

Ceccato, P., Gobron, N., Flasse, S., Pinty, B. & Tarantola, S. 2002a. Designing a spectral index to estimate vegetation water content from remote sensing data: Part 1 Theoretical approach, Remote Sensing of Environment, Vol. 82, Elsevier Science Inc., New-York, USA: 188-197.

Ceccato, P., Flasse, S., Tarantola, S., Jacquemoud, S. & Gregoire, J-M. 2001. Detecting vegetation leaf water content using reflectance in the optical domain, Remote Sensing of Environment, Vol. 77, Elsevier Science Inc., New-York, USA: 22-33.

Chuvieco, E., Deshayes, M., Stach, N., Cocero, D. & Riano, D. 1999. Short-term fire risk: foliage moisture content estimation from satellite data. Remote sensing of large wildfires in the European Mediterranean Basin, E. Chuvieco (Ed.), Berlin: Springer (University of Alcala, Spain): 17-38.

Chuvieco, E., Riano, D., Aguado, I. & Cocero, D. 2002. Estimation of fuel moisture content from multitemporal analysis of Landsat Thematic Mapper reflectance data: applications in fire danger assessment. International Journal of Remote Sensing, Vol. 60 (N°5), Taylor & Francis, New York: 563-570.

Deshayes, M., Chuvieco, E., Cocero, D., Karteris, M., Koutsias, N. & Stach, N. 1998. Evaluation of different NOAA-AVHRR derived indices for fuel moisture content estimation: interest for short term fire risk assessment. III International Conference on Forest Fire Research, 16/20 November 1998, Vol I, Luso, Portugal: 1149-1167.

Fourty, T. & Baret, F. 1998. On spectral estimates of fresh leaf biochemistry. International Journal of Remote Sensing. Vol. 19 (N°7), Taylor & Francis, New York: 1283-1297.

Hartford, R.A. & Rothermel, R.C. 1991. Fuel moisture as measured and predicted during the 1988 fires in Yellowstone Park. USDA, Forest Service, Missoula.

Hunt E. R. and Rock B. N., 1989. Detection of Changes in Leaf Water Content Using Near- and Middle-Infrared Reflectances. In Remote Sensing of Environment, Vol. 54, Elsevier Science Inc., New-York, USA, pp 43-54.

Pearson, R.L. & Miller, L.D. 1972. Remote mapping of standing crop biomass for estimation of the productivity of the short-grass Prairie, Pawnee National Grasslands, Colorado. 8th International Symposium on Remote Sensing of Environment, ERIM, Ann Arbor, MI: 1357-1381.

Roldan, A., Dauriac, F., Deshayes, M. & Gonzalez, F. 2003. Cartografia de la variacion de la humedad de la vegetacion mediterranea a partir de imagenes Spot-HRVIR, X Congreso Nacional de Teledeteccion, 17-19 September 2003, Madrid, Spain, submitted.

Rothermel, R.C., Wilson, R.A., Morris, G.A. & Sackett, S.S. 1986. Modelling moisture content of fine dead wildland fuels: input to BEHAVE fire prediction system. Research Paper INT-359, USDA Forest Service Intermountain Research Station, Odgen, Utah.

Simard, A.J. 1968. The moisture content of forest fuels – A review of the basic concepts. Forest Fire Research Institute Information report FF-X-14, Ottawa, Ontario: 47.

Viegas, D.X., Viegas, T.P., Ferreira, A.D. 1992. Moisture content of fine forest fuels and fire occurrence in Central Portugal. The International Journal of Wildland Fire, Vol. 2 (No.2): 69-85.

Viney, N.R. 1991. A review of Fine Fuel Moisture Modelling. International Journal of Wildland Fire, Vol. 1 (N°4): 215-234.

# Use of optical, thermal infrared and radar remote sensing for monitoring fuel moisture conditions

B. Leblon, K. Abbott, L. Gallant & G. Strickland
*Faculty of Forestry and Environment Management, University of New Brunswick, Canada*
bleblon@unb.ca or Brigitte.leblon@agrorennes.educagri.fr

M. Alexander
*Northern Forestry Complex, Canadian Forest Service, Edmonton, Canada*

Keywords: optical, thermal infrared, radar, fuel moisture, NOAA-AVHRR, ERS-1, RADARSAT-1

ABSTRACT: Our study presents results acquired over boreal coniferous forests located in the Mackenzie River basin, Northwest Territories, Canada. NOAA-AVHRR optical and thermal infrared images and SAR images from ERS-1 and RADARSAT were correlated to the Canadian Forest Fire Danger Rating System (CFFDRS) Fire Weather Index (FWI) codes and indices, which were used here as a surrogate of fuel moisture. Results showed that FWI codes and indices were related to optical and thermal infrared NOAA-AVHRR data or SAR data, but the relationship was more or less strong with either fast-drying fuel codes or slow-drying fuel codes and indices, depending on the case The study suggests that the most promising use of satellite images for fire danger monitoring is through the combination of optical and thermal infrared images to radar images.

## 1. INTRODUCTION

As reviewed in Leblon (2001, 2003), fuel moisture studies using remote sensing have been primarily used indices derived from NOAA-AVHRR NDVI images like the relative greenness (RG) (e.g., Burgan et al; 1998). Leblon (2001, 2003) also listed several problems related to the use of NDVI images in fuel moisture mapping, namely the saturation of relationships, the influence of site wetness on relationships and the difficulty of using NDVI over forests, due to the spectral mixture of the overstory with the understory, both being different in nature and in moisture content. In fact, NDVI and associated vegetation indices are only indirectly related to fuel moisture, because it rather measures the greenness and the chlorophylleous activity of the vegetation. Thermal infrared data are more related to moisture variables, since surface temperatures ($T_s$) increase with droughtness levels (e.g., Pierce et al., 1990). NOAA-AVHRR surface temperature data were correlated to fuel moisture variables (e.g., Dominguez et al., 1994; Chuvieco et al., 1999; Strickland et al., 2001). Indices combining NDVI and thermal infrared NOAA-AVHRR images, like the Vegetation and Temperature Condition Index (VT) of Kogan (2001) and the index of Chuvieco et al. (2001), were also proposed. The one primary disadvantage of the optical or thermal infrared-derived information is that coverage is restricted to cloud-free conditions, a limitation that can be overcome using data acquired by active microwave sensors, like those onboard the ERS and RADARSAT satellites. For northern Alaskan boreal forests, Canadian Forest Fire Danger Rating System (CFFDRS) Fire Weather Index (FWI) codes and indices, which were used as a surrogate of fuel moisture, were correlated to $\sigma^o$ derived from SAR images (Bourgeau-Chavez et al. 1999, 2001).

Our study presents results gathered over northern boreal coniferous forests located in the Mackenzie River basin, Northwest Territories, Canada. NOAA-AVHRR optical and thermal infrared images and SAR images from ERS-1 and RADARSAT were correlated to the CFFDRS FWI codes

and indices, which were used here as a surrogate of fuel moisture. Details of the study on NOAA-AVHRR images can be found in Leblon et al. (2001) and in Strickland et al (2001). The one on RADARSAT images is detailed in Abbott et al. (2002) and on ERS-1, in Leblon et al. (2002).

## 2. MATERIALS AND METHODS

NOAA-AVHRR optical and thermal infrared images and ERS-1 SAR images were acquired during the 1994 fire season over 18 stands of jack pine, black spruce and white spruce distributed among 6 sites located in the Mackenzie River basin, Northwest Territories, Canada (57º36' Lat. N. to 71º27' Lat. N. and 110º39' Long. W to 135º18' Long. W). NOAA-11 AVHRR images consisted of NDVI and surface temperature ($T_S$) images acquired, from snowmelt to snowfall. The time of acquisition was between 22 and 24 UT, which means that the corresponding local time was afternoon. Each image has a ground spatial resolution of 1 km and was georeferenced to a Lambert conic conformal projection. They were corrected for radiometric and atmospheric effects following the method described in Strickland *et al.* (2001). On each corrected image, a 3-by-3 pixel window was extracted for each stand based on its geographical coordinates and mean NDVI and $T_S$ values were computed. They were used as follows: (i) estimation of NDVI for cloudy days using polynomial interpolations and computation of the accumulated NDVI over the fire season (ΣNDVI) and (ii) estimation of daily ratios between actual and potential evapotranspiration (AET/PET) following the method of Vidal et al. (1994) developed for Mediterranean forests. In the method, AET is calculated from $T_S$-$T_a$, through an analytical model derived from the energy budget equation, while PET is calculated by the Penman-Monteith equation. In both AET and PET computations, NDVI is used to account for the effect of ground cover on some model parameters.

The second spectral data set acquired over the 18 stands consisted of twenty-two ERS-1 SAR images which have a nominal ground resolution of 30 m. Only daytime ERS-1 SAR images (descending orbit) were considered because they were acquired closed to the time of FWI indices estimation. SAR images were georeferenced and radar backscatters ($\sigma^o$) were extracted to compute mean backscatters of each stand. In this study, data from Alaska sites were also used (see Bourgeau-Chavez *et al.* 1999). In addition to these 1994 data sets, the study used 11 descending orbit RADARSAT-1 SAR images acquired in 2000 over black spruce and jack pine forests located at the International Crown Fire Modelling Experiment (ICFME) site, Northwest Territories (61º35'Lat.N., 117º10'Long.W). The images were acquired almost daily, over a 15 day period in June 2000, between 6h30 and 7h45 am (LST), but at different incidence angles and different spatial resolutions. For both SAR image types, selected sites were ideal, because they do not have significant topography which may affect radar backscatter. Fuel moisture conditions were assessed through the FWI codes and indices. They were computed using the WeatherPro™ package of Remsoft Inc. based on the CFFDRS equations from weather stations records located close to the stands.

## 3. RESULTS

### *3.1 Optical images*

The correlation between NDVI or ΣNDVI and FWI codes and indices was positive, and was better with CFFDRS variables corresponding to slow-drying fuels, like the duff moisture code (DMC), the drought code (DC) (Fig. 1) and the buildup index (BUI), than to CFFDRS variables related to fast-drying fuels, like the fine fuel moisture code (FFMC) and the fire weather index (FWI)). Strong correlations have previously been observed with DC, but they were negative, because NDVI data were acquired not only on forests, but also on grasslands, for which drought reduces vegetation greenness and thus NDVI, while in the same time, it increases FWI variables. In our case, NDVI images were

acquired solely on coniferous stands, for which NDVI increases until mid-summer and then decreases, because of understory deciduous phenology. Thereby, the seasonal variation of NDVI did not reflect possible drought increasing throughout the season, as shown by the seasonal trends of FWI variables. These results suggest that red and near-infrared-based vegetation indices, like ΣNDVI, are better indicators of chlorophyll activity of vegetation rather than indicators of actual drought. For this reason, a better use of NDVI images over boreal forests in fire management will be to map timing of deciduous leaf flushing, which is critical for fires in mixed deciduous-boreal forests.

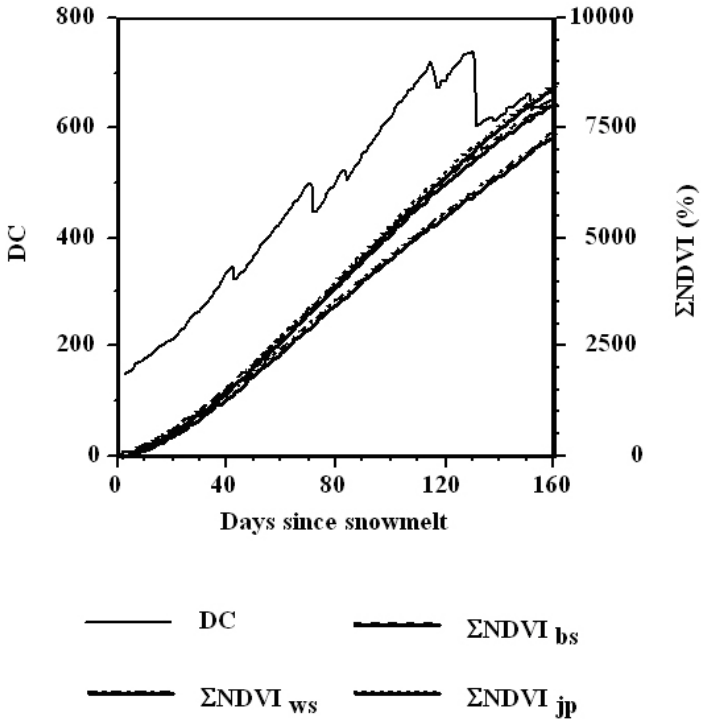


Figure 1. An example of seasonal variation for DC and ΣNDVI for the three stands of Hay River (bs: black spruce, ws: white spruce and jp: jack pine) (after Leblon et al. 2001)

### *3.2 Thermal infrared images*

Thermal infrared AVHRR bands are possible better drought indicators than the red and near-infrared ones, because the difference between surface and air temperatures ($T_s$-$T_a$) is analytically related to AET. Because a better indicator of drought levels and thus of fire potentials is the ratio between actual and potential evapotranspiration (AET/PET), correlations between AET/PET and each FWI code and index were computed for each stand, each species, each site and for all the cases. FFMC and FWI were most correlated with AET/PET, except in the northern site, where DC, DMC, and BUI were the most correlated. The difference at this site may be related to the sparser and shorter forest canopy occurring at this site, which makes satellite signals sensitive not only to the surface level, but also to the forest floor level. To define a fire danger index based on the AET/PET ratio, AET/PET values were categorized into classes ranging from 0.0 to 1.0 by steps of 0.1. For each class of AET/PET, a mean value for each FWI index and code was estimated. These categorized ratios were plotted against mean FWI index or code. AET/PET was well related to FWI in most of the sites, but it was related to fast-drying fuel codes or to slow-drying fuel codes and indices, depending on the site. A negative trend was also found when pooling all the mean values for the different sites (Fig. 2). However, there was some variability around the trend, which means that other fire danger factors

should be considered, like the wind. Also, since AET/PET can be computed only under clear sky, the use of SAR images has also been investigated.

### *3.3 SAR images*

Mean radar backscatters ($\sigma^o$) extracted from the ERS-1 images were first correlated to weather variables which was measured at the time of satellite overpasses over the study sites. $\sigma^o$ exhibits a decreasing trend with increasing air temperatures, probably because high air temperatures induces plant water stress that can lower radar backscatter from the canopy. In each case, $\sigma^o$ increases with the rainfall, as already shown in other studies. The good correlation $\sigma^o$ and weather variables, which are used to compute the various FWI codes and indices, may expect that these indices and codes are also well related to $\sigma^o$. For each site, there was no systematic relationship between the FWI codes and observed radar backscatter, except in the site where the cumulative precipitation before image acquisition was the highest. When one examines correlation coefficients when specific forest types are considered across all regions, some significant patterns do emerge. Within black spruce stands, there does appear to be statistically significant negative correlations between radar backscatter and DMC, DC (Fig. 3), and BUI. Indeed, northern boreal black spruce stands have open canopies, with much of the ground layer exposed to the incoming microwave radiation. Therefore, variations in the moisture conditions of the ground layer (DC and DMC) would be expected to alter the amount of energy scattered from these surfaces. A significant negative correlation was also found with FFMC for the white spruce stands and with FWI for the jack pine stands. A similar trend was observed over the ICFME site with the RADARSAT-1 images (Abbott et al. 2002).

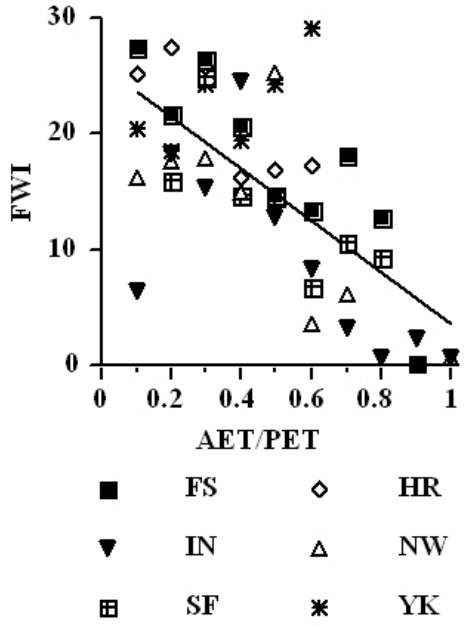


Figure 2. Relationships between the AET/PET ratio and FWI for all the sites together. Each site is marked by a different symbol. The trend is indicated by a solid line (after Strickland et al. 2001)

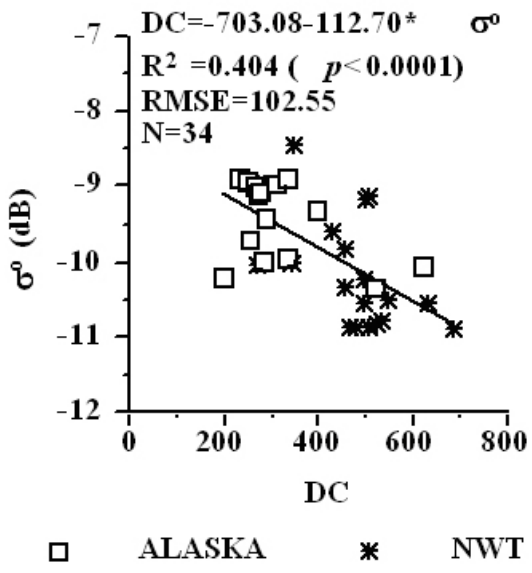


Figure 3. Relationship between $\sigma^o$ and slow-drying fuel moisture (DC) for the black spruce stands located both in Alaska and in Northwest Territories. Data from Alaska stands are from Bourgeau-Chavez *et al.* (1999). Data from Northwest Territories stands are from Leblon *et al.* (2002).

## 4. CONCLUSIONS

Our study over northern boreal forests showed that FWI codes and indices were correlated to optical and thermal infrared NOAA-AVHRR images or SAR images, but the relationship was more or less strong with either fast-drying fuel codes (FFMC) or slow-drying fuel codes and indices (DMC, DC and BUI), depending on the case. Because of the inherent operational limitations of each kind of images (image availability due to either poor weather conditions or long revisiting periods), the study suggests that the most promising use of satellite images for fire danger monitoring is through the combination of optical and thermal infrared images to radar images, the first kind of images being acquired by the same satellite in the same time, whereas the second kind can be seen as a complementary data source.

## 5. REFERENCES


Abbott, K., Leblon, B., Staples, G., Alexander, M.E., & MacLean, D. 2002. Use of RADARSAT-1 images to map forest fuel moisture over boreal forests. 24th Canadian Remote Sensing Symposium, Toronto,Canada, June 2002.

Bourgeau-Chavez, L.L., Kasischke, E.S., & Rutherford, M.D. 1999. Evaluation of ERS SAR data for prediction of fire danger in a boreal region. International Journal of Wildland Fire 9(3): 183-194.

Bourgeau-Chavez, L. L., Brunzell,S., Nolan, M., & Hyer, Ed.: 2001. Analysis of SAR data for fire danger prediction in boreal Alaska. Final Report, ASF-IARC Grant NAS-98-129, 59 pages.

Burgan, R.E., Klaver, R. W., & Klaver, J.M. 1998. Fuel models and fire potential from satellite and surface observations. International Journal of Wildland Fire 8(3): 159-170.

Chuvieco, E., Aguado, I., Cocero, D. & Riaño, D. 2001, Design of an empirical index to estimate fuel moisture content from NOAA-AVHRR analysis in forest fire danger studies, 3rd International Workshop of the European Association of Remote Sensing Laboratories (EARSel) on Remote Sensing and GIS applications to Forest Fire Management, Paris, France, pp. 36-39.

Kogan, F.N. 2001. Operational space technology for global vegetation assessment. Bulletin of the American Meteorological Society 82(9): 1949-1964.

Leblon, B. 2001. Forest wildfire hazard monitoring using remote sensing. Remote Sensing Reviews 20(1): 1-43.

Leblon, B. 2003. Using remote sensing for fire danger monitoring Natural Hazards (in press)

Leblon, B., Chen, J., Alexander, M.E., & White, S. 2001. Fire danger monitoring using NOAA-AVHRR NDVI images in the case of northern boreal forests. International Journal of Remote Sensing 22(14): 2839-2846.

Leblon, B., Kaschike, E.S., Alexander, M.E., Doyle, M, & Abbott M. 2002. Fire danger monitoring using ERS-1 SAR images over northern boreal forests. Natural Hazards 27: 231-255.

Strickland, G, Leblon, B., Chen, J., & Alexander, M. 2001. A model to assess fire danger using NOAA-AVHRR images in the case of northern boreal forests, 23th Canadian Remote Sensing Symposium, Québec, Canada, August 2001, pp. 667-676.

Vidal, A., Pinglo, F., Durand, H., Devaux-Ros, C. & Maillet, A. 1994. Evaluation of a temporal fire risk index in Mediterranean forests from NOAA thermal IR. Remote Sensing of Environment 49: 296-303.

# Contribution of image treatment and analysis in study of vegetal flammability

A.Madoui
*Department of Biology, Faculty of Sciences, University Ferhat Abbas – Sétif, SETIF, Algérie*
mado_amar@yahoo.fr

M. Bouafia
*Department of Applied Optics*

D. Alatou
*Department of Biology, University Mentouri - Constantine*

Keywords: flammability, forest fires, image treatment, optical density

ABSTRACT: the images capture and treatment of vegetal material during thermal process application has been applied to study the flammability of *Hedera helix*. The aim of experimental investigation is to prove the existence of quantitative and qualitative relation between the optical distribution density and flammability of the vegetal.
The experimental setup consists of optical system composed of a vertical microscope associated to a CCD camera and interface card (Matrox). This one allows visualising the image of the vegetal heated progressively by oven. A regulator and thermocouple controlled the temperature until 350°C.
The paper describes the experimental procedure and the image treatment and analysis using Image Pro-Plus software. As results, the images of *Hedera helix* in two states, dry and fresh, show the behaviour of the heated vegetal in dependence on temperature. The optical density deduced from the images can be related to water content of vegetal.

## 1. INTRODUCTION

The part of vegetal combustible is important in release and propagation of fires. All studies on flammability and combustibility of vegetal species have been done by exposed samples to the radiation of an epiradiator (Trabaud, 1976; Delabraze & Vallette, 1974; Forgeard, 1989; Vallette, 1990). But thermal analysis can be used for study the behaviour of plants during heating (Philpot, 1970). Water content of combustible has a major influence on flammability and combustibility (Mutch, 1964; Montgomery & Cheo, 1969; Pompe & Vines, 1966; Countryman & Philpot, 1970; Fosberg & Schroeder, 1971; Nord & Countryman, 1972; in Trabaud, 1976). In the same way, according to (Kaloustian, 1997), in middle infrared domain, the reflectance of plants is affected by their water content. We try to follow the different states of vegetal during heating with capture its image in different temperature and different water content.

## 2. MATERIALS AND METHODS

The study was realized on *Hedera helix* which grown in the University campus of Setif. The samples were collected in the morning during July 2002. Some leaves were tested immediately as fresh samples, the other one were put in drying oven at 80°C during 48 hours in order to eliminate all

its water before to use it in the experience. The water content was evaluated on three samples of leaf in order to have an average and minimize the errors. Following equation was used:

**WC = fW – dw / fW * 100** (**WC =** Water content**; fW =** fresh weight**; dW =** dry weight**)**

For *Hedera helix*, we have found: Weight of fresh leaf = 4.562 g., Weight of dry leaf = 1.568 g. Content water = 4.562 -1.568 / 4.562 * 100 = **65.63 %**

The samples are cut with scissors and put in the ceramic melting pot. It is important to note that the apical part of leaf was kept to reduce a loss of water during experience. The experimental setup of our thermal processing system is shown in figure 1.

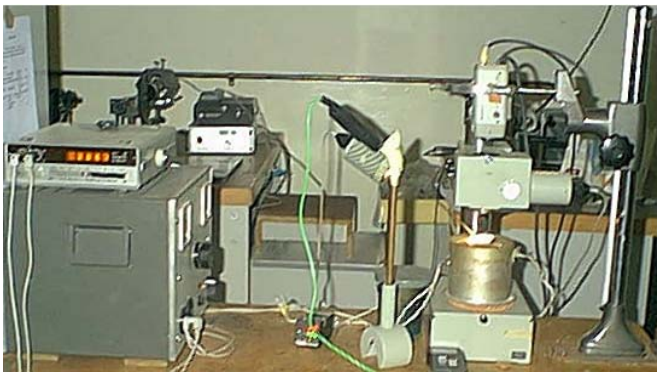

Figure 1. Experimental setup for thermal processing application.

The absolute temperature was measured by a thermocouple (type "C"), which was welded into the middle of the ceramic melting pot, which contains sample, providing an intimate measure of leaf temperature. The oven is adapted for light reflection measurement and regulator controls its temperature. The oven is situated under vertical microscope, which observed the image of sample during thermal processing. The image was captured in the exit pupil of the microscope by a camera CCD (SSC-108P, Sony). The figure 2 shows some states of fresh and dry *Hedera* leaves during heating. The optical signal depends on the temperature was analyzed by using the Image Pro Plus software. Because the detected optical signal depends on temperature and water content of the vegetal, the image and optical signals of all samples are first measured at initial temperature corresponding to fresh leaf state. The thermal process has been then applied over the range of initial temperature to 350°C for fresh and dry *Hedera* leaves.

**a) Fresh leaf**

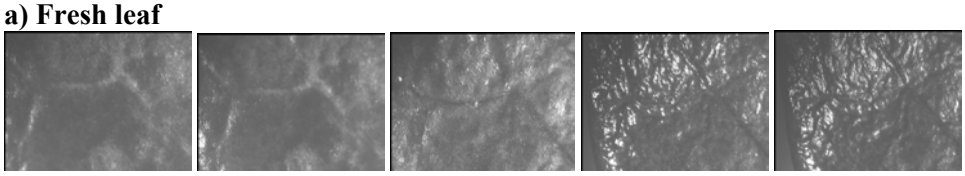

T= 59°C T= 100°C T= 160°C T=200°C T=300 °C

**b) Dry leaf**

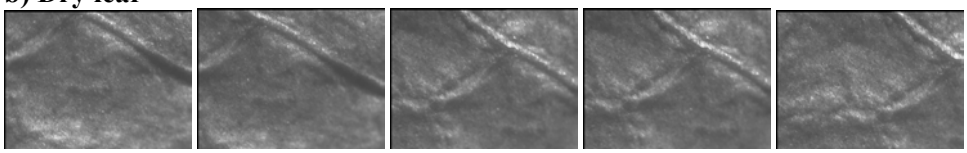

T= 39°C T=100°C T =160°C T=210°C T=300°C

Figure 2. Some fresh (a) and dry (b) *Hedera* leaves images during heating process.

## 3. RESULTS AND DISCUSSION

It is known that, during heating, the vegetal passes by different states until the total calcinations (TRABAUD, 1976). So, it takes several colors, from green (fresh state), passing by yellow (without pigments) and ending with dark color that corresponds to the calcination. Figure 3 shows clearly the behavior of *Hedera* leaf versus the temperature and the water content.

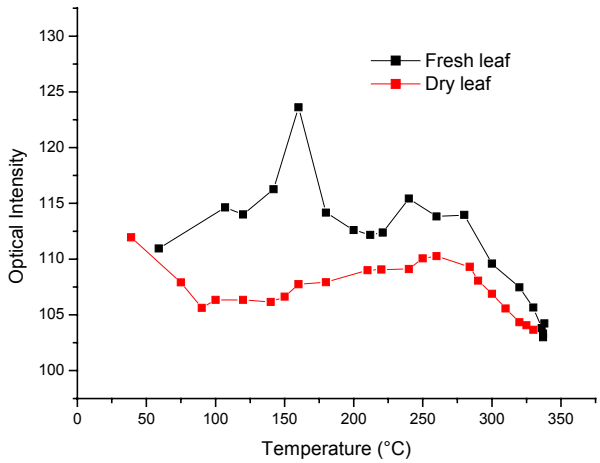


Figure 3. Reflected optical intensity as a function of the temperature

The reflected optical intensity at heating states has been deduced from image treatment using Image Pro Plus Software. According to FORGEARD (1989), dry leaf of plant became dark rapidly than fresh one. This explains the look of dry *Hedera* leaf curve. After heating, the optical intensity decreases until 100°C, then stabilize around 100 and 150 °C, increases slightly at 250°C and finish with lower value at 320°C. Because, the dry leaf become yellow (without pigments) so the reflectance is more important than in fresh leaf at the beginning of heating process. On the other hand, the fresh *Hedera* leaf curve is characterized by three states corresponding to colors and water content. In this situation, the change of color and moisture of leaf are progressively. A green state is seen at the beginning heating, brown and yellow at 150°C, and dark over 200°C.

A lack of chlorophyll pigmentation can be shown to reduce drastically the absorption of visible light by a leaf (GATES & *al*., 1965), the reflectance will be very important which explains the pick appearing at 150°C in our case. According to PHILPOT (1970) and BERNARD & NIMOUR (1994), the gas give off during the pyrolyze of plants between 175 and 350°C were responsible of flammability.

From 200°C, the two curves show the same tendency. At this temperature, both dry and fresh *Hedera* leaves submit the same effect of heating and show the same behavior until 320°C.

## 4. CONCLUSION

In summary, a new method for the behavior of leaves during heating based on light reflectance microscopy and imaging treatment has been proposed and demonstrated. It has been found that the optical reflected intensity is related to the water content of vegetal. The dry leaf show less variance in its behavior during heating, but the fresh one passes by several states before burning. This result will be having an important role in combating forest fires but more investigations for other natural plants must be done.

## 5. ACKNOWLEDGMENT

The authors greatfully acknowledge the financial support given by the ADRU, Algeria.

## 6. REFERENCES

Bernard M. & Nimour N., 1994. Science Technique Technologie, 26, 24.

Delabraze P. & Vallette P.C., 1974. – *Inflammabilité et combustibilité de la végétation forestière méditerranéenne*. R.F.F. n° special. 1: 171-177.

Forgeard, F. 1989. – *Inflammabilité et combustibilité des principales espèces végétales des landes de Bretonnes*. Bull. Ecol., t. 22 (3-4): 389-404.

Gates D.M., Keegan H.J., Schleter J.C., Weidner V.R., 1965. – *Spectral properties of plants*. Appl. Optics., 4 :11-20.

Kaloustian J., A. M. Pauli et J. Pastor, 1997. – *Etude comparative par analyses thermique et chimique de quelques végétaux méditerranéens*. Journal of Thermal Analysis 50: 795-805.

Philpot C. W., 1970. – *Influence of mineral content on the pyrolysis of plant materials*. Forest Sciences., 16: 461-471.

Trabaud, L., 1976. – *Inflammabilité et combustibilité des principales espèces des garrigues de la region méditerranéenne*. Oecol. Plant., 11 : 117-136.

Vallette J.–C., 1990. – Inflammabilité des espèces forestières méditerranéennes. Conséquences sur la combustibilité des formations forestières. R.F.F., XLII, n° sp. 76-92.

# The GOFC/GOLD-Fire Program: a mechanism for international coordination

Chris Justice, Ivan Csiszar
*Geography Department, University of Maryland*
cjustice@umd.edu

Johann Goldammer
*World Fire Monitoring Center, Freiburg University*

Bryan Lee
*Natural Resources Canada / Canadian Forest Service of Biology*

Emilio Chuvieco
*Geography Departament, University of Alcalá, Madrid, Spain*

Keywords: fire monitoring, international coordination, satellites

ABSTRACT: The Global Observation of Forest Cover/Global Observation of Landcover Dynamics (GOFC/GOLD) program is providing international coordination to put in place the long-term observing systems needed for global environmental monitoring. Environmental monitoring requirements include satellite and ground observations for global change scientific research, as well as for natural resource management and the associated policy and decision support systems.

## 1. BACKGROUND

It is recognized that the range of global observations necessary to understand and monitor earth processes, to assess human impacts and support natural resource management, exceeds the capability of any one country and therefore necessitates an international program (Ahern et al. 2001). GOFC/GOLD was formed under the Committee on Earth Observation Satellites (CEOS) to bring together data providers and information users to improve access to and use of satellite and ground based observations on forests and fire. GOFC/GOLD has recently become part of the Global Terrestrial Observing System (GTOS), which is sponsored by the International Global Observing System Partners (IGOS), including the UNEP and UN/FAO (Figure 1). GOFC/GOLD is currently helping GTOS secure the global observation needed for carbon and biodiversity monitoring.

The GOFC/GOLD program currently has two implementation teams focusing on two land cover and fire. Fire is a global phenomenon with many aspects; it is a major ecosystem disturbance, a land use management tool, a significant source of trace gases and aerosols and a natural hazard. Fire and its effects cross national boundaries. Large amounts of money are spent each year to monitor and manage wildfires. GOFC/GOLD has a Secretariat, maintained by the Canadian Forest Service. The GOFC/GOLD-Fire Implementation Team has developed program goals and strategic partnerships with a number of international programs, to help meet those goals, including the CEOS Working Group on Land Product Validation, the CEOS Disaster Management Support Group (DMSG), the IGBP International Global Atmospheric Chemistry (IGAC) Biomass Burning Experiments (BIBEX) program, the EARSeL Special Interest Group (SIG) on Forest Fires, the UN International Strategy for Disaster Reduction, Working Group 4 on Wildland Fire. The latter is helping to increase the awareness of fire issues, strengthen fire monitoring within the UN System, to improve national collation of fire

information and the standardization of national reporting and articulation of the information needs of policy makers with respect to fire information.

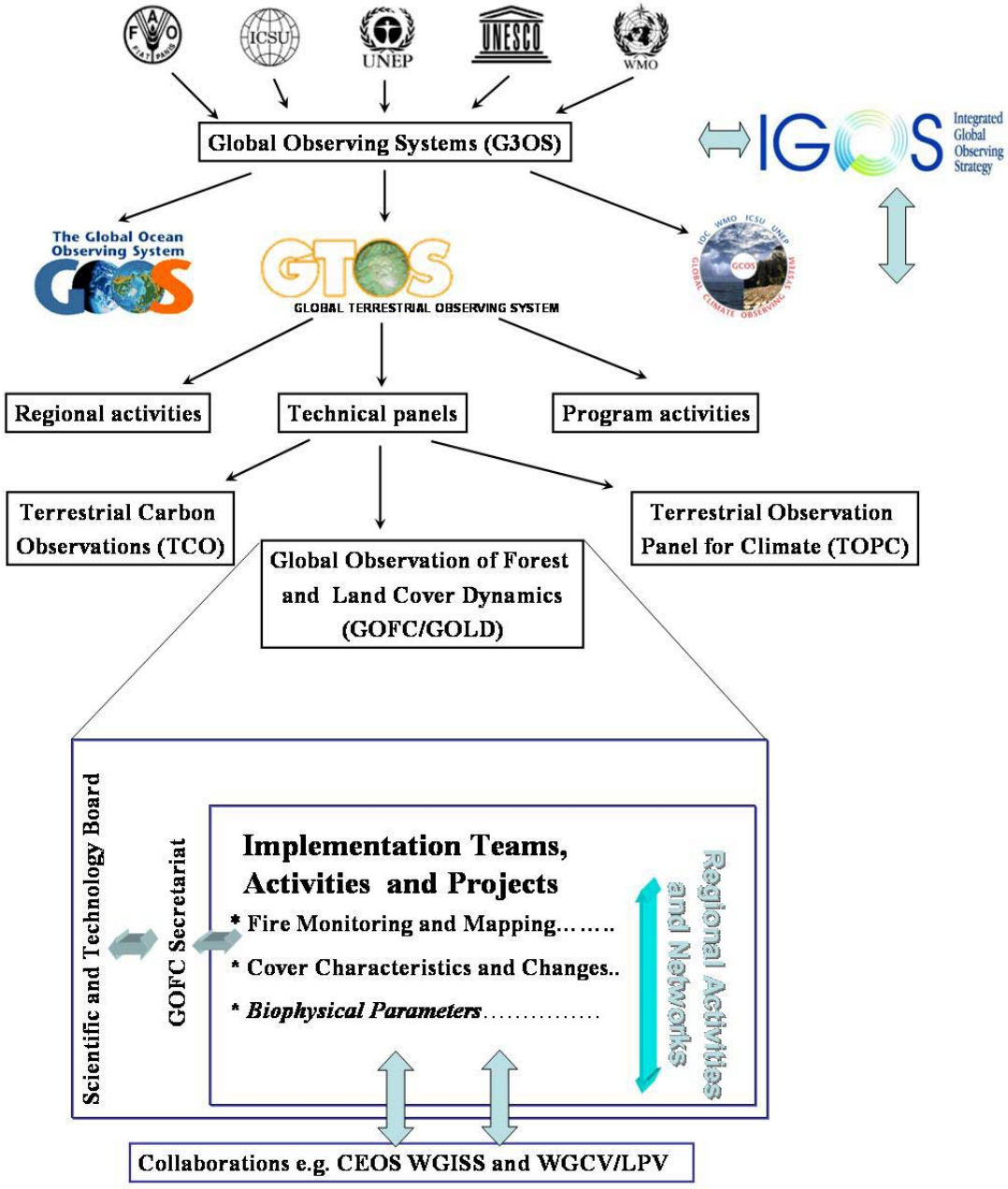


Figure 1. Organizational status of GOFC/GOLD

## 2. PROGRAM GOALS FOR GOFC/GOLD-FIRE

The GOFC/GOLD-Fire program has a number of stated goals which cover the broad range of perceived needs of the fire community. The goals are as follows:

*2.1 To increase user awareness by providing an improved understanding of the utility of satellite fire products for resource management and policy within the United Nations and at regional national and local levels.*

One of the largest problems for satellite data users is to gain an understanding of the products that are available and how they can be used. This includes satellite data and information, as well as data collected by more conventional means at the national and international level. Clearly a dialogue needs to be developed, providing feedback from users as to what is needed and from providers as to what they can deliver (UN FAO 1999, Justice et al. 2003). Open sharing of data and information is a prerequisite for effective global monitoring and will be one of the underpinnings of the IGOS. Encouraging organizations and institutions to assess, articulate and provide advocacy for their long-term information requirements, evaluate the effectiveness of the current monitoring systems and to adopt policies of open data and information sharing will be primary challenges for GOFC/GOLD in this area.

*2.2 To encourage the development and testing of standard methods for Fire Danger Rating suited to different ecosystems and to enhance current fire early warning systems.*

Early warning of fires provides a means by which resources can be allocated for fire management and fire policies can be put in place to mitigate hazardous fires. There are several fire danger rating systems currently in use around the World. There is a need to better document these systems and to understand their performance and reliability and the relationship between the different methods and their applicability to different fire and management regimes. Currently, the most effective of these systems combine meteorological and satellite observations in a modeling context. Timely delivery of meteorological and satellite data at the appropriate spatial scales is an important prerequisite for operational fire risk mapping. Developing easy access, data delivery systems, user oriented models and clear probability estimates will be the primary challenges for GOFC/GOLD in this area.

*2.3 To establish an operational network of fire validation sites and protocol,, providing accuracy assessment for operational fire products and a test-bed for new or enhanced products, leading to standard products of known accuracy.*

For data products to be used in numerical models or in a decision-making framework, it is critical for users to understand their reliability and accuracy. Up until recently, satellite fire products or national fire statistics have been generated with little or no indication of accuracy. In the framework of the CEOS Land Product Validation Working group, GOFC/GOLD is promoting the development of quantitative methods for quality assessment (QA) and to determine the accuracy of global and regional satellite fire products and maps (Roy et al. 2002, Morisette et al. 2002). This involves comparison with other airborne or satellite products and analysis of independent observations of known accuracy. Validation of global products is a labor intensive and costly activity and there are real advantages in cost and resource sharing between national and regional programs. A number of Test Sites around the World are being established as a focus for fire product validation (Justice et al. 2000). The primary challenge for GOFC/GOLD in this area will be to encourage satellite data providers to assess the accuracy of the products that they are delivering and to involve the user community in the accuracy assessment process. It is important for data providers to recognize that quantitative product validation is not an option but is an integral part of the data and information delivery system and must be included as part of the overall mission costs.

*2.4 To enhance fire data product use and access, for example by developing operational multi-source fire data and combined with GIS data and making these available over the Internet.*

One of the obstacles to using satellite data is the accessibility and cost of data products. Information on how to access, read and interpret the products needs to be made more readily available. At present, data from different systems are provided by different means and in different formats. Different satellite systems provide different information on fires and are provided by different groups and agencies. GOFC/GOLD is promoting ease of access to multiple archives and standard data formats. Similarly when the data are obtained they need to be readily combined with other geospatial data. The availability of WEB-GIS data will lead to an advance in current capabilities (Justice et al. 2002). Examples of recent advances in this area for fire monitoring can be found at (http://www.sentinel.csiro.au/, http://firemaps.geog.umd.edu). The Internet is allowing improved, timely and automated access to data and removing the need for data handling charges. However until there is global connectivity, there will also remain the need for more traditional information delivery in some regions. Promoting the provision of timely and affordable data in standard formats by the operational agencies and data providers will be a primary challenge for GOFC/GOLD.

*2.5 To develop an operational global geostationary fire network providing observations of active fires in near real time.*

The diurnal cycle of fire activity means that polar orbiting satellite systems provide only a sample of the daily fire activity. In some regions fires are short-lived, lasting no more than a couple of hours. In other systems fires will burn throughout the day and night. Geostationary systems, providing frequent acquisitions give perhaps the best opportunity to detect active fires from space. However in the past, these systems have been limited by their spatial resolution and geographic extent and have not been designed for fire applications. The new generation of geostationary systems with 1km spatial resolution or higher and with temporal resolutions of 15-30 minutes, provide an enhanced capability for operational monitoring (Prins and Schmetz 2001). Developing an international network of geostationary satellites with standard fire products, will provide an important advance for monitoring active fires and fire scars. Scientists from the US, Europe and Japan are working together in the framework of GOFC/GOLD to develop such a global network.

*2.6 To establish operational polar orbiters with fire monitoring capability, providing i) operational moderate resolution long-term global fire data and products to meet user requirements and distributed ground stations providing enhanced regional products. These products should include fire danger, fuel moisture content, active fire, burned area and fire emissions, ii) operational systematic high resolution data acquisition allowing fire monitoring and post-fire mapping and assessment, thereby continuing the long-term records from Landsat and SPOT.*

Moderate resolution polar orbiters are an important source of data provision for fire monitoring. Ensuring that the current and future operational sensors include the capability to detect fires and generate reliable fire products is an important goal. The lead-time between project concept, instrument design and operation is long and there is a need for a well articulated set of requirements from the user community. Improvements to the current systems for fire monitoring can be envisioned and need to be shared with instrument design engineers and data providers. The next generation of operational polar orbiters need to benefit from the advances made and the lessons learned using experimental systems such as the Moderate Resolution Imaging Spectroradiometer (MODIS) and SPOT VEGETATION (Townshend and Justice 2002). Transitioning the research advances made using experimental systems into the operational domain is a challenge for scientists and space agencies. A combination of global moderate data acquisition, production and archive and free access regional direct broadcast systems will continue to be needed. Global data products and archives are needed for global change research

and monitoring long-term trends. Regional direct broadcast capabilities enable custom near real time products to be generated for local applications.

Currently there is no operational high resolution polar orbiter for land monitoring. The Landsat Enhanced Thematic Mapper (ETM) is providing science quality, high resolution observations with unprecedented global coverage but the Landsat series is coming to an end and there are no plans for additional ETM instruments. Although plans for a Landsat Continuity Data Mission are being reviewed by NASA and USGS for launch in 2006, there is no long term commitment for operational data provision. SPOT high resolution data provide an additional long term record of high resolution data and have been widely promoted and used for resource management applications. For land managers and scientists alike, it is essential that high resolution satellites become operational and a continued data stream be established as part of an open global information infrastructure and an integrated global observing strategy. There is the need for a strong and effective lobby by the user community to secure these observations. In the design of such a system the instrument calibration, acquisition strategy and affordable data pricing are of critical importance to the user community. Experimental systems such as EO1, ASTER and BIRD provide a number of technological advances in imaging for fire and burned areas that could be transitioned to a new generation of operational high resolution sensors (Yamaguchi et al 1998, Briess et al. 2002).

.

*2.7 To create emissions product suites, developed and implemented to provide annual and near real-time emissions estimates including the associated input data sets.*

The research community is developing the methods to include satellite information on fires and area burned in models of fire emissions (Scholes et al. 1996, van der Werf 2003, Justice et al. 2003, Kaufman et al. 2003, Korontzi et al. 2003). The combination of satellite time series data on the timing and areal extent of burning and indicators of vegetation, state dynamically modeled fuel load, and ground based emission factors provide the basis for emission products. Information on fire energy provides input for fire emissions calculations (Wooster 2002). As part of the emission product suite, it will be important to provide the users with the data inputs used and an estimation of the output product accuracy.

## 3. THE GOFC/GOLD REGIONAL NETWORKS

A major role of GOFC/GOLD is to provide a coordinating mechanism for national and regional activities. GOFC/GOLD is developing a number of regional networks of data providers, data brokers and data users, in close partnership with the UN ISDR WG IV. This UN interagency program is bringing together fire managers to help develop and implement the regional fire policies. Strong networks of resource managers and scientists provide the key to sustained capability for improving the observing systems and ensuring that the data are being used effectively. Wherever possible these networks should build on existing regional structures and activities. A series of workshops are being held to engage the user community to raise and address regional concerns and issues. The aim of the regional networks is to provide a strong voice for regional needs and foster lateral transfer of technology and methods within and between regions. GOFC/GOLD networks are currently being developed in Central Africa (OSFAC), Southern Africa (MIOMBO), Russia and the Far East, South America and Southeast Asia (SEARIN).

Further information on the GOFC/GOLD-Fire program can be found at http://gofc-fire.org, where the core information is also available in Spanish and Russian (Fig. 2).

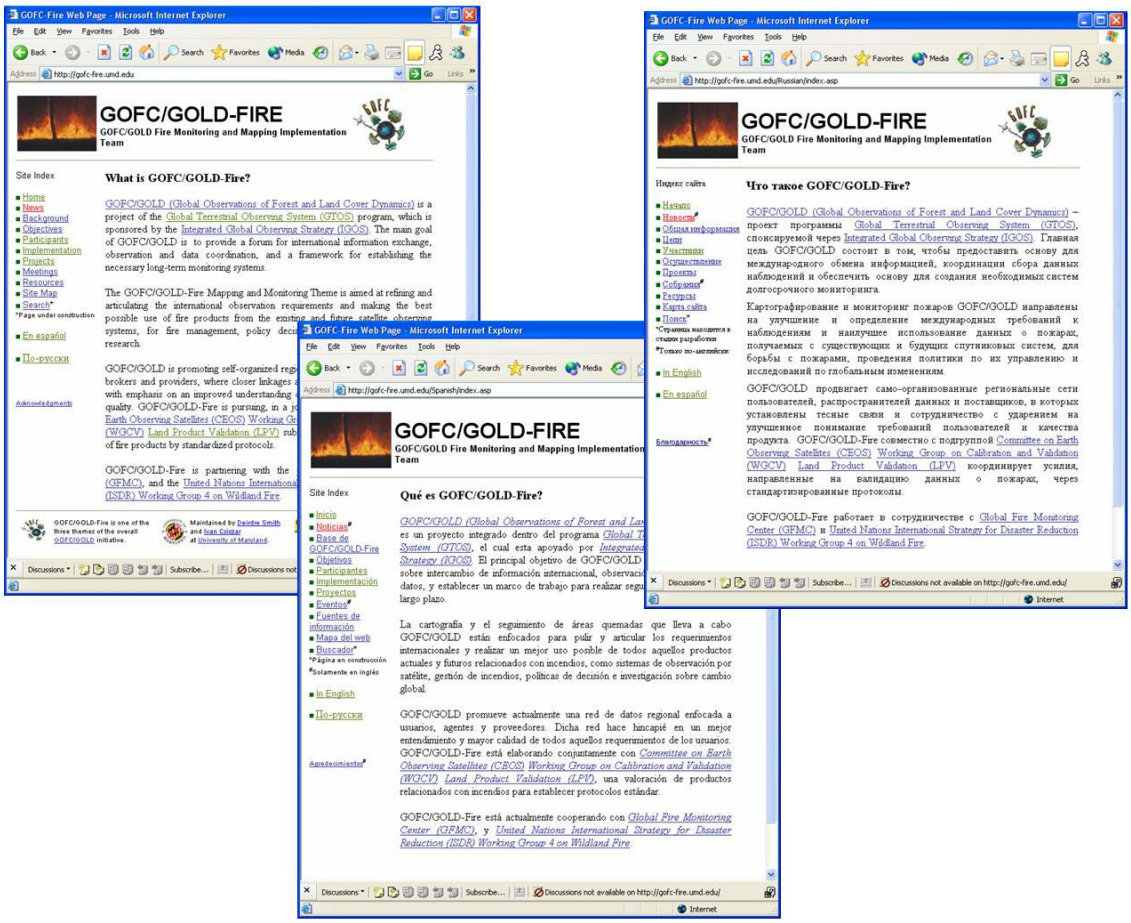


Figure 2. Home page of the GOFC/GOLD-Fire website

## 4. REFERENCES


Ahern, F., Goldammer, G., Justice, C.O. (Editors), 2001. Global and Regional Vegetation Fire Monitoring From Space: Planning a Coordinated International Effort. SPB Academic Publishing, The Hague, The Netherlands. ISBN 90-5103-140-8, 250pp.

Briess, K., E. Lorentz, D. Oertel, W. Skrbek and B. Zhukov, 2002. Fire Recognition Potential of the Bi-spectral InfraRed Detection (BIRD) Satellite. DLR, TN-BIRD-2000-Working Paper 115.

UN FAO 1999. FAO Meeting on Public Policies Affecting Forest Fires. FAO Forestry Paper 138, 365pp.

Justice, C.O., Smith, R., Gill, M., Csiszar, I. 2003. Satellite-based Fire Monitoring: current capabilities and future directions, International Journal of Wildland Fire, in press.

Justice, C. O., Giglio, L., Korontzi, S., Owens, J., Morisette, J. T., Roy, D., Descloitres, J., Alleaume, S., Petitcolin, F., and Kaufman, Y., 2002. The MODIS Fire Products. Remote Sensing of Environment, 83:244-262.

Justice C.O., Belward A., Morisette J., Lewis P., Privette J., Baret F., 2000. Developments in the validation of satellite products for the study of the land surface. International Journal of Remote Sensing, 21, 17, 3383-3390.

Kaufman, Y., Ichoku, C., Giglio, L., Korontzi, S., Chu, D. A., Hao, W. M., Li, R.-R., and Justice, C. O., 2003, Fires and smoke observed from the Earth Observing System MODIS instrument – products, validation, and operational use. International Journal of Remote Sensing, 24:1765-1781.

S. Korontzi, C. O. Justice and R. Scholes (2003). Influence of timingand spatial extent of vegetation fires in southern Africa on atmospheric emissions, Journal of Arid Environments, 54(2), 395-404.

Prins E. and Schmetz J. 2001. Diurnal active fire detection using a suite of international geostationary satellites. In Ahern, F., Goldammer, G., Justice, C.O. (Editors), 2001. Global and Regional Vegetation Fire Monitoring From Space: Planning a Coordinated International Effort. SPB Academic Publishing, The Hague, The Netherlands. ISBN 90-5103-140-8, p139-148.

Roy, D., Borak, J, Devadiga, S., Wolfe, R., Zheng, M., Descloitres, J., 2002b, The MODIS land product quality assessment approach, Remote Sensing of Environment, 83:62-76.

Scholes, R.J., Ward, D. and Justice, C.O., 1996. Emissions of trace gases and aerosol particles due to vegetation burning in southern hemisphere Africa. Journal of Geophysical Research, 101:23677-23682.

Townshend, J.R.G. and Justice, C.O., 2002. Towards operational monitoring of terrestrial systems by moderate-resolution remote sensing, Remote Sensing of Environment, 83:351-359.

van der Werf, G., Randerson, J. T., Collatz, G. J., and Giglio, L., 2003, Carbon emissions from fires in tropical and subtropical ecosystems. Global Change Biology, 9:547-562.

Wooster, M.J., 2002, Small-scale experimental testing of fire radiative energy for quantifying mass combusted in natural vegetation fires. *Geophysical Research Letters*, 29:2027-2034.

Yamaguchi, Y., A.B. Kahle, H. Tsu, T. Kawakami and M. Pniel, 1998, Overview of Advanced Spaceborned Thermal Emission and Reflection Radiometer (ASTER). *IEEE Transactions on Geoscience and Remote Sensing*, 46:1062-1071.

# The LANDFIRE Project: Developing critical spatial data and modeling tools for implementing the USA National Fire Plan and the Cohesive Strategy

Robert E. Keane
*USDA Forest Service, Rocky Mountain Research Station, Fire Sciences Laboratory, Missoula, Montana, USA*

Keywords: fuels mapping, biophysical modeling, condition class, ETM+

ABSTRACT: The National Fire Plan's Cohesive Strategy developed by the USDA-Forest Service and the Department of the Interior and the Ten-Year Comprehensive Plan establish a national commitment to restore and maintain ecosystem health in fire-adapted ecosystems for priority areas across the interior West. In 2000, a series of maps for the lower 48 states were developed at 1 $km^2$ pixel resolution that characterized vegetation cover, historical fire regimes and departures from the historical regimes, known as fire regime condition classes (FRCC). FRCC provided a basis for assessing fire risk and valuable information for national prioritization and planning and made significant contributions to the Cohesive Strategy. It became apparent that finer scale information was critically needed nationally, regionally and locally to effectively implement the National Fire Plan.

## 1. INTRODUCTION

The LANDFIRE (LANDscape and FIRE Management Planning System) project was initiated to provide scientifically credible, comprehensive and critical mid-scale data for prioritization and planning to implement the National Fire Plan, both at the national and local level. The objective of LANDFIRE is to provide the spatial data and predictive models needed by land and fire managers to prioritize, evaluate, plan, complete, and monitor fuel treatment and restoration projects, essential to achieving the goals targeted in the Cohesive Strategy and National Fire Plan of the United States.

## 2. METHODS

The data will eventually be mapped using consistent, standardized, and comprehensive methods across the contagious United States at 30 meter resolution. Maps of condition class will be developed from an integration of spatial data layers of vegetation, biophysical setting, and fuels using simulation models of fire and succession. Vegetation composition and structure are being mapped at the USGS EROS Data Center using regression tree analysis on three TM scenes (leaf-on, leaf-off, peak season) and a variety of biophysical and pattern variables. Fuels, FRCC, and a myriad of other maps and tools are being developed at the USDA Forest Service Rocky Mountain Research Station Fire Sciences Laboratory. Critical to LANDFIRE is a comprehensive database of georeferenced field data used 1) as reference for mapping, 2) as an assessment of map accuracy, 3) to initialize computer models, and 4) to parameterize computer models

## 3. RESULTS

Currently, LANDFIRE is only funded for prototype development in two areas of the western US (western Montana/eastern Idaho and central Utah). Vegetation maps and models for the 10 million hectare central Utah area have been completed using 15,000 ground reference plots and over 30 new fire behavior fuel models are currently being mapped for this area. About 20 million additional hectares in the northern Rocky Mountains will be available by summer 2004. Methods and protocols developed from LANDFIRE can be used to map fuels and fire regimes for anywhere in the world. Information and products from LANDFIRE are available at www.landfire.gov

## 4. CONCLUSION

The process developed through this project has proven successful in the two pilot areas and will be applied throughout the United States. These maps will provide land managers with the information they need to make decisions about fire and fuels programs.

## 5. REFERENCES

Keane, R. E., Long, D. G., Schmidt, K. M., Mincemoyer, S. A., and Garner, J. L. 1998. Mapping fuels for spatial fire simulations using remote sensing and biophysical modeling. *In*: Natural resource management using remote sensing and GIS: proceedings of the Seventh Forest Service Remote Sensing Applications Conference - April 6-10, 1998.Nassau Bay, Texas. American Society for Photogrammetry and Remote Sensing, Bethesda, Maryland *pages:* 301-316.

Keane, R. E., Burgan, R. E., and van Wagtendonk, J. W. 2001. Mapping wildland fuels for fire management across multiple scales: integrating remote sensing, GIS, and biophysical modeling. Int. J. Wildland Fire 10(3&4): 301-319.

# The European Forest Fire Information System (EFFIS)

J. San-Miguel-Ayanz , P. Barbosa, G. Schmuck, G. Libertà

*European Commission, Directorate General Joint Research Centre, Institute for Environment and Sustainability*
jesus.san-miguel@jrc.it

Keywords: fire, risk, burnt area, remote sensing, geographic information system, OpenGis, spatial database, map-overlay, raster-vector integration, space-temporal analysis.

## 1. INTRODUCTION

Europe has suffered in the last years a large number of forest fires that has caused enormous losses in terms of human life and environmental damage. Forest fires in Europe are nowadays the result of strong landscape strains for its use and management. High population density in suburban or tourist areas increase the risk of fires due to negligence or accident. Also, rural exodus, extensification of agriculture and livestock breeding, and the increase of agricultural practices and burning to enlarge pastures are some of the causes of the increasing number of fires in Europe. Economically not very profitable, the Mediterranean forests are often used as recreational an area, which aggravates the problem. In the last decade the growth of cities in their neighbor natural areas has resulted in an increase of a particular type of damaging fires, those that take place in the urban-forest interface.

Although the devastating effect of fires at the regional (supra-national) and global scales is widely acknowledged, the mechanisms to estimate fire risk or the effect of fires on the landscape at these scales are not yet developed. Moreover, in Europe, no system exists to store the information and the knowledge on forest fires.

The European Commission, aware of the problem that forest fires pose on people and the environment, set up the necessary mechanisms to develop coherent forest fire information for Europe. Several services of the European Commission (EC), including the EC Joint Research Center, are working to establish the so-called European Forest Fires Information System (EFFIS). The present article describes this system, which will store the existing information on forest fires at the European level, and will incorporate on-line derived information on fire risk and fire damages assessment retrieved through the use of advanced methods. An example of these latter data is the information derived by two of the existing modules. The first one is referred to as the European Forest Fire Risk Forecasting System (EFFRFS) that provides forest fire risk forecast during the peak of the fire season, i.e. from May to October every year. A second module, referred to as the European Forest Fire Damage Assessment System (EFFDAS), evaluates, through the processing of satellite imagery, the damage caused by forest fires. Fire risk and burnt area mapping methodologies in the systems are harmonized at the European scale, which permits the extraction of coherent information for Europe, and the inter-comparison of fire risk and fire damages between European countries or regions. The EFFIS is a dynamic system that incorporates information on forest fires as it becomes available. It is intended as a web interface system in which users can retrieve information for any area of interest in Europe.

The EC reinforced this action in 1997 by setting up a research group to work specifically on the development and implementation of advanced methods for the evaluation of forest fire risk and the estimation of burnt areas at the European scale. This group is since 1999 working at the EC DG Joint

Research Centre and its activities are coordinated through DG ENV to reach the final users in the Member States.

The forest fire activities comprise the different phases of fire monitoring. i.e. before, during and after the fire event. Only fire behavior, for which very detail local information is required is not considered. On the prevention phase, the work has focused both on the development of systems to provide forest fire risk forecast based of existing fire risk indices, and on the development of new integrated forest fire risk indicators. Five types of forest fire risk indices, from long-term (static) risk indicators to short-term (dynamic) risk indicators have been implemented. All these indices permit the harmonized assessment of forest fire risk at the European scale. They may be used as tools for the assessment of risk situations in cases in which international cooperation in the field of civil protection is needed. In all cases, the indices were calibrated and validated using a five-year fire (1992-1997) event dataset.

In addition to evaluating the fire risk, an activity to estimate the annual damage caused by forest fires in the south of the EU was established. This activity has produced, for the years 2000 and 2001 the first cartography of forest fire damages in the south of the EU. All the burned areas larger than 50 ha, which account for an average 75 % of the total area burnt every year, were mapped using satellite imagery. Further, the analysis of which types of land cover classes were affected was performed. In order to centralize the existing information on forest fires in Europe, the EC General Directorate for Environment and the Joint Research Centre have initiated a collaboration for the creation of the so called European Forest Fire Information System EFFIS.

It has been decided to establish the integrated system at Joint Research Centre in Ispra, Italy within the Natural Hazards Project. The system, as well as the information to be entered, are coordinated by the EC Directorate General of Environment, and are accessible to all the representatives of the civil protection and forest fire services of the EU Member States.

## 2. THE EUROPEAN FOREST FIRE RISK FORECASTING SYSTEM (EFFRFS)

As mentioned above, the EFFRFS has been designed for computing several types of forest fire risk indices varying from dynamic indices to long-term indices. Once the indices are computed, they are distributed to the civil protection and forest fire services via Internet. Forest fire risk is influenced by many variables. These variables have a wide range of spatial and temporal variability. According to this variability forest fire risk can be classified into long-term prediction and short-term prediction (Vorissis, 1999**)**. The methods as well as the applications of the derived fire risk maps vary with this time frame. Long term prediction is provided by indices that are referred to as static or long-term. Short time prediction is provided by the so-called dynamic indices. Long-term fire risk prediction is intended for long term planning, which may serve to characterized regions as subject to high or low risk of fires. On the other hand, short-term prediction is more related to fire fighting and extinction and it can be seen as a decision support mechanism for the allocation of forest fighting resources by operational fire fighting centers.

The following forest fire risks are being computed:

1. Long-term (static) indices
    - 1.1 Probability of fire occurrence (Chuvieco *et al.* 1998)
    - 1.2 Likely damage

2. Dynamic indices
    - 2.1 Meteorological fire risk (6 indices) (Bovio & Camia, 2000)
    - 2.2 Vegetation stress fire risk (Illera et al. 1996)

3. Fire Potential Index (Sebastian et al. 2002)

## 3. THE EUROPEAN FOREST FIRE DAMAGE ASSESSMENT SYSTEM (EFFDAS)

Burnt area mapping and forest fire damage assessment are performed as a support activity for the European Commission Directorate General of Environment. First, burnt areas are identified and classified on satellite imagery, then the damage is assessed intersecting these maps of burnt areas with a land-use / land-cover database. The CORINE land-cover is used since it is the only land-use map with a harmonized legend for all the European countries.

Currently, the method used in EFFDAS is based on change detection techniques using satellite imagery from IRS WiFS. Although WiFS presents an optimal ground spatial resolution for the analysis of fires at the European scale (180 meters), it is fairly limited in spectral resolution as it provides only a NIR and Red spectral bands. Enhancement of the spectral resolution with other sensors such as MODIS has been tested with very promising results (Barbosa et al. 2001). It is there foreseen that a combination of this two sensors may be used in the future for the operational mapping of burnt areas. This current methodology is explained in detail in Barbosa *et al.* (2002).

Once the perimeter of the burnt area is identified on the satellite image, the next step is the evaluation of the forest fire damage. This is performed in a GIS environment by intersecting the classified image with a land cover database. The process involves the geo-coding of the image (warping) to the map projection of the land cover map. Warping is performed until sub-pixel registration between the two data layers is achieved.

## 4. QUERIES AND ANALYSIS

All this information generated (alphanumeric, vector and raster) are stored in an object-related database using OpenGis Simple Features Specification for vector data (Oracle) and an image extension for raster data, the raster extension has been developed in-house. Moreover a set of geographic layers are stored, i.e. administrative boundaries (communes, provinces and regions), CORINE land-cover, river network, etc.

Based on this common spatial data infrastructure a set of analysis functions has been developed to perform queries and extract data from the database. A wide variety of queries can be done to extract data from the database, any information layer present in the database can be query as is or in combination with any other layer, map-overlay queries. Also a time scale condition can be introduced for those layers like “Dynamic indices” or “Fire Potential Index” with time dimension, on a base of weekly, decade, month and year statistics. The main objective is to have the capability to perform any space-temporal combination of queries using vector or raster layers and their attributes.

All these geo-processing functionality have been implemented as services at middle-tier level or at database-tier level using Java and C programming languages and open source software components and/or libraries.

A web based client user interface is used to present the results of user queries; the main service is based on the standard OpenGIS Web Map Server Specification 1.1.1. The main effort has been dedicated to develop within a common framework a set of GIS tools for spatial analysis that can allow the user the possibility to work with data coming from fire risk index models, remote sensing data, meteorological data and geo-spatial data.

The users can access the results of his analysis and/or queries as a unique object, it is possible to see and download a maps and graphics that show the results in a classic image formats line JPEG, PNG or similar. But at the same time there is the possibility for the users to download the data produced by the analysis functions, and this is achievable for all kinds of data stored in the database or produced during the work (alphanumeric, vector and raster).

A pre-operational version of this system is active since spring 2000 and servers the community with a day-based service from May to October for the fire risks maps and available on the web as a tool for data analysis.

## 5. REFERENCES


Barbosa, P. M., San-Miguel-Ayanz, Martinez, B. & Schmuck, G., 2002, Barbosa, P. M., Burnt area mapping Southern Europe using IRS - WiFS imagery, IV International Conference on Forest Fire Research, Luso-Coimbra.

Barbosa, P. M., San-Miguel-Ayanz, J. & Schmuck, G., 2001, Remote sensing of forest fires in Southern Europe using IRS - WiFS and MODIS data, SPIE Remote Sensing Symposium, Toulouse, France, 17-21 September.

Bovio G. & Camia A., 2000, 'Description Eudic software for fire danger indices calculation', final report to JRC, Computation of meteorological fire danger indices for southern Europe, p. 14.

Burgan, R.E., Klaver, R.W. & Klaver, JM., 1998, 'Fuel Models and Fire Potential from Satellite and Surface Observations', International Journal of Wildland Fire, Vol. 8: 159-170.

Chuvieco, E., Salas, J., Barredo, J. I., Carvacho, L., Karteris, M. & Koutsias, N., 1998, IV International Conference on Forest Fire Research, Luso-Coimbra.

Illera P., Fernandez A., Calle A. & Casanova J. L., 1996: "Temporal evolution of the NDVI as an indicator of forest fire danger"; International Journal of remote sensing, Vol. 17: 1093-1105.

Vorissis, D., 1999, Definition of the needs of suppress groups as concern of the prediction of the behavior of the wild land fires, in DELFI Proceedings, Athens, pp. 159-163.

Sebastian Lopez, A., San-Miguel-Ayanz, J. And R. Burgan, 2002, Integration of satellite sensor data, fuel type maps and meteoralogical observations for the evaluation of forest fire risk at the pan-European scale, International Journal of Remote Sensing, Vol. 23, No. 13, pp. 2713-2719.

# Session 2. Fuel type mapping

# Deriving canopy structure for fire modeling from Lidar

B. Peterson, P. Hyde, M. Hofton, R. Dubayah
*University of Maryland*
Dubayah@geog.umd.edu

J. Fites-Kaufman, C. Hunsaker
*United States Forest Service*

J. B. Blair
*NASA/Goddard Space Flight Center*

Keywords: lidar, canopy structure, fire behavior modeling, FARSITE

ABSTRACT: The ability to accurately predict the spatial spread and intensity of forest fires has become increasingly important. One of the major roadblocks in the application of spatial models is the difficulty in obtaining the required forest structural characteristics over the domain of interest and at suitable resolution. Lidar remote sensing has demonstrated the potential to accurately estimate needed forest structure such as canopy height, crown density, aboveground biomass and canopy cover. This paper provides a brief background on the derivation of canopy structure characteristics predicted to be important for fire behavior modeling from lidar data. We provide an overview of lidar remote sensing, including the general characteristics of small-footprint and large-footprint systems and review results from previous studies using large-footprint lidar systems for the derivation of forest structure. We then summarize our research with the United States Forest Service to assess the efficacy of marrying lidar data to the FARSITE forest fire model for the Sierra Nevada mountains in California.

## 1. INTRODUCTION

Forest fires pose large-scale ecological and economical problems (Schmoldt et al. 1999). Canopy fires in particular can be devastating to the natural environment and to human settlements (Roberts et al. 1998; Scott and Reinhardt 2001). Forest management practices in the United States over the last century have promoted the suppression of forest fires (United States Forest Service (USFS) 2000). It is argued that this policy of suppression has altered the natural patterns of fire frequency and extent in the ecosystem and has caused changes in fuel loads, creating potentially hazardous conditions that need to be addressed through altered fire policy (USFS 2000). These altered fuel loads, combined with several years of drought conditions throughout much of the United States, has stimulated interest in predicting the behavior and effects of proscribed fire and wildfires. Because of the difficulties involved in studying wildfires *in situ*, fire behavior models are used instead.

Several models have been developed to predict fire behavior. One such model, FARSITE, has been identified by Federal land management agencies in the United States as the best model for predicting fire growth (Keane et al. 2000). One advantage of FARSITE is its ability to model crown fires. Crown fires pose particular problems to forest managers because they are difficult to control, spread rapidly and their post-fire effects are more severe than surface fires (Scott and Reinhardt 2001). For accurate predictions of fire growth (surface and canopy) FARSITE depends on the “consistency

and accuracy of the input data layers needed to execute spatially explicit fire behavior models" (Keane et al. 2000). Having input parameters derived from high quality remote sensing data would therefore be a great asset to fire modeling endeavors.

FARSITE is a GIS-based fire model that is in common use with government agencies in the USFS as well as other government agencies in the United States. In all, FARSITE has eight input layers (Finney 1998). The first five: elevation, slope, aspect, fuel model and canopy cover are all that are needed to simulate surface fires. The last three: canopy height, canopy bulk density and canopy base height are needed to model crown fires. Several of these inputs are canopy structure characteristics that are difficult and labor intensive to measure on the ground.

There is intense interest in obtaining the measurements needed for accurate fire modeling using remote sensing techniques. The data need for modeling crown fires are related to the vertical structure of canopy (height, density and base height) and conventional passive optical and radar techniques have had difficulty recovering such structure. Of the different remote sensing technologies currently available large-footprint, waveform-digitizing lidars are proving to be the best-suited tools for forest mensuration (Blair et al. 1994; Blair et al. 1999) and, therefore, for obtaining the input parameters for the fire modeling (Salmon and Dubayah 2002). Lidar directly measures the vertical structure of vegetation canopies. Canopy height, canopy cover, basal area and biomass, among others, have all been successfully derived from large-footprint lidar (Lefsky 1997; Lefsky et al. 1999a; Lefsky et al. 1999b; Dubayah and Drake 2000; Lefsky et al. 2001, Drake et al. 2002). In addition, digital elevation models for sub-canopy topography (Hofton et al. 2002) from which slope and aspect can be calculated have also been obtained from lidar.

Lidar is a proven method for deriving elevation, slope, aspect, canopy cover and canopy height - each important for fire behavior modeling. Furthermore, lidar derived metrics are expected to be correlated with canopy bulk density and canopy base height. In this paper we summarize our efforts to derive these important variables using lidar for fire modeling. We first give a brief background on lidar remote sensing, describing its basic physical principles, as well as the various types of commercial and research systems available. We then describe the different types of forest structure that may be recovered using lidar, and give some examples from our own field efforts in different biomes. Lastly we provide an overview of our research with the United States Forest Service to assess the efficacy of marrying lidar data to the FARSITE forest fire model for the mountains of the Sierra Nevada in California.

## 2. LIDAR REMOTE SENSING

Lidar (often used synonymously with the term "laser altimetry") is an active remote sensing technique in which a pulse of laser light is sent to the Earth's surface from an airborne or spaceborne laser. The pulse reflects off of canopy materials such as leaves and branches and the ground surface beneath the canopy. The surface area illuminated by the laser pulse is referred to as a "footprint". As the laser pulse interacts with all the surface elements within the footprint (both canopy and ground) it is shape becomes distorted according to the distribution of intercepting canopy and ground materials. The energy in this waveform pulse is then collected back at the instrument by a telescope. The time it takes for the pulse to travel from the laser, reflect off of the surface and be collected at the telescope is recorded. This travel time provides a distance or range from the instrument to the reflecting surface.

Lidar systems typically used for forest mensuration are classified according to the following characteristics: (1) whether they record the complete reflected laser pulse (or "waveform digitizing)" or just the first or last portion of the returned signal (or "single return"); (2) whether they are small footprint (less than 1 m diameter) or large-footprint (tens of meters in diameter); and (3) their sampling rate or scanning pattern. Most commercial lidar systems are low-altitude, small-footprint,

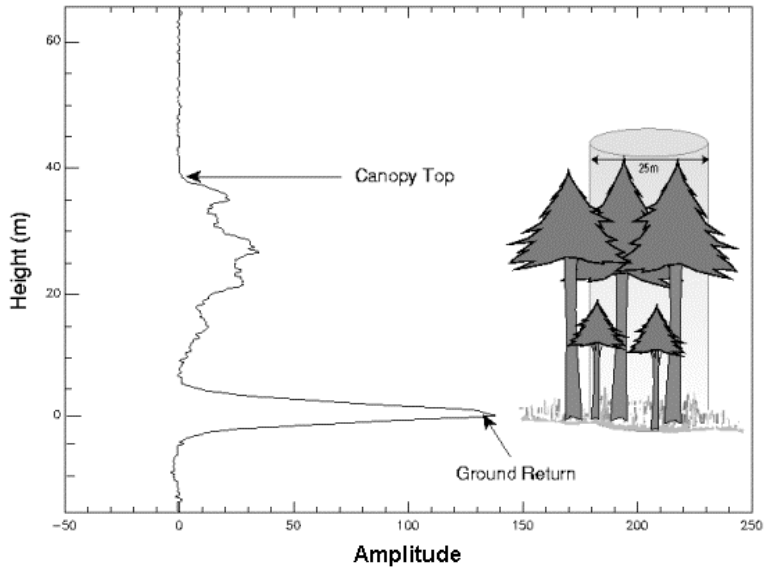


Figure 1. Conceptual basis for large-footprint lidar remote sensing. A pulse of laser energy reflects off canopy (e.g. leaves and branches) and the ground beneath, resulting in a waveform. The amplitude of individual peaks in the waveform is a function of the number of reflecting surfaces at that height. The canopy height is determined by subtracting the range to the ground (defined as the midpoint of the last peak) from that of the first detectable canopy return above noise.

high sampling rate (1,000-25,000 Hz), multiple (first and last) return systems that either provide profiles of canopy or ground topography along a transect or rely on a dense coverage of footprints to map an area.

Small-footprint lidar systems are not optimal for mapping forest structure. Firstly, the narrow beams tend to oversample tree crown shoulders and miss the tops of trees (Nelson 1997). Therefore, unless the footprints are in close proximity to each other and blanket an area, the actual canopy surface must be reconstructed statistically. Secondly, the small footprint size necessitates extensive flying to cover large areas. Finally, for single return systems, it is difficult to ascertain whether or not a given footprint has penetrated though the canopy and reached the ground below. If the ground topography cannot be determined, accurate canopy heights are impossible to measure because height is measured relative to the ground.

Large-footprint systems have been designed to address these problems. The increased footprint size is closer to the diameter of a typical canopy-forming tree (10-25 m), and therefore the return signal is guaranteed to include the tops of tree crowns. The larger footprint size also increases the likelihood of gaps in the canopy being included in the signal, ensuring that the laser energy will penetrate through the canopy and reach the ground. Furthermore, larger footprints allow large areas to be mapped efficiently, reducing flight and operations costs. Finally, large-footprint lidar systems are waveform-digitizing. They provide a record of the vertical structure of vegetation within the footprint (Figure 1). Other remote sensing systems, such as passive optical and radar, have been used to measure forest structure. These systems, however, typically require complex models to recover forest structure characteristics such as height and biomass. In contrast, lidar, and especially waveform-digitizing lidar, provides a direct and elegant means to measure canopy structure. The two basic

canopy measurements that can be made with lidar are canopy height, i.e. the top of the canopy within the footprint, and the vertical distribution of intercepted surfaces within the canopy. At any given height in the canopy, the amplitude of the return waveform is a measure of the strength of the return. Therefore, for forest stands with similar composition of canopy elements within a footprint, larger amplitude indicates more canopy material and smaller amplitude less.

## 3. FOREST STRUCTURE FROM LIDAR

Measurements from small-footprint lidar systems have been successful in estimating canopy heights (Nelson 1997), percent canopy cover (Weltz et al. 1994), timber volume and in some cases aboveground biomass (Nelson et al. 1988; Naesset 1997). Large-footprint, waveform-digitizing lidar systems have been optimized for the measurement of forest canopies (Blair et al. 1994; Blair et al. 1999). Subcanopy topography, canopy height, basal area, canopy cover and biomass have all been successfully derived from large-footprint lidar waveform data in a variety of forest types (Hofton et al. 2002; Lefsky et al. 1999a; Lefsky et al. 1999b; Means et al. 1999; Dubayah and Drake 2000; Peterson 2000; Drake et al, 2002). For example, results from Hofton et al. (2002) show that large-footprint lidar measured subcanopy topography in a dense, wet tropical rainforest with an accuracy better than that of the best operational digital elevation models (such as USGS 30 m DEM products). Means et al. (1999) used large-footprint lidar to recover mean stand height ($r^2 = 0.95$) for conifer stands of various ages in the Westerns Cascades of Oregon. Drake et al. (2002) found that metrics from a large-footprint lidar system were able to model plot-level biomass ($r^2 = 0.93$) for a wet tropical rainforest. Dubayah et al. (2000) and Lefsky (2002) provide a thorough overview of forest structure derived using large-footprint lidar.

## 4. FIRE MODELING IN THE SIERRA NEVADA

Our work has concentrated on deriving fire-modeling-specific forest structure measurements from large-footprint lidar waveform data. Working with the USFS in California we have experimented with using lidar data to predict canopy structure variables that are of special interest to forest fire modelers. For example, parameters (e.g. canopy base height and crown bulk density) that are key to determining the spread of low-intensity ground fires to more devastating crown fires are not easily derived from passive optical remote sensing systems, if at all. Because of its ability to measure canopy structure characteristics, large-footprint lidar has been identified as a key instrument for obtaining these variables.

Based on previous and concurrent studies, the use of lidar data to obtain elevation, slope, aspect, canopy cover and canopy height has been adequately (for example see Figure 2). However, in this study, the primary concentration is on deriving canopy bulk density and canopy base height as these are critical to determining the behavior of possible canopy fires using the FARSITE model and have not yet been successfully derived from lidar data. Our overall approach is to assess (a) the accuracy with which lidar, perhaps in conjunction with other remote sensing data and models, can retrieve these variables, and; (b) evaluate the effects of lidar-derived spatial maps of these input variables on FARSITE model outputs in terms of total area burned, spotting rate, and the spatial distribution of area burned relative to outputs using field-based inputs.

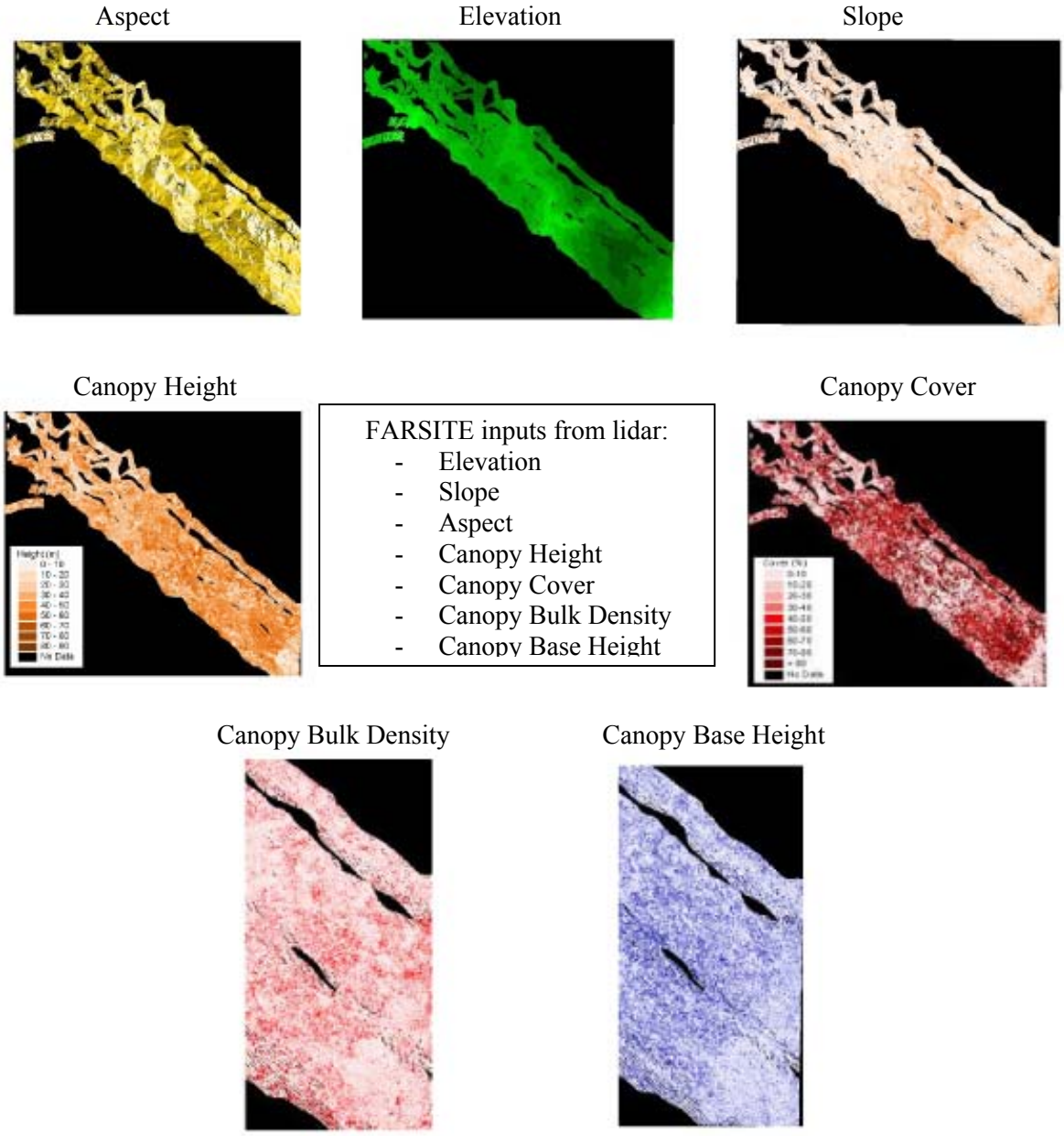


Figure 2. Images of LVIS-derived forest structure characteristics gridded for input into FARSITE. Canopy bulk density and base height are shown for a subset of the area imaged by LVIS. Gaps between lines are caused by irregularities in the airplane trajectory.

### *4.1 Lidar Data*

The lidar data used in this study were collected by the Laser Vegetation Imaging Sensor (LVIS). The LVIS instrument mapped a large area of the Sierra National Forest in October 1999. LVIS is a large-footprint, waveform-digitizing lidar system (Blair et al. 1999). The system has a vertical precision of approximately 30 cm. The ranging data are combined with airplane roll, pitch and bearing data as well as GPS data to locate each individual footprint on the surface. Flying onboard a NASA C-130 at 8 km above ground level and operating at 320 Hz, LVIS produced 25 m-diameter footprints at the surface, overlapping by 50% across track and contiguous along track.

*4.2 Field Data*

Field data were collected during two campaigns in the summers of 2000 and 2001 in the Sierra National Forest and are a representative sample of the different vegetation types found in the area. Circular plots centered on lidar footprints measured 30 m in diameter. Within these plots all trees over 10 cm dbh were sampled. Measurements included: tree height, height to partial crown, partial crown wedge angle, height to full crown, four crown radius measurements and distance and azimuth relative to the plot center. Tree crown shape and species were also recorded. For a subset of the plots, leaf area index (LAI) measurements were taken at 61 points located every 3 m up to 15 m on transects radiating from the plot center at every 30 and at the plot center. The LAI measurements were taken with two LICOR LAI-2000 instruments – one in the plot taking the below-canopy measurements at the 61 points (four measurements at each point) and one located a short distance away logging open sky data. The data from the two sensors were merged using the LICOR C2000 software and used to calculate LAI for each of the 61 points.

The field data were used to calculate crown bulk density and canopy base height using equations developed by Elizabeth Reinhardt of the USFS's Rocky Mountain Research Station. A common method for calculating canopy bulk density from field data is to generate a vertical profile of canopy bulk density and then finding the maximum of a 4.5 m-deep running average for horizontal layers of canopy approximately 0.3 m thick (Scott and Reinhardt 2001). Additionally, canopy bulk density has also been estimated by establishing relationships with LAI (Scott and Reinhardt 2001).

Canopy base height is difficult define and to measure (Scott and Reinhardt 2001). Canopy base height is "the lowest height above the ground at which there is sufficient canopy fuel to propagate fire vertically through the canopy" (Scott and Reinhardt 2001). For fire modeling purposes canopy base height is commonly defined as the lowest height above which a threshold (commonly at least 0.011 kg $m^{-3}$) of available canopy fuels is present (see Scott and Reinhardt for more detail on how this threshold was derived).

For FARSITE modeling a common practice has been to calculate canopy bulk density and canopy base height as described above from measurements made in field sampling plots. Because the field measurements are point data the canopy bulk density and canopy base height estimates must be extrapolated to cover the entire area to be modeled. Typically, canopy bulk density and canopy base height values for given forest types are applied to entire stands of the same forest type. Therefore, within-stand variability of canopy bulk density and canopy base height is not adequately represented in the model.

*4.3 Results: Lidar-Derived Inputs for the FARSITE Model*

In this section we briefly discuss the success we have had generating FARSITE inputs from lidar data. The LVIS-generated DEM of the Sierra Nevada shown in Figure 2 was generated by gridding the elevation measurements for each footprint. Slope and aspect were then calculated from the DEM in a GIS. Canopy height and canopy cover retrievals from LVIS in the Sierra Nevada are currently being validated in another study (Hyde et al. in prep) and preliminary results are encouraging. The methods used to derive canopy height and cover from LVIS are explained in that paper. Gridded images of LVIS-derived canopy height and canopy cover are shown in Figure 2.

There are several ways in which canopy bulk density can be derived from lidar waveform data. One method we used mimics the way in which the running mean approach is used with field data. The maximum of a 4.5 m thick running mean of a waveform is easily calculated. Alternatively, other metrics were derived from the waveform that were assumed to be good predictors of canopy bulk density. These different metrics were compared to field-derived canopy bulk density using multiple linear regression. Initial exploration of different lidar metrics for the derivation of canopy bulk density showed that peak amplitude, total canopy energy and the ratio of canopy energy to total energy collectively were the best predictors. The results of regression analysis between field-derived canopy bulk density and canopy bulk density derived from these LVIS metrics are shown in Figure 3. Based

on these results an input grid of lidar-derived canopy bulk density was generated for a subset of the entire study area (Figure 3).

The simplest way of deriving canopy base height from lidar waveform data is to apply an energy threshold to the waveform or a plot of cumulative canopy energy – similar to the method used to derive canopy base height from the field data. An input grid for FARSITE was created using the height of a 10% cumulative energy threshold as a surrogate for field-derived canopy base height.

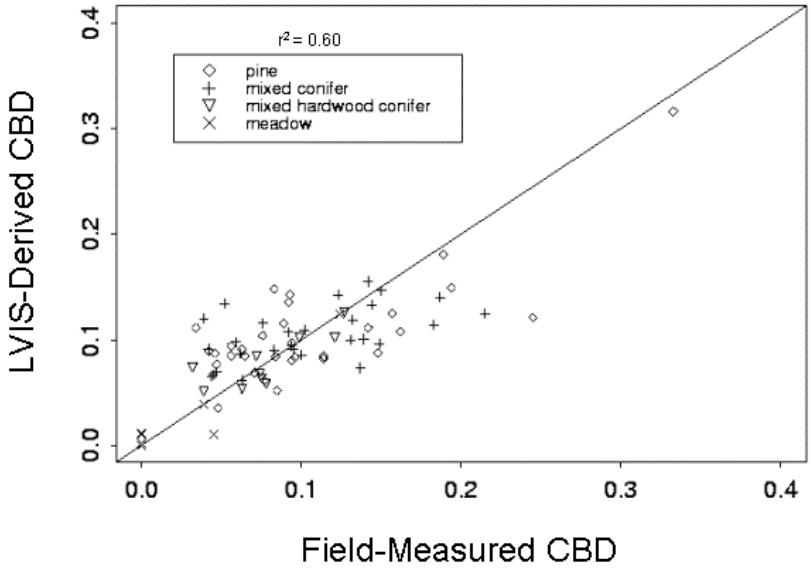


Figure 3. Results of a regression analysis between field-based canopy bulk density and lidar metrics (total canopy energy, canopy energy/total energy ratio and peak amplitude) for plots representing different forest types in the Sierra Nevada.

*4.4 Running FARSITE*

The FARSITE model was run twice (Figure 4), first using canopy bulk density and canopy base heights derived from field data and second using lidar-derived canopy bulk density and canopy base height. All other inputs - including the location of the ignition point - were kept the same for both model runs and were generated by the USFS from sources other than lidar. The model was run for a subset of the study area for a period of approximately 9 hours. A comparison of the two model runs shows that the total area burned in the first model run was much less than that in the second, though the relatively amount of passive crown fire between the two appears to be similar. The model run using lidar data shows areas of active crown fire not apparent in the first run. The differences between the two are likely caused by higher canopy bulk densities and lower canopy base heights in the lidar-derived inputs. Analysis will be needed to determine whether or not the FARSITE outputs based on lidar data reflect actual fire behavior more accurately than field-based inputs.

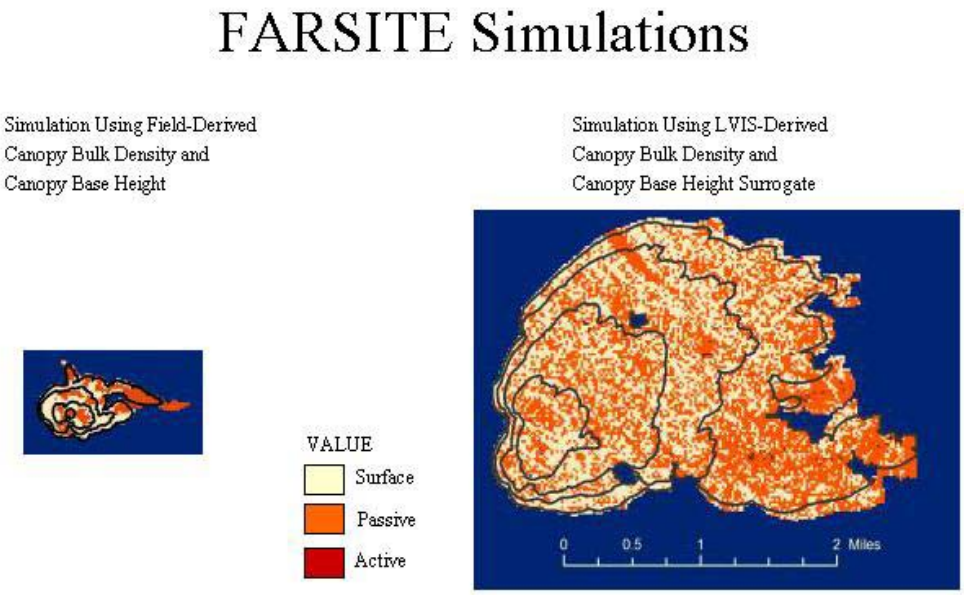


Figure 4. Results from two FARSITE runs. The left portion of the figure shows the output of FARSITE run with field-based canopy bulk density and canopy base height. The right portion of the figure shows the output of FARSITE run with lidar-derived canopy bulk density and lidar-derived canopy base height.

## 5. CONCLUSION

Large-footprint, waveform-digitizing systems specifically designed to characterize the structure of forest canopies have had success in recovering forest structure characteristics for large areas in a comparatively simple and direct manner. In this study we have shown how lidar may be used to provide the spatially explicit forest structure data needed by a commonly used fire behavior model. Specifically, we have demonstrated that inputs for the FARSITE fire behavior model can be obtained directly from the LVIS instrument or modeled from the lidar data.

We continue to explore methods for deriving fire modeling specific forest structure data from lidar. It is possible that lidar alone is not the best predictor of canopy bulk density and/or canopy base height. Therefore, other options must be considered. One such option is to incorporate the use of a radiative transfer model to better understand the relationship between waveform shape and canopy geometry. Another approach is to investigate the use of fusion of lidar data from different types of remote sensors (such radar and passive optical) that are more readily available and complement the vertical structure data provided by lidar.

## 6. ACKNOWLEDGEMENTS

We wish to express our gratitude to Wayne Walker of the University of Michigan for all his work planning for and conducting the two field campaigns in the Sierra Nevada as well as the rest of the field crew: Michelle West, Josh Rhoads, Meghan Salmon, Sharon Pronchik, Bryan Emmett, John Williams and Aviva Pearlman. Steve Beckwitt provided assistance in transforming the gridded LVIS

data into data layers ready for input into FARSITE. This work was supported by a NASA grant (Dubayah) for the implementation of the Vegatation Canopy Lidar mission, and by the US Forest Service.

## 7. REFERENCES

Blair, J.B., D.B. Coyle, J. Bufton and D. Harding. 1994. Optimization of an airborne laser altimeter for remote sensing of vegetation and tree canopies. IEEE International Geoscience and Remote Sensing Symposium, vol. 2:939-941.

Blair, J.B., D.L. Rabine and M.A. Hofton. 1999. The Laser Vegetation Imaging Sensor (LVIS): A medium-altitude, digitization-only, airborne laser altimeter for mapping vegetation and topography. ISPRS Journal of Photogrammetry and Remote Sensing, vol. 54:115-122.

Drake, J.B., R.O. Dubayah, D. Clark, R. Knox, J.B. Blair, M. Hofton, R.L. Chazdon, J.F. Weishampel, S. Prince. 2002. Estimation of tropical forest structural characteristics using large-footprint lidar. Remote Sensing of Environment, vol. 79:305-319.

Dubayah, R. and J. Drake. 2000. Lidar remote sensing for forestry. Journal of Forestry, vol. 98: 44-46.

Dubayah, R., R. Knox, M. Hofton, and B. Blair, Land surface characterization using lidar remote sensing, in Spatial Information for Land Use Management, edited by M. Hill and R. Aspinall, pp. 25-38, Gordon and Breach, 2000.

Finney, M.A. 1998. FARSITE: Fire Area Simulator-Model. Development and Evaluation. USDA Forest Service Research Paper. RMRS-RP-4.

Hofton, M., L. Rocchio, J.B. Blair and R. Dubayah. 2002. Validation of Vegetation Canopy Lidar sub-canopy topography measurements for dense tropical forest, Journal of Geodynamics, 34:491-502.

Keane, R.E., S.A. Mincemoyer, K.M. Schmidt, D.G. Long and J.L. Garner. 2000. Mapping Vegetation and Fuels for Fire Management on the Gila National Forest Complex, New Mexico. USDA Forest Service General Technical Report RMRS-GTR-46-CD.

Kimes, D., J. Gastellu-Etchegorry and P. Esteve. 2002. Recovery of forest canopy characteristics through inversion of a complex 3D model. Remote Sensing of Environment, vol. 79:320-328.

Lefsky, M.A. 1997. Application of Lidar Remote Sensing to the Estimation of Forest Canopy and Stand Structure. PhD. Dissertation, University of Virginia.

Lefsky, M.A., D. Harding, W.B. Cohen, G. Parker and H.H. Shugart. 1999a. Surface lidar remote sensing of basal areas and biomass in deciduous forests of eastern Maryland, USA. Remote Sensing of Environment, vol. 67:83-98.

Lefsky, M.A., W.B. Cohen, A. Hudak, S. Acker and J. Ohmann. 1999b. Integration of lidar, Landsat ETM+ and forest inventory data for regional forest mapping. ISPRS Workshop: Mapping Surface Structure and topography by Airborne and Spaceborne Laser, November 9-11, 1999, La Jolla, CA.

Lefsky, M.A., W.B. Cohen and T.A. Spies. 2001. An evaluation of alternate remote sensing products for forest inventory, monitoring, and mapping of Douglas-fir forests in western Oregon. Canadian Journal of Forest Research, vol. 31:78-87.

Lefsky, M.A., W.B.Cohen, G.G. Parker and D.J. Harding. 2002. Lidar remote sensing for ecosystem studies. BioScience, vol. 52:19-30

Means, J.E., S.A. Acker, D.J. Harding, J.B. Blair, M.A. Lefsky, W.B. Cohen, M.E. Harmon and W.A. McKee. 1999. Use of large-footprint scanning airborne lidar to estimate forest stand characteristics in the western Cascades of Oregon. *Remote Sensing of Environment*, vol. 67:298-308.

Naesset, E. 1997. Determination of mean tree height of forest stands using airborne laser scanner data. *Remote Sensing of Environment*, vol. 61:246-253.

Nelson, R., R. Swift and W. Krabill. 1988. Using airborne lasers to estimate forest canopy and stand characteristics. *Journal of Forestry*, vol. 86:31-38.

Nelson, R. 1997. Modeling forest canopy heights: the effects of canopy shape. *Remote Sensing of Environment*, vol. 60:327-334.

Peterson, B. 2000. *Recovery of Forest Canopy Heights Using Large-Footprint Lidar*. Master's Thesis, University of Maryland.

Roberts, D., M Gardner, J. Regelbrugge, D. Pedreros and S. Ustin. 1998. Mapping the distribution of wildland fire using AVIRIS in the Santa Monica Mountains. *Proceedings of the 7th AVIRIS Earth Science and Applications Workshop*.

Salmon, J. and R. Dubayah. 2002. *Mapping wildland fuels in the Sierra Nevada using lidar remote sensing*. Ninth Biennial Remote Sensing Applications Conference, San Diego, CA, April 2002.

Schmoldt, D.L., D.L. Peterson, R.E. Keane, J.M. Lenihan, D. McKenzie, D.R. Weise and D.V. Sandberg. 1999. Assessing the Effects of Fire Disturbance on Ecosystems: A Scientific Agenda for Research and Management. USDA Forest Service General Technical Report PNW-GTR-455.

Scott, J. H. and E. D. Reinhardt. 2001. *Assessing Crown Fire Potential by Linking Models of Surface and Crown Fire Behavior*. USDA Forest Service Research Paper. RMRS-RP-29.

United States Forest Service. 2000. An Agency Strategy for Fire Management, January 12, 2000, Washington, D.C.

Weltz, M. A., J.C. Ritchie and H.D. Fox. 1994. Comparison of laser and field measurements of vegetation height and canopy cover. *Water Resources Research*, vol. 30:1311-1319.

# Hyperspectral technologies for wildfire fuel mapping

D.A. Roberts & P.E. Dennison
*University of California, Department of Geography, Santa Barbara, California, USA*
dar@geog.ucsb.edu

Keywords: AVIRIS, Spectral Mixture Analysis, Wildfire Fuels, canopy moisture

ABSTRACT: Wildfire is one of the most significant forms of natural disturbance, impacting a wide range of ecosystems ranging from boreal forests to Mediterranean shrublands and tropical rainforest. One of the greatest uncertainties in assessing fire danger is our knowledge of fuels. Fuel properties vary at fine spatial scales, change depending on stand age and prior disturbance history and vary seasonally and interannually depending on moisture availability. Remote sensing has the potential of reducing uncertainty in mapping fuels and improving our ability to assess spatially and temporally varying fuel characteristics. One very promising technology for wildfire fuels mapping is hyperspectral remote sensing. Hyperspectral remote sensing systems measure reflected or emitted electromagnetic radiation over a large number of contiguous spectral bands. Detailed spectral information allows researchers to fully characterize atmospheric properties, thereby removing atmospheric contamination to retrieve high quality surface reflectance. Fine spectral information also facilitates mapping of biophysical and chemical information that is directly related to the quality of wildfire fuels, including above ground live biomass, canopy moisture etc. In this paper, we present examples of mapping wildfire fuel properties derived from Airborne Visible/Infrared Imaging Spectrometer (AVIRIS) data acquired over Southern California. Examples are presented from two chaparral dominated ecosystems, one along the Santa Ynez front range near Santa Barbara, the other the Santa Monica Mountains. Important fuel properties are divided into four broad categories, including fuel type, fuel moisture, green live biomass and fuel condition. Fuel types are mapped using Multiple Endmember Spectral Mixture Analysis, which has the ability to map vegetation to the species level. Live fuel moisture and green live biomass are assessed using remotely sensed measures of canopy moisture, derived from the expression of liquid water in the reflectance spectrum of plants. Fuel condition is mapped using spectral mixture analysis, in which a spectrum composed of a mixture of surface types is decomposed into green vegetation, soil, senesced material (non-photosynthetic vegetation) and shade. Seasonal changes in fuel characteristics, and longer term changes following wildfire are assessed by analysis of time series AVIRIS, acquired between 1994 and 2001.
A hyperspectral system is best used in concert with other data sources, which provide greater temporal and spatial coverage than are currently available from airborne systems, such as AVIRIS. To explore the potential of other sensors, we present results comparing the performance of AVIRIS to Hyperion, a spaceborne hyperspectral system with 242 spectral channels. To explore synergisms with coarser resolution, broad band data we compare AVIRIS measures of fuels to measures provided by ETM and MODIS over the same region in southern California.

## 1. INTRODUCTION

Wildfire is one of the most significant forms of global disturbance, impacting community dynamics, biogeochemical cycles and local and regional climate across a wide range of ecosystems ranging from boreal forests to tropical rainforest (Pyne et al., 1996). Within the wildland urban interface, wildfire represents one of the most serious economic and life-threatening natural disasters.

For example, in Southern California average annual costs due to home and property loss are estimated at $163 million dollars (California State Board of Forestry, 1996). In these regions, the potential of catastrophic wildfire is exacerbated by extreme weather events (i.e., Santa Ana Winds), more than 70 years of fire suppression, and periods of extended drought (Radtke et al., 1982). Postfire effects, such as erosion and mud slides from fire-burned slopes often exceed the cost of the original fire in damage (Barro and Conard, 1991).

One of the greatest uncertainties in assessing fire danger is a lack of knowledge of fuels. Fuels vary at fine spatial scales, change depending upon stand age and prior disturbance history and vary seasonally and interannually depending on moisture availability. Remote sensing has the potential of reducing uncertainty in mapping fuels and improving our ability to assess spatially and temporally varying fuel characteristics. Hyperspectral remote sensing is a relatively new technology that has considerable promise for improving our ability to map wildfire fuels. These systems measure reflected or emitted electromagnetic radiation over a large number of contiguous spectral bands. This detailed spectral information allows researchers to fully characterize atmospheric properties, thereby removing atmospheric contamination to retrieve high quality surface reflectance. Subtle spectral differences between plant species also enables improved fuel type mapping, distinguishing land-cover classes with distinct fuel properties. Fine spectral information also facilitates mapping of biophysical and chemical information that are directly related to the quality of wildfire fuels, such as canopy moisture and improved estimates of surface cover (e.g. exposed soils, senesced and live vegetation). In this paper we present research results from two regions in Southern California, in which hyperspectral data from the Airborne Visible Infrared Imaging Spectrometer (AVIRIS) and Hyperion are used to map important fuel properties.

## 2. BACKGROUND

Fire behavior is a product of fuels, terrain and weather, which vary in importance depending upon fire regime and season (Pyne et al., 1996). Wildfire fuels, because of high spatial and temporal variability, represent one of the greatest sources of uncertainty in predicting fire danger. Currently, fire danger is most often assessed using broad band sensors such as the Advanced Very High Resolution Radiometer (AVHRR), and Thematic Mapper (TM), through some combination of classification to map fuel types, meteorology and ancillary GIS information such as slope, aspect, elevation and fire history (e.g. Chuvieco and Congalton, 1989; Chuvieco and Salas, 1996). In the United States, fire danger is typically quantified by assigning land-cover to fuel categories described by the National Fire Danger Rating System (Bradshaw et al., 1978), while behavior is predicted using fuels described by Anderson, 1982.

Much of the potential of hyperspectral remote sensing for mapping wildfire fuels is illustrated by plant spectra (Figure 1). In this figure, four spectra are shown, senesced grass, coast live oak (*Quercus agrifolia*), chamise (*Adenostoma fasciculatum*) and bigpod Ceanothus (*Ceanothus megacarpus*). Spectral absorptions by water (1), chlorophyll (2), and ligno-cellulose (4) are numbered and marked by arrows. The strong spectral contrast between high Near-infrared reflectance (3) and strong chlorophyll absorption at 680 nm is the basis for most vegetation indices such as the Normalized Difference Vegetation Index (NDVI= ($\rho_{NIR}$-$\rho_{red}$)/($\rho_{NIR}$+$\rho_{red}$). The depth of liquid water bands at 980, 1200, 1350 and 1900 nm depend upon the number of leaves present in a canopy and the moisture content of leaves, and thus are sensitive to green live biomass and live fuel moisture. Ligno-cellulose bands (4) in the short-wave infrared (SWIR) indicate the presence of dry plant material and are thus a measure of dead fuels. They are particularly important for separating senesced grass from bare soil. Subtle spectral differences between chaparral species make it possible to map them separately when they are dominant within a stand.

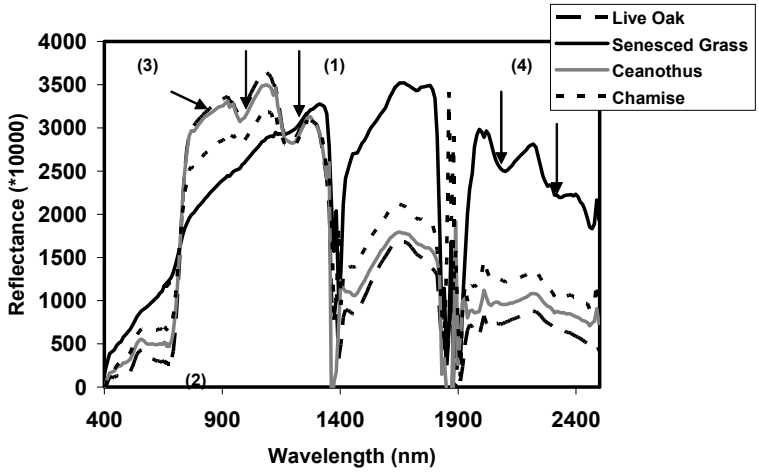


Figure 1. AVIRIS spectra of two chaparral dominants, coast live oak and a senesced grass.

Enhanced spectral information available through imaging spectrometry led Dennison et al. (2000) to develop an alternate framework for assessing fuel properties. In this framework, standard mapping of fuel types is augmented with other important fuel properties including: 1) canopy moisture; 2) green live biomass; and 3) measures of live to senesced canopy components, called fuel condition. Canopy moisture and green live biomass can be assessed through expression of the liquid water bands. Indices developed for estimating moisture include equivalent liquid water thickness (EWT; Green et al., 1993; Roberts et al., 1997), the Normalized Difference Water Index (NDWI= $(\rho_{857}- \rho_{1241})/( \rho_{857}+ \rho_{1241})$ ;Gao, 1996) and the Water Index (WI= $\rho_{895}/ \rho_{972}$; Peñuelas et al., 1993). EWT is estimated from at sensor radiance or reflectance data using a Beer-Lambert approach in which the spectral expression of liquid water is modeled as the exponential of the absorption coefficient of liquid water modified by the pathlength within the medium (Roberts et al., 1998a). Ustin et al. (1998) evaluated the potential of EWT as a measure of canopy moisture in chaparral ecosystems. Serrano et al. (2001) expanded this analysis to compare the NDWI, EWT and WI as measures of relative water content (RWC) in chaparral, concluding that WI was most sensitive to RWC, while EWT was more sensitive to canopy structure.

Fuel condition can be estimated using Spectral Mixture Analysis (SMA) to map green vegetation (GV) and non-photosynthethic vegetation (NPV) fractions (Roberts et al., 1993). The fractions respond to the relative proportions of live (GV) and senesced (NPV) vegetative land cover. Vegetation communities and species can be mapped using Multiple Endmember Spectral Mixture Analysis (MESMA). MESMA is an extension of SMA, in which the number and types of endmembers are allowed to vary on a per-pixel basis (Roberts et al., 1998b). In many cases it is possible to discrimination vegetation spectra to the species level. For wildfire fuels mapping, vegetation maps produced by MESMA are typically reclassified to standard fuel models such as those presented by Anderson (1982), providing species-specific fuels information otherwise inaccessible through remote sensing.

## 3. METHODS

### *3.1 Study Sites*

Examples are provided for two regions of Southern California, the Santa Ynez front range (34˚ N, 120˚ W) and the Santa Monica Mountains (34˚ N, 118.7˚ W). Both regions have Mediterranean climates, characterized by winter precipitation, summer droughts and relatively moderate temperature ranges due to their close proximity to the ocean. Both ranges are approximately east-west oriented,

resulting in strong environmental gradients between warm/dry south facing slopes and more mesic, cooler north facing slopes. Vegetation in more xeric locations is dominated by three chaparral species, chamise and big-pod Ceanothus at lower elevations and manzanita (*Arctostaphylos* sp) at higher elevations. More mesic locations are dominated by coast-live oak and greenbark Ceanothus (*Ceanothus spinosus*). Senesced grasslands occur primarily on more shallow slopes. Both regions have experienced major fires over the past 12 years, including the Painted Cave Fire (1990: Santa Barbara), Green Meadows (1993: SMM), Old Topanga (1993: SMM) and Calabasas Fires (1996: SMM).

### *3.2 Remote Sensing Data*

Time-series AVIRIS data were acquired over both study sites. AVIRIS is an airborne imaging spectrometer that acquires 224 spectral channels between 350 and 2500 nm at a nominal sampling interval of 10 nm with a ground-instantaneous field of view (GIFOV) of 20 meters and a swath of 12 km when flown on the ER2 at 20 km altitude (Green et al., 1998). Typically AVIRIS data are acquired within 2 hours of solar noon. In the Santa Monica Mountains, 16 AVIRIS flightlines were acquired between 1994 and 2002, including several acquisitions that included both spring and fall. Along the Santa Ynez front range, 5 scenes were acquired between 1998 and 2002, with two scenes acquired in May, one in June and two in September. In addition to AVIRIS, we have analyzed one EO-1 Hyperion scene, acquired on June 12, 2001. Hyperion is a spaceborne imaging spectrometer that samples 242 channels at a nominal sampling interval of 10 nm with a GIFOV of 30 m and a swath of 7 km (Ungar et al., in press). It follows the Landsat Enhanced Thematic Mapper (ETM) in its orbit, and thus acquires data at approximately 10:30 AM DST.

AVIRIS data were radiometrically calibrated by the Jet Propulsion Laboratory then georectified by UCSB. Surface reflectance was retrieved using the approach described by Green et al., (1993), in which radiance, modeled using Modtran radiative transfer code for a specific latitude, longitude, date and visibility condition, is fit to radiance measured by AVIRIS. Initial estimates of apparent surface reflectance were further adjusted using homogeneous ground reflectance targets located in each region. Hyperion data were radiometrically calibrated by TRW using Level 1b processing. then corrected using post-launch calibration equal to a 1.08 multipier applied to radiance for the VNIR and 1.18 multiplier in the SWIR (Green et al., in press). Surface reflectance was retrieved for Hyperion using Atmospheric Correction Now VERSION (3.12) (ACORN:Analytical Imaging & Geophysics, Boulder, CO).

### *3.3. Image Analysis*

Hyperspectral data were processed to map dominant vegetation types, fuel condition, and estimate canopy moisture. Dominant vegetation types were mapped using MESMA, using spectra extracted from relatively pure stands of specific land-cover dominants described in the field. Six land-cover types were described, including; manzanita, chamise, big-pod Ceanothus, coast-live oak, senesced grass and bare soil. Spectra were extracted from over 95 field polygons with uniform cover and composition and a minimum size criterion of 60 by 60 meters. For each polygon, species composition was categorized based on percent of total cover: 0-10%, 10-25%, 25-50%, 50-75%, 75-90%, 90-100%. Several important land-cover categories, including greenbark Ceanothus, could not be mapped at 20 meters resolution because of small spatial extent.

Fuel condition was mapped using SMA to map green vegetation (GV:green leaves), non-photosynthetic vegetation (NPV; stems, wood and litter), shade and soil. Reference endmembers used in this study were derived from field and laboratory spectra and are the same as described by Roberts et al. (in press).

A variety of measures can be employed to estimate live fuel moisture and green live biomass. Here we present results based primarily on EWT and the NDWI. EWT is potentially the most viable measure of moisture in that it provides physical units of water thickness (typically in micrometers or

millimeters). NDWI, in contrast, is of value because this index can be applied to hyperspectral data and broad-band systems, such as MODIS.

## 4. EXAMPLES DERIVED FROM AVIRIS

### *4.1 Live fuel moisture and green live biomass*

A subset of examples is presented in this paper. In Figures 2 and 3, applications of EWT are shown. In the first example, EWT is used to estimate leaf area index. The relationship to the left (Fig 2a), was developed by merging data from conifer and broadleaf plants (Roberts et al., 1998a). This example shows a near-linear relationship between LAI and EWT up to LAIs exceeding 10. The example on the right (Fig 2b) shows LAI estimated using this relationship applied to EWT mapped using AVIRIS over the Santa Monica Mountains. LAI estimates are fairly reasonable, including ~3-4 for chamise and up to 6 for Ceanothus. The lowest LAI is estimated for senesced grasslands and drought deciduous soft chaparral.

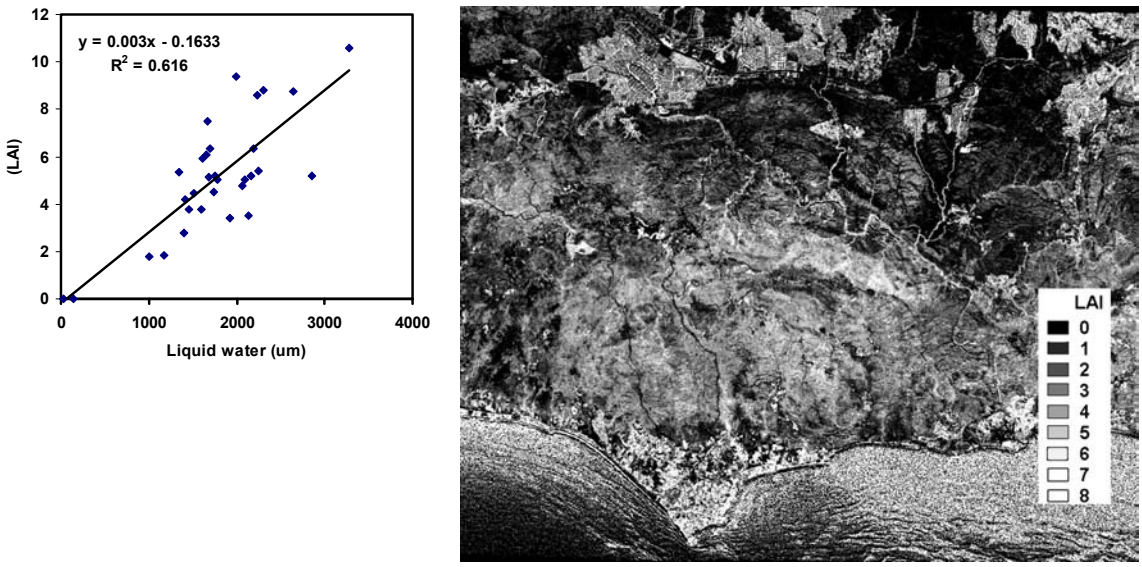


Figure 2. The relationship between EWT and LAI for conifer and broadleaf deciduous plants (left). Estimates of LAI derived from AVIRIS using this EWT/LAI relationship applied to data acquired over the Santa Monica Mountains.

Figure 3 shows the relationship between EWT and live fuel moisture estimated by the Los Angeles County Fire Department through destructive harvests of chamise. Data points were derived from 16 AVIRIS data sets acquired over the Santa Monica Mountains between 1994 and 2002.

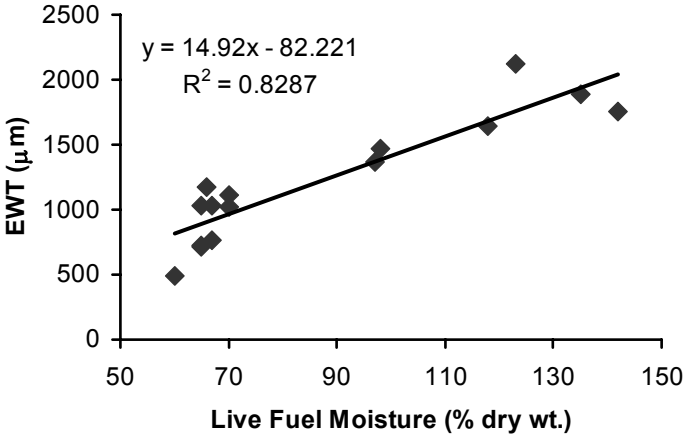


*4.2*

Figure 3. Relationship between EWT and Live Fuel Moisture (Dennison and Roberts, 2003)

Fuel condition was mapped using SMA and reference endmembers derived from the Santa Monica Mountains applied to the Santa Barbara data sets. An example of how fuel condition changes depending on soil water balance is shown in Figure 4. In this example, soil water balance was estimated as the difference between precipitation and potential evapotranspiration (Dennison and Roberts, 2003). The highest positive soil water balance occurred in May, 1998 during a very strong El Niño. The lowest (most negative) soil water balance was calculated for a September 11, 1999. This example shows a near-linear decrease in the GV fraction and a non-linear increase in NPV as the season progresses from moist to dry conditions.

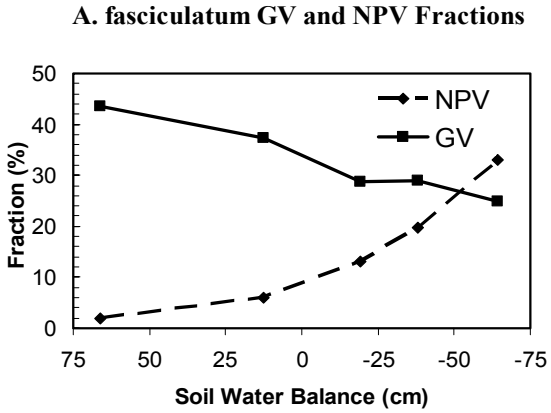


Figure 4. Relationship between NPV and GV fractions and soil water balance for chamise (Dennison and Roberts, 2003)

## 5. SCALING UP FROM AVIRIS

A major limitation of a hyperspectral, airborne system such as AVIRIS is its limited temporal and spatial coverage. This limitation can be partially addressed using spaceborne data. One option is to use a spaceborne imaging spectrometer, such as Hyperion. While this sensor has a limited swath width (7 km), it can acquire an image with a down-track length of up to 185 km. More importantly, as an imaging spectrometer it has the potential of providing many of the fuel measures derived from AVIRIS and can do this globally. A second alternative is to use hyperspectral data to improve the analysis of broad-band data such as ETM and MODIS. For example, AVIRIS can be used to develop spectral libraries needed for the analysis of MODIS or ETM. In addition, AVIRIS can be used to help develop relationships between measures of moisture, such as EWT and measures that can be applied to broad band data, such as SMA used to map GV and NPV fractions. The following examples show some of the capability of Hyperion for mapping important fuel properties including moisture and fuel condition. In these examples, Hyperion data acquired on June 12, 2001 were evaluated by direct comparison to AVIRIS data acquired on June 14, 2001. The last example shows temporal changes in NPV derived from MODIS using the same endmembers used to analyze AVIRIS.

Figure 5 shows plots of moisture estimated from Hyperion (x) plotted against AVIRIS (y). The data points were derived from 79 polygons that occurred in the overlap region between the two scenes (Roberts et al. 2003). Two measures, NDWI and EWT are shown. The latter estimate of moisture was derived from liquid water bands centered at 1200 nm, rather than 980 nm which is more typically used. This became necessary because of the very low Signal to Noise ratio of Hyperion at 980 nm. Both measures show that Hyperion is highly sensitive to canopy moisture. A slope less than one suggest that Hyperion may be more sensitive to moisture, although numerous artefacts in Hyperion may also account for differences in performance.

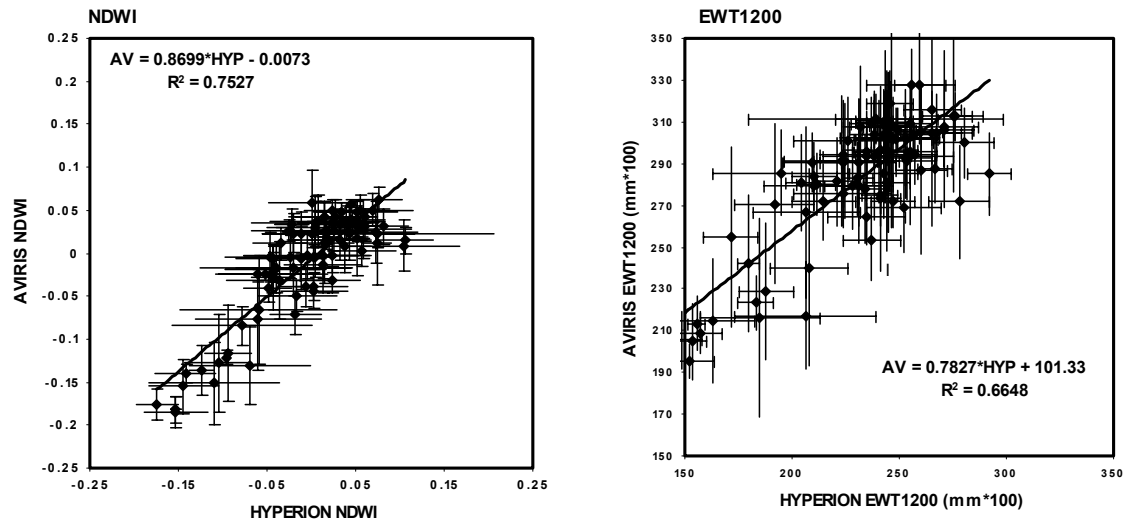


Figure 5. Scatterplot of NDWI and EWT1200 showing the estimates derived from Hyperion (x) plotted against AVIRIS estimates (y). Adapted from Roberts et al., 2003.

Figure 6 shows the relationship between Hyperion and AVIRIS for GV, NPV, soil and shade fractions. The NPV and soil fractions derived from these two sensors show near 1:1 relationships, suggesting that Hyperion has the capability to discriminate senesced vegetation from soils at high accuracy. A slope greater than one for GV, and less than one for the shade fractions is caused by the higher solar zenith angle for the Hyperion data sets. Because the sun was lower in the sky when the Hyperion data were acquired, vertically oriented structures such as plants cast more shadows, resulting in a higher shade fraction, and lower GV fraction relative to AVIRIS. This demonstrates the sensitivity of the shade fraction to canopy structural properties.

Figure 7 shows NPV time series data derived by applying SMA to MODIS time series data acquired in 2001 from Southern California. SMA was applied to the MODIS 0.5 km reflectance product using endmembers derived from AVIRIS and convolved to MODIS wavelengths. Grasslands (ecv_l) stand out as having the most pronounced increase in NPV fraction, starting near Julian day 100. Woodlands (ecv_h) show an initial decrease in NPV, followed by a modest increase. All chaparral communities (lpnf_oj, fr and si) show an initial seasonal decrease to Julian day 100-150, followed by a gradual increase.

## 6. CONCLUSIONS

Hyperspectral data from systems such as AVIRIS provide a diversity of unique wildfire fuel properties including direct measures of live fuel moisture and green live biomass, improved fuel type mapping and improved separation of soils and senesced materials. In this paper, we present examples in which AVIRIS data are used to map live fuel moisture, live green biomass and fuel condition, a measure of live vs senesced material. Examples are provided for time series data acquired over two regions of southern California, the Santa Ynez front range and the Santa Monica Mountains. Some of the potential of scaling up AVIRIS results, is shown using data acquired from the spaceborne imaging spectrometer, Hyperion, and through time series analysis of MODIS.

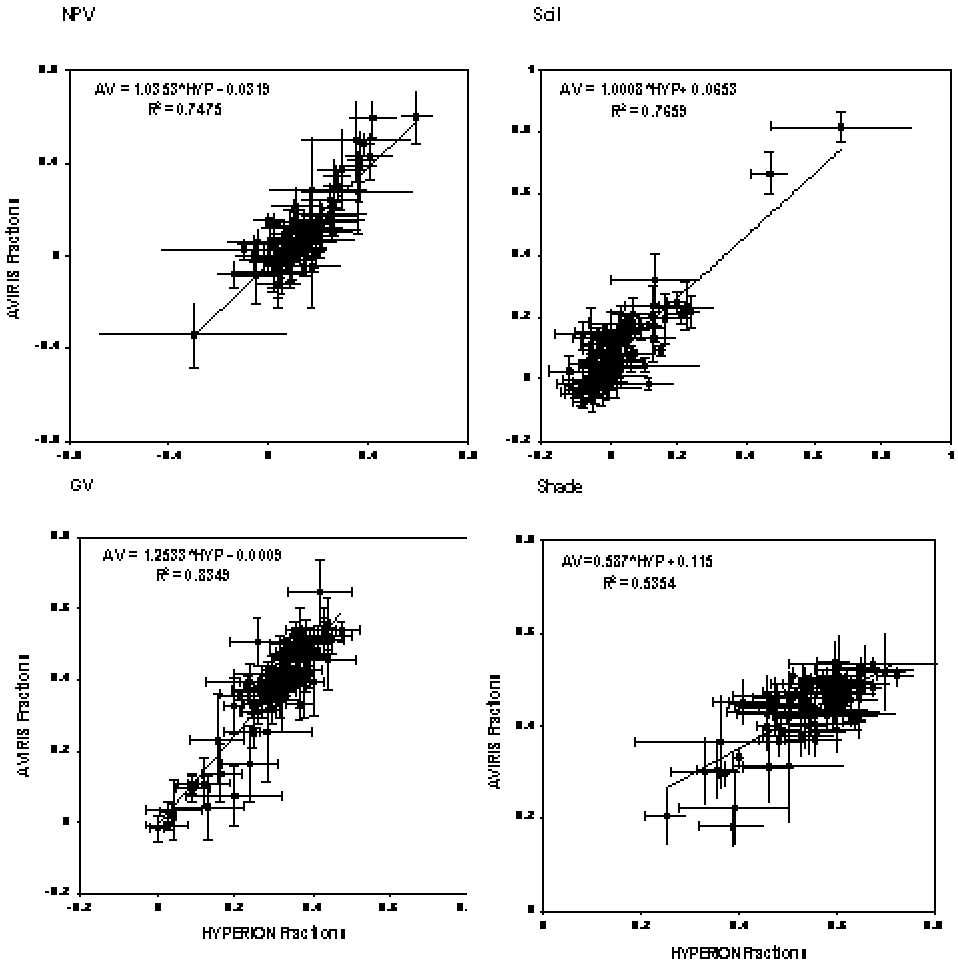


Figure 6: Showing the relationship between AVIRIS and Hyperion spectral fractions for NPV, Soil, GV and Shade. Adapted from Roberts et al., 2003.

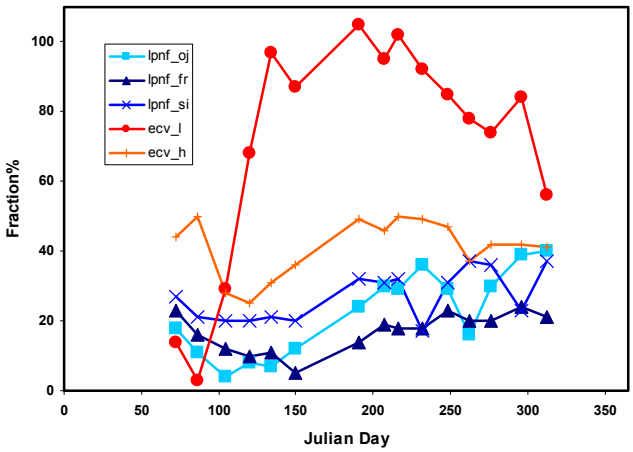


Figure 7. NPV time series derived from MODIS 0.5 km reflectance data acquired in 2001.

## 7. ACKNOWLEDGEMENTS

This research has been supported by a diversity of research grants including the NASA Solid Earth and Natural Hazards program, the Regional Earth Science and Applications Center (RESAC) program and the Joint Fire Science program. Hyperion data and analysis were supported by the funding from the EO-1 SVT program. Support for Phil Dennison was provided, in part, through a NASA Earth System Science Fellowship.

## 8. REFERENCES

Anderson H.E. 1982, Aids to Determining Fuel Models for Estimating Fire Behavior, USDA Forest Service, Intermountain Forest and Range Experiment Station, INT-122, 22 p.

Barro S.C., and Conard, S.G., 1991, Fire effects on California chaparral systems: an overview. Environ. Int. 17: 135-149, 1991.

Bradshaw L.S., Deeming, J.E., Burgan, R.E., Cohen, J.D., 1978. The 1978 National Fire-Danger Rating System: technical documentation". Gen. Tech. Rep. INT-169. USDA Forest Service Intermountain Forest and Range Experiment Station. 44 pp.

California State Board of Forestry, 1996, California Fire Plan : a Framework for Minimizing Costs and Losses from Wildland Fires, the Board, Sacramento, Calif.

Chuvieco, E., and Congalton R.G., 1989, Application of remote sensing and geographic information systems to forest fire hazard mapping, Rem. Sens. Environ, 29:147-159.

Chuvieco E., and Salas. J., 1996, Mapping the spatial distribution of forest fire danger using GIS, Int. J. of GIS, 10(3): 333-345.

Dennison, P.E., Roberts, D.A. and Regelbrugge, J.C., 2000, Characterizing chaparral fuels using combined hyperspectral and synthetic aperture radar data, Proc. 9th AVIRIS Earth Science Workshop, JPL, Pasadena, CA Feb 23-25, 119-124.

Dennison, P.E. and D.A. Roberts, 2003. Endmember Selection for Multiple Endmember Spectral Mixture Analysis, Proc. 12th JPL Airborne Earth Science Workshop, Jet Propulsion Laboratory, Pasadena, CA.

Gao, B.-C., 1996, NDWI-A normalized difference water index for remote sensing of vegetation liquid water from space, Remote Sens. Environ. , vol. 58, 257-266.

Green, R.O., Chrien, T.G., and Pavri, B., in press, On-orbit Determination of the Radiometric and Spectral Calibration of Hyperion Using Ground, Atmospheric and AVIRIS Underflight Measurements, IEEE Trans. Geosci. Remote Sens.

Green, R.O., Conel, J.E., and Roberts, D.A., 1993, Estimation of aerosol optical depth and calculation of apparent surface reflectance from radiance measured by the Airborne Visible-Infrared Imaging Spectrometer (AVIRIS) using MODTRAN2, SPIE Conf. 1937, Imaging Spectrometry of the Terrestrial Environment, 12p.

Green, R.O., Eastwood, M.L., Sarture,C.M., Chrien T.G., et al., 1998, Imaging spectroscopy and the Airborne Visible Infrared Imaging Spectrometer (AVIRIS). Remote Sens. Environ. 65(3): 227-248.

Peñuelas, J., Filella, I., Biel, C. Serrano L., and Save, R., 1993, The reflectance at the 950-970 nm region as an indicator of plant water status, Int. J. Remote Sens., vol. 14, 1887-1905.

Pyne, S.J., Andrews, P.L. and Laven, R,D., 1996, Introduction to Wildland Fire 2nd edition, John Wiley and Sons, Inc, NY, 769 pp.

Radtke, K.W.H., Arndt, A. and Wakimoto, R.H., 1982, Fire history of the Santa Monica Mountains, In C.E. Conrad and W.C. Oechel (Eds.) Dynamics and Management of Mediterranean-type Ecosystems, USDA FS Tech. Report PSW-58, pp. 438-443.

Roberts, D.A. Brown, K.J., Green, R., Ustin, S., and Hinckley, T., 1998a, Investigating the relationship between liquid water and leaf area in clonal Populus, Proc. 7th AVIRIS Earth Science Workshop JPL 97-21, Pasadena, CA 91109, 335-344.

Roberts, D.A., Dennison, P.E., Gardner, M., Hetzel, Y., Ustin, S.L., and Lee, C., in press, Evaluation of the potential of Hyperion for fire danger assessment by comparison to the Airborne Visible Infrared Imaging Spectrometer, IEEE Trans. Geosci. Remote Sens.

Roberts, D.A., Gardner, M., Church, R., Ustin, S., Scheer, G., and Green, R.O., 1998b Mapping Chaparral in the Santa Monica Mountains using Multiple Endmember Spectral Mixture Models, Remote Sens. Environ. 65: 267-279.

Roberts, D.A., Green, R.O., and Adams, J.B., 1997, Temporal and Spatial Patterns in Vegetation and Atmospheric Properties from AVIRIS, Remote Sens. Environ., 62: 223-240.

Roberts, D.A., Smith, M.O., and Adams, J.B., 1993. Green vegetation nonphotosynthetic vegetation and soils in AVIRIS data, Remote Sens. of Environ., 44 (2-3), 255-269.

Serrano, L. Ustin, S.L. Roberts, D.A., Gamon, J.A., and Penuelas, J., 2000, Deriving water content of chaparral vegetation from AVIRIS data, Remote Sens. Environ., vol. 74:570-581.

Ungar, S., Pearlman, J. Mendenhall J., and Reuter D., in press, Overview of the Earth Observing One (EO-1) Mission, IEEE Trans. Geosci. Remote Sens.

Ustin, S.L., D.A. Roberts, D.A., Pinzon, J., Jacquemoud, S., Gardner, M., Scheer, G., Castaneda, C.M., and A. Palacios, 1998, Estimating Canopy Water Content of Chaparral Shrubs Using Optical Methods, Remote Sens. Environ., vol. 65:280-291

# Scaling-up based on Radiative Transfer Modeling in a Pine (Pinus Montana ssp. arborea) dominated canopy for forest fire fuel properties mapping using Imaging Spectrometer Data

B. Kötz, M. Schaepman, F. Morsdorf, K. Itten
*Remote Sensing Laboratories (RSL), University of Zurich*
bkoetz@geo.unizh.ch

P. Bowyer
*Telford Institute of Environmental Systems, School of Environment and Life Sciences, University of Salford*

B. Allgöwer
*Geographic Information Systems, University of Zurich*

Keywords: forest fire fuel properties, radiative transfer model, imaging spectroscopy

## 1. INTRODUCTION

Accurate information of fuel properties of forests must be available in high spatial and spectral resolution to be able to understand the processes involved in initiation and propagation of forest fires. Imaging spectroscopy has been proven to be a quantitative data source that may provide spatially distributed information on biomass, canopy structure, and fuel moisture to assess fire risk and to mitigate the impact of forest fires.

Research on the application of radiative transfer models (RTM) for coupling leaf and canopy models showed promising results to derive accurately the structure as well as the biochemistry of generally homogeneous canopies (Fourty and Baret 1997; Weiss and Baret 1999). Yet, the application of these models to a heterogeneous canopy, such as a coniferous forest, where the complex canopy structure dominates the interaction of incident radiation with the individual scatterers (e.g., needles, stems, branches, understory), still needs extensive research (Ceccato, Flasse et al. 2001).

The modeling of canopy reflectance using appropriate RTM and an explicit characterization of the radiative transfer from the needle to canopy level will enhance our understanding on the radiative processes involved within a heterogeneous canopy. This approach will help to identify the key parameters most sensitive within the radiative transfer model and to assess ambiguities within the model parameterization leading to instability of the model inversion (Combal, Baret et al. 2002). In addition to the above, the potential of integrating ancillary information on the canopy structure into the retrieval process is discussed.

## 2. METHODOLOGY

Radiative transfer modeling is applied at different scales to investigate the link between needle optical properties using ground measurements and canopy reflectance derived from imaging spectrometer data. This scaling-up approach focuses on the potential of airborne imaging spectroscopy to map biophysical and biochemical parameters relevant for forest fires. Radiative transfer models of different levels of complexities (e.g., GeoSAIL, FLIGHT) are employed to simulate top of the canopy reflectance for a representative range of canopy parameters derived from detailed field measurements.

Precise parameterization of the RTM is necessary to evaluate the effect of modeling assumptions at needle and canopy level. Subsequently simulated canopy reflectance is compared to actual canopy reflectance acquired by two imaging spectrometers (DAIS 7915, ROSIS) to evaluate the performance of the different RTM. This analysis supports the identification of the the key model parameters, and shall outline the most relevant model uncertainties. Based on this, the need for further restrictions in form of ancillary information within the retrieval process can be derived.

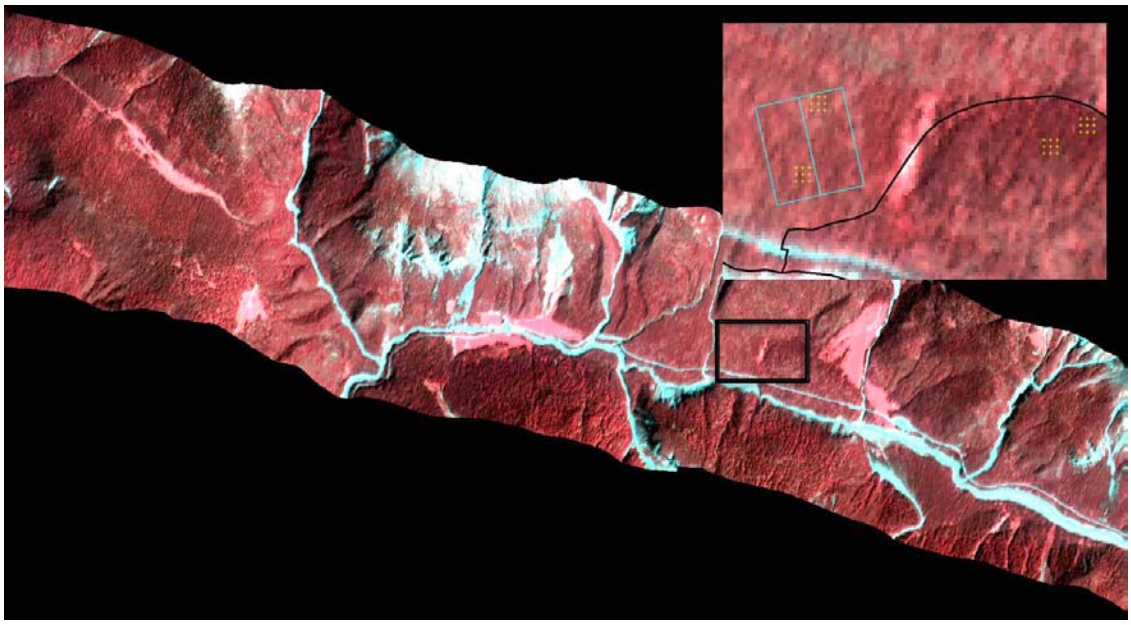

Figure 1. Geocoded DAIS 7915 image of the Swiss National Park (data acquired on August 14, 2002). The zoom window represents the core test sites (indicated using crosses), as well as the plot of the Long Term Forest Ecosystem Research site of the Swiss Federal Institute for Forest, Snow and Landscape Research (WSL).

This study is based on an extensive field campaign in the Swiss National Park (SNP) during summer 2002[1]. Unique ground based characterization of the canopy structure, biochemistry and optical properties of the canopy elements were measured using various measurement instruments, ranging from non-destructive spectroradiometric measurements to dry biomass estimation of needles (cf., Table 2). The core equipment for this activity was composed of four different types of spectroradiometers, measuring the diffuse and total hemispherical irradiance, downward transmittance, ground reflectance, needle transmittance, and understory reflectance. In addition, hemispherical photos, and LAI meters were used simultaneously. The imaging spectrometer data was acquired in parallel to the ground measurements with the two above-mentioned sensors (cf., Figure 1). The imaging spectrometer data was calibrated to absolute radiances. Subsequently they were georeferenced and atmospherically corrected, resulting in canopy reflectances.

## 3. RESULTS AND DISCUSSIONS

A coupled approach of two RTM's, PROSPECT on the needle level and the complex ray-tracing canopy model FLIGHT, demonstrated the general potential of imaging spectrometer data to map forest canopy parameters. Uncertainties in both the ground measurements of the canopy parameters as well in the imaging spectrometer data have been assessed and taken into account.

The radiative transfer has been parameterized on the needle and canopy level by the average field data of the four core test sites (in the following labeled LWF1 and 2, STA1 and 2) each

[1] The measurements in the SNP have been carried out in the framework of the EC SPREAD project (01.0138/EVG1-CT-2001-00043), in work packages 1.1 and 1.2 respectively. This contribution focuses on the activities of the work package 1.2, while the on going research of work package 1.1 is presented in a separate contribution to this workshop by Morsdorf *et al*.

characterized by 9 subplots spaced in a grid of 10 meters. The tree geometry is based on WSL's long term monitoring inventory describing tree height, crown radius and length of single trees of the study area. The uncertainty in the radiative transfer parameterization introduced by measurement and instrument errors have been included in the model simulations by the relative standard error for each parameter (cf.,Table 1). Standard error propagation is applied assuming linear independency of the input parameters to assess the effect of ground data uncertainties on canopy reflectance. An approximation of the model uncertainty (relative standard error of 1.9%) as a function of the photon number was also included in the error propagation.

A thorough assessment of the imaging spectrometry data was carried out at radiance level to describe and quantify the radiometric quality of the data. The assessment revealed a list of bad bands affected by measurement noise or highly non-linear behavior, which were excluded from the further data analysis. The quality assessment of radiometric correction yielded relative deviations compared to ground reflectance of –8 % close to 550 nm and ~2.5 % in the nIR. The calibration errors and the spatial variability of canopy reflectance over the core test sites, expressed as relative standard deviation, described the uncertainty associated with the imaging spectrometer data.

Figure 2 demonstrates finally the ability of the RTM approach to scale up canopy parameters from the leaf to canopy level characterizing canopy reflectance within model and measurement uncertainties. Radiative transfer modeling consequently proofs to be a versatile and valuable tool for a range of forest fire fuel properties.

Table 1. Canopy parameter of the core test sites and their relative measurement error. The spectral properties of bark and understory were characterized by field measurements. Additional model parameters used for all plots are: fraction of bark (0.4), crown form (cone), leaf structure (N: 2), aerosol optical thickness: (0.08).

| | LWF1 | LWF2 | STA1 | STA2 |
|---|---|---|---|---|
| LAI | 1.23 (13%) | 1.01 (22%) | 2.2 (19%) | 2.25 (17%) |
| Fcover | 0.55 (13%) | 0.46 (22%) | 0.77 (19%) | 0.79 (17%) |
| Cab [µg/cm$^2$] | 61.80(1.54%) | 75.10 (1.54%) | 59.00 (1.54%) | 62.80 (1.54%) |
| Cw [g/cm$^2$] | 0.047 (7.5%) | 0.045 (7.5%) | 0.049 (7.5%) | 0.042 (7.5%) |
| Cdry [g/cm$^2$] | 0.038 (7.5%) | 0.036 (7.5%) | 0.038 (7.5%) | 0.035 (7.5%) |

Figure 2. Simulated and measured canopy reflectance of the four core plots. Error bars represent the uncertainties of the RTM approach (solid grey), and DAIS measurements (bars with gaps).

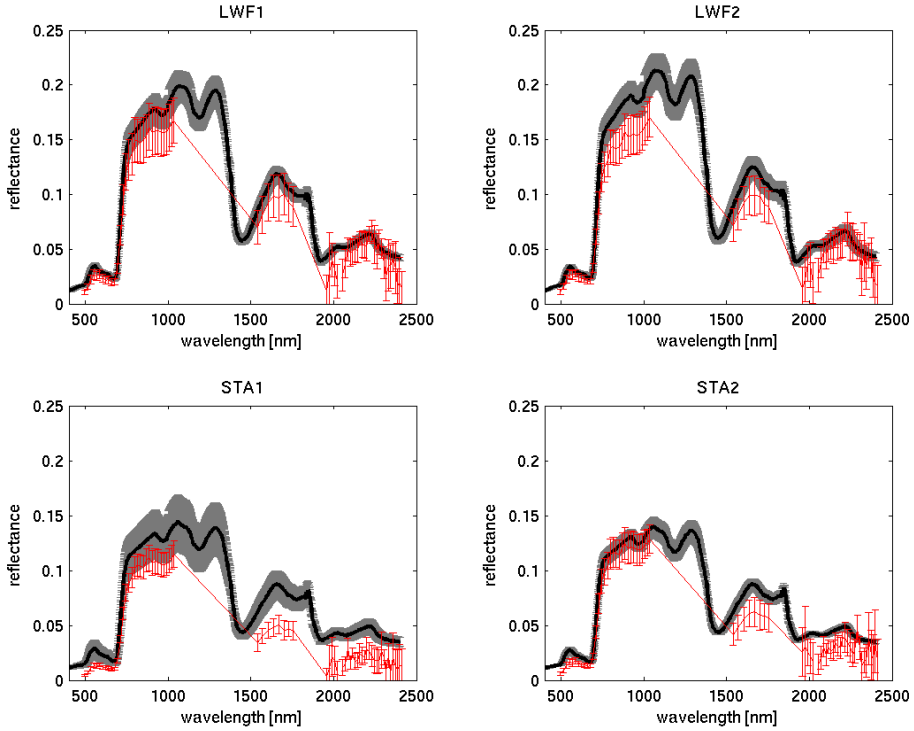

Table 2: List of acquired canopy parameters during the field campaign in the Swiss National Park (OF+x: time of overflight + x days)

| Parameter | Instrument | Time | Sampling |
|---|---|---|---|
| **Optical properties** | | | |
| L□ (Leaf reflectance) | ASD + Licor1800 sphere | OF | Species |
| Lt (Leaf transmittance) | ASD + Licor1800 sphere | OF | Species |
| Cab (chlorophyll content) | CAD-As. | OF | Spatial |
| Cw (water content) | Balance, Licor3100 | OF | Spatial |
| S□ (Soil reflectance) | ASD field spectrometer | OF | Type |
| U□ (Understory reflectance) | GER1500 radiometer | OF | Spatial |
| □ (ground reflectance) | ASD field spectrometer | OF | Spatial |
| Canopy transmission, FAPAR/FIPAR | GER1500 radiometer + MFR7 sun photometer | OF | Spatial |
| **Structural properties** | | | |
| LAI / LAD | Licor2000, Hem. photographs | OF | Spatial |
| Tree height | Terrestrial survey, Theodolite | OF+14 | Spatial |
| Crown height/ shape | Terrestrial survey, Theodolite | OF+14 | Spatial |
| Tree density | Field survey | OF+14 | Spatial |
| Fraction of branch (wood) | Hem. photographs | OF+7 | Spatial |
| Fraction of senescent | Hem. photographs | OF+14 | Spatial |
| Vegetation cover | Hem. photographs | OF+14 | Spatial |
| Atmospheric properties | | | |
| Horizontal visibility | MFR7 sun photometer | OF | |
| Water vapour | MFR7 sun photometer | OF | |
| **Geometric information** | | | |
| GCP | DGPS | OF/+14 | Spatial |

## 4. REFERENCES


Ceccato, P., S. Flasse, et al. (2001). "Detecting vegetation leaf water content using reflectance in the optical domain." Remote Sensing of Environment **77**(1): 22-33.

Combal, B., F. Baret, et al. (2002). "Improving canopy variables estimation from remote sensing data by exploiting ancillary information. Case study on sugar beet canopies." Agronomie **22**(2): 205-215.

Fourty, T. and F. Baret (1997). "Vegetation water and dry matter contents estimated from top-of-the-atmosphere reflectance data: A simulation study." Remote Sensing of Environment **61**(1): 34-45.

Weiss, M. and F. Baret (1999). "Evaluation of canopy biophysical variable retrieval performances from the accumulation of large swath satellite data." Remote Sensing of Environment **70**(3): 293-306.

# Generation of crown bulk density for *Pinus sylvestris* from LIDAR

D. Riaño & E. Chuvieco
*Geography Department, University of Alcalá, Madrid, Spain*
David.riano@uah.es

S. Condés
*Dept. de Economía y Gestión Forestal, ETS de Ingenieros de Montes. Madrid, Spain*

J. González Matesanz
*Servicio de Geodesia. Instituto Geográfico Nacional, Madrid, Spain.*

Keywords: LIDAR, crown bulk density, foliar biomass

## 1. INTRODUCTION

One of the most critical variables in fire behavior modeling of crown fires is the estimation of crown bulk density (CBD) (Scott, 1999). CBD is computed as the foliage biomass (FB) over the crown volume. Brown (1965) showed that it is possible to obtain crown weight base on other measurements of trees. LIDAR does not saturate at high biomass and it would be easier to separate tree crown information from other canopy data than with optical data. LIDAR systems have been tested for estimating other critical forest parameters such as tree height, cover or total biomass (Hyyppa et al., 2001; Magnussen et al., 1999; Means et al., 1999; Naesset, 1997), which have produced better results than aerial photography, airborne hyperspectral sensors (e.g. AVIRIS), and airborne profiling radar (Hyyppa et al., 2000; Hyyppa et al., 2001; Lefsky et al., 2001).

This paper explores the utility of LIDAR to produce a crown bulk density estimation for *Pinus sylvestris* once we found a specific relationship between foliage biomass and crown volume of this species versus LIDAR.

## 2. METHODOLOGY

The test site is located about 50 Km North of Madrid. The Toposys II system (www.toposys.com) recorded high-density first and last LIDAR returns. The accuracy of the LIDAR was validated using Differential GPS (DGPS) and a total station.

The data provider generated the digital terrain model (DTM) based on the bisection principle (von Hansen and Vögtle, 1999). The height above the ground for the raw LIDAR data was generated using this DTM and spline function interpolation (figure 1).

The LIDAR heights above the ground were validated with measurements of trees in the field. A total of 10 plots were located with a DGPS (outsite the forest) and a total station (in order to locate the plot in the forest). We measured each tree height which was in a radius <10 m to the center of the plot (figure2).

We performed destructive sampling (figure3) in order to test an allometric equation relating foliar biomass and various forest parameters such as diameter at breast height (DBH), tree height, crown volume, crown height or crown area. 10 trees of different size-class were cut down weighting all branches. We also weighed foliar biomass of three branches (one from the upper part of the crown, another one from the middle and a third one from the lower crown) in order to find a relationship

between the weight of braches and foliar biomass. We followed the methodology proposed by Lopez-Serrano (2000).

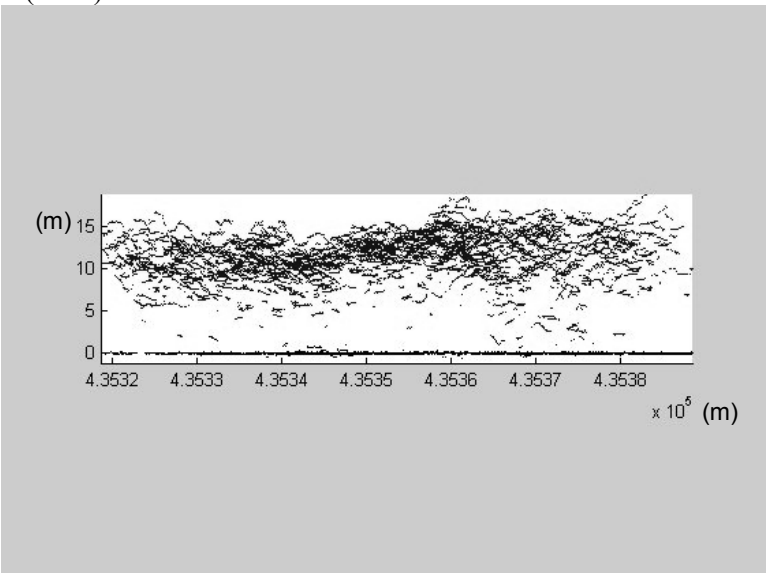


Figure 1. We used this DTM as true ground height above the sea level to interpolate the raw LIDAR data. We obtained for each laser pulse (X, Y) the interpolated ground height referenced to the sea level (Z´). Therefore Z-Z´ was the vegetation height above the ground. The algorithm used was spline function interpolation

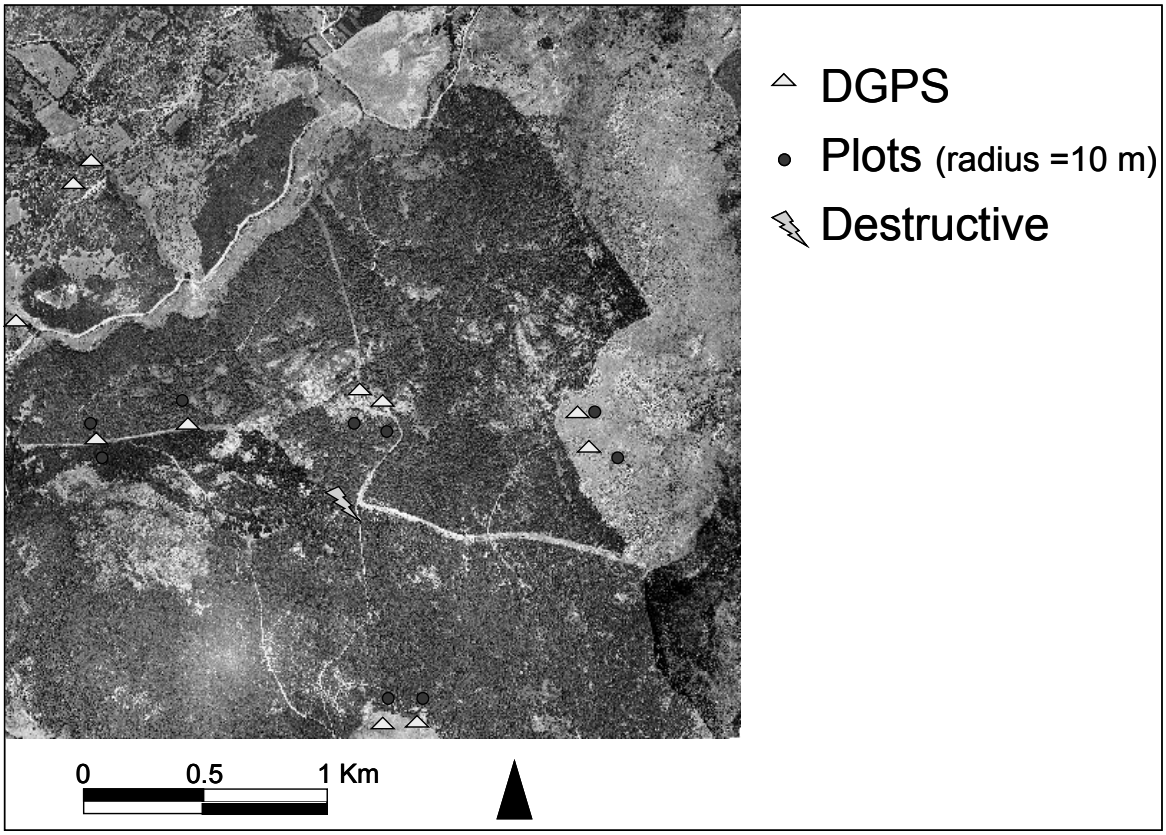


Figure 2. Location of plots.

Figure 3. Destructive sampling.

Foliar biomass was calculated for all trees of the 10 plots according to this allometric equation. The total foliar biomass of each plot was related to various parameters extracted from LIDAR data (percentile 50, 75, 95; mean and maximum of all lasers pulses within the plot, percentage of canopy hits (height >3 meters),percentile 1, 5, 50, 95, 99; mean, standard deviation and total number of crown laser pulses).

Crown volume was calculated for each tree measuring crown width in N, E, S and W directions and assuming an ellipsoid form. The total crown volume was compared to the crown volume obtained from the LIDAR data. We used the crown height times the percentage of crown laser hits. The crown height was calculated from percentiles 1 and 95 of crown hits.

## 3. RESULTS AND DISCUSSIONS

We obtained an absolute average difference between LIDAR data and ground reference DGPS measurements of 0.24 m using 28 points.

The height above the ground obtained from LIDAR (figure 4) was very accurate with a relationship 1:1. There were some outliers due to cutting of some trees in one of the plots. The field measurements were carried in June 18th for this plot whereas the flight was done in August 20th. The rest of them were carried out the beginning of September. Some other errors could be due to mislocations of trees in the field.

The following allometric equation was obtained relating DBH and foliar biomass:

$$Foliar\ biomass\ of\ a\ tree = 0.000485\,DBH^{3.1518} \quad (1)$$

$R^2$=0.88 P-value<0.01

The best LIDAR predictor of total foliar biomass of each plot was the mean laser height (MLH):

$$Foliar\ biomass = 127.81 * e^{0.1422 * MLH} \quad (2)$$

$R^2$=0.82 P-value<0.01

The crown volume estimated from the crown volume obtained from the LIDAR data (crown height times the percentage of crown laser hits) (VC) rendering the following equation:

$$Crown\ volume = 0.974 * VC - 0.129 \quad (3)$$

$R^2$ = 0.88 P-value<0.01

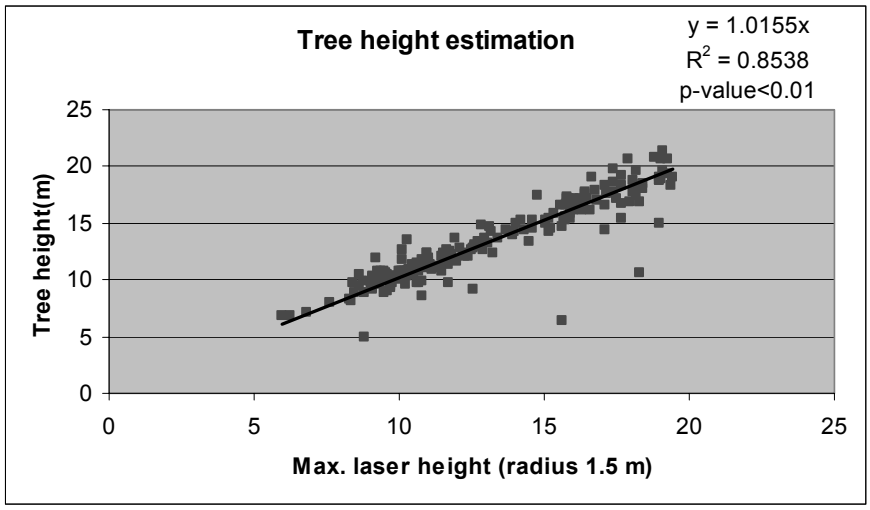


Figure 4. Tree height estimation from LIDAR.

This equation involves nine of the ten plots. The plot removed from the equation had the problem that there was only one low tree and the rest were much higher, causing overestimation of crown height, since estimated crown base height was too low. There is no bias and this relationship is 1:1.

LIDAR provides accurate estimation of crown bulk density. An allometric equation relating DBH or other forest parameter could be used in other to obtain a relationship between foliage biomass for a specific species and LIDAR data. Besides LIDAR can provide a direct estimation of crown volume although further research is needed to obtain automatic crown base height estimation in order to solve the problem of trees with very different size.

## 4. ACKNOWLEDGEMENTS

We wish to acknowledge the Autonomous Region of Madrid (Spain) for financing project number: 07M/0067/2001. We also thank all the people in the Department for helping in the field work.

## 5. REFERENCES

Brown, J.K. (1965). Estimating Crown Fuel Weights of red pine and jack pine. Research Paper LS-20, USDA, Forest Service.

Hyyppa, J., Hyyppa, H., Inkinen, M., Engdahl, M., Linko, S. and Zhu, Y.H. (2000), Accuracy comparison of various remote sensing data sources in the retrieval of forest stand attributes, *Forest Ecology and Management*. 128(1-2): 109-120.

Hyyppa, J., Kelle, O., Lehikoinen, M. and Inkinen, M. (2001), A segmentation-based method to retrieve stem volume estimates from 3-D tree height models produced by laser scanners, *IEEE Transactions on Geoscience and Remote Sensing*. 39(5): 969-975.

Lefsky, M.A., Cohen, W.B. and Spies, T.A. (2001), An evaluation of alternate remote sensing products for forest inventory, monitoring, and mapping of Douglas-fir forests in western Oregon, *Canadian Journal of Forest Research*. 31(1): 78-87.

Lopez-Serrano, F.R., Landete-Castillejos, T., Martínez-Millán, J. and Cerro-Barja, A. (2000), LAI estimation of natural pine forest using a non-standard sampling technique, *Agricultural and Forest Meteorology*. 101: 95-111.

Magnussen, S., Eggermont, P. and LaRiccia, V.N. (1999), Recovering tree heights from airborne laser scanner data, *Forest Science*. 45(3): 407-422.

Means, J.E., Acker, S.A., Harding, D.J., Blair, J.B., Lefsky, M.A., Cohen, W.B., Harmon, M.E. and McKee, W.A. (1999), Use of large-footprint scanning airborne lidar to estimate forest stand characteristics in the Western Cascades of Oregon, *Remote Sensing of Environment*. 67(3): 298-308.

Naesset, E. (1997), Determination of mean tree height of forest stands using airborne laser scanner data, *ISPRS Journal of Photogrammetry and Remote Sensing*. 52(2): 49-56.

Scott, J.H. (1999), NEXUS: A System for Assessing Crown Fire Hazard, *Fire Management Notes*. 59(2): 20-24.

von Hansen, W. and Vögtle, T. (1999), Extraktion der Geländeoberfläche aus flugzeuggetragenen Laserscanner-Aufnahmen, *Photogrammetrie, Fernerkundung, Geoinformation*. 4: 229-236.

# Deriving Geometric Properties of Single Trees from High Resolution Airborne Laser Scanning Data

Felix Morsdorf, Erich Meier, Benjamin Koetz, Klaus Itten
*Remote Sensing Laboratories (RSL), University of Zurich*
morsdorf@geo.unizh.ch

B. Allgöwer
*Geographic Information Systems, University of Zurich*

Keywords: forest fire fuel properties, lidar

## 1. INTRODUCTION

The potential of airborne laserscanning for mapping forest stands has been intensively evaluated in the past few years, and algorithms deriving structural forest parameters in a spatial context from laser data have been successfully implemented by a number of researchers [2], [3], [4].

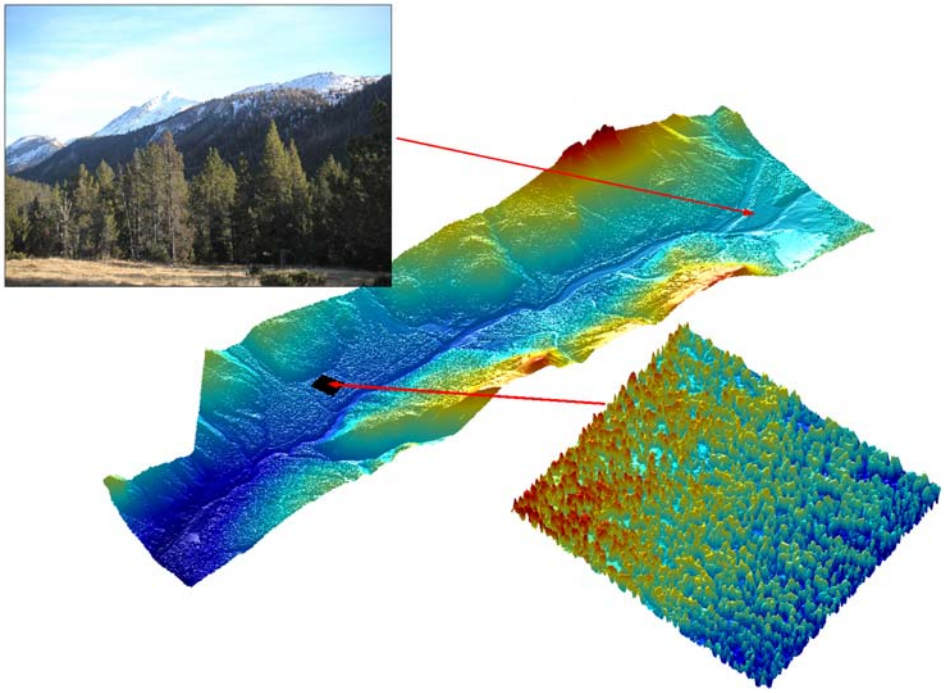

Figure 1. Shaded representation of DSM (Digital Surface Model) from the test site in the Swiss National Park. The area covered by the WSL field measurement database is enlarged.

Deriving parameters as tree height, crown volume and crown base height that are also critical for wildland fire modeling has been accomplished for two-dimensional cells or small stands [5]. However, with very high point density laser data one could pursue the approach of deriving these parameters on a singletree basis. This was carried out by using standard image processing tools on the

vegetation model (**D**igital **S**urface **M**odel, DSM) by [1], but so far not for LIDAR raw data. One of the main obstacles has been the validation of such an approach, mainly because of the cost in time and effort in gathering ground truth data and uncertainties in these measurements.

## 2. METHODS

We explore the potential of delineating single trees from laser scanner raw data (x,y,z-triples) and validate this approach with a dataset of more than 2000 georeferenced trees, including tree height and crown diameter, gathered on a long term forest monitoring site by the Swiss Federal Institute for Forest, Snow and Landscape Research (WSL). In addition to this, an extensive field campaign was carried out in summer 2002 measuring biophysical properties like LAI, fcover, and biomass for various stands[1]. The LIDAR system used is the FALCON II sensor by the german company Toposys. This system delivered more than 20 points per $m^2$ with a footprint size of about 20 cm in diameter. The sensor recorded both first and last echo from the ground, thus being able to resolve well vegetation top and ground surface in this boreal like vegetation type. The test site is located in the Swiss National Park and covers an area of roughly 14 $km^2$, with mainly mountain pine trees (Pinus Montana ssp. arborea). The accuracy of the laser scanner is evaluated trough 6 reference targets, being 3x3 m in size and horizontally plain, for validating both the horizontal and vertical deviations of the laser scanner using the raw data.

Table 1. Number of points on target, mean height difference, standard deviation of points on target and distance offsets for the 6 laser targets.

| Target Identifier | Number of Points | Mean Height Difference [cm] | σ Height [cm] | Δ x [cm] | Δ y [cm] |
|---|---|---|---|---|---|
| 1000 | 215 | 3 | 6.8 | 9 | 7 |
| 2000 | 266 | -2 | 5.9 | 24 | -11 |
| 3000 | 151 | -2 | 6.6 | 6 | 6 |
| 4000 | 381 | 1 | 5.6 | 15 | -3 |
| 5000 | 302 | -2 | 5.8 | 4 | 15 |
| 6000 | 276 | 2 | 5.2 | 25 | -18 |

The LIDAR data is segmented using a *k-means* clustering algorithm in all three coordinate dimensions with the *z*-axis being compressed in order to accommodate for the aspect ratio of pine trees. As starting cluster centroids, the local maxima derived from the DSM as in [1] are used. The resulting tree clusters are used to derive tree height, crown volume and eventually crown base height of the single tree.

*The measurements in the SNP have been carried out in the framework of the EC SPREAD project (01.0138/EVG1-CT-2001-00043), in work packages 1.1 and 1.2 respectively. This contribution focuses on the activities of the work package 1.1, while the ongoing research of work package 1.2 is presented in a separate contribution to this workshop.*

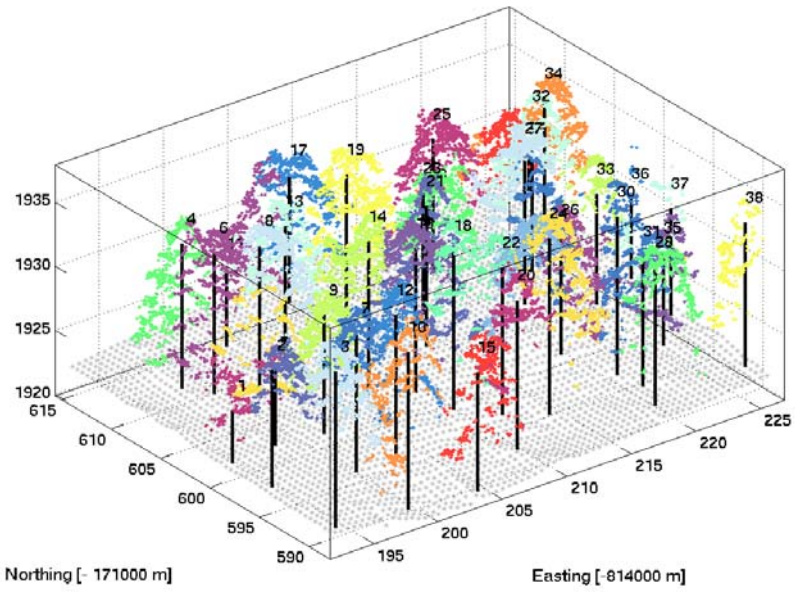


Figure 2. Single trees segmented by cluster analysis from the test site in the Swiss National Park. The horizontal axes describe the distance in the swiss coordinate system (CH1903+), the vertical denotes absolute height. Numbers on trees are tree identifiers assigned during clustering analysis.

## 3. RESULTS

The LIDAR data is successfully segmented into single trees using cluster analysis. Tree height derived from the tree clusters is well matched with the field data, if only dominant overstory trees are used in the matching process.

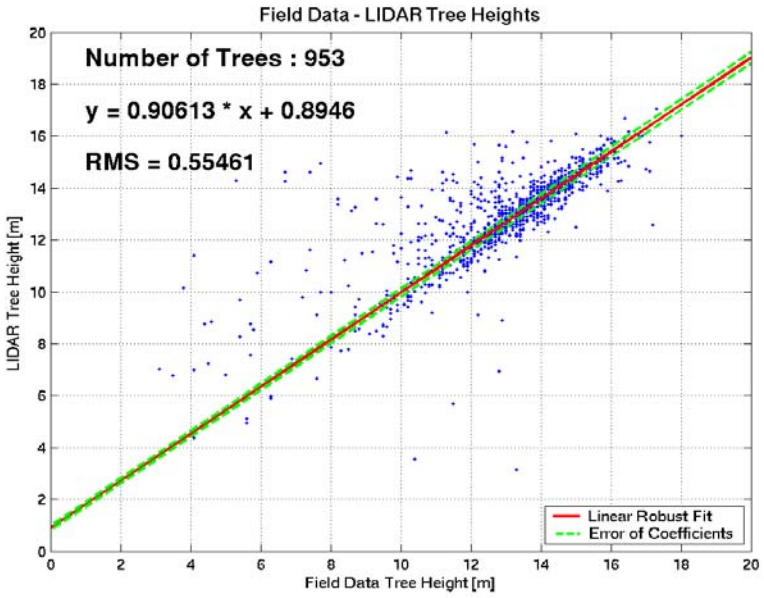


Figure 3. Robust regression of LIDAR derived tree heights versus field measured tree heights, for dominant overstory trees only.

Smaller trees very close (distance < 1 m) to the overstory trees can not yet be automatically detected. Computing the convex hull of each tree cluster directly yields the crown volume, with some uncertainties regarding the base of the crown, which might be overcome using a percentile base approach on the tree clusters as in [5].

## 4. REFERENCES


[1] Juha Hyyppä, O. Kelle, and M. Lehikoinen, and M. Inkinen. A segmentation-based method to retrieve stem volume estimates from 3-D tree height models produced by laser scanners. *IEEE Transactions on Geoscience and Remote Sensing*, 39:969-975, 2001

[2] Jason B. Drake, Ralph O. Dubayah, David B. Clark, Robert G. Knox, J. Bryan Blair, Michelle A. Hofton, Robin L. Chazdon, John F. Weishampel, and Stephen D. Prince. Estimation of tropical forest structural characteristics using large-footprint lidar. *Remote Sens. Environ.*, 79:305-319, 2002.

[3] Joseph E. Means, Steven A. Acker, Brandon J. Fitt, Michael Renslow, Lisa Emerson, and Chad Hendrix. Predicting Forest Stand Characteristics with Airborne Scanning Lidar. *Photogrammetric Engineering & Remote Sensing*, 66(11):1367-1371, 2000.

[4] M. A. Lefsky, W. B. Cohen, S. A. Acker, G. G. Parker, T. A. Spies, and D. Harding. Lidar Remote Sensing of the Canopy Structure and Biophysical Properties of Douglas-Fir Western Hemlock Forests. *Remote Sens. Environ.*, 70:339-361, 1999.

[5] David Riano, Erich Meier, Britta Allgöwer, Emilio Chuvieco. Generation of Vegetation Height, Vegetation Cover and Crown Bulk Density from Airborne Laser Scanning Data, *In: Proceedings of the 4th International Conference on Forest Fire Research and Wildland Fire Safety, D.X. Viegas (ed.), Luso, Portugal, November, 18 - 23, Millpress Science Publishers, Rotterdam, Netherlands*

# Session 3. Fire risk mapping methods

# Human fire causes: a challenge for modeling

V. Leone & R. Lovreglio
*University of Basilicata, Potenza, Italy*
leone@unibas.it

Keywords: arson, ash seeding, human fires, motivation, natural disaster, NCAVC, negligence, ritual fires, swidden, slash and burn, vandalism

ABSTRACT: Forest fires are neither a natural disaster nor a natural calamity or a fatality, but rather an anthropogenic phenomenon with an exclusive, direct dependence on social behavior, whether voluntary or involuntary. Despite the progress in knowledge about the physical facets of the phenomenon, its causes remain scarcely known or unknown. The outcome is often an over-emphasis on fire suppression, but inadequate attention to addressing the underlying causes of harmful fires. Filling this gap is crucial to mount significant prevention efforts.
Paper proposes a classification of motivations of voluntary fires, which could help in constructing a conceptual model of wildland fires.

## 1. INTRODUCTION

The current research literature in the social sciences offers an extensive body of findings about the human dimensions of wildland fires (Machlis *et al.*, 2002). Humans are considered responsible for about 90% of biomass burning, with only a small percentage of natural fires contributing to the total amount of vegetation burned. Since lightning regime is strongly related to geographical position and may be considered as stable, under current climatic conditions, the increase in the amount of fires around the world can only be explained by human factors. Surprisingly, wildfires are still considered among natural hazards, even by some authoritative sources (NASA, 2003); the UE too, in different Frame Programmes, includes fires among natural hazards.

Natural causes do not justify the scale, nor the clamorous evolution of the number of anthropic fires, defined as a "*social aggression to the forest*" (CFS, 1992). Sentences such as: "*wildland fires are inevitable natural events*" (Cleaves, 2001) are, therefore, somehow misleading and restrictive, focussing on the natural impacts, but avoiding to consider the human causality of most fires. In addition, they could induce a sort of resigned acceptance of the phenomenon, considered a cyclic, ineluctable event.

Forest fires are neither a natural disaster nor a natural calamity or a fatality, with the exception of those started by natural agents (maybe not even these fires, since they often spread in seminatural, cultural environments); rather, they are an anthropogenic phenomenon with an exclusive, direct dependence on social behaviour, whether voluntary or involuntary.

Regarding fires, today we have an excellent knowledge of what happens, when and where. Knowledge of fire, as a complex physic-chemical reaction, results excellent and allows good prediction of its behaviour, through the use of a wide set of fire behaviour /spread models produced since the 50-60's in the States. Remote sensing and satellite imagery can show the time, place and extent of selected active fires around the world, with special emphasis on their distributive pattern, on energy and gas release etc. But we do not yet know enough about who start wildfires and why. We still have, on the subject, mainly a list of credible, sometimes obvious motivations for starting fires,

without the capacity of filling the gap between the advanced knowledge of the physical facets of the phenomenon and the very reasons of its genesis.

Putting some emphasis on prevention and removal of causes, we recall Macmillan (1911, in Murphy, 1990): "… *the measures adopted to protect the forest from fire are now generally understood: they are removal by education or legislation adequately enforced of the causes of fires...*" (emphasis added).

About ninety years afterwards, FAO (1999) notes that "*It is next to impossible to design specific fire prevention campaigns if one cannot identify the causes of wildfires in a systematic way. If critical fire starting causes remain unknown, then it becomes extremely difficult to mount a significant prevention effort.*»

Similarly, it has been stated that "*Until our ability to determine the causes of forest fires improves, our efforts at prevention will essentially remain shots in the dark…*" (E.P, 2003).

## 2. FIRE CAUSES

Causes are more diverse than is often assumed, and fire initiation is neither as random, nor, in some cases, as meaningless as some analyses suggest. Understanding the reasons why fires start is crucial when determining what to do to prevent or reduce their incidence, avoiding the piecemeal approach to fire, concentrated mainly on fire suppression (Wilson, 1976), and hence mainly focused on fighting fires and developing the infrastructure to detect and facilitate access to fire.

In many countries forest and fire management Authorities are actually unable to cope effectively with increasing problems created by forest fires. The outcome is often an over-emphasis by governments on fire suppression, whereas inadequate attention is given to addressing the underlying causes of harmful fires (Jackson & Fisher, 2001)

Surely we perceive fires as a negative factor, menacing the forest and its several recognized values and functions of great importance for the human life, apart from and in addition to the classical functions of protection and production of material resources. All these new, global functions (such as carbon fixation, maintenance of the biological diversity, stabilization of soils and regulation of the hydrological cycle, recreation), justify the new approach toward fire: mainly a destructive process/force that needs to be managed.

Fires are today thought of as a misfortune, a tragedy inflicted by human malice, greed or carelessness (Grove & Rackham, 2001), as a "*environmental horror*" (Pyne, 2000) and summer by summer interpretation of ignition causes seems a major theme for newspapers and TV. A list of possible culprits is absolutely varicolored and imaginative, with bizarre interpretations and includes shepherds, arsonists, beekeepers, madmen, developers, speculators, foreign agents, smugglers distracting preventive officers, right-wing politicians taking revenge against the estates of rich Communists etc. (Grove & Rackham, op. cit.).

But while regarding fires as a destruction factor and an ecological crime, a man made disaster, we should remember that, in a rather recent past, people considered the forests like an obstacle for development, without any special attention for their ecological values and conservation. The effort to use and subdue the forest, rather than to conserve it, has been a constant theme at most times. Fire, on the contrary, was considered a positive tool of victory over hostile lands, a good and efficacious instrument for colonizing new lands.

It seems strange, but in the era of monstrous artificial memory, we are loosing the memory of our former way of life, when fire was embedded in human history. Two of the first ten European proverbs, in order of diffusion, make reference to fire (Paczolay, 1995). The long-established use of fire in agriculture, sylviculture and livestock-breeding is well documented, as well as being testified by ritual customs, such as the capillary diffusion of bonfires and ritual use of fire all over the Old Continent. In the past, the presence of vast areas of forest to be colonized, in a time of "*land hunger*", called for an almost complacent attitude in man's victory over a hostile, powerful nature. Destruction, with an efficient and easy-to-use tool (fire), was therefore engaged in, without excessive disquiet so as to increase the productive base of agricultural activity.

For centuries forest destruction was considered a neutral operation, until proved otherwise (Vecchio, 1974), since people only recognised the value of alternative uses for the space that the forest occupied: if they burned it, there would be more space for agriculture and farming. Even violent destruction of forests with fire were very frequent and well known in period of social and political turbulence (Armiero & Palmieri, 2002).

Burning is, therefore, a universal human cultural trait, and a number of motivations for starting fires, are ancient patterns that have remained the same throughout the ages. These include: facilitation of travel and improved visibility when hunting in forests; improvements of grazing for game and increases in yields of seeds in grasslands; setting vegetation on fire as an act of war (Stewart, 1953); hunting drives and attack/defense; increase yields in seeds; creating better pasture for livestock, clearing for agricultural fields (*slash and burn* agriculture) (Aschmann, 1977). Many native populations selectively used fire, in an "intermediate-scale disturbance regime that promoted a heterogeneous mosaic of different vegetation types", consciously managing their environment for long-term benefits (Timbrook, *et al.* 1982; Delcourt & Delcourt, 1997).

Pastoral fire probably helped the process by which wildlife was domesticated; the seasonal herding of livestock between two pastures (transhumance) in environments such as those of Iberia, the Balkans, South of Italy, Britain and Algeria has almost universally been accompanied by seasonal firing for the improvement of pasture. Fire and fallow, too, constituted an endless cycle. Part of the agricultural revolution that preceded Europe's industrial revolution involved the conversion of "wasteland" through a regimen of cutting and burning. Even in northern Europe, "*swidden*" persisted into recent times: in Germany to the late 1890s; in Belgium to 1908; in France to the mid-1920s; in Finland, burdened with war refugees, to the 1950s. As late as 1957, it was estimated that at least one-quarter of the earth was subjected to swidden agriculture, with perhaps one-seventh of that amount, or over three per cent of the earth's land area, burned annually (Pyne, 2000).

Regarding Italian forest, as late as the 1930s, in the forests of Calabria, in the South of Italy, burning the forests and "*ash seeding*" of barley, wheat and rye was a traditional, common practice of the Region, where arson fires now represent an enormous problem. Fire, in this context, was the traditional instrument for the management of ecosystems, an efficacious tool for colonizing new lands, when flattening trees with axe was an enormous effort, in times of dramatic alimentary scarcity.

## 3. MOTIVATIONS AND THEIR CLASSIFICATION

The change of fire from an instrument of agricultural management to an element of assault and alteration is, therefore, obvious and intuitive.

After the period of colonization for agricultural and settlement purposes, today we are witnessing a drop in fires of agricultural origin and their large-scale replacement with involuntary fires, testifying the slight familiarity and scarce respect towards nature.

At the same time the worrying, increasing trend in voluntary fires has become more marked. This is an undeniable reality, grown to enormous proportions, proved by the capture of confessed criminal incendiaries and by the finding of primitive (but not for this less efficient) timer devices, indicating the wish to carry through the destructive act, carefully choosing the place, time and method of ignition (Leone, 2000). But, which are the impulses that prompt people to destroy their environment?

The reply is normally a list of possible motivations, for instance (Jackson & Fisher, op.cit.):

- Perverse economic and social incentives that encourage the inappropriate use of fire.
- Greed and corruption.
- Land and resource conflicts.
- Weak or ineffective bureaucracies and governments.
- Economic necessity.
- Political motives.

Also more detailed list of less usual arson motivations, such as that given in Table 1, put into evidence that without a classification or analysis of the inner drives, the list remains merely descriptive.

Literature offers interesting exemples of classification. For instance, FAO (De Meo, 1986) identified:

- Causes external to the forestry sector;
- Causes internal to the forestry sector.

Among the former, there is voluntary, direct, conscious intervention, dictated by needs connected with agricultural and grazing practices; with hunting; with soil use; conflicting interests.

Involuntary intervention external to the forestry sector comprises: farming and agricultural activities without cautionary measures; recreational activities and the increased urban pressure in general. Among the causes internal to the forestry sector: increasing marginality of forest resources; a widespread disregard for forest preservation; the outbreak of fires connected with job creation.

The motivation classification formerly adopted in Spain by I.C.O.N.A and now widely adopted by D.G.C.N. (Vélez, 2000) is very similar, distinguishing:

- Fires from which the starter hopes to benefit;
- Fires from which the starter assumes he will not draw tangible benefit;
- Fires caused for political reasons.

Under the first group come motives ranging from destroying the forest cover in order to obtain land for grazing, to the use of fire for transforming rural terrain into building plots, to fire which generates jobs (in fire-fighting and rehabilitation activities).

In the second group we find resentment against acts carried out by public authorities, ill feelings between private citizens and groups, conflicting interests, opposition to hunting reserves, resentment against administrative sanctions, vandalism, or irrational acts. Mentioned in a separate category are pyromaniacs, individuals affected by a rare personality disorder, namely Impulse Control Disorders (Lejoyeux *et al*., 2002).

This paper discusses only about fires started deliberately, i.e. by someone intending to destroy an area of forest for whatever motive. Fires started by accidental causes or negligence, i.e. whose origins are connected directly or indirectly with a human activity, but the person concerned did not act with the intention of destroying an area of forest, are, therefore, neglected.

Negligent fires have some specific features and characteristics of repetition, concentration, distribution pattern, relationship with human seasonal activities (agricultural, recreation activities etc.). Many findings lead to the hypothesis that conditions in the forest environment could determine fire risk levels, since site attributes would also determine the human activities that could take place. Studies are, therefore, focusing on where fires were located in relation to roads, trails, towns, vegetation, rivers, topographic (elevation, slope, aspect) data, power lines, train ways, industries, forestry operation sites and many more geographic variables.

Much more difficult is the analysis of arson fires, generally considered as a symptom of problems linked to a complex series of socio-economic circumstances: the depopulation of vast areas, the abandonment of agriculture, the distribution of new settlements in rural settings, the diffusion of transportation infrastructures, the burgeoning of interests which often conflict with the conservation of natural resources etc. (Leone, 2000).

A very interesting taxonomy of arson motivations, able to identify the inner drives, the personal traits and characteristics exhibited by offenders, has been proposed by the National Center for the Analysis of Violent Crime (NCAVC), located at the FBI Academy in Quantico, Virginia. The NCAVC has determined that the identification of the offender's motive is a key element in crime analysis (Sapp *et al*., online). The NCAVC reviewed arson research literature, actual arson cases, and interviewed incarcerated arsonists across the nation, producing a motive classification which proves very effective in identifying offender characteristics:

- Vandalisme
- Excitement
- Revenge
- Crime concealment
- Profit
- Extremist

In Table 2 we synthesize the main elements of NCAVC classification, adapted with the purpose to give attributes to motivations, defined as the inner drive or impulse that is the cause, reason or incentive that induces or prompts a specific behavior .We have of course discarded elements which are site, culture and country specific.

## 4. CONCLUSION

NCAVC classification, with minor modifications, seems applicable to forest fires in different countries and covers a wide specter of situations, to which it gives a plausible interpretation. Understanding of the typology of arsonists, particularly typological classification based on motivations, may enhance investigative efforts and provide a focus for intervention efforts.

In conclusion: causes of fires arise undoubtedly from many complex social, environmental, political, organizational and economic forces. But the importance of social, cultural variables is likely to vary by country or region and over time. Further research is, therefore, needed to support understanding the multiple independent and intervening factors, in order to construct a conceptual model of wildland fires, with the goal of modeling the human dimension of the phenomenon.

## 5. REFERENCES


Armiero, M. & Palmieri, W. 2002. Boschi e rivoluzioni nel Mezzogiorno. La gestione, gli usi e le strategie di tutela nelle congiunture di crisi di regime (1799-1860). In: Lazzarini, A. (ed.) *Diboscamento montano e politiche territoriali*. Alpi e Appennini dal Settecento al Duemila. Franco Angeli Storia, Milano, pp. 598

Aschmann, H. 1977. Aboriginal Use of Fire. In: Proceedings of the Symposium on the Environmental Consequences of Fire and Fuel Management in Mediterranean Ecosystems, General Technical Report WO-3, U.S. Department of Agriculture, Forest Service, Washington D.C.

CFS, 1992 Aspects sociaux, economiques et culturels des incendies de forêts en Italie. Proceed. Seminar on Forest Fire Prevention, Land Use and People. ECE/FAO/OIT, Athens, Apr. 1987.

Cleaves, D. 2001. Fires in The Wildland Urban Interface: Dilemmas of Duality and the Role of National Science Leadership. Natural Disasters Roundtable, January 26, 2001Washington
http://www7.nationalacademies.org/ndr/cleaves_abstract.pdf

Delcourt, H.R. & Delcourt, P.A. 1997. Pre-Columbian Native American Use of Fire on Southern Appalachian Landscapes. *Conservation Biology* 11: 1010-1014

De Meo, G. 1986 Riflessi economici della distruzione boschiva. *Cellulosa e Carta*, 3: 6-7.

E.P (Environment Policy) 2003 Putting out the Fire: Saving Greece's Forests
http://www.greece.gr/ENVIRONMENT/EnvironmentalPolicy/AttackingTheRoot.stm

FAO 1999 FAO meeting on public policies affecting forest fires. FAO Forestry Paper 138, Rome, UN Food and Agriculture Organization.

Groves, A.T. & Rackham, O. 2001 *The Nature of Mediterranean Europe-An Ecological History*. Yale University Press, New Haven and London, 217-240

Jackson, J.W. & Fisher, R.J. 2001. Keynote address, Communities in Flames Conference, Balikpapan, Indonesia, http://www.iucn.org/info_and_news/press/cifjackson.pdf.

Lejoyeux, M., Arbaretaz, M., McLoughlin, M. & Ades, J. 2002 Impulse control disorders and depression. *Journal of Nervous and Mental Disease*. 190 (5): 310-314

Leone, V. 2000 Sociological aspects in the phenomenology of forest fires. In: Ciancio, O.(ed.) *The forest and man.* Acc. Ital. Sc. For., 305-324

Machlis, G.E., Kapolan, A.B., Tuler S.P., Bagby, K.A. & McKendry, J.E. 2002. *Burning questions. A Social Science Research Plan for Federal Wildland Fire Management*. Idaho Forest, Wildlife and Range Experiment Station, College of Natural Resources, University of Idaho, pp.253

Murphy, P.J. 1990 The art and science of fire management. In: Alexander M.E. & Bisgrove G.F. The art and Science of Fire Management, INF. REP. NOR-X-309 Forestry Canada

NASA, 2003 Natural Hazards http://earthobservatory.nasa.gov/NaturalHazards/

Paczolay, G. 1995. European Proverbs http://www.vein.hu/library/ve/proverbs/european.htm

Pyne, S. 2000 The Corner House Briefing 18 - Fire Planet: The Politics and Culture of Combustion http://cornerhouse.icaap.org/briefings/18.html

Sapp, A.D., Huff, T.G., Gary, G.P. & Icove, D.J. Motive-based Offender Analysis of Serial Arsonist http://www.interfire.org/features/serialarsonists/Motive_based/cover.htm

Stewart, O.C. 1956 Fire as the First Great Force Employed by Man. In: *Man's Role in the Changing Face of the Earth*, edited by W. L. Thomas, pp. 115-133. University of Chicago Press, Chicago.

Timbrook, J., Johnson, J.R. & Earle, D. E. 1982. Vegetation Burning by the Chumash.. *Anthropology* 4: 163-186.

Vecchio B., 1974 *Il bosco negli scrittori italiani del Settecento e dell'età napoleonica*. Piccola Biblioteca Einaudi, PBE 235, Torino, pp. 276

Vélez, R. 2000. *La defensa contra incendios forestales. Fundamentos y experiencias*. McGraw-Hill/Interamericana de España S.A.U., Madrid.

Wilson, C.C. 1976 Detection and control of forest fires for the protection of the human environment. Project 0206-74-003 with The Food and Agriculture of the United Nations as co-operate agency.

Table 1. An example of list of possible arson motivations

| Motivation | Geographic context | Author |
|---|---|---|
| Clearing forest for oil palm cultivation | Indonesia | Barber & Schweithelm, 2000 |
| Excitement seeing the air tankers and trucks | Canada | Jones, online |
| Fire as a weapon | Indonesia | Colfer, 1999, |
| Fire used to illegally degrade forest so that it becomes eligible for conversion. | Indonesia | Barber & Schweithelm, 2000 |
| Fires connected with job research in fire-watching, fire-fighting and reforestation activity (*fire industry*), | Italy,Spain, USA | Leone & Vita, 1982; Vélez , 2000; Bertrand & Baird, 1975; Doolittle & Lightsey, 1979 |
| Government support for large-scale land clearing for industrial plantations, | Indonesia | Moore, online |
| Hired torch | USA | NCAVC, online |
| Hunting with fire | Kalimantan | IFFM Project, online |
| Improvements of grazing for game | | Stewart, 1953 |
| Increases in yields of seeds in grasslands | | Stewart, 1953 |
| Intentional fires related to land claims | Indonesia | Moore, online |
| Land speculation | Indonesia | IFFM Project, online |
| Land use conflicts | Indonesia | IFFM Project, online |
| Lighting a fire to foster a cause | Canada | Jones, online |
| No reason other than “hey let’s do it”; | Canada | Jones, online |
| Nomadic cultivation | Indonesia | Barber & Schweithelm,2000 |
| Preparation of garden plots | Indonesia | Barber & Schweithelm, 2000 |
| Profit from transporting water to remote stretches of forest during a fire | N. Carolina | online |
| Protest against imposed land-use changes | Portugal | W.R.M.,1998 |
| Protest against protected areas | Italy | Leone et al., 2003 |
| Resentment against Authorities | Spain | Velez, 2000 |
| Setting brush fires to enhance hunting game | USA | Sapp et al. 1993, 1994. |
| Setting fire to forests to rent equipment | USA | Huff, 1994 |
| Unemployed labourers seeking employment as loggers to salvage burned timber. | USA | NCAVC, online |
| Unsettled land tenure system | Indonesia | Lachowski et al, online |
| Use of fire to clean agricultural plots | Indonesia | Barber & Schweithelm, 2000 |
| Use of fire to improve hunting | Indonesia | Barber & Schweithelm, 2000 |
| Vandalism | Canada | Jones, online |

Table 2. Taxonomy of arson fires (adapted and modified from NCAVC)

| Motivation | Definition | Type of target and selection | Main interest | Distance from home | Damage | Scenario | Return to scene |
|---|---|---|---|---|---|---|---|
| VANDALISM | Malicious or mischievous fire setting that results in damage to property | School property<br>Educational facilities.<br>Abandoned structures,<br>Vegetation | Setting fire, not watching | 0,5-1 mile | Nuisance fires | | No return. |
| EXCITEMENT | Seeking of thrill, attention, recognition, sexual gratification (rare), relieve of boredom.<br>Fires are set to gain attention and to meet the needs of being important. (author is sometimes the "hero " type) | Nuisance fires<br>Occupied apartments<br>Vegetation<br>Fire planned and premeditated | Fires that result in major conflagrations; bigger and bigger fires over time, more severe and more dangerous to fire-fighters and residents. | 1-2 miles | Major fires to provide thrills | Familiar | Within 24 hours to briefly observe the damage. |
| REVENGE | Fires set in retaliation for real or perceived injustice or wrong | Buildings (other than residences), vegetation and vehicles.<br>Fire intentional, planned, pre-meditated and targeted. | | Within walking distance of his home | | Familiar | No return. |
| a. personal revenge | Use of fire to retaliate for a one-to-one or personal grievance, argument, fight, personal affront or any of infinite arrays of events perceived by the offender to warrant retaliation. | Victim's vehicle, home or personal possession<br>Single fires. | | 1-2 miles of home or workplace. Fire usually set after work or on days off and weekends. | | Familiar | After 2 days. |
| b. societal retaliation | Use of fire in revenge against the society that the author perceives has wronged him | Random but multiple fires<br>Structures other than residences and businesses, vehicles and vegetation.<br>Fires premeditated and intentional | | 1-2 miles of home or workplace | | Familiar | Within 24 hours. |
| c. institutional | Fire against institutions as | Building housing. | | Institutional | | | Within 24 |

| | | | | | | | |
|---|---|---|---|---|---|---|---|
| retaliation | government, education, military service(s), medicine, religion, or any other entity reflecting and representing the establishment. Use of fire to settle grievances with the institution and to intimidate those associated with the institution. | More than one fire at a location.<br>Number of fires set and reset in the same building or facility.<br>Fires may be set in varied locations, including work spaces. | | facilities within 1-2 miles of their home or workplace. | | | hours of the fire. |
| d. group retaliation | Fire as expression of anger towards the group or its members rather than anger at a specific individual within the group. | Group headquarters building, church, meeting place, or symbolic targets such as emblems or logos.<br>Fires are set in the area where the group lives or works. | | | | | |
| CRIME CONCEALMENT | Fire set to hide or conceal the primary crime activity. | Residences, businesses, vehicles and other structures to conceal thefts or to destroy evidence. | | 1-2 up to 10 miles from home. | | | Within 1-2 days return to view the damage. |
| PROFIT | Profit from fire setting, either directly for monetary gain or from a goal other than money.<br>"torches for hire". | Pre-selected. | | | | | Within 1-2 days after the fire. |
| EXTREMIST | Fire set to further social, political or religious causes. | Targets reflect the focus. | | | | | |

Table 3. Taxonomy of arson fires (second part)

| Motivation | Ignition material | Use of D.A.I.D.s | Use of combustion accelerants | Material left on the scene | Behaviour after fire |
|---|---|---|---|---|---|
| VANDALISM | Matches, Lighter. | | | | |
| EXCITEMENT | Matches, Lighter. | Yes (to delay ignition of the fire until the author gets in position to respond to the fire). | Available materials | Matches. | Author remains at the scene or goes to another location to observe the fire and fire suppression efforts.<br>He is sometimes described as the "hero" type, often remaining at the scene to warn others, to report the fire or to assist in fire fighting efforts.<br>Once the fire is over, the excitement-motivated arsonist loses interest. After returning to the scene, he does not follow the case in the media nor does he take souvenirs |
| REVENGE RETALIATION | Matches. | | Available materials | Matches. | The author leaves as soon as the fire is set. He usually does not return to the scene. |
| personal retaliation | Matches. | Yes | Available materials or gasoline | Gas cans and matches. | After setting the fire, the author leaves the scene and only returns after 1-2 days. |
| societal retaliation | Matches, Lighter. | | Available materials | | After setting the fire, author leaves the scene and does not attempt to watch the fire.<br>He will typically return to the scene within 24 hours to view the damages. |
| institutional retaliation | | | | | After the fire, the author remains at the scene, or goes to another location to observe the fire, sometimes no return to the scene at anytime or return to the scene within 24 hours of the fire. |
| group retaliation | Matches. | | Available materials | | After setting the fires, the author remains at the scene and then returns later to view the damages. |
| CRIME CONCEALMENT | Matches, Lighter. | | Available materials | Authors avoid leaving evidence | No attempt to follow the case in the media, to contact the media, police or the victim. |
| PROFIT | Gasoline, Matches. | Yes | | . | Author does not remain at the scene although he often goes to another location to watch the fire. |
| EXTREMIST | Incendiary Devices, Molotof cocktails. | | | Unexploded incendiary or explosive devices. | |

# The use of the Nearest Neighbour Method to predict forest fires

A. Felber
*Swiss Federal Institute for Forest, Snow and Landscape Research, 7260 Davos Dorf, Switzerland*
felber@slf.ch

P. Bartelt
*Swiss Federal Institute for Forest, Snow and Landscape Research, 7260 Davos Dorf, Switzerland*
bartelt@slf.ch

Keywords: forest fire risk, nearest neighbour method

ABSTRACT: Based on a statistical approach, the nearest neighbour method is used to predict the occurrence of natural hazards like forest fires or avalanches. The following extended abstract discusses the application of the nearest neighbour method to asses forest fire danger of the Swiss Southern Alps. Beside a short introduction explaining the method the different output possibilities are shown.

## 1. INTRODUCTION

The increase in the number of forest fires in southern Switzerland since the 1960s has made it necessary to improve forest fire management methods. The development of fire danger prediction methods is considered to be one of the most important elements of an effective forest fire management strategy (Conedera et al. 1997).

Nearest neighbour models attempt to compare similar situations in the past with current data and assume that similar events are likely to occur in similar conditions. It is used in forest fire forecasting at a meso and local scale where it assumed that weather factors and possibly fuel factors can be extrapolated successfully over the area of interest and are representative of forest fire events. Nearest neighbour models generally output a list of similar days in the past along with associated events. Beside this list information the user also gets back a graphical description of the events. Past fires are showed on a geo-referenced map which allows the forecaster to visualise relationships between neighbours in terms of clustering in meteorological/fuel variables and the identification of spatial clusters of forest fire occurrence as a function of location, altitude, exposition, slope angle, forest type, for example.

The following extended abstract presents some aspects of the development of a nearest neighbour model that is used to forecast the forest fire hazard in southern Switzerland. The emphasis is planned on the integration of meteorological and socio-economic data for fire danger modelling and several aspects of forest fire mapping methods.

## 2. METHODOLOGY

The study area covers the region of Ticino (4000km$^2$ ~ 10% of Switzerland). The typical vegetation in this region consists of chestnut forests on acid soils, deciduous mixed broad-leafed forests on limestone and beech forests at altitudes between 800 and 1300 m a.s.l. (Conedera et al. 1996). Average annual temperatures are closely dependent on the altitude, ranging from less than

5°C to 13°C. The annual rainfall amount also shows large differences – partly exceeding more than 2000mm. The climate is characterized by dry and sunny winters with periods of north-foehn (wind) but occasionally strong snowfalls, by wet springs and autumns and by sunny summers with heavy periods of rain (thunderstorms).

Most forest fires (surface fires) break out during the dry winter period (December – April) and less in the summer months. In the past 35 years an average around 65 forest fires occurred burning about 800ha of forests and pasture land annually. 90% of all fires are caused directly (15% - arson fires) or indirectly (e.g. train) by humans.

Because of the importance of meteorological factors in forest fire activity, a large number of fire danger evaluation methods, based on current meteorological properties, have been developed. Because the lack of a general theory to explain the complex interactions between the various factor involved, most methods are based on empirical approaches (Viegas et al. 1999). Another approach which has been shown to be successful in avalanche forecasts is the use of a nearest neighbour model as originally developed by Buser (1983). Because of a more or less analogous problem – many influence variables, not knowing the exact process of ignition, interdependencies between the main variables, etc. - we adapted the model to use it for the prediction of forest fires in southern Switzerland.

Nearest neighbour models work on the simple principle of finding the most similar days in the past to the forecast conditions and allowing the forecaster to compare the resulting events. Either some predetermined rule is then used to determine the likelihood of forest fire occurrence, or the forecaster may simply use the model as an *aide-memoire* (Purves et al. 2002). Nearest neighbour models are attractive since they are intuitive in their operation and their data requirements are relatively modest, in general being homogenous fuel, weather and forest fire data over a period of some years (Purves et al. 2002).

As already mentioned an advantage of the nearest neighbour model is the fact that variables considering human behaviour which can play an important role in forest fire outbreaks can also be taken into account (Felber and Bartelt 2002). By the analysis of past fires in southern Switzerland one can see, that e.g. the distance between a camping site, fire place or railway track and the outbreak point of the fire is significant. Another example that represents the influence of human beings on forest fires can be seen by the analysis of the time and date of fire outbreaks. Most fires start in the early afternoon and there exists a slight preference for weekends (Koutsias et al. 2002; Conedera et al. 1996). By the analysis and interpretation of the output made by the nearest neighbour model, the user of the program can take some of these facts into consideration (Felber and Bartelt 2002).

## 3. RESULTS

The nearest neighbour model was used operationally in Switzerland for the first time during the early forest fire season 2003.

The output of the model can be interpreted in different ways, with the three most common descriptions being:

- Binary: Some rule is used to interpret the events on the basis of a threshold value. If more than a threshold number of events have occurred then the event is forecast.
- Probabilistic: The number of events in the total number of neighbours is transformed into a probability, generally in a linear transformation.
- Descriptive: The results are interpreted by the forecaster who utilises them as an *aide-memoire* to identify similar conditions in the past.

Beside a table output of your nearest neighbours including the meteorological and other relevant information (e.g. type of fire, duration, area, etc.), Figure 1 shows the ignition points of the forecasted neighbours on a geo-referenced map. Further on one can use the spatial information about the forecasted fires by simple queries in Geographic Information Systems (GIS) to analysis more specific questions like e.g. spatial patterns or the influence of socio- economic changes. This advanced GIS tool which is separated from the nearest neighbour model has the ability to manage effectively spatial and temporal information in widespread applications (Kalabokidis et al. 2002, Chou 1992, Chuvieco & Congalton 1989, Salas & Chuvieco 1994, Salas et al. 1994).

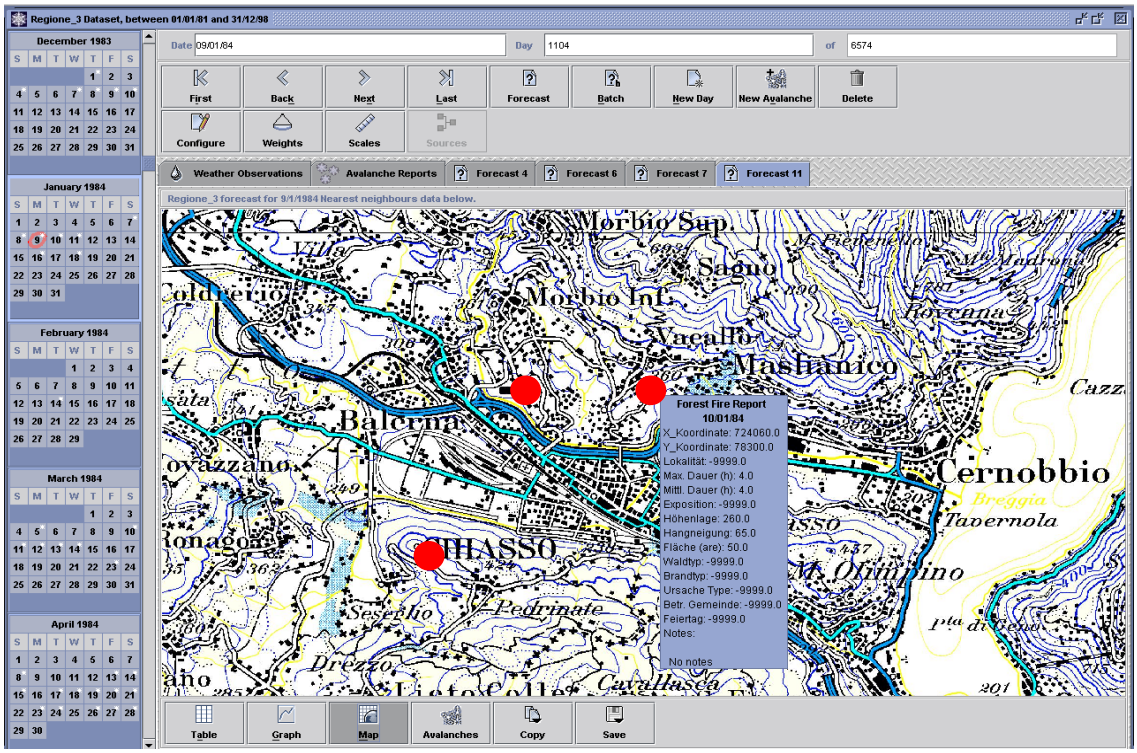


## 4. REFERENCES


Buser, O. 1983. Avalanche forecast with the method of Nearest Neighbours: an interactive approach. Cold Regions Science Technology. (No. 8): 155-163.

Chou, Y.H. 1992. Management on wildfires with a Geographical Information System. International Journal of Geographic Information Systems. Vol. 6: 123-140.

Chuvieco, E. & Congalton, R.G. 1989. Application of Remote Sensing and Geographic Information System to Forest Fire Hazard Mapping. Remote Sensing of Environment. Vol. 29: 147-159.

Conedera, M.; Marxer, P.; Hofmann, C.; Tinner, W. & Amman, B. 1996. Forest Fire Research in Switzerland: Fire Ecology and History Research in the Southern Part of Switzerland. International Forest News. Vol. 15: 13-20.

Conedera, M.; Mandallaz, D.; Bolognesi, R. & Ambrosetti, P. 1997. Forest Fire Research in Switzerland: Fire Danger Prediction in the Southern Part of Switzerland . International Forest News. Vol. 16: 2-6.

Felber, A.; Bartelt, P. 2002. Definition of Forest Fire Hazard Variables of the Nearest Neighbour Forecasting Method. In: Proceedings of the 4th International Conference on Forest Fire Research & Wildland Fire Safety, edited by D.X. Viegas. Luso, Portugal.


[1] Cornice: Nearest Neighbour Program by Ross Purves, University of Zurich.

Kalabokidis, K; Konstantinidis, P. & Vasilakos, C. 2002. GIS analysis of physical and human impact on wildfire pattern. In: Proceedings of the 4th International Conference on Forest Fire Research & Wildland Fire Safety, edited by D.X. Viegas. Luso, Portugal.

Koutsias, N.; Allgöwer, B. & Conedera, M. 2002. What is common in wildland fire occurrence in Greece and Switzerland – Statistics to study fire occurrence pattern. In: Proceedings of the 4th International Conference on Forest Fire Research & Wildland Fire Safety, edited by D.X. Viegas. Luso, Portugal.

Salas, F.J. & Chuvieco, E. 1994. Geographic Information System for wildland fire risk mapping. Wildfire. Vol. 3(2): 7-13.

Salas, F.J.; Viegas, M.T.; Kyun, I.A.; Chuvieco, E. &Viegas D.X. 1994. A local risk map for the Council of Poiares central Portugal: Comparison of GIS and field work methods. 2nd International Conference on Forest Fire Research. Coimbra, Portugal. pp. 691-702.

Viegas, X.; Bovio, G.; Ferreira, A.; Nosenzo, A. & Sol, B. 1999. Comparative Study of Various Methods of Fire Danger Evaluation in Southern Europe. International Journal of Wildland Fire Vol. 9(4): 235-246.

# Model for Forest Fire Risk Estimation in Estado Miranda (Venezuela)

L.G. García-Montero, C. Pascual, D. Bravo and J. Urbano
*Madrilenian Bureau for Agricultural and Food Research (I.M.I.A)*
Cristina.pascual@imia.madrid.org

J. García-Cañete
*Ministery of Education of Madrid's Region.*

Keywords: forest fire risk, tropical forest

ABSTRACT: Based on the Council for Environment of Madrid Region model, forest fire risk in Barlovento (Estado Miranda, Venezuela) was assessed. The following extended abstract explains how the model was adapted to tropical environment, where available information is limited. Besides environmental impact of forest fires was analysed.

## 1. INTRODUCTION

In December 1999, rain broke Guapo´s dam and Barlovento Region (Venezuela, Estado Miranda) was flooded. As consequence, Madrid Government, the Madrilenian Bureau for Agricultural and Food Research (I.M.I.A.) and Estado Miranda agreed to develop a preliminary land planning project for that area.

In land planning process, "real environmental capacity" must consider "potential environmental capacity" and "risk evaluation" (Ramos, 1979). Long-term forest fire risk indices include variables that are fairly static. They are used to determine areas with high risk of fire due to their intrinsic conditions (San Miguel-Ayanz, 2002).

The objective of this study was to assess the risk of forest fires in Barlovento, where available cartography and territorial information is limited. The developed model was based on Council for Environment of Madrid´s Region model (J.M. Nicolás Zabala, 2002; pers. com.). Also environmental impact of forest fires in Barlovento was analysed.

## 2. METHODOLOGY

In Barlovento Region, a corridor of 55 km x 37 km was defined inside the flooded area. Several maps (i.e. DTM, slope and aspect) were obtained. Besides, a land use map was carried out by means of remote sensing. Supervised classification of digital orthophoto Cartocentro (2,5m pixel) was performed in order to classify forest, shrubs, farming/grazing lands and burned areas. Rural roads, villages, quarries, etc. were also added by photointerpretation from Cartocentro (García-Montero *et al.*, 2003). A forest fuel map was also prepared. Different vegetation types and uses were assigned to different BEHAVE type models, taking into account field work, fire fighter's advice and vegetation and land used maps. Final fuel types were: high tropical forest, low tropical forest, high deciduous forest, evergreen bushes, natural deciduous bushes and grazing land (Vegetation map of Venezuela, E:1:100000).

The model for forest fires risk estimation has the same steps as Council for Environment of Madrid Region model (J.M. Nicolás Zabala, 2002; pers. com.) (fig 1), but model variables were adapted to Barlovento environmental parameters.

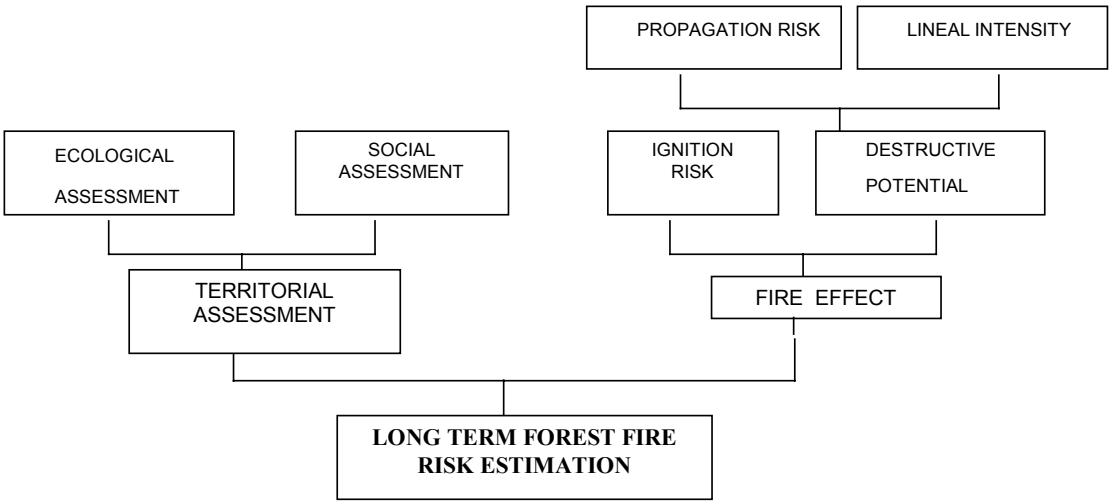


Figure 1. Phases and components of Council for Environment of Madrid Region model. Model variables were adapted to Barlovento environmental parameters.

Different weights were assigned to each model parameter according their potential contribution to long term fire risk. Spatial analysis with GIS was applied in order to obtain each component, which was finally reclassified into 4 risk levels: Low (L), Moderate (M), High (H) and Very High (VH).

Table 1. Components integration was performed by matrix combination

| | COMPONENT B | | | |
|---|---|---|---|---|
| COMPONENT A | L | M | H | VH |
| L | L | L | M | H |
| M | L | M | H | H |
| H | M | H | VH | VH |
| VH | H | H | VH | VH |

In order to check the model, the burned land map obtained by means of remote sensing was compared with the forest fire risk model.

Tables adapted from Council for Environment of Madrid Region model

## PROPAGATION RISK

**PR = 3F + 4S + 3As – A – Fl**

| F = Forest fuel | weight |
|---|---|
| urban areas and reservoirs | - |
| high tropical forest | 2 |
| low tropical forest | 4 |
| high deciduous forest | 5 |
| evergreen bushes | 8 |
| natural deciduos bushes | 10 |
| grazing lands | 20 |
| dumps | 9 |
| | |
| **S = Slope (%)** | |
| 0 a 6 | 4 |
| 6 a 12 | 6 |
| 12 a 25 | 8 |
| 25 a 35 | 10 |
| | |
| **As = Aspect** | |
| Sunny place | 5 |
| Shady (NW, N, NE, E) | 1 |
| | |
| **A = Altitude** | |
| 0 - 500 (26 - 25 ºC) | 0 |
| 500 - 1000 (24 ºC) | 10 |

## LINEAL INTENSITIY

LI = 12,4 x W x R

W = forest fuel density (Tm/ha)

R = propagation speed (m/min)

| F = Forest fuel | W | R |
|---|---|---|
| urban areas and reservoirs | - | - |
| high tropical forest | 1 | 9 |
| low tropical forest | 2 | 15 |
| high deciduous forest | 2 | 15 |
| evergreen bushes | 5 | 20 |
| natural deciduos bushes | 10 | 25 |
| grazing lands | 1 | 7 |
| dumps | | |

## IGINITION RISK

IR = 4 H + 3 F+ 2 As - A

| H = Human risk | Weight |
|---|---|
| **100 m buffer from roads-** | |
| highway | 2 |
| Secondary road | 3 |
| Forest roads | 10 |
| Dumps | 9 |
| **F = Forest fuel** | Idem |
| **As = Aspect** | Idem |
| **A = Altitude** | Idem |

## ECOLOGICAL ASSESMENT

| | weight |
|---|---|
| **Natural Areas, Natural Parks** | 3 |
| **Mountain areas preserving from floods** | |
| Level 1 (public) | 2 |
| Level 2 (private) | 1 |
| **Farming-forest exploitation areas** | 1 |

## SOCIO-ECONOMIC ASSESMENT

| | weight |
|---|---|
| **1000 m buffer from urban areas** | |
| **1.5 km buffer from reservoirs** | 3 |
| **100m buffer from (airport, petrol station and roads)** | |

On the other hand, as part of the land planning process, the natural quality of study area was evaluated considering habitat quality, landscape assessment and vegetation quality. Vegetation quality was obtained as a combination of three variables: singularity, fragmentation and natural value. Guatopo National Park and different protected areas were also considered in the natural quality assessment (Ramos, 1979; Aguiló *et al*., 2000).

## 3. RESULTS

The distribution area of risk categories and the percent of the sensed burned land in each risk category were obtained (fig1).

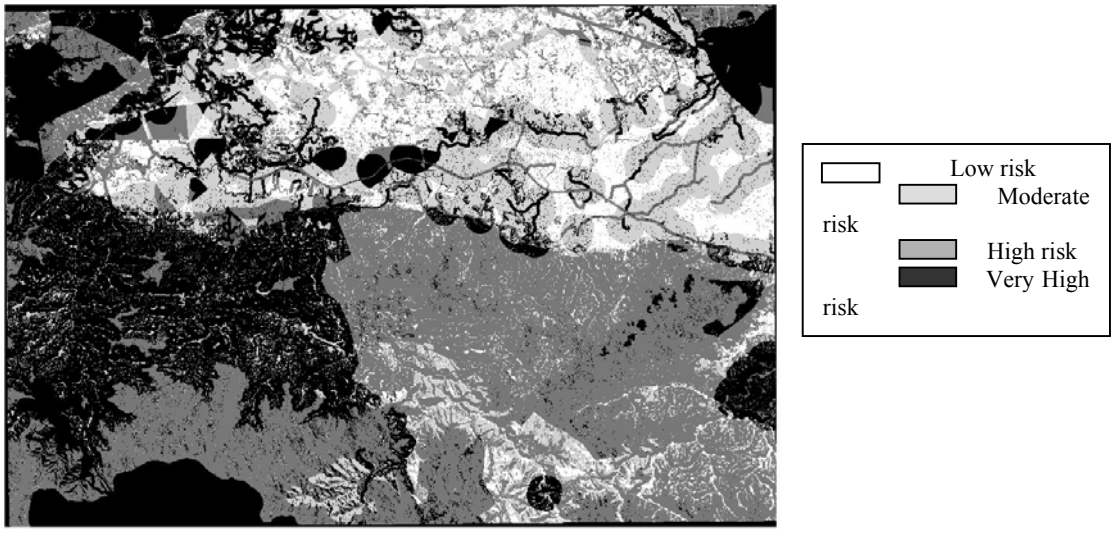


Figure 2. Forest fire risk estimation.

Table 2. Area distribution for each risk category in study area and percent of burned land sensed and their distribution in each risk class.

| Risk Category | Percent of area | Percent of burned land (<0.5 ha) | Percent of burned land (>0.5 ha) |
|---|---|---|---|
| Low | 12.4 % | 2 % | 0 % |
| Moderate | 18.3 % | 5 % | 2 % |
| High | 39.0 % | 27 % | 10 % |
| Very high | 30.3 % | 67 % | 87 % |

In Estado Miranda, farmers are used to burn forest areas in order to get farming places (shifting cultivation). This land management has caused vast extensions of burned land, bushes and grazing land that represent the 11% of the study area.

Table 3: Area distribution of land uses obtained by remote sensing (1st and 2nd columns). Impact assessment of the forest fires in natural quality classes of study area: surface of burned land (3rd and 4th columns)

| Land uses | Percent of relative area | | Natural quality classes | Percent of area burned areas |
|---|---|---|---|---|
| Forest | 89 % | | without protection areas | 12% |
| Farming/grazing pasture | 3 % | | low protection areas | 29% |
| Burned land | 0.30 % | | medium protection areas. | 15% |
| Bushes | 7 % | | high protection areas | 10% |
| | | | areas under legal protection | 33% |
| Total study area | 100 % | | Total surface of burned areas | 100% |

## 4. DISCUSSION AND CONCLUSSIONS

The final model was checked with burned land map achieved by remote sensing. 87% of burned land whose area was bigger than 0.5 ha, were in zones of *very high* fire risk. 94% of burned land whose area was smaller than 0.5 ha were in *high* and *very high* risk zones (Table1). Previous figures were considered to have validated the model, and the fire risk model was incorporated into the land planning process.

The 43% of sensed burned land were in *high* and *very high quality* areas (areas under legal protection). This might suggest a low impact of forest fires in this tropical ecosystem, but taking into account that natural vegetation regenerates itself very quickly in tropical forest, this 43% shows only forest fires effect for a short period of time.

Fires can be monitored and analysed over large areas in a timely and cost-effective manner by using satellite sensor imagery in combination with spatial analysis as provided by (GIS) (Sunar & Ozkan, 2001). Remote sensing and GIS have shown to be particular useful tools to assess forest fire risk in zones, as Barlovento region, where available cartography and territorial information is limited.

## 5. REFERENCES


Aguiló et al., 2000. Guía para la elaboración de estudios del medio físico. Ministerio Medio Ambiente. Madrid.

García-Montero, L.G., Bravo, D., Pascual, C., García-Cañete, J.; García, A.; Urbano, J., 2003. Análisis del medio con teledetección y SIG y participación social: primera fase de una planificación territorial en el Estado Miranda (Venezuela). Revista Forestal Española, 32:22-29

Ramos, A., 1979. Planificación física y Ecología. Modelos y métodos. E.M.E.S.A. Madrid.

Sunar, F. & Ozkan, C., 2001. Forest fire analysis with remote sensing data. International-Journal of Remote Sensing. Vol 22: 2265-2277.

San-Miguel-Ayanz, J., 2002. Methodologies for the evaluation of forest fire risk: from long-term (static) to dynamic indices, in Forest Fires: Ecology and Control, Edited by Anfodillo T.and Carraro, V. Univesity degli Studi di Padova.

# Mapping forest fire prone areas in Lebanon

T. Masri, M. Khawlie, G. Faour & M. Awad.
*National Council for Scientific Research/National Center for Remote Sensing. Beirut, Lebanon*
tmasri@cnrs.edu.lb

Keywords: Lebanon, forest fire mapping, parameters, GIS

## 1. INTRODUCTION

In Lebanon, forest fires recur annually between mid summer and the beginning of winter. According to the Lebanese civil defense statistics, a total number of 1413 forest fire events took place in 1997 alone. The Ministry of Agriculture estimated about three thousand burned hectares in the two years 1998 and 1999. More than 35 percent of the initial forest cover is deteriorated during the last 40 years (Masri et al. 2002) leading to a green cover reduction to less than 7% of the Lebanese territory. Forest fires are responsible, along with land mismanagement, for the expansion of desertification. For this reason, the Lebanese government has started taking action to prevent the accelerated deterioration of green cover including grazing restrictions over burned areas, implementation of new "forests protection" law, training forest engineers for adequate forest management, institutional capacity building for forest fire protection, and allocation of twenty billion Lebanese pounds for reforestation.

In this context, mapping forest fire prone areas in Lebanon, which is the purpose of this paper, can provide decision-makers an objective means for allocation of endangered areas. The adequate use of these maps would be a necessity for planning forest fire management including detection, prevention and protection.

Knowing the most vulnerable sites is the first essential step to cope with forest fires in preparing an adequate infrastructure such as forest road network, water and survey towers. However, a georeferenced map is a must for proper planning and management logistics, as well as, for knowing their distribution over the Lebanese territory. In such a way the human and material damages can be reduced or even may be excluded.

## 2. METHODOLOGY

Forest fire risk evaluation in Lebanon did not exist before due to the lack of some dynamic and structural indices or parameters needed for this purpose (Van Wagner, 1987). Some of those major indices, i.e, land cover type are taken from the recently produced land cover/use map of Lebanon (NCRS, 2002) based on Indian Satellite image of 5 m. resolution, the Normalized Difference Vegetation Index (NDVI) was extracted from Landsat TM taken in September 2000, the aspect and slope gradient indices were extracted from digital elevation model (D.E.M.) 20 m. vertical accuracy. The evapotranspiration taken from existing meteorological stations spread all over the country. Other needed indices such as fuel thickness, humidity and fire history are lacking.

For this reason, the approach used here is restricted only to five structural and dynamic parameters, following the recommendations of Space Application Institute (San Miguel-Ayanz and.

Schmuck, 2002). They are: Aspect NDVI, land cover, slope gradient and evapotranspiration. The linear overlay process known as "rating and weighting" is used for evaluation based on expert judgment. The total "weight" given for all parameters is 100 points (table 1). This value is distributed among the parameters according to their relative importance in possible starting forest fire. The aspect of "rate", however, is ranked from 0 given to the least important factor, to 4 given to the most important one as shown in the table. Calculation of each final value was made according to classification formula cited below. This is a commonly used procedure when dealing with several variables of different character all affecting or leading to a certain end result. The geographic information system, Arc - View software, was used for data manipulation and to define fire prone areas into 6 classes: no risk, very low, low, medium, high and very high risk.

Table 1. Weighting and rating of forest fires parameters in Lebanon

| **Parameter (*i*)** | **Weight** | **Rate (*x*)** | | | | |
|---|---|---|---|---|---|---|
| | **%** | **0** | **1** | **2** | **3** | **4** |
| **Aspect** | ***20*** | **(X)** | N-E | N-W | S-E | S-W |
| **NDVI** | ***30*** | 0 | 0-0.2 | 0.2-0.4 | 0.4-0.6 | >0.6 |
| **Land cover** | ***30*** | Nonvegetated (rock, bare land, urban…) | Agriculture | Shrub, sparse, degenerated &grassland | Coniferous, broadleaves, & mixed | **(X)** |
| **Slope gradient %** | ***10*** | flat | <8 | 8-30 | 30-60 | >60 |
| **Evapotranspiration ( Eto)** | ***10*** | **(X)** | >0.6 | 0.6-0.4 | < 0.4 | **(X)** |

Classification formula: Fire risk index = $\Sigma^{n}_{1} w_i \times x_i$
Where: $w_i$ = weight of the parameter *i*
$x_i$ = rate of the parameter *i*

## 3. RESULTS AND DISCUSSION

Based on the calculation explained in table 1, the thematic map of the forest fire prone areas classifies the Lebanese territory into six categories of potential hazard: very high, high, moderate, low, very low and not risky. Every category is represented on the map by polygons having precise geographical coordinates and acreage. The map can be produced in different scales, from 1/200000 to 1/20000, depending on the degree of detail needed (see fig 1 and 2).

Although it is common to consider coniferous forests more susceptible to fires than broadleaved ones, the map classifies these two forest types at the same high level of risk. This can be justified by the fact that the broadleaved forests in Lebanon are mostly composed of evergreen *Quercus calliprinos*, which is a highly combustible material in late summer, while the coniferous forests are mostly composed of pruned *Pinus pinea* trees.

The map reveals that most of the very high and high potential hazard of about 8 $km^2$, are located in the southern exposure slope of western Mount Lebanon chain. The region includes forested broadleaved and coniferous areas. Another 183 $km^2$ from the same green cover type, but located mostly on the northern aspect, is shown in the map under low to medium risk category areas.

Because horticultural areas and open agricultural fields are also prone to fire, the map also includes these areas in the classification. For this reason, the large territory of Bekaa agricultural valley, where wheat and barely cover about 20000 hectares, as well as the Akkar plain in the north and the large grassland areas of the south, appear in this map within the very low risk category, with a total area of about 4116 $km^2$. The coastal strips, the degenerate and denuded northeast areas, as well as the high mountainous and barren rocky areas are shown in this map within the no risk category, with a total area of about 6145 $km^2$.

## 4. REFERENCES


Masri T., Khawlie M., and Faour G. (2002). Land-use/cover change, water resources and driving forces during 40 years in Lebanon . RICAMARE Workshops in I.R.D. Medenine, Tunisie 20-21 avril 2001. Published in*: MEDIAS Newsletter*. Mars 2002- N°13 bis P.p.9.

NCRS (2002) Land cover/use map of Lebanon scale 1/20000. Project done by NCSR, Ministry of Environment and Ministry of agriculture.

Van Wagner (1987) Elaboration et structure de la méthode canadienne de l'indice Foret- météo. Serv. Can. For, Inst. For. Nat. Petawawa, Chalk River (Ont.), *Rapp. Tech. For*. 35F, 34 p.

San Miguel-Ayanz J. and. Schmuck G. (2002). Forest fire activities of SAI (Space Application Institute of JRC) in support to STRIM. *1st Land –Water Med Network Workshop.* 15-16/4/2002 , Joint Research Center , Ispra,Italy.

# Forest Fire Hazard Map of Lebanon

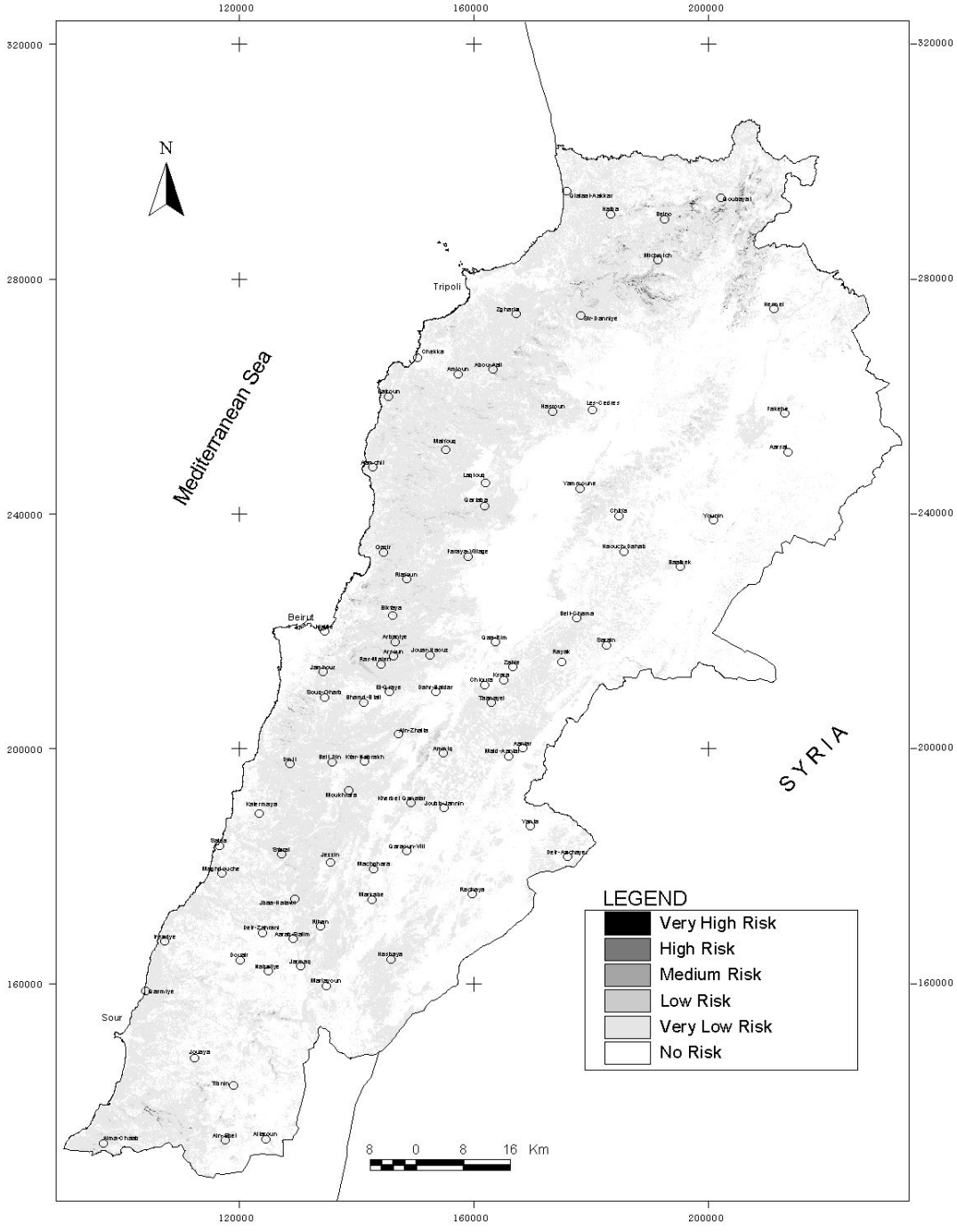

# Mapping forest fire occurrence at a regional scale

J. de la Riva, F. Pérez & N. Lana-Renault
*Dept. of Geography, University of Zaragoza, Spain*
delariva@posta.unizar.es

N. Koutsias
*Dept. of Geography, University of Zurich, Switzerland*

Keywords: Fire occurrence pattern, spatial modelling, kernel density estimation, Spain

ABSTRACT: Within the framework of fire danger, spatialisation of the dependent variable -historic fire occurrence- is required in order to correlate with human and environmental factors. Considering that fire ignition points contain positional uncertainties, a "moving window" of fixed dimensions can be used for estimating the intensity at each grid cell. Kernel estimation is an extension to the "moving window" concept where the fixed size window is replaced by a three dimensional function.
Kernel density interpolation can provide an alternative approach to define fire occurrence patterns by converting the point data to continuous density surfaces. Moreover, the method considers the relative position of points within the "moving window" which results to more realistic estimates.

## 1. INTRODUCTION

Within the framework of fire danger modelling, spatialisation of the dependent variable -historic fire occurrence- is required in order to correlate with human and environmental factors. Considering that fire ignition points contain positional uncertainties, a regular grid superimposed over the point distribution, as frequently done in pattern analysis, does not allow their correct spatialisation and proper study (Gatrell *et al.*, 1996). Substantial differences can be observed depending on the grid size and the extent of the positional inaccuracies. Increasing the grid size, the influence of the incorrect points can be minimized, however, followed by loss of spatial variability due to generalization. To overcome such deficiencies, a "moving window" of fixed dimensions can be used for estimating the intensity at each grid cell. Kernel estimation is an extension to the "moving window" concept where the fixed size window is replaced by a three dimensional function. Kernel density interpolation can provide an alternative approach to define fire occurrence patterns by converting the point data to continuous density surfaces. Moreover, the method considers the relative position of points within the "moving window" which results to more realistic estimates (Koutsias *et al.*, 2002).

## 2. OBJECTIVES AND STUDY AREA

The goal of this paper is to spatially define historic fire occurrence using a kernel density interpolation method and to present it as a categorical variable. Spanish fire occurrence data are recorded both at a UTM 10x10 km grid and at municipality level, which introduces an enhanced degree of uncertainty in the fire location. In order to ameliorate the accuracy of the fire location, a new spatial reference system is designed. Furthermore, it is applied in two areas with similar physical characteristics but different administrative structure and fire pattern, the Central Spanish Pre-Pyrenees (9301 $km^2$) and the East-central Iberian Range (9112 $km^2$) (Figure 1), so that the results will be more consistent.

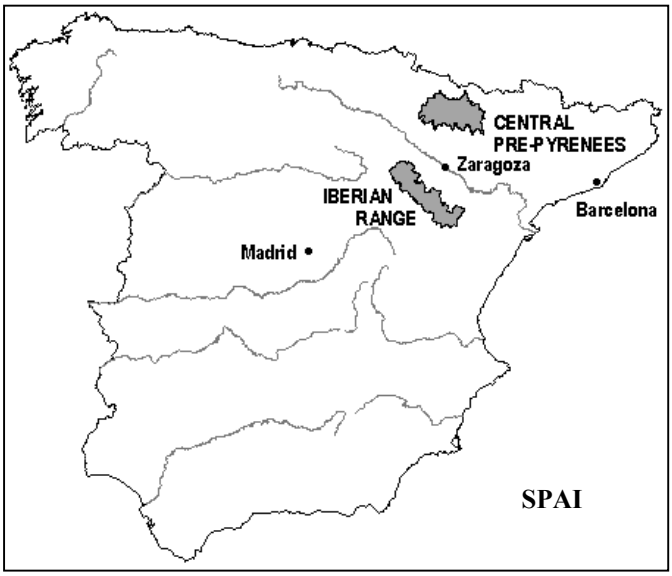


Figure 1. Study areas

Both areas are located in medium mediterranean mountain environments and are characterized by a great diversity of relief (between 800 to 1700 m) and vegetational communities dominated by *Pinus* (*sylvestris*, *pinaster*, *nigra*, most of them afforested), *Quercus ilex rotundifoliae*, *Q. faginea*, *Q. coccifera*, *Buxus sempervirens*, etc.

The two areas present a high number of fires, favoured by such characteristics and the human activity (Pérez Cabello & de la Riva, 2001): 1120 fires in the Pre-Pyrenees and 1134 fires in the Iberian Range between 1983 and 2001. Finally, the mean acreage of the municipalities is quite different: 104.8 $km^2$ and 39.8 $km^2$ respectively.

## 3. MATERIAL AND METHODS

Fire occurrence data were obtained from the Spanish official database. They are referenced within a new spatial unit (polygons) created from the overlaying of the UTM grid and the municipality boundaries in order to have a more accurate fire spatialisation. Because there is no information of the exact x/y UTM position of the ignition points, the fire ignition data were located using a random sampling design over the forested area within each polygon using ArcView 3.2.

Fire densities were calculated by applying a kernel density interpolation method implemented in CrimeStat® (Levine, 2002)[2]. A 100x100 m grid was obtained by using a fixed kernel approach and a normal distribution function. The size of the smoothing parameter or 'bandwidth' (standard deviation of the normal distribution) is critical because it determines the density results. Its value depends on the specific characteristics of the study case, specially the mean polygon area and the mean number of ignition points within each polygon. Consequently, several methods have been tested to choose the bandwidth size: the first method considers solely the mean polygon size; the second one is based on mean random distance calculations (using both polygon and total area mean size and number)[3]; in the

[2] CrimeStat® V. 2.0 is available on http://www.icpsr.umich.edu/NACJD/crimestat.html

[3] Mathematically defined as:

- Length of a theoretical radius (r) = D/2, where D is the diagonal of a theoretical square.
- Mean random distance (RDmean): $RDMean=1/2\sqrt{A/N}$

where A is the mean size polygon, and N is the mean number of ignitions points falling inside the polygons.

Since it is more accurate to consider the distance between two theoretical points, data are calculated using the double of the RDmean.

third one the influence of the random distribution points is evaluated; and finally, a visual-subjective approach is considered. Fire data from a wider area were introduced so that to preserve the influence of the external points and to minimize the edge effect problems.

A correlation analysis was applied not only to categorize the variable but also to check the goodness of the kernel density interpolation.

## 4. RESULTS AND DISCUSSION

Results obtained from the mean polygon size and the mean random distance calculations indicate the range of values that are appropriate to be used for defining the bandwidth size. For the Pre-Pyrenees case, those values are 3781 m for the mean polygon size calculation, 2757 m for the mean random distance and 2761 m for total mean random distance while for the Iberian Range case they are 3049 m, 2842 m and 2835 m respectively.

The influence of the randomly distributed ignition points was also considered. To evaluate which smoothing parameter is less influenced by the localisation of the ignition points, three random sampling schemes were designed. Fire densities were then calculated using the different bandwidth sizes. For each chosen bandwidth, a regression analysis was applied between the three random fire densities results. In both areas, Pre-Pyrenees and Iberian range, density values obtained with a 2500 m bandwidth are more affected by the random points distribution ($R^2 = 0.89$ and $R^2 = 0.86$ respectively ) than the values obtained with the other bandwidths ($R^2 > 0.93$).

As a result of the methodologies mentioned above, the effective range of bandwidth sizes in the Pre-Pyrenees case is between 2750 m and 3800 m, while for the Iberian range is between 2800 m and 3100 m. Figures 2 and 3 show densities values calculated in the Pre-Pyrenees (bandwidth 3250 m) and the Iberian range (bandwidth 3000 m).

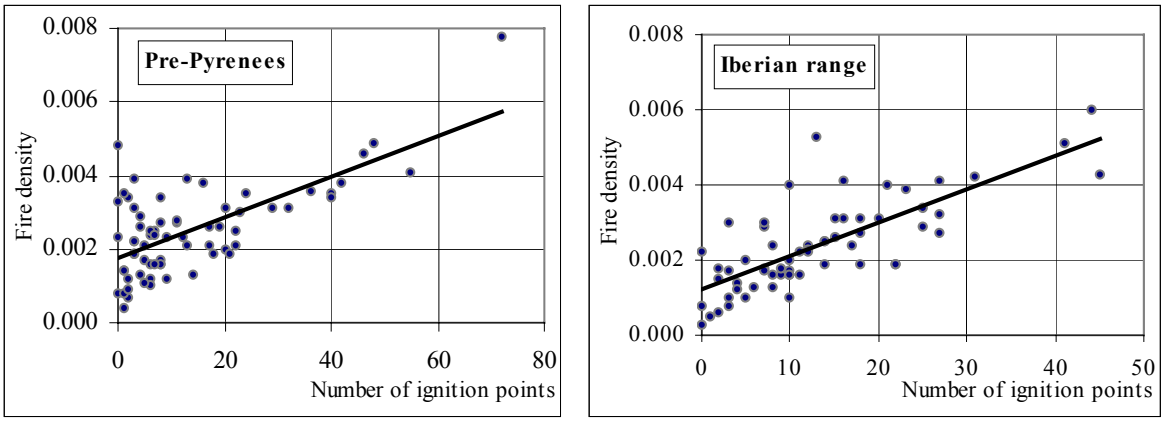


Figure 2. Correlation densities -maximum values- and fire ignition points.

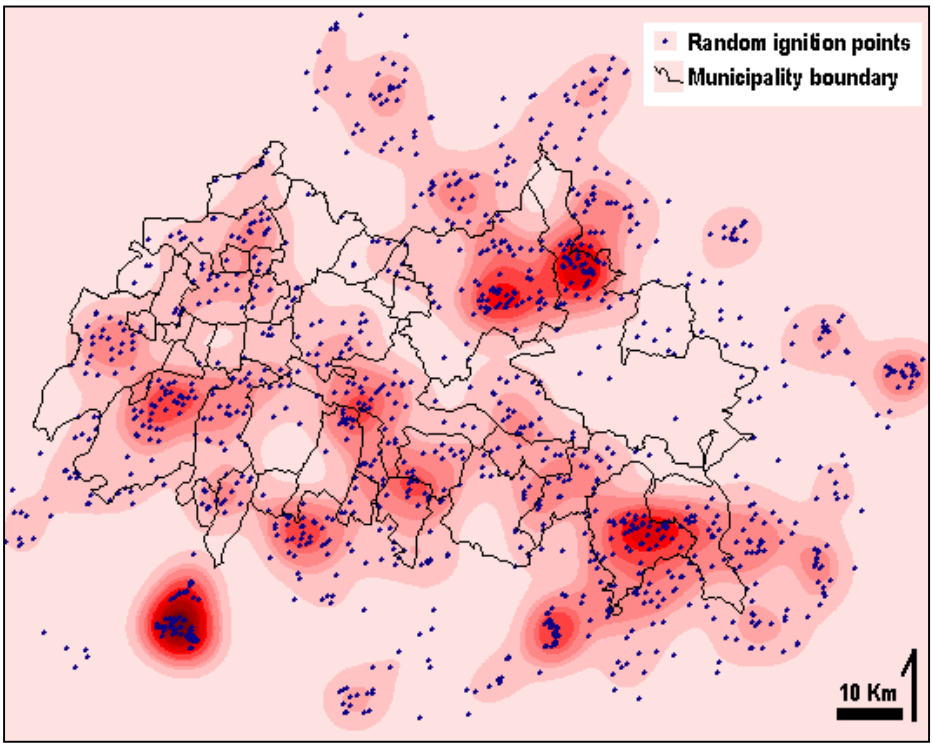


Figure 3. Fire densities using 3250 m bandwidth and random ignition points. Pre-Pyrenees area.

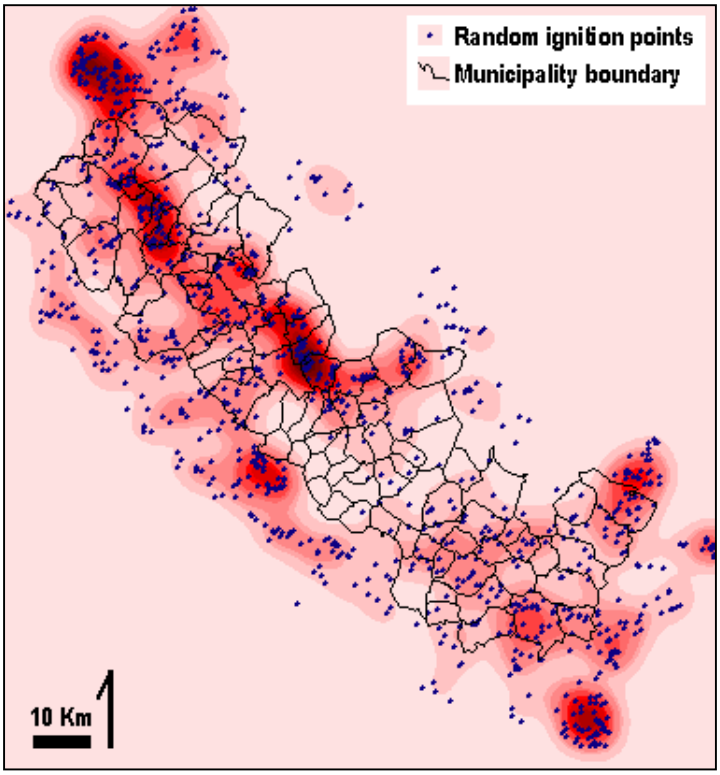


Figure 4. Fire densities using 3000 m bandwidth and random ignition points. Iberian range area.

To categorise the density values, the correlation coefficient between the number of fire ignition points and the kernel estimates was considered. According to the bandwidth definition, three standard deviations were considered and a 10x10 km grid was used. As expected, correlations, although statistically robust ($P < 0.001$), offer a $R^2 = 0.46$ and 0.58 for the maximum value per raster units and $R^2 = 0.33$ and 0.65 for the mean value in Pre-Pryrenees and Iberian range respectively (Figure 4).

Categories can be established from these correlations in order to map fire danger according to number of ignition points: very high (> 40), high (30-40), medium (20-30), low (10-20), very low (< 10).

## 5. ACKNOWLEDGEMENTS

This research was supported by the Spanish Ministry of Science and Technology (contract AGL2000-0842): FIRERISK project (*Remote Sensing and Geographic Information Systems for forest fire risk estimation: an integrated analysis of natural and human factors*).

## 6. REFERENCES

Gatrell, A.C., Bailey, T.C., Diggle, P.J. & Rowlingsont, B.S. 1996. Spatial point pattern analysis and its application in geographical epidemiology. *Transactions of Institute of British Geographers* 21: 256-274.

Koutsias, N., Kalabokidis, K. & Allgöwer, B. 2002. Fire occurrence patterns at landscape level: beyond positional accuracy of ignition points with kernel density estimation methods. Poster presentation in 2002 *World Conference on Natural Resources Modeling, "Modeling Natural and Biotic Resources in a Changing Planet"*, Sigri, Lesbos, Greece.

Levine, N. 2002. CrimeStat II: *A Spatial Statistics Program for the Analysis of Crime Incident Locations (V. 2.0)*. Washington, DC: Ned Levine & Associates, Houston, TX, and the National Institute of Justice.

Pérez Cabello, F. & de la Riva, J. (2001): Forest fires and land degradation in Spain. The Huesca Western Pre-Pyrenees case study. Key-Note in the workshop "*Landnutzungswandel und Landdegradation in Spanien*", Frankfurt am Main, Germany.

# An Empirical Fire Danger Model for Tropical Humid Areas (East Kalimantan, Indonesia)

G. Rücker
*ZEBRIS GIS and Consulting, München, Germany*
gruecker@zebris.com

Keywords: Fire Danger, Tropical Rain Forest, Decision Support System, Indonesia, NOAA-AVHRR

ABSTRACT: An empirical fire danger model for humid tropical areas is presented. Through analysis of historical fire data from NOAA-AVHRR hotspot detections during a reference fire season and their spatial relation to the main factors supposed to influence fire occurrence an empirical model is derived through weights-of-evidence analysis. The factors analyzed are height above sea level, land-cover, accessibility (roads, rivers and settlements), the Keech-Byram drought index from meteorological stations and vegetation vigor represented through Normalized Difference of Vegetation Index (NDVI) data from NOAA-AVHRR satellite images. The results of the analysis show that all factors at least have a moderate influence on fire occurrence and that the results of the analysis can be extrapolated to other periods of time. However, more and more accurate data would help to improve the model to become a highly useful tool for decision makers in fire management.

## 1. INTRODUCTION

Until recently, forest fires in tropical rainforest climates were seen as exceptional events with only limited consequences at a local level. Because of the ongoing destruction and degradation of rainforests, the formerly rare phenomenon of forest fires became an important ecological agent in areas of tropical humid climate (Nepstadt et al. 1999, Siegert et al. 2001) and its consequences are of global impact (Page et al. 2002). Contrary to boreal or Mediterranean forests, evergreen tropical rainforest vegetation is not well adapted to fire, and repeated fire events lead to rapid and irreversible degradation already after few fire events. This has been shown to be especially true for East Kalimantan's rainforest (Siegert et al., 2001). The Indonesian-German co-operation project Integrated Forest Fire Management (IFFM) in Samarinda (East Kalimantan) has been working on a Fire Information System (FIS) for several years to co-ordinate prevention and control actions. In order to establish an efficient FIS, it is crucial to identify regions with elevated fire danger induced through natural geographic conditions or human intervention. Although this problem is of global significance, there are still few experiences with fire danger estimations for tropical rainforest areas. Objective of the study presented here was therefore to develop a simple empirical model for fire danger based on existing or easily available data, e.g. land-use and vegetation, terrain and meteorological conditions. The map should be dynamic, i.e. reflect short-term changes due to meteorological and vegetation conditions in order to give a realistic estimate of fire danger.

In North America and Europe several approaches to fire danger modelling have been developed over the past decades. Based on the United States Department of Agriculture (USDA) National Fire Danger Rating System (Deeming et al 1974), Burgan et al. (1998) developed a Fire Potential Index, combining ground and space-borne observations derived from NOAA-AVHRR NDVI data. The fire potential Index uses relative NVDI values (also called relative greenness, an index comparing historical maxima to actual NDVI values) and live and dead fuel loads derived from ground-based fuel moisture maps to define this index. This approach is being adopted by the European Commission to develop a fire danger model for the Mediterranean (Sebastián-López et al., 2002). Kogan (1997)

represents a Vegetation Condition Index (VCI) and a Temperature Condition Index (TCI) and presents the use of this index to monitor droughts on a global scale. Malingreau (1990) also points out the correlation between fire potential and surface temperature measured by NOAA satellites, as temperature increases when vegetation desiccates. Chuvieco et al. (2002) related fuel moisture to NDVI and other indexes derived from Landsat TM satellite images. They showed that NDVI was related to fuel moisture and thus to the flammability of the vegetation. Currently, agencies from Canada are adapting the Canadian Forest Fire Weather Index System, a subsystem of the Canadian Fire Danger Rating System to the conditions prevalent in Indonesia.

## 2. DATA AND METHODS

Existing fire danger models, e.g. those in use in the United States or Canada are based on a dense observation network and sometimes decades of research into the fire behaviour of different vegetation formations. In the tropics, little is known about fire behaviour, nor fuel models, nor is there a dense network of meteorological stations or fire weather observations available. Fuel types prevalent in the Northern latitudes cannot be easily transferred to the tropics. However, it has been shown that fire potential can be observed with earth observation satellites through drops in NDVI or a rise in surface temperature before the fire (Malingreau 1990). This makes observations in remote areas with no meteorological stations feasible. In order to get a preliminary fire danger model for the province of East Kalimantan, we decided to develop this model purely on statistical relationships with data that are available for the whole province. There were several data sets available for fire danger modelling (table 1). Using these data an empirical algorithm was established based on fire behaviour in past fire events. This algorithm should calculate a fire danger index for any location in the province based on the given input data. The model was to be validated with hotspot data and through simulation of historical fire occurrences.

Table 1. Available Data at IFFM

| Dataset | No. of Classes for WofE Analysis | Source |
|---|---|---|
| Simple land cover map (ERS-2 Radar interpretation) | 5 | IFFM (Siegert et al. 2001) |
| 1km Digital Elevation Model | 6 | USGS |
| Roads, rivers and settlements (Accessibility) | 2 | IFFM/BAPPEDA (see text) |
| Keech-Byram-Dryness Index (KBDI) | 4 | IFFM (Deeming 1994) |
| NOAA-satellite images relative greenness | 4 | IFFM (see text) |
| Historical fire occurrence (NOAA Hotspots) | - | IFFM |
| **Number of possible factor combinations** | **960** | |

Relative greenness was calculated based on NOAA satellite images of the 1-km AVHRR global land data set (Eidenshink and Faundeen, 1994) and data collected at the Samarinda ground station. From these data historical maxima and minima were calculated and relative greenness was then derived from a comparison to a 30-day maximum composite dataset. Accessibility was calculated by buffering roads, rivers and settlements with a buffer of 5 km for rivers and settlements and 2 km for roads.

The applied method is based on derivation of weights for the different factors based on a statistical analysis of historical fire behaviour. Probability of fire occurance (i.e. fire danger) is then calculated according to the Weights of Evidence model (WoE) presented by Bonham-Carter (1994). The empirical data set of historical fire occurrences during a reference period was used for model

development. The fire danger model consists of a weighted overlay of the different input factors that give a map of probabilities for fire occurrence. This map can then be used as a fire danger map in early warning systems.

## 3. RESULTS

We calculated the weights of evidence for several months during the fire season of 1997. We chose this period because it was a severe fire season and is thought to represent severe, but not yet catastrophic conditions. Furthermore, it was one of the few periods in the 1990'ies with a good record of several meteorological stations and a complete coverage with NOAA satellite images received at the Samarinda ground station. From this analysis we conclude that all of the input factors had at least a moderate predictive capacity. As to be expected, land-cover and related land-use were closely related to fire occurrence. Thus, grasslands and clear-cut areas were strongly associated with the presence of fires. Also it did not come as a surprise that at a height above sea level superior to 220m, very few fires occurred since the elevated areas of East Kalimantan are still little prone to fires. The dynamic elements KBDI and relative greenness were of moderate to strong predictive influence: depressed NDVI values were moderate to strong predictors for fires, and a high KBDI was related to presence of fires, whereas a low KBDI was strongly related to absence of fires. Vicinity to settlements and traffic networks was only moderately predictive for fire occurrence. However, we believe from experience that accessibility greatly determines fire probability. The relatively low predictive capability of this factor may be due to the relatively poor quality of our road network data on the one hand, and on the more subtle interaction between man, vegetation and fire, that cannot be expressed in simple terms of accessibility, on the other. We then calculated a fire danger map for time periods that were not in our input dataset of autumn of 1997 and assessed its predictive capability with historical hotspot data. It turned out that there was a strong difference in hot spot occurrence between low estimated probabilities and higher estimated probabilities, while there was no difference between high and extreme estimated probabilities, indicating some need for refinement of the model.

## 4. CONCLUSIONS

The presented model is based on historical fire occurrence. We can draw several conclusions from the weights calculated for the different factors. Land-cover has the strongest influence on fire occurrence. The land cover map derived from ERS-SAR data, although very basic, includes sufficient information to identify endangered areas. The areas with the highest predictive capacity were grasslands and clear-cut areas. This may be related to the fuel types, since the pyrophytic grasslands that frequently represent the fire climax in East Kalimantan are easily flammable and fires spread rapidly. On the other hand, high occurrence of fires in those areas may also be related to land-use since fire is a frequently used, e.g. for hunting. Fires are also frequent in oil-palm and plantation areas as well as in secondary forest and agricultural areas. This is supposed to be related to the type of land-use and land-management on these areas as well as to the ease of ignition of the vegetation. Dipterocarp forest generally indicates low fire occurrence. However, with the available map it is not possible to differentiate between closed and opened Dipterocarp forests. From our own research (Siegert et al. 2001) it is known that opened forests are much more fire prone. Height above sea level is also an important indicator. Higher elevations have a strong negative association with fire occurrence, which may be due to a number of reasons: first, population density and land-use intensity is low in these areas, resulting in an almost closed forest cover, and second, rainfall and humidity is higher and temperatures are lower. Vicinity to settlements and rivers (the accessibility grid) is only of moderate importance. This may be due to the fact that our buffer is too uniform, because there are also large areas within the buffer zone that are only infrequently visited. However, in the more densely populated areas, vicinity to traffic networks and thus better accessibility may be of higher predictive value than

in the areas with sparse population. NDVI is an important dynamic element, although the calculated weights are not very high. From interpretation of the calculated fire danger maps, we can conclude that a depression of NDVI especially in forested areas precedes fires that frequently spread from other highly endangered areas into the forest. KBDI is strongly related to fire occurrence, however we only have very little reliable data to calculate serious estimates for the whole province, since there are only very few stations and only few of these are fully operational and ready to exchange data with IFFM on a continuous basis. Overall, the statistical model performs well within the limitations imposed by the method and data availability. The basic assumption that fire occurrence is governed by a set of independent variables and probabilities of fire events can therefore be calculated from the combination of these factors proved to be valid. Due to the easy adaptability of the weights of evidence parameters, the model can easily be adapted as new data sets become available. For instance, there is still little knowledge about how fuels were altered due to the fires of the last big El Niño event. As soon as data on fire behaviour in the areas affected become available, they can readily be integrated into the model.

## 5. REFERENCES


Bonham-Carter, G.F., 1994, Geographic Information Systems for Geoscientists: Modelling with GIS. Pergamon, Oxford, 398 p.

Burgan, R.E., Klaver, R.W., Klaver, J.M., 1998, Fuel models and fire potential from satellite and surface observations. International Journal of Wildlife Fire, 8, 159-170.

Chuvieco, E., Riaño, D., Aguado, I., Cocero, D. (2002): Estimation of fuel moisture content from multitemporal analysis of Landsat Thematic Mapper reflectance data: Applications in fire danger assessment. International Journal of Remote Sensing, Vol 23, No. 11: 2145-2162

Deeming, J.E.; Lancester, J.W., Fosberg, M.A., Furman, W.R., Schroeder, M.J. (1974): The National Fire-Danger Rating System. USDA, Forest Service. Research Paper RM-84, Fort Collins, Colorado. 165 pages

Deeming, J.E.(1995): Development of a fire danger rating system for East Kalimantan, Indonesia., IFFM Doc. No. 02, Samarinda

Eidenshink, J. C., and Faundeen, J. L., 1994: The 1-km AVHRR global land data set: first stages in implementation. International Journal of Remote Sensing, 15, 3443-3462.

Kogan, F.N. (1997): Global Drought Watch from Space. Bulletin of the American Meteorological Society, 78, 621-636.

Malingreau, J.-P. (1990): The contribution of remote sensing to the global monitoring of fires in tropical and subtropical ecosystems. In: Goldammer, J.G.: Fire in the tropical biota. Ecological Studies 84, Springer, Berlin a.o.: 337-370

Page, S.E., Siegert, F., Rieley, J.O., Boehm, H.D.V., Jaya, A. , Limin, S.: The amount of carbon released from peat and forest fires in Indonesia during 1997. *Nature*, 420: 61-65

Sebastián-López, A., An Miguel-Ayanz, J., Burgan, R.E. (2002): Integration of satellite sensor data, fuel type maps and meteorological observations for evaluation of forest fire ris at the pan-European scale. International Journal of Remote Sensing, Vol 23, No. 13: 2713-2719

Siegert, F., Ruecker, G., Hinrichs, A., and Hoffmann, A.A.(2001): Increased damage from fires in logged forests during droughts caused by El Niño, Nature, 414: 437-440

# Fire Threat Analysis in West Kutai District of East Kalimantan, Indonesia

Solichin
*South Sumatra Forest Fire Management Project, Palembang, Indonesia*

J. G. Goldammer & A. A. Hoffmann
*Fire Ecology Research Group Fire Ecology & Global Fire Monitoring Center (GFMC), Max Planck Institute for Chemistry, Biogeochemistry Department, Freiburg University, Freiburg, Germany*
jggold@uni-freiburg.de

G. Rücker
*ZEBRIS GIS and Consulting, München, Germany*

Keywords: fire threat, fire danger rating, fire risk, Indonesia

ABSTRACT: Severe vegetation fires have been a common event in Indonesia in the past two decades. In various countries a number of early warning methods have been introduced to support fire prevention and suppression activities but not yet in tropical areas. The study aims to the development of a Fire Threat Analysis (FTA) map in West Kutai District of East Kalimantan, Indonesia by incorporating Risk of Ignition (RoI), Potential Fire Behavior (PFB), Values at Risk (VaR) and Fire Suppression Capability (FSC). Integration of FTA and fire danger rating allow fire managers to conduct tactical suppression planning and prioritization and could be used to evaluate the existing management capacity in relation to fire threat level.

## 1. INTRODUCTION

Severe vegetation fires have been a common event in the tropical ecosystem of Indonesia in the past two decades, where East Kalimantan was the province worst hit. The combination of recurring El-Niño events, and the ongoing forest coverage as well as socio-economic changing, will cause additional intense fires in the future (Goldammer, 1990, Hoffmann et al., 1999, Siegert et al., 2001). It is therefore important to improve and intensify the early warning efforts within private and government land management institutions for more effective and efficient measures in anticipating the reoccurring fire event.

A number of early warning methods have been introduced to support fire prevention and suppression activities. Many countries are applying Fire Danger Rating (FDR) to assess the level of dryness based on daily weather observations. Keetch-Byram Drought Index (KBDI) and Fire Weather Index (FWI) are the common indices used as Fire Danger Rating. In the latter development, a more comprehensive method of Fire Threat Analysis (FTA) that incorporates several factors such as Risk of Ignition (RoI), Potential Fire Behavior (PFB), Values at Risk (VaR) as well as Fire Suppression Capability (FSC), has been introduced in Australia, Canada and New Zealand, but not yet in tropical countries (Borger, 1999; Majorhazi et al, 1998; Hawkes et al, 1996).

The aim of this study is to develop Fire Threat Analysis maps in West Kutai District of East Kalimantan, Indonesia (Fig.1)


Figure 1. Location of the study area

## 2. METHODOLOGY

Total of 12 layers that contribute to FTA were identified. RoI consists of 2 layers, namely accessibility and human settlement. Differ to those in Canada and USA where lightning is the main cause of starting fires, all RoI layers in this process are related to human causes, which are the major causes in most fire events in Indonesia (Bowen *et al.*, 1999; Hoffmann, 1999).

Altitude, annual precipitation, and vegetation type (digitized from Landsat images) are involved to generate PFB. VaR consider all valuable factors that are economically and ecologically important to the community. This includes life and property (represented by human settlements), timber in forest concessions and protected areas. FSC consists of 4 layers, such as the capacity of fire personnel and equipment, trained villages, accessible roads and rivers as water sources during the dry period. FTA is then generated based on these datasets (Fig.2).

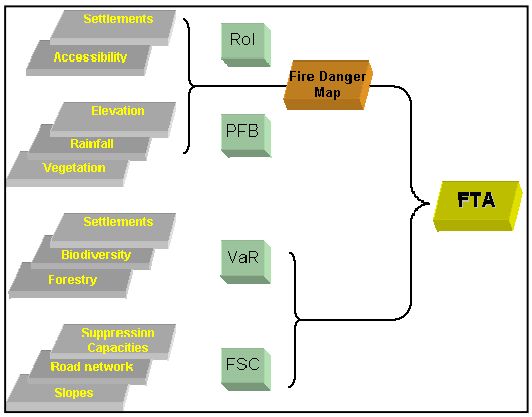


Figure 2. Fire Threat Analysis processing.

RoI and PFB components were processed by means of Weight of Evidence model (see Kemp *et al*, 1999), because they are related to fire occurrence and intensity. Incorporating all factors from RoI and PFB components simultaneously into this model was done to generate Fire Danger Map (FD). The historical NOAA hotspots, acquired in 1997-1998, were used in this model as "training points" to determine the frequency of fire occurrence in a specific area. The output of the Weight of Evidence model is a map showing the probability of each unit cell that a fire hotspot will occur (Rücker, 2002). All factors of FSC and VaR components were scored and combined with GIS operation. In the next step the three components (FD, VaR and FSC) were adjusted with specific value so that they are comparable.

## 3. RESULTS

Four main components Risk of Ignition, Potential Fire Behavior, Values at Risk, Fire Suppression Capability were generated to be further used for creating FTA for West Kutai District, Fire Danger, and Fire Threat Analysis.

### *3.1 Risk of Ignition*

The RoI map (Fig. 3) shows the relatively well distributed Risk of Ignition potential where 0 means low and 0.09 high ignition potential of the West Kutai district. Because almost all fires in Kalimantan are human-induced, the ignition potential in the district follows the extent of the river Mahakam and its tributaries, which play an important role in distribution of population and supporting transportation throughout the district. Moreover, the risk of ignition in the southern part of the district is higher than that in northern part. This is because the population and road networks in the southern part are denser.

### *3.2 Potential Fire Behavior*

Annual precipitation, vegetation types, and elevation are important factors that contribute to PFB map. The northern part has again lower fire hazard level than in the southern part. Mountainous forest and dense still mainly undisturbed *Dipterocarp* forest dominate the northern part, while intensive land for agriculture, degraded peat swamp and grassland are common in the southern part. Moreover, the northern part has higher amount of precipitation and higher elevation than in the southern part. Figure 4 shows the Potential Fire Behavior map where 0 means low and 0.9 high fire hazard.

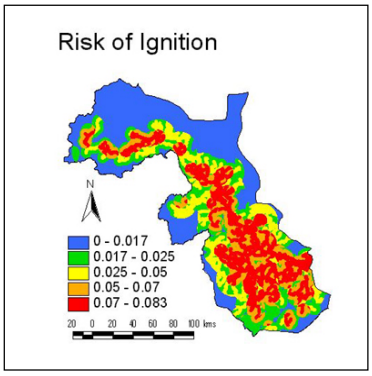


Figure 3. Risk of Ignition map

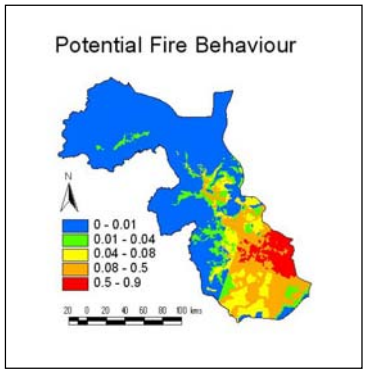


Figure 4. Potential Fire Behavior map

### *3.3 Values at Risk*

The process involved three factors e.g. life and properties that are represented by a settlement layer, timber forestry and biodiversity. These areas should be objective to be protected from fires due to their economical and ecological values. In contrast to PFB and RoI, the northern part has more valuable areas than in the southern part, because undisturbed forests, that support high biodiversity and timber values, still dominate the area. Figure 5 shows the Value at risk map with low (5), medium (10), high (15) and very high (25) values at risk areas.

### *3.4 Fire Suppression Capability*

Four factors contribute to FSC, namely slope, road network, water resources, and preparedness of fire fighters and equipment. As shown in Figure 6, only small area of the district has sufficient capability in conducting fire suppression measures. Red color indicates the low capability in fire suppression and the green colour indicates high capability in fire suppression. Most of road networks in East Kalimantan were constructed by timber concessions for their own purposes and therefore usually are not connected to district main roads or have dead end in a log pond near big river. Besides, results from a workshop on capacity assessment in the district show that there is still a lack of fire fighter and equipment for fire suppression measures.

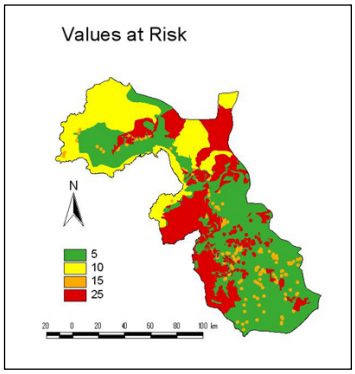

Figure 5. Values at risk map

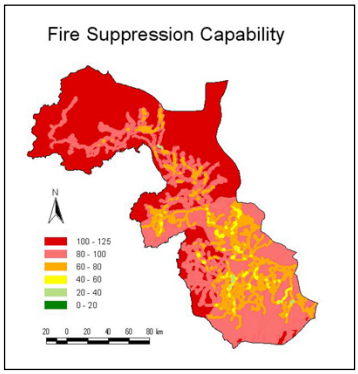

Figure 6. Fire suppression capability

### *3.5 Fire Threat Analysis*

Fire Threat Analysis (FTA) is combination between Fire Danger (FD), Values at Risk (VaR) and Fire Suppression Capability (FSC). Figure 6 shows the fire threat map of West Kutai. About 6% in the district shows extreme fire threat. Mostly near the river Mahakam basin area where peat vegetation is dominant. 10% of the district has a high fire threat level. A very low and low fire threat level dominates the district by 43 % and 30 % respectively, while only nine percent of the district is rated moderate level. This very low level mostly occurred in northern part where the altitude is more than 1000 metres and the annual precipitation more than 3600 mm.

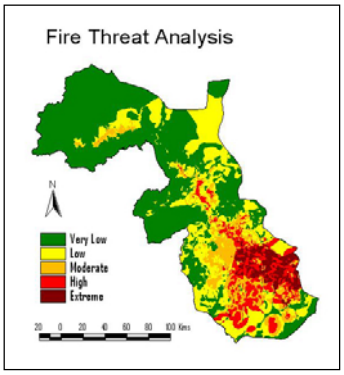

Figure 7. Fire Threat Analysis map of West Kutai District

## 4. CONCLUSION

The FTA information can support fire management planning at a strategic level. Integration of FTA and fire danger rating allow fire managers to conduct tactical suppression planning and prioritization. FTA could also be used to evaluate the existing management capacity of particular area

in relation to fire threat level. However, because Fire Threat reflects the four components previously mentioned it is therefore not easy to determine which combination of factors has more influence in some particular threat level. Fire managers, should carefully interpret the map taken into consideration advance knowledge about the local environment. A Fire Threat Analysis map should not be interpreted without examining the four components and the factors that contribute to each of them. Otherwise the interpretation will lead to confusion. Hence, it is sometimes necessary to display all components and their factors in the same occasion. This would make interpretation easier.

## 5. REFERENCES


Borger, B. 1999. New Zealand Wildfire Threat Analysis Project: The Analysis Phase. National Rural Fire Authority. New Zealand. http://www.fire.org.nz/rural/ publications/WTAanalysisreport/index.html.

Bowen, M.R., Bompard, J.M., Anderson, I.P, Guizol, P. and Gouyon, A. 1999. Anthropogenic Fires in Indonesia: A View from Sumatra. In Radojevic and Eaton (Eds). Forest Fires and Regional Haze in South East Asia. Nova Science. New York.

Goldammer, J. G. and Seibert, B. 1990. Droughts and Fires in Tropical Lowland Raind Forest. In: Fire in the Tropical Biota. Springer Verlag. Berlin.

Hoffman, A., Hinrichs, A. and Siegert, F. 1999. Fire Damage in East Kalimantan in 1997/1998 related to Land Use and Vegetation Classes: satellite radar Inventory Results and Proposal for further Actions. IFFM-SFMP Report No.1a. MOFEC. GTZ and KFW. Samarinda.

Majorhazi, K. 1998. Wildfire Threat Analysis for New Zealand. Online. National Rural Fire Authority. http://www.fire.org.nz

Ruecker, G. 2002. Consulting and Software Development to Produce a Dynamic Fire Danger Map for East Kalimantan. Consultancy Report-IFFM/GTZ. Munich.

Siegert, F., Ruecker, G., Hinrichs, A. and Hoffmann, A. 2001. Increased Damage from Fires in Logged Forests during droughts caused by El Niño. Nature Volume 414.

# Multicriteria Decision Analysis for Forest Fire Risk Assessment in Galicia, Spain

J. Varela, J. E. Arias, I. Sordo & A. Tarela
*Technological Research Institute, University of Santiago de Compostela, Galicia, Spain*
eljpet@usc.es

Keywords: Geographical Information Systems (GIS), Multicriteria Decision Analysis (MCDA), Decision Support Systems (DSS), environmental risk assessment

ABSTRACT: Many environmental factors contribute to the appearance of forest fires in Galicia (Spain). The severe socio-economic consequences of wildfires demand Information Systems (IS) for supporting diverse decision making problems related to the main fire fighting actions (planning, prevention, surveillance, extinction, and the like). We do believe that the integration of MCDA techniques and GIS frameworks can decisively improve the management of all available resources for fire fighting: Geographical Information Systems spatially enable the expert's judgments, whereas MCDA procedures allow the GIS to become a true Decision Support System.

## 1. INTRODUCTION

Every year, thousands of hectares of forest soil are burned by wildfires in Galicia (geographically located in the NW corner of the Iberian Peninsula, Galicia is one the 19 Autonomous Communities in Spain), mostly during the summer months. Among the multiple reasons for this fact, we must emphasize the summer weather conditions, the state of the vegetation and many socioeconomic issues (in this sense, the high frequency of man-caused fires must be highlighted). On the other hand, the extinction of forest fires is strongly conditioned by the physical environment, characterized by a complex topography, a high dispersion of the population and a wide forest surface.

As a result, the Government of Galicia (Xunta de Galicia) devotes to fire fighting a growing number of human and material resources, whose coordination from a hierarchy of control centres is being more and more complex [1]. This situation requires information systems (IS) adapted to the Forest Fire Fighting Service (SDCIF).In this sense, among several IS implanted for the last years, we can stand out a Geographical Information System (GIS) that keeps up-to-date a complete cartographic database, an Automatic Vehicle Location (AVL) System which tracks all the aerial resources, and a centralized database where all the available data about active and historical fires are stored.

Given the main role that the cartographic database plays within this organization, we intend to apply Multicriteria Decision Making (MCDM) techniques to evaluate a static fire risk index for the whole region. This index will be built starting from all those structural factors that influence the appearance and spread of fire, as considered by the Service's experts. We believe that such an index can be especially useful for planning tasks (infrastructure enabling and the like) and organization of surveillance and extinction operations (for instance, the index layers can directly feed the AVL system).

## 2. METHODS

The term *decision analysis* designates a broad group of systematic procedures for analyzing problems that require complex decisions. The basic strategy consists of dividing the problem in well-defined small pieces, analyzing each part separately and integrating them in a logical way to obtain a meaningful solution that allows the selection among several action lines. The decision making typically implies a high number of possible alternatives and many conflicting evaluation criteria. The alternatives must be valued by diverse individuals and interest groups, each one characterized by different preferences with regard to the relative importance of each evaluation criterion.

Nowadays it is commonly accepted that Multicriteria Decision Analysis (MCDA) procedures and Geographical Information Systems (GIS) can mutually benefit: MCDA techniques will this way overcome their classic spatial limitation and, reciprocally, GIS, initially conceived as decision support tools, can systematically incorporate the user preferences revealed by MCDA procedures.

We will confront here a descriptive approach based on permanent criteria, therefore we will refuse to compute a transitory fire risk index. In that sense, we could assert that our index is *static* or *structural*.

As Malczewski [2] has already suggested, two main categories of MCDA procedures can be considered: Multiobjective Decision Making (MODM) and Multiattribute Decision Making (MADM). The first class better suits design problems and the vector data model, whereas the second group fits evaluation problems and the raster data model. Given that we only intend to describe the current scenario, a set of MADM techniques will be encoded within ArcView 3 (whose object-oriented programming language is Avenue [3]), making full use of the GRID data model and the Spatial Analyst extension [4].

If we now focus in our decision problem, the *goal* is to compute a fire risk index from five secondary indexes, each one depicting a different viewpoint of wildfire fight. Thus, our *objectives* are established as the calculation of the detection, ignition, spread, protection, and inherent value indexes.

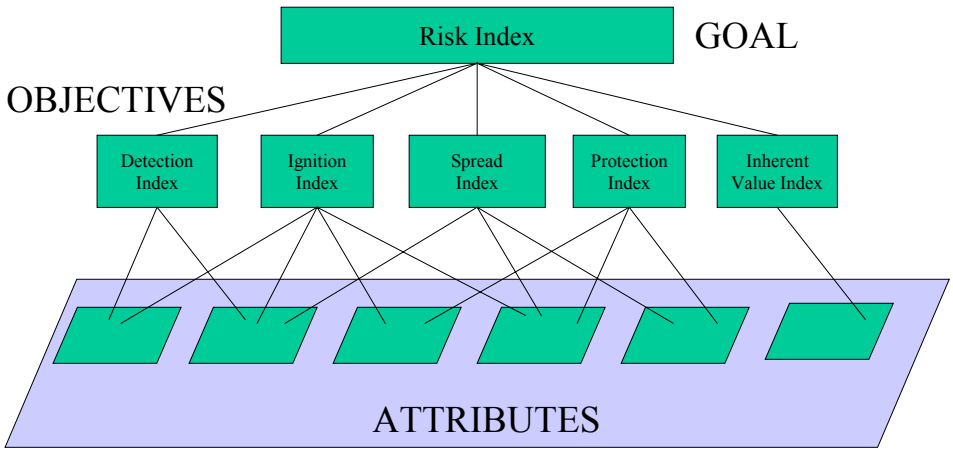


Figure 1. Construction of the risk index.

Each secondary index is built from a set of *attributes* or thematic layers established by the recommendations of SDCIF experts (mainly retrieved from questionnaires) and relevant literature. Given the variety of scales on which attributes are in fact measured, the values contained in the criterion map layers must be transformed to comparable units before an aggregation is made. Each attribute is standardized either as a *benefit criterion*, when higher values of the attribute yield higher values of the index, or otherwise as a *cost criterion*. A brief description of each secondary index follows:

- **Detection index**: measures the difficulties that the Service finds to promptly detect the fires. Obviously, the response time must minimize in order to decrease the damaged surface.
- **Ignition index**: takes into account variables that set the probability of fire start. A prominent occurrence of man-caused fires must be here remarked.

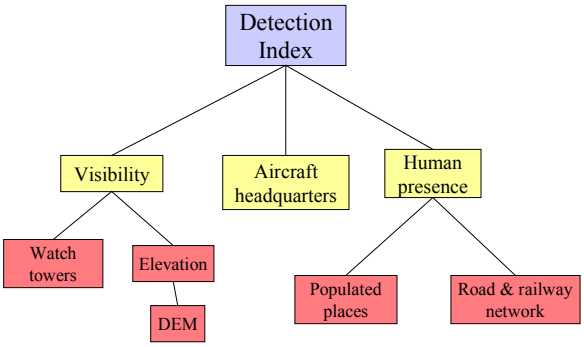


Figure 2. Construction of the detection index.

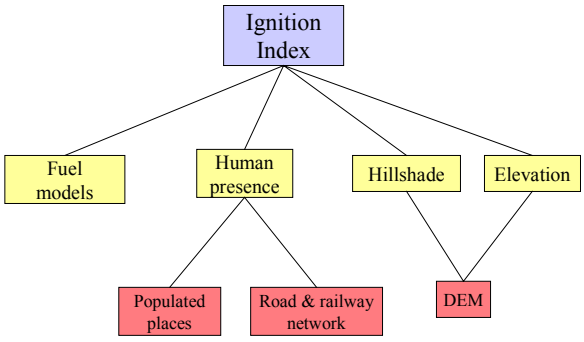


Figure 3. Construction of the ignition index.

- **Spread index**: combines the fire's advance ability over each fuel model, the distance to the closest firewall, and slope (the fire spreads quicker over higher gradients) and elevation (used here as an indirect and permanent measurement of humidity and temperature) values.
- **Protection index**: joins some SDCIF infrastructure efforts to protect the territory. A long distance to the closest aircraft headquarters certainly reveals a weak protection score.

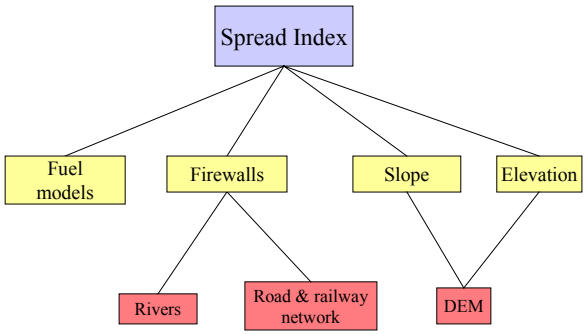


Figure 4. Construction of the spread index.

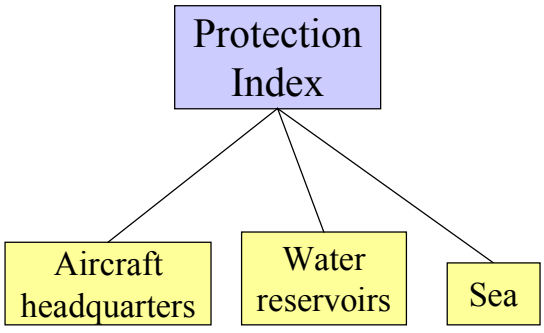


Figure 5. Construction of the protection index.

- **Inherent value index**: this index gathers human and environmental viewpoints to artificially emphasize the risk index within several areas that require a special watch.

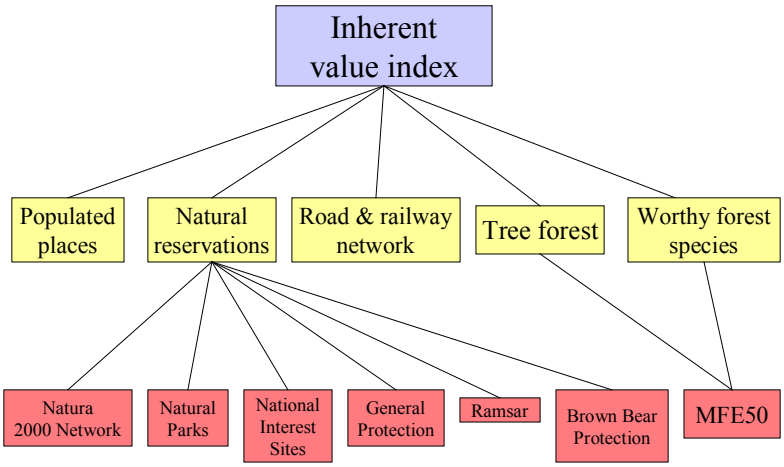


Figure 6. Construction of the inherent value index.

The *alternatives* to be valued are the total of 738,944 pixels yielded by a 200 by 200 metres partition of the Community bounds, as defined in the Numerical Cartographic Database 1:200,000 scale (BCN200) by the National Geographical Institute (IGN) of Spain.

The general framework proposed by Jankowski [5] for multiple criteria decision making has been followed to develop our decision problem. In this scheme, we have to highlight three main steps: *standardization* of layers, in order to transform all criteria to comparable units (this way we derive commensurate maps); incorporation of *user preferences*, typically carried out by means of relative importance weights; finally, an *aggregation function* or decision rule combines the standardized and weighted layers to compute each secondary index. Further aggregation procedures yield the structural fire risk index starting from the five secondary indexes.

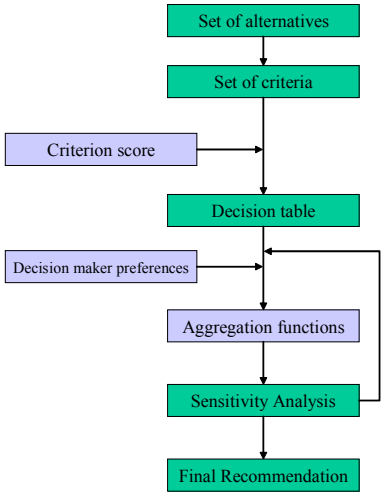


Figure 7. Jankowski's framework for MCDM.

The selected MADM techniques for standardization, weighting, and aggregation have been, respectively, *score range*, *pairwise comparison* [6] and *TOPSIS* (an ideal point method) procedures.

## 3. RESULTS

We can focus, for instance, on the pairwise comparison for weighting all the criteria involved in the protection index (the fourth secondary index). This method sets the relative importance of the criteria taking them in a one-on-one basis. As a result, a weight for each criterion is extracted, as well as an overall *consistency ratio* (CR). A CR greater than 0.1 reveals the existence of inconsistent judgments and a revision of the process is suggested.

Table 1. Pairwise comparison for the protection index, and resultant weights of the involved criteria.

| | H | R | S |
|---|---|---|---|
| Proximity to extinction aircraft headquarters (H) | 1 | 3 | 4 |
| Distance to water reservoirs (R) | | 1 | 2 |
| Distance to the sea (S) | | | 1 |

| | |
|---|---|
| $w_H$ | 0.623 |
| $w_R$ | 0.239 |
| $w_S$ | 0.137 |

CR = 0.016

The five resulting indexes are also weighted by means of a new pairwise comparison and aggregated to achieve the final fire risk index.

Table 2. Pairwise comparison for the final fire risk index.

| | DI | II | SI | PI | VI |
|---|---|---|---|---|---|
| Detection Index (DI) | 1 | 1/2 | 1/4 | 1/3 | 1/2 |
| Ignition Index (II) | | 1 | 1/3 | 1/2 | 1 |
| Spread Index (SI) | | | 1 | 2 | 3 |
| Protection index (PI) | | | | 1 | 2 |
| Inherent value index (VI) | | | | | 1 |

| | |
|---|---|
| DI | 0.079 |
| II | 0.137 |
| SI | 0.402 |
| PI | 0.244 |
| VI | 0.137 |

CR = 0.007

We can visualize below the look of all secondary indexes and the final fire risk index. The darker red shades illustrate a greater fire risk index.

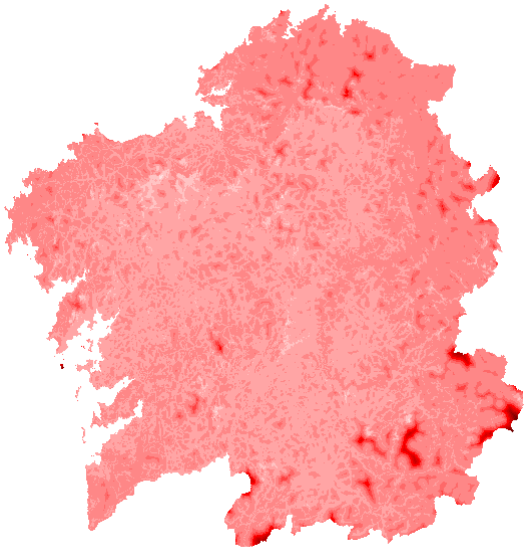

Figure 8. Detection index.

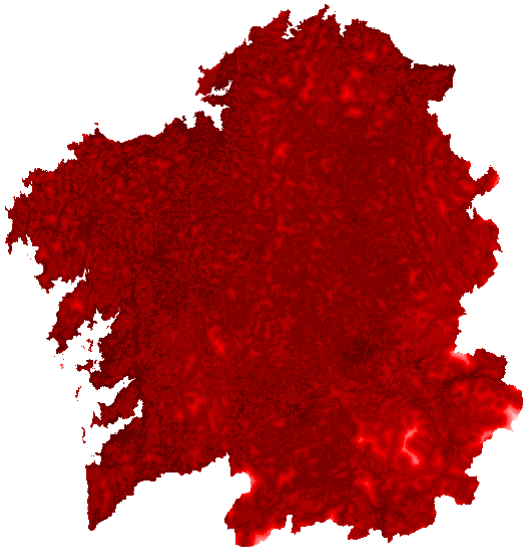

Figure 9. Ignition index.

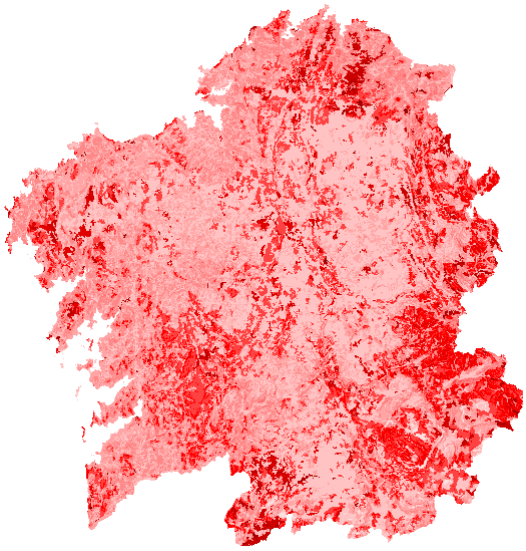

Figure 10. Spread index.

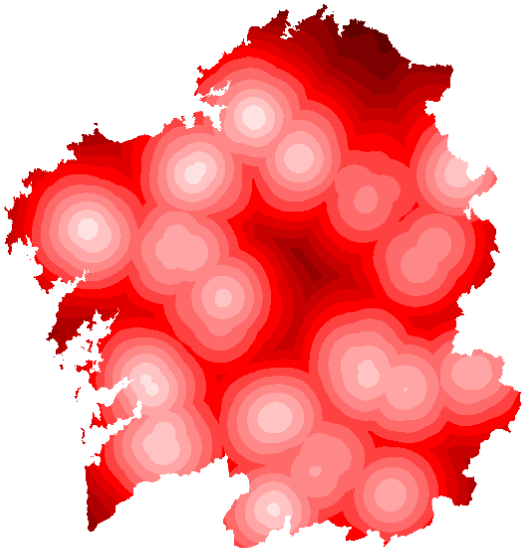

Figure 11. Protection index.

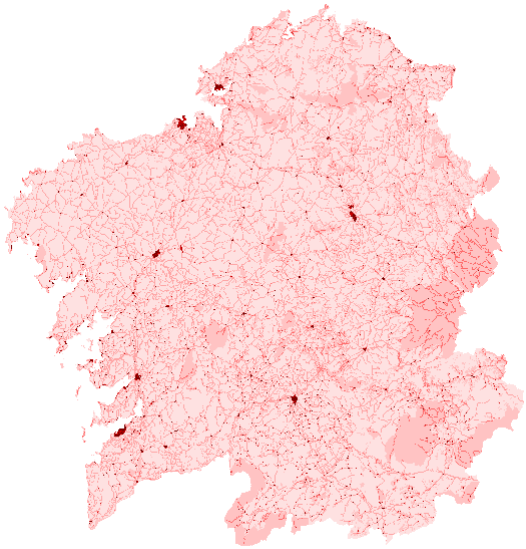

Figure 12. Inherent value index.

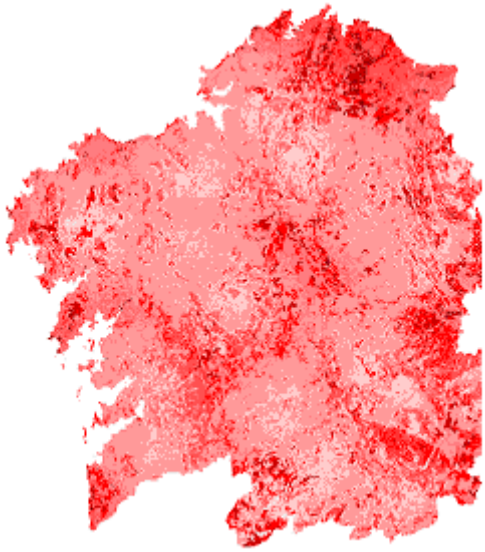

Figure 13. Final fire risk index.

## 4. CONCLUSION

The validation of the risk index leans on 1997, 1998, and 1999 wildfire boundaries. A supervised classification of LANDSAT imagery was accomplished in order to extract these contours. The construction of zonal histograms followed to reveal a spatial pattern of the risk index for the whole region, as well as the yearly distribution of the index for the burned areas. The figure below shows zonal histograms for Galicia and for the burned surface in 1999; the overlay of fire risk index (grey shades) and burned surface (red tone) is also displayed.

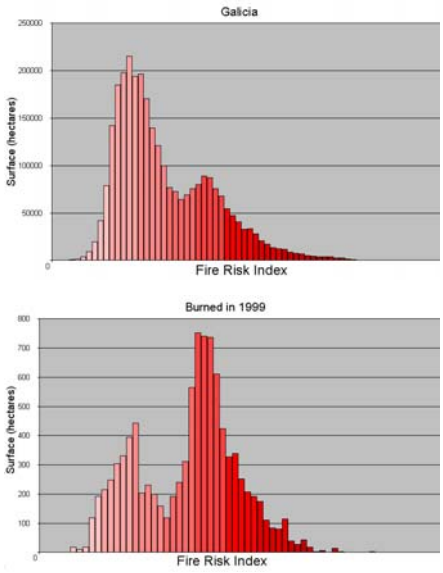


Figure 14. Fire risk zonal histograms.

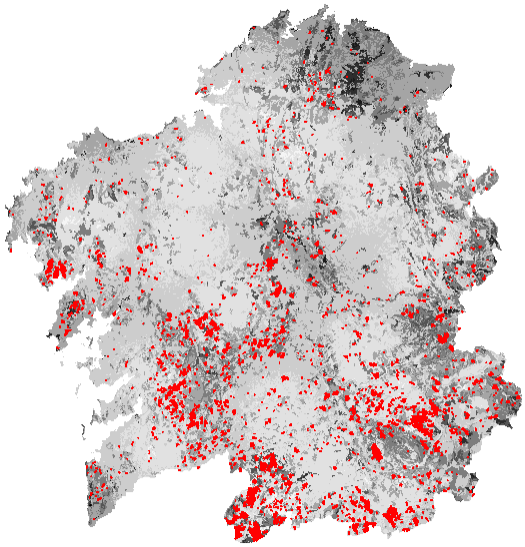

Figure 15. Spatial pattern of risk index & burned area.

As a matter of fact, at the time of writing this paper, the risk index is being used in planning tasks such as vegetation clearing, or firewall and forest trail arrangement. The direct involvement of SDCIF experts in the process (especially, throughout criteria choice and pairwise comparison) makes them quite confident about the index worth.

On the other hand, an integration of the index layers inside the AVL system has been foreseen for the next summer's fire fight campaign. This way, the user will be provided with real time reports about fires and aerial resources evolution. The information offered by the risk index will be completed by current meteorological data (precipitation, temperature, wind, and relative humidity) sent from weather stations hosted by the Natural Environment Department (which spread all over the territory).

In the near future, we intend to upgrade the risk index value collecting new criteria and improving the quality of some of the existing layers. An expert-guided revision of the contribution of all factors is also expected. A final challenge is to incorporate Multiobjective Decision Making (MODM) procedures in order to face a mandatory approach that enables the recommendation of infrastructure tuning.

## 5. REFERENCES

[1] Vélez Muñoz, R. 2000. La defensa contra incendios forestales – Fundamentos y experiencias. Madrid: McGraw-Hill.

[2] Malczewski, J. 1999. GIS and Multicriteria Decision Analysis. New York: John Wiley & Sons, Inc.

[3] ESRI. 1996. Using Avenue – Customization and Application Development for ArcView. Redlands (California): Environmental Systems Research Institute, Inc.

[4] ESRI. 1996. Using the ArcView Spatial Analyst – Advanced Spatial Analysis Using Raster and Vector Data. Redlands (California): Environmental Systems Research Institute, Inc.

[5] Jankowski, P. 1995. Integrating geographical information systems and multiple criteria decision-making methods. International Journal of Geographical Information Systems. Vol. 9, # 3: 251-273

[6] Saaty, T. L. 1990. Multicriteria Decision Making: The Analytic Hierarchy Process. Pittsburgh: Expert Choice Inc.

# Session 4. Burned land mapping

# Fire regimes in protected areas of Sub-Saharan Africa, derived from the GBA2000 dataset

I. Palumbo, J-M. Grégoire, L. Boschetti & H. Eva
*European Commission Joint Research Centre, Ispra, Italy*
jean-marie.gregoire@jrc.it

Keywords: fire regimes, protected areas, SPOT-VEGETATION, Africa

ABSTRACT: Fire is known to play a central role in natural ecosystems of sub-Saharan Africa and its management is of basic importance in protected areas. A SPOT-VGT dataset has been used for the temporal and spatial analysis of three fire parameters during the 1999-2000 period: the length of the fire season, the peak activity period and the area burned per type of vegetation cover. Based on these 3 parameters, the parks have been clustered and regional patterns identified. When considering the length of the fire season, the parks North of the equator are grouped in 3 clusters: most of Western Africa's parks show a burning season distributed over 4 months (November to February); the central Africa's parks show a longer burning season, from November to April; the parks from 22 degrees Eastwards show usually a fire season duration of 6 months (November to April). South of the equator the situation appears much more complex and fragmented.
In terms of the peak period, the Western Africa's parks show a peak of fire activity in the early dry season (November-December). Most of the central Africa's parks show a peak in the second half of the dry season (January-February). South of the equator, one can consider 3 main groups: parks from the Eastern part of the Democratic Republic of Congo and from the neighbouring regions show a peak in May-June; parks in Angola and Western Zambia show a peak in July-August; the third group (Eastern part of Southern Africa) shows a peak in September-October.
The percentage of vegetated area burnt in the parks, regardless of the vegetation cover type, is quite variable: from 1% to 70%. North of the equator, the values range from 15 to 70%; while the range is between 15 to 50% for the parks South of the equator.
Finally, a synthetic index is proposed for providing the park managers with a tool to assess the fire impact on the encroachment dynamics by woody vegetation. South of the equator, 48% of the parks show an index value between 8 and 10 (high encroachment risk), whereas only 9% of them show values of 4 and 5 (medium risk). North of the equator, 21% of the parks show low values of the index (4-5) while 29% have an index value higher or equal to 8.

## 1. INTRODUCTION

Over most regions of the African continent, fires are known to affect significantly the vegetation cover, both in terms of structure and of species composition. The magnitude of the phenomena is particularly large in the protected areas where burning is the technique most commonly used for illegal hunting. Park managers as well as scientists are therefore aware that improving the control of fire practices is one of the key issues in any management scheme for protected areas. There is a need for accurate and quantitative information on the extent of burning, on the vegetation cover affected by burning and on the fire seasonality within the protected areas. However, it is only recently that

continental inventories of vegetation fires have been available (http://shark1.esrin.esa.it). Very few of these inventories provide information on the area actually burnt per type of vegetation cover [Eva and Lambin, 1998; Barbosa *et al*., 1999]. It is in this context that the *Global Burnt Area–2000 initiative* (GBA2000) has been launched by the Global Vegetation Monitoring (GVM) Unit of the Joint Research Centre (JRC) in partnership with several institutions around the world, with as specific objectives to produce a map of the areas burnt globally for the year 2000, using the medium resolution (1 km) satellite imagery provided by the SPOT-Vegetation system and to derive statistics of area burnt per main type of vegetation cover [Grégoire *et al*., 2003]. The present study is based on the analysis and interpretation of the GBA2000 products for assessing the fire regimes in the main protected areas of sub-Saharan Africa.

## 2. METHODOLOGY AND DATA

A data set of 14 months of daily global imagery acquired by the VEGETATION (VGT) instrument, onboard the SPOT-4 satellite, was assembled in the context of the *Millennium Ecosystem Assessment* operation. The acquisitions started on October 20$^{th}$ 1999 and ended on December 31$^{st}$ 2000.

National institutions from 6 countries (Australia, Canada, Italy, Portugal, Russia, and the UK) and two international institutions (JRC and UNEP-GRID) contributed to the GBA2000 project. Seven regional algorithms were developed by the GBA2000 partners and integrated into a global processing chain developed by the JRC [Tansey, 2002]. The African subset of the satellite dataset was processed to burnt area maps using the algorithm developed by Silva *et al*. [2003]. The final version of the global burnt area map, made accessible to the user community in December 2002 [http://www.gvm.jrc.it/fire/gba2000/index.htm], was used in this study. The areas burnt were computed from the number of SPOT VGT pixels classified as being burnt, considering the area covered by the pixel as entirely burned. This is obviously an approximation, as a 1 km$^2$ pixel can be classified as burnt even if the area effectively affected corresponds only to 50% of the area covered by the pixel. However, this approximation is the same for all the protected areas analysed and should not introduce a bias for the analysis, which is done in a relative way.

The UNEP/WCMC [1997] database has been used for the identification of the African protected areas larger than 100000 ha. The resulting 107 areas have been studied in the present work. The information on the vegetation cover type was derived from the University of Maryland's 1km Global Land Cover Product [Hansen *et al*., 2000].

A GIS package dedicated to the post-processing of burnt area products [Palacios-Orueta *et al*., 2002] was used to derive the information required for assessing the fire regimes over the protected areas. Three characteristics of the fire season have been considered: the length of the fire season, the peak of fire activity and the area burnt per type of vegetation cover. To avoid background noise, values of burnt area per month and per vegetation cover type lower than 400 ha (4 pixels) have been excluded from the analysis. Moreover, statistics on burned area have been computed considering only the vegetated area and not the total area of the parks.

## 3. ANALYSIS AND RESULTS

### *3.1 Fire seasonality*

The potential fire season shows usually a 6-months duration: November to April and May to October, for the Northern and Southern hemispheres respectively. Based on the meteorological information provided by the Global Precipitation Climatology Centre (http://www.dwd.de/research/gpcc/e23.html), we have considered three periods of 2 months each starting in November 1999 for the Northern hemisphere and in May 2000 for the Southern

hemisphere: the first period corresponds to the early dry season; the second one shows precipitations lower or equal to 10mm/month; the last period corresponds to the start of the rainy season.

### *3.2 Length of the fire season*

When considering the length of the fire season we refer to the number of periods affected by fire. A period is defined as burned if at least 1 month over the 2 considered is detected as burned.

The parks north of the equator are clearly grouped in three clusters (figure 1a). The Western Africa's parks (from Senegal to the western border of Nigeria), belong to the first cluster, which shows a burning season distributed over 4 months (November to February). A few parks, located in Mali, Burkina Faso, Togo and Nigeria, show a 2 months fire season (November and December). The second cluster corresponds to the parks of Eastern-Nigeria, Cameroon, Chad and the border region with the Central African Republic. They show a longer burning season, lasting from November to April. The third cluster corresponds to the parks from around 22 degrees Eastwards. They show a more variable duration of the fire season: from 4 months (November – February) to 8 months (November-June), with a majority of parks showing a fire season duration of 6 months (November to April).

South of the equator (figure 1b) the situation appears much more complex and fragmented. It is quite difficult to group the parks on the basis of the length of the fire season only. The situation observed in Angola gives a good example of this heterogeneity. The 5 parks considered in this country show 4 different fire seasons: May to August, May to October, May to December and July to October. However in the whole area 2 periods seem to be recurring: the first one is in the central region (Democratic Republic of Congo and part of Zambia); it covers 6 months (May to October). The second one, in the Eastern part of the continent (Eastern Zambia, Eastern-Tanzania, Zimbabwe and Mozambique), is characterised by a shorter fire season: 4-months, from July to October.

### *3.3 Peak of the fire season*

We define the peak-period as the one with the highest values of burned area (expressed in percentage) among the 4 time periods studied.

North of the equator (figure 2a), the parks can be grouped in two categories. The Western African parks belong to the first group (Côte d'Ivoire, Ghana, Togo and Benin). They show a peak of fire activity in the early dry season, during the November-December period. In a sense, this confirms the "western" specificity observed when considering the length of the fire season. In fact, the western cluster which burns "only" during 4 months from November to February corresponds here to the Western exception which shows a peak early in the season, in November-December. The second cluster corresponds to the central Africa region (Eastern-Nigeria, Cameroon, Chad, Central African Republic and Southern Sudan). Most of the parks of the region show a peak of fire activity in the second half of the dry season, during the January-February period. There are few exceptions of peak in the early dry season, during the November-December period, in the border region between the Central African Republic and Sudan, and in the South of Chad. The parks which show a peak during the January-February period correspond largely to the cluster characterized by a long burning season (November to April). These temporal patters are quite important as they certainly help assessing the impact that fires have on the vegetation cover.

South of the equator, the clustering of the parks is less clear than in the North, but one can still consider 3 main groups (figure 2b). Parks from the Eastern part of the Democratic Republic of Congo and from the neighbouring regions show a peak in May-June. In Angola and Western Zambia the peak period shifts to July-August. This reflects the progressive moving of the dry season, South of the Congo basin. The third group includes parks which show a peak later, in September-October. They are mainly located in the Eastern part of Southern Africa: Eastern Tanzania, Eastern Zambia, Zimbabwe, Mozambique, Botswana and South Africa.

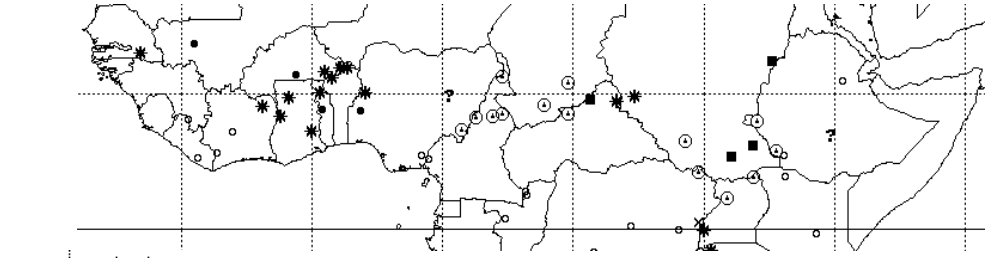

| | |
|---|---|
| ○ | non-burning area |
| ● | Nov99-Dec99 |
| ✱ | Nov99-Feb00 |
| ⊙ | Nov99-Apr00 |
| ■ | Nov99-Jun00 |
| × | Jan00-Apr00 |
| ? | unclassified |

a) 10ºW 0ºE 10ºE 20ºE 30ºE 40ºE 50º E

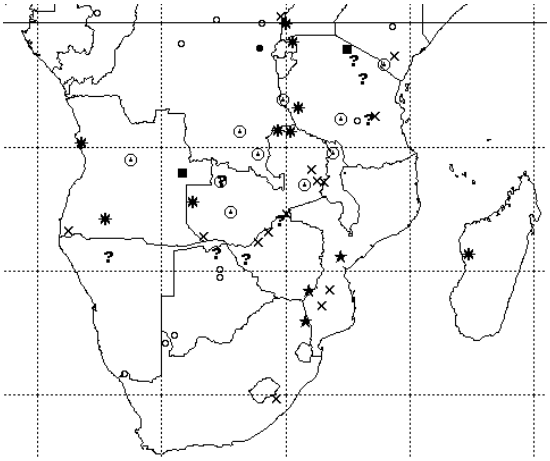

| | |
|---|---|
| ○ | non-burning area |
| ● | May00-Jun00 |
| ✱ | May00-Aug00 |
| ⊙ | May00-Oct00 |
| ■ | May00-Dec00 |
| × | Jul00-Oct00 |
| ★ | Jul00-Dec00 |
| ? | unclassified |

b) 10º E 20º E 30º E 40º E 50º E

Figure 1. Duration of the fire season in the African parks North (a) and South (b) of the equator

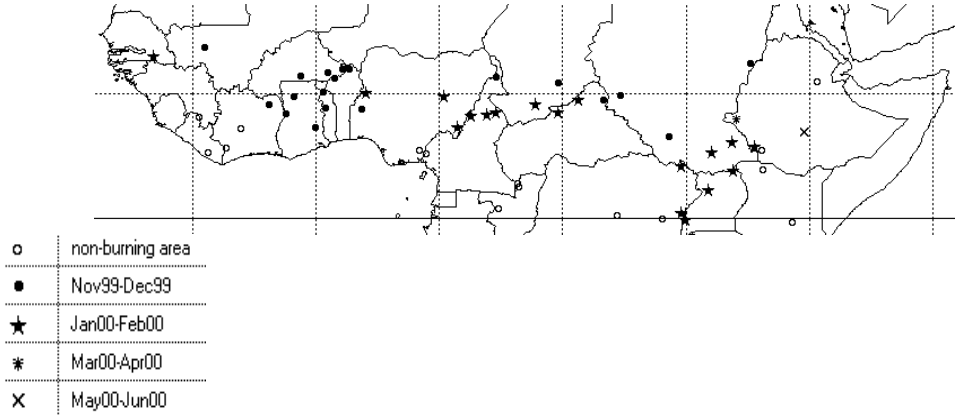


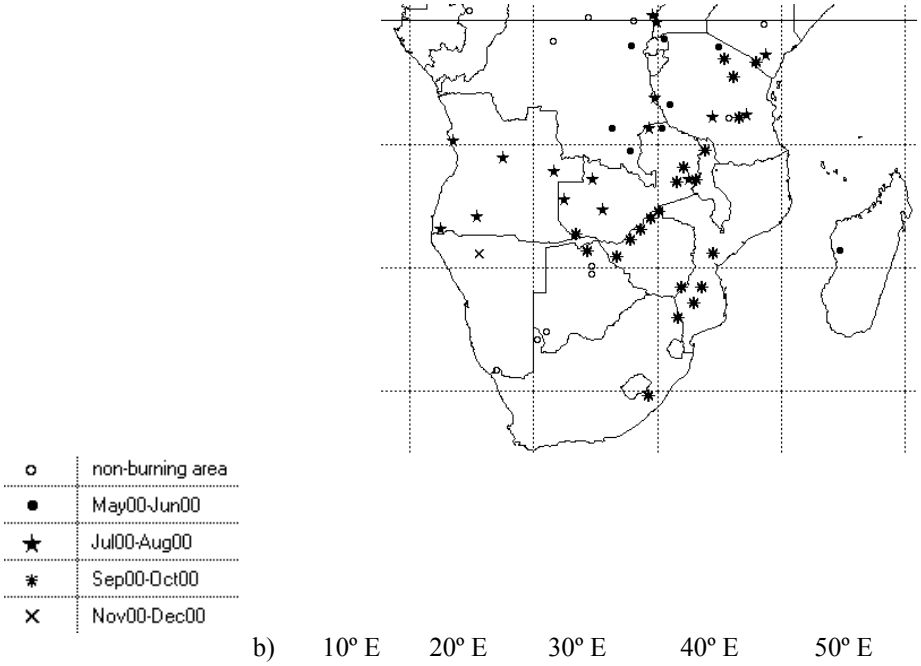


Figure 2. Peak of the fire season in the African parks North (a) and South (b) of the equator

*3.4 Overall burnt area and area burnt per type of vegetation cover*

The percentage of vegetated area burnt in the parks, regardless of the vegetation cover type, is quite variable: from 1% to 70%. The parks North of the equator tend to be more affected, with values ranging from 15 to 70%, while the range is between 15 to 50% for the parks South of the equator. There is a positive correlation between the percentage of area burnt and the length of the fire season. It must be noticed that high percentage values correspond to late season fire-peaks. These observations appear more clearly when considering the type of vegetation cover affected by burning.

As already explained we focused on the major vegetation classes using the UMD's Global Land Cover product. We aggregated the original 13 classes into 3 main categories of vegetation cover.

The *Grassland* category has been obtained by merging the *Cropland* and the *Grassland* classes; the *Shruland* category is composed by *Wooded Grassland, Closed Shrubland* and *Open Shrubland*; the last category considered is the *Woodland* which includes the *Evergreen Needleleaf Forest, Evergreen Broadleaf Forest, Deciduous Needleleaf Forest, Deciduous Broadleaf Forest, Mixed Forest* and *Woodland* classes. Our analysis focused on the impact of fire on *Shrubland* and *Woodland* categories, as the final objective is to assess the encroachment risk by woody vegetation.

*3.5 Area burnt in the woodland category*

The area burned is found to be quite variable but in general terms higher for the parks of the northern hemisphere (figure 3a) than for those of the Southern hemisphere (figure 3b). In the former, at least 5% of the woodland area is affected by burning and many parks show values between 30% and 75%, with a general increase of this percentage from West to East. While most of the parks South of the equator show values between 5% and 30% of the woodland area affected by burning, and even less than 5% for a number of parks. Only three parks have more than 30% of the woodland area burnt.

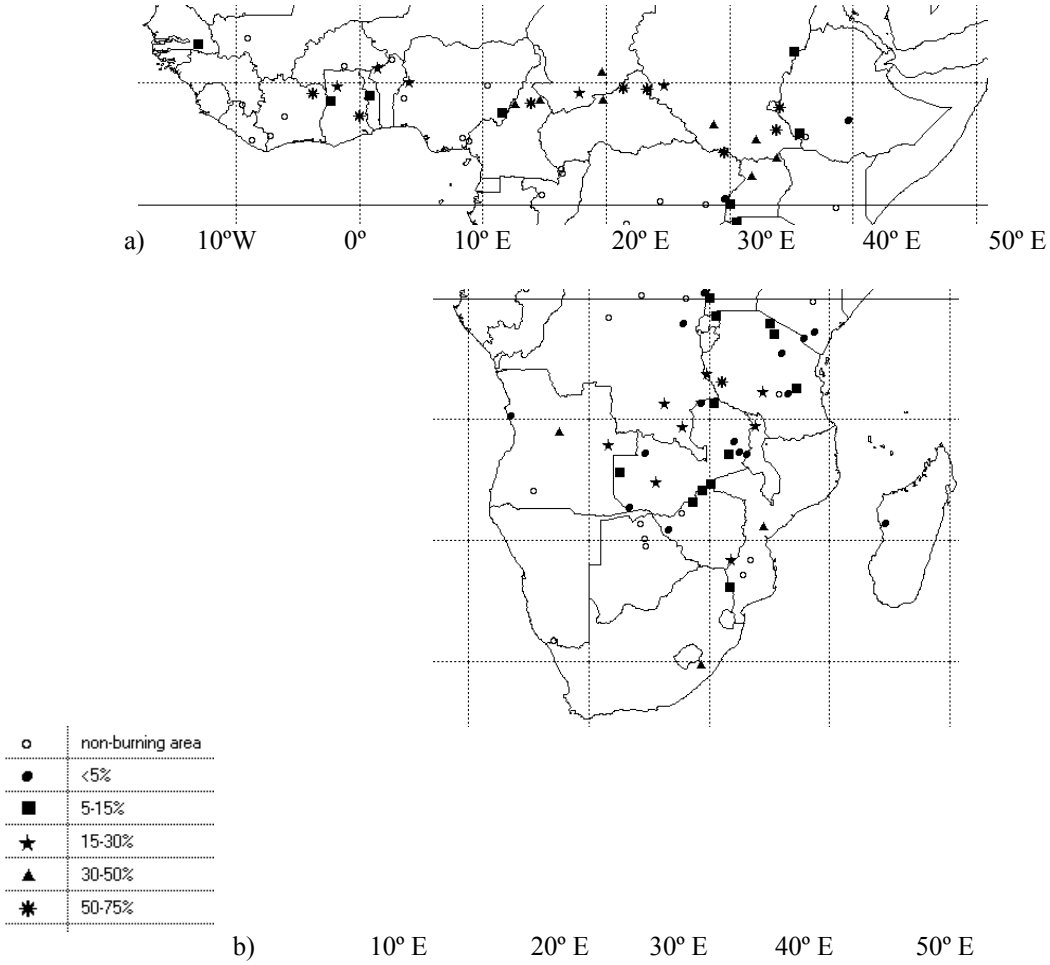


Figure 3. Percentage of the woodland area burnt in the African parks North (a) and South (b) of the equator

*3.6 Area burnt in the shrubland category*

The shrubland category shows more or less the same situation: on average, the percentage of this land cover type which is affected by burning is higher in the parks north of the equator (figure 4a) than in those South of the equator (figure 4b).

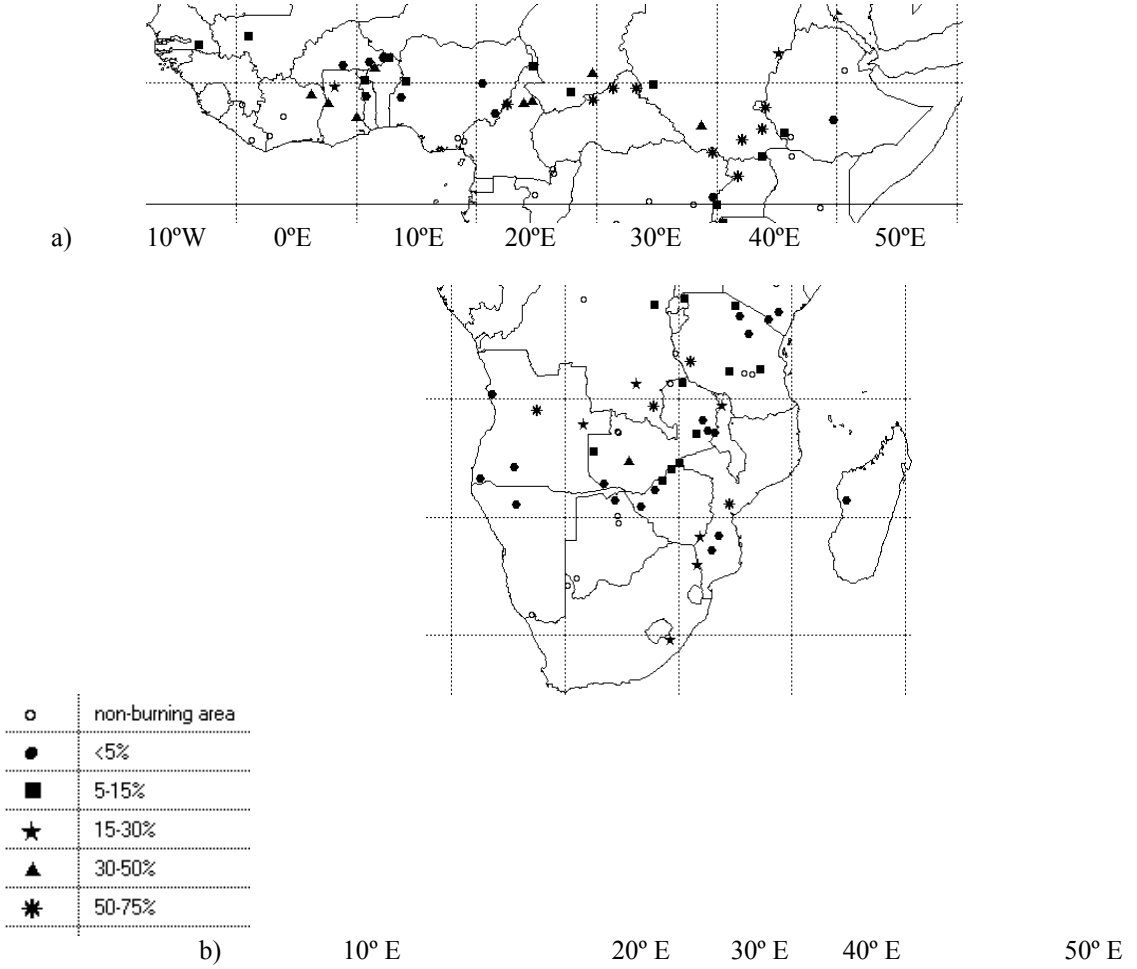


Figure 4. Percentage of the shrubland area burnt in the African parks North (a) and South (b) of the equator

## 4. INDEX OF ENCROACHMENT PROBABILITY

In the previous sections, we have assessed three key characteristics of the fire regimes in the African protected areas: the length of the fire season, the peak period of fire activity and the area burnt per type of vegetation cover. An index is now proposed for providing the park managers with a possibility to assess the fire impact on the encroachment dynamics by woody vegetation. Although other factors, such as the density of herbivores, play a key role in woody encroachment (Van Wilgen and Scholes, 1997), we focus our analysis on the role of fire.

The control of encroachment by woody vegetation is a key issue in park management. For instance, woody expansion shades out the understory forage in the naturally open forest and grassland areas and results in diminished habitat quality for wildlife and livestock. (British Columbia Forest Service, 1998).

Five parameters have been considered (Table 1) with a specific weighting and rating. The peak period of the fire season is probably the main factor influencing the development of the woody vegetation: “late fires” are known to limit considerably the development of trees and shrubs because they have a higher burning efficiency. In a similar way, the smaller the area burnt, the higher the encroachment by woody vegetation.

The index is a linear combination of the five parameters listed above; for each of them we have considered a fixed number of intervals corresponding to a score value, increasing with the risk of encroachment: 8 intervals for the first 2 parameters (length of the fire season and peak period) and 5

for the last three parameters (area burnt, area burnt in the shrubland, area burnt in the woodland). The scores are then normalised and weighted.

Table 1. Fire parameters considered for the *Encroachment Probability Index*

| Parameter | Weight | Score | | | | | | | |
|---|---|---|---|---|---|---|---|---|---|
| **Length** burning season (month) | 0.20 | | | | | | | | |
| **Peak** burning season (top: North; bottom: South) | 0.40 | un | ay | pr | ar | eb | an | ec | ov |
| | | ec | ov | ct | ep | ug | ul | un | ay |
| Total veg. **area burnt (%)** | 0.10 | 0-70 | 0-50 | 5-30 | -15 | -5 | | | |
| **Shrubland area burnt (%)** | 0.10 | 0-75 | 0-50 | 5-30 | -15 | -5 | | | |
| **Woodland area burnt (%)** | 0.20 | 0-75 | 0-50 | 5-30 | -15 | -5 | | | |

The *Encroachment Probability Index* is computed as follows:

$$\mathbf{EP} = \mathbf{L}*a*\text{Weight}_{\mathbf{L}} + \mathbf{P}*a*\text{ Weight}_{\mathbf{P}} + \mathbf{A}*b*\text{ Weight}_{\mathbf{A}} + \mathbf{S}*b*\text{Weight}_{\mathbf{S}} + \mathbf{W}*b*\text{ Weight}_{\mathbf{W}}$$

where
**L** represents the score assigned to the length of the fire season
**P** is the score applied for the peak parameter
**A** represents the score assigned to the total area burned
**S** and **W** represent the scores for the Shrubland and Woodland area burned parameter
a= 10/8 b= 10/5 normalization factors

The index has values ranging from 1 to 10, corresponding respectively to the lowest and the highest probability of encroachment by the woody vegetation. The EP values for each park are presented on Figure 5. It must be noticed that no park shows EP values lower than 4. All non-burning parks have been excluded from the index computation and they are represented as a separate class on Figure 5. Being the index linear in its parameters, parks with different regimes might of course have the same EP value. For instance, the Saint Floris (CAR; 9.53N, 21.36E) and Garamba parks (DRC; 4.25N, 29.63E) show a fire season duration of 4 and 7 months respectively, but the same value of the index [5], which is indicator of a medium level probability of encroachment by the woody vegetation. The reason for that being that the peak of the burning season is in the late dry season for St. Floris Park, while it occurs in the early dry season for Garamba Park. The peak period has a higher weight in the calculation of the index than the length of the burning season; the probability of encroachment by woody vegetation is higher for the early season fires than for those occuring late in the dry season.

The frequency distribution of the 107 protected areas considered in this study (figure 6a) shows that most of them have values between 6 and 8, which corresponds to a medium to high encroachment risk; two of them reach the highest possible value of the index. High as well as low values are reached by the same number of parks. A comparison between the situation North and South of the equator (figures 6b and 6c) shows that most parks with a high index value are located in Southern Africa. South of the equator, 48% of the parks show an index value between 8 and 10, whereas only 9% of them show values of 4 and 5. The situation at North appears quite different: 21% of the parks show low values of the index (4-5) while 29% have an index value higher or equal to 8.

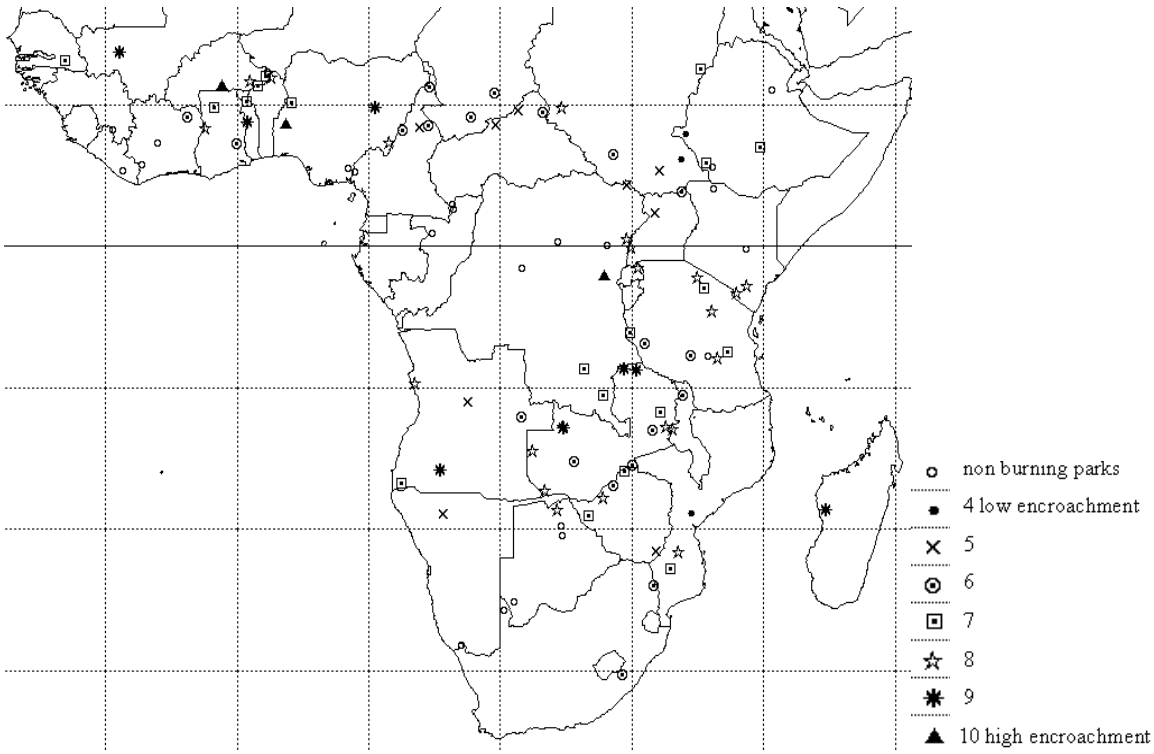


Figure 5. EP index value, computed for the 1999-2000 burning season, for the 107 protected areas

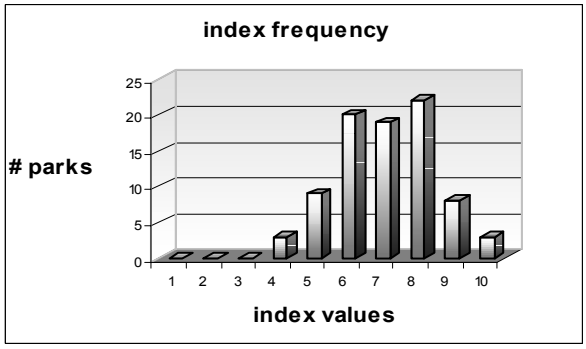


(a)

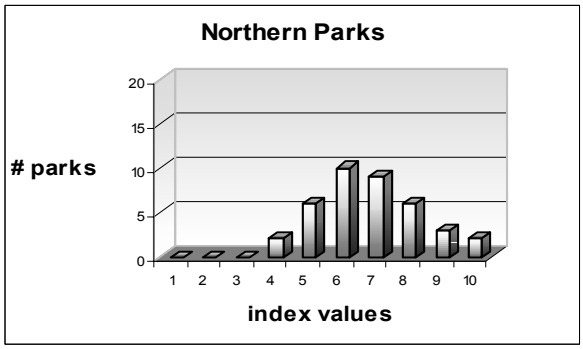


(b)

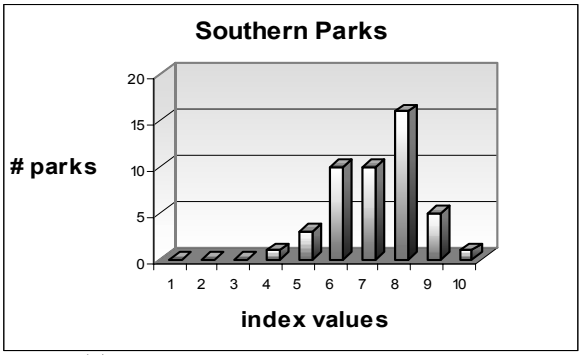


(c)

Figure 6. Frequency distribution of the 107 protected areas as a function of the Encroachment Index: all parks (a), parks north of the equator (b) and South of the equator (c)

## 5. CONCLUSIONS

The present study aimed at analysing and interpreting the GBA2000 products for assessing the fire regimes in the main protected areas of sub-Saharan Africa. A GIS package dedicated to the post-processing of burnt area products was used to derive, for the 1999-2000 fire season, three parameters representing the length of the fire season, the peak period of fire activity and the area burnt per type of vegetation cover for a selection of 107 protected areas.

When considering only the length of the fire season, the parks North of the equator are clearly grouped in 3 clusters with variable fire-duration: from 4 to 6 months. South of the equator, the situation appears much more complex or fragmented.

When considering the peak-activity period, the analysis shows that the parks North of the equator are divided into 2 groups with peak in the early and late dry season; a correspondence with the clusters from length of fire season analysis is noticed for Western and Central African parks.

In terms of total area burned, higher values are found in the Northern hemisphere where maximum values reach the 70% whereas in the South they do not exceed 50%.

Finally an encroachment risk index has been introduced as a synthetic representation of the three parameters previously presented. The objective being to provide the park managers with a tool for fire management. The protected areas north of the Equator show lower values of encroachment risk than those in the Southern region. It must be noticed that this preliminary version of the encroachment index is built on fire related parameters with empirical weights which will improved in future work. Moreover, rainfall data and longer time-series of fire information should be used for a better understanding of the fire temporal dynamics per type of vegetation cover and for an improved assessment of the risk of encroachment by woody vegetation. Last but not least, the availability of medium resolution (250 m) maps of burnt area and land cover type would greatly increase the quality and usefulness of this fire related encroachment index. Future work will be done to test the possibilities offered by the medium resolution satellite imagery (TERRA-MODIS and ENVISAT-MERIS).

## 6. ACKNOWLEDGEMENTS

The GBA2000 dataset would not be a reality without the contribution of all the co-investigators in the development of the regional algorithms and the constant effort of Kevin Tansey to develop the global burnt area products. The authors would also like to acknowledge Steffen Fritz for his support in the spatial analysis and Philippe Mayaux for his contribution to the reflection on parks management.

## 7. REFERENCES

Barbosa, P.M., Stroppiana, D., Grégoire, J-M. & Pereira, J.M.C. 1999. An assessment of vegetation fire in Africa (1981-1991): burned areas, burned biomass and atmospheric emissions. *Global Biogeochemical Cycles*, 13(4): 933-950.

British Columbia Forest Service. 1998. http://www.for.gov.bc.ca/research/ecoearth/ordroad/ingrow.htm

Eva, H. & Lambin, E.F. 1998. Burnt area mapping in Central Africa using ATSR data. *International Journal of Remote Sensing* 19(18): 3473-3497.

Grégoire, J-M., Tansey, K. & Silva, J.M.N. 2003. The GBA2000 initiative: Developing a global burned area database from SPOT-VGT imagery. *International Journal of Remote Sensing* 24(6): 1369-1376.

Hansen, M., DeFries, R., Townshend, J. R. G. & Sohlberg, R. 2000. Global land cover classification at 1km resolution using a decision tree classifier. *International Journal of Remote Sensing* 21:1331-1365.

Palacios-Orueta, A., Parra, A. & Chuvieco, E. 2002. *FUEGO II Project - Development of Global Fire Analysis GIS Modules – Technical Report*. University of Alcalà, Spain.

Silva, J.M., Pereira, J.M., Cabral, A.I., Sà, A.C., Vasconcelos, M.J., Mota, B. & Grégoire, J-M.. 2003. An estimate of the area burned in southern Africa during the 2000 dry season using SPOT-VEGETATION satellite data. *Journal of Geophysical Research* in press.

Tansey, K. 2002. Implementation of regional burnt area algorithms for the GBA2000 initiative, *Publications of the European Commission* (20532), Luxembourg.

UNEP/ WCMC. 1997. *Digital Chart of the World (DCW)*; scale 1:1'000'000.

van Wilgen, B.W. & Scholes, R.J. 1997. *The Vegetation and Fire Regimes of Southern Hemisphere Africa. Fire in Southern african Savannas, Ecological and Atmospheric Perspectives*. Edited by BW van Wilgen, MO Andreae, JG Goldammer, JA Lindesay. Witwatersrand University Press.

# Assessing vegetation condition through biomass burning smoke by applying the Aerosol-Free Vegetation Index (AFRI) on SPOT-VEGETATION and TERRA-EOS MODIS images

E. Ben-Ze'ev, A. Karnieli
*Remote Sensing Laboratory, Jacob Blaustein Institute for Desert Research, Ben-Gurion University of the Negev, Israel*
benzeev@bgumail.bgu.ac.il

Y. Kaufman
*NASA/GSFC Greenbelt, MD, USA*

Keywords: AFRI, smoke, biomass burning, SPOT VEGETATION, MODIS

ABSTRACT: The Aerosol Free Vegetation Index (AFRI) is based on the correlations between SWIR spectral bands and the visible red spectral band and its main advantage is in penetrating an opaque atmosphere influenced by biomass burning smoke. The index was employed on SPOT-VEGETATION and TERRA-EOS MODIS images in order to assess its functionality on low-resolution satellite sensors. For both 1X1 km spatial resolution images the index showed moderate results and thus a mathematical correction was proposed and when employed, showed better AFRI values. We assume that the index's primary values were influenced by the atmosphere and by the satellite viewing zenith angle.

## 1. INTRODUCTION

Previous studies revealed high correlations between the SWIR 1.6 and 2.1μm spectral bands and the visible blue, green, and red spectral bands (Kaufman and Remer, 1994; Kaufman *et al*., 1997). These correlations led to linear relationships, such as $\rho_{0.469} = 0.25\rho_{2.1}$; $\rho_{0.55} = 0.33\rho_{2.1}$; $\rho_{0.645} = 0.5\,\rho_{2.1}$; and $\rho_{0.645} = 0.66\,\rho_{1.6}$, where ρ is the ground reflectance and 0.469, 0.55, and 0.645 are the blue, green, and red wavelengths, respectively, were found to be significant and consistent with previous findings(Karnieli, 2001). Based on these relationships, a modified vegetation index, namely Aerosol-Free Vegetation Index (AFRI) was proposed. Two versions of the index were formulated:

$$AFRI_{1.6} = (\rho_{NIR} - 0.66\rho_{1.6})/(\rho_{NIR} + 0.66\rho_{1.6}) \quad (1)$$

and

$$AFRI_{2.1} = (\rho_{NIR} - 0.5\rho_{2.1})/(\rho_{NIR} + 0.5\rho_{2.1}) \quad (2)$$

where NIR (near infrared) is the 0.8μm band. Like other vegetation indices, such as the Normalized Difference Vegetation Index (NDVI), AFRI was proven to be sensitive to the green, photosynthetic active vegetation. However, its advantage is penetrating an opaque atmosphere influenced by biomass burning aerosols. Consequently, it produces a realistic vegetation condition image.

Under clear sky conditions the AFRI, especially the $AFRI_{2.1}$, closely resembles the NDVI. The values of both indices are almost identical (Karnieli et al., 2001). It is thus possible to assess vegetation conditions without using the visible bands that are more sensitive to atmospheric scattering. The index was tested on an image of Cuiábá, Brazil, taken during the Smoke Clouds and Radiation –

Brazil (SCAR-B) experiment by the airborne hyperspectral imager - Airborne Visible/Infrared Imaging Spectrometer (AVIRIS). Implementation of the AFRI on the image gave true vegetation values for the vegetated area covered by biomass burning smoke.

Due to its accomplishment we decided to check the index's performance from a higher orbit. Two sensors with the SWIR bands were chosen. The SPOT VEGETATION (VGT) and the Moderate Resolution Imaging Spectroradiometer (MODIS) onboard Terra-EOS. . The former has a 1.6 μm band while the latter has both 1.6 and 2.1μm bands.

## 2. METHODS

Several sets of VGT and MODIS images were investigated. Fire sites were located using the Global Burnt Area – 2000 initiative web site (http://www.grid.unep.ch/activities/earlywarning/preview/ims/gba/test.htm) and smoke was verified using the Aerosol Robotic Network (AERONET). Among these, a VGT image of a boreal forest fire in the Virginia Hills, central Canada, during the spring of 1998, characterized by large smoke plumes (Fig. 1) and a MODIS image of the Rodeo-Chdiski forest fire in Arizona during June-July 2002. Since NDVI has a major disadvantage over areas of biomass burning smoke, and AFRI was found not to work properly over water bodies and snow, a combined use of the two VIs was done on the VGT image. Due to a moderate correlation between the red and SWIR channels, a correlation was performed between the two VIs in order to calculate their offset.

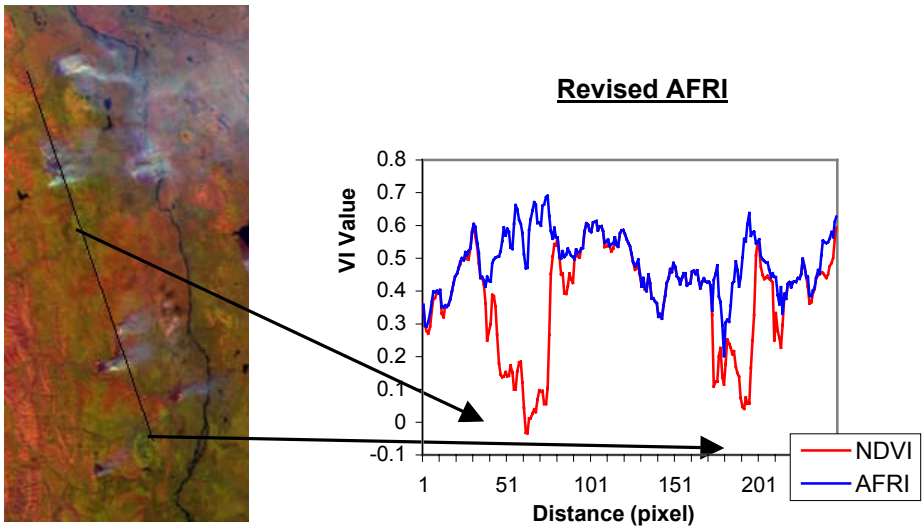


Figure 1. A False-color composite image (RGB=SWIR, B3, B0) of the fires at Virginia Hills (Canada) with a cross-section over vegetation and smoke covered areas. The arrows show the smoke covered pixels. The graph on the right illustrates the large fluctuations in the NDVI along the cross-section due to the smoke. Note the generated upper envelope, which was formulated and uses the high AFRI values on the smoke-contaminated pixels.

This correlation was done using smoke-free pixels, which constituted 60% of the sampled pixels. The offset from the linear relationship between the indices was then used for calculating the Revised AFRI by adding it to the AFRI value for every pixel. This procedure was applied to match the AFRI values with those of the NDVI over smoke-free areas. However, in the smoke-affected areas, where the NDVI values drop, the AFRI values were used instead and functioned as an envelope (Fig. 1). The procedure was further tested on the satellite image, using Integrated Design Language

(IDL) programming on the Environment for Visualizing Images (ENVI) software, in order to restore it and to enhance vegetation signals beneath smoked areas. Fig. 2 shows the NDVI, AFRI and Revised AFRI images generated from the raw image.

Fig 3. shows a similar method of smoke free pixels which was used with the Level 1B MODIS image.

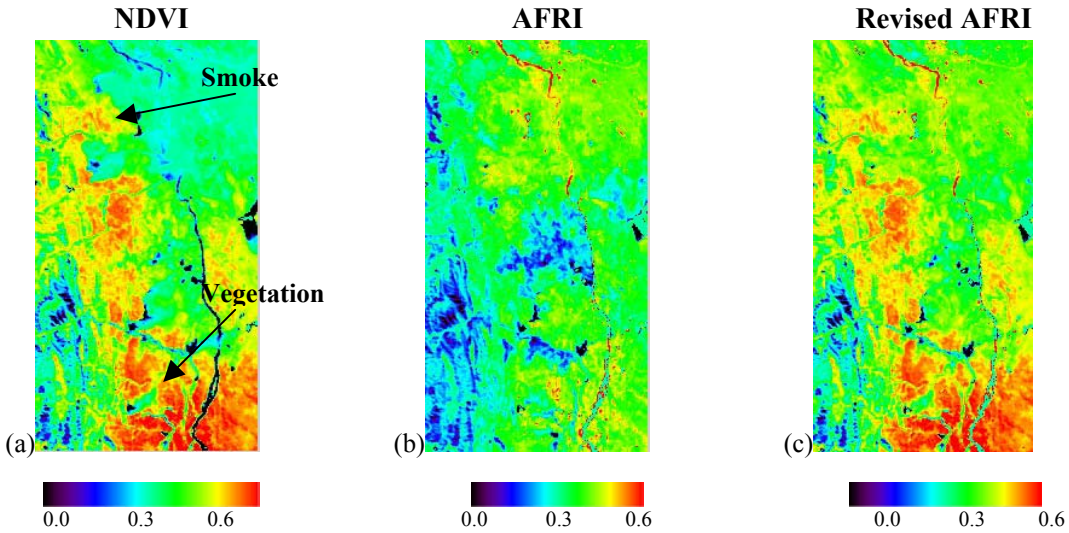


Figure 2. (a) A colored NDVI image. Note the light blue hues at the upper right corner of the image, which represent the smoke. (b) A colored AFRI image. The index penetrated the smoke but did not give correct vegetation values as seen at the bottom right side of the figure. (c) The Revised AFRI procedure managed to penetrate the smoke and at the same time calculate the high vegetation values.

## 3. RESULTS AND CONCLUSIONS

The Aerosol Free Vegetation Index was formulated and tested on the Airborne Visible/Infrared Imaging Spectrometer and showed promising results. When tested with the VEGETATION and the MODIS instruments, the index did not manage to present vegetation values equal to the NDVI values although it did penetrate the smoke. We suspect that the difference between the NDVI and the AFRIare due to the influence of the atmosphere (the level 1B does not undergo an atmospheric correction) as well as the influence of the sensors viewing angle (Gatebe et al., 2001). However, by employing the new procedures in conjunction with the AFRI, better results were achieved. The revised index managed to penetrate the biomass burning smoke and to show a true vegetation-condition value through both images.

We conclude that the AFRI index and its revised predecessors can aid in monitoring vast areas of vegetation during periods of a smoke contaminated atmosphere. Airborne sensors can use the AFRI as is, whereas for low-resolution spaceborne platforms such as the SPOT VGT and the MODIS the revised AFRI may produce better results.

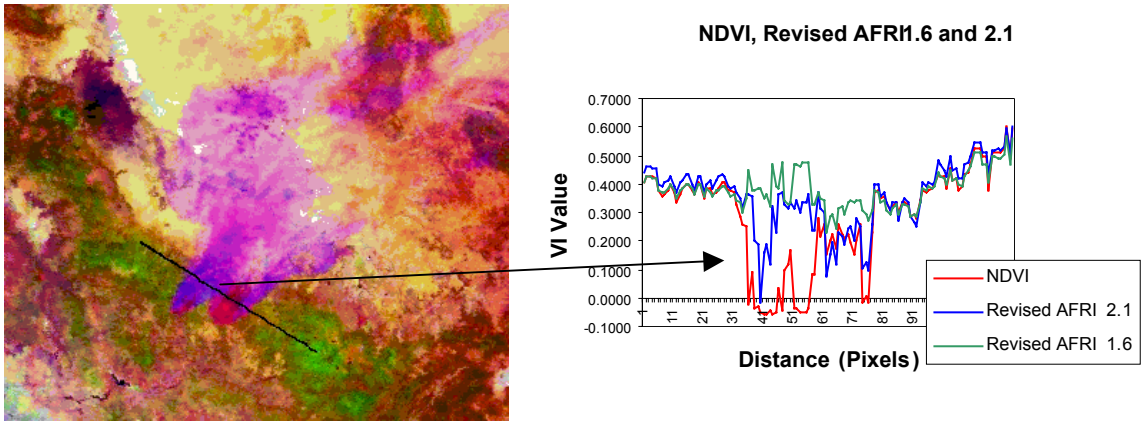


Figure 3. A MODIS false color (RGB=SWIR, NIR, blue) image of the Rodeo-Chedeski fire, June 2002, with a cross-section over vegetated and smoke contaminated areas. The graph on the right illustrates the VIs values along the cross-section. Note the drop in NDVI value (arrow) due to the smoke, whereas the AFRIs maintain higher values because of their ability to penetrate the aerosols. The drop in AFRI2.1 values is assumed to occur due to the wavelength's proximity to the thermal emission from the fire.

## 4. REFERENCES


Gatebe, C. K., King, M. D., Tsay, S. C., Ji, Q., Arnold, G. T., and Li, J. Y. (2001). Sensitivity of off-nadir zenith angles to correlation between visible and near-infrared reflectance for use in remote sensing of aerosol over land. *IEEE Trans. Geosci. Remote Sens.* **39**(4): 805-819.

Karnieli, A. (2001). AFRI - Aerosol Free Vegetation Index. *Remote Sensing of Environment*, 77, 10-21.

Kaufman, Y.J. and Remer, L.A. (1994), Detection of forests using mid-IR reflectance - an application for aerosol studies. *IEEE Trans. Geosci. Remote Sens.* 32: 672-683.

Kaufman, Y.J., Wald, A.E., Remer, L.A., Gao, B.-C., Li, R.-R., and Luke, F. (1997), The Modis 2.1-µm band correlation with visible reflectance for use in remote sensing of aerosol. *IEEE Trans. Geosci. Remote Sens* . .1298-1286 ,35

SPOT IMAGE, VEGETATION Overview
http://www.spotimage.fr/data/images/vege/vegetat/ book_1/1/11/e11a.htm

Joint Research Center European Commission, Global Burnt Area 2000 Project
http://www.grid.unep.ch/activities/earlywarning/preview/ims/gba/test.htm

# Hemispheric fire activity characterization from the analysis of global burned surfaces time series (1982-1993)

C. Carmona-Moreno & J.P. Malingreau
*European Commission, Joint Research Centre, Ispra (VA), Italy*
cesar.carmona-moreno@jrc.it

M. Antonovski
*Institute of Global Climate and Ecology, Moscow, Russia*

V. Buchshtaber & V. Pivovarov
*National Research Institute of Physical-Technical and Radiotechnical Measurements, Moscow, Russia*

Keywords: global burned surfaces time series, spatio-temporal analysis, global fire activity seasonality.

ABSTRACT: The Earth Observation data appear as a good opportunity for the Global Change Community for the analysis of global phenomena having an important impact in this issue. In this way, this paper proposes the analysis of a long time series of global burned surfaces detected from NOAA-AVHRR-8km data at low resolution (from January 1982 to December 1993) for the characterization of the global fire activity seasonality (average seasonal cycle and the inter-annual variability). The analysis of this data at global scale allows a spatial decomposition of the phenomenon: Northern hemisphere presents a stable behaviour of the seasonal cycle in contrast with the Southern fire activity that is characterised by important high frequencies and instabilities; local and absolute seasonal peaks are identified for each hemisphere; and, have been detected a quasi-biennial periodicity in the Southern Hemisphere that could be correlated with the Southern Oscillation episodes.

## 1. INTRODUCTION

Some experts (Andreae, 1991; Crutzen & Carmichael, 1993) consider CO2 emissions as a result of fires in savannas (these represent about 45% of the global burned biomass a year) have little impact on the atmospheric CO2 concentration trend, the justification being that a similar amount of the CO2 emitted returns from the atmosphere back to vegetation during re-growth. However, other products-emissions from this fire activity remain in the atmosphere for a long period influencing the "greenhouse process". Additionally, some vegetation classes that burn do not reabsorb CO2 in a short period (for example, boreal and temperate forests), and therefore, the CO2 and other gases emitted into the atmosphere might participate in the "greenhouse process" for decades, even centuries. The fluctuation of the global biomass burning (excluding savannas contribution) could be the origin of the disturbance of global carbon cycle on the scale of several years. On long time scales (several hundreds of years), the contribution of the biomass burning could be neglected only if the burned surfaces (land use/cover) would not be anthropogenicaly affected during this temporal cycle, but this is not the case in the industrial and maximisation exploitation context of the natural resources nowadays. In this perspective, regular computations of global burned surface maps play a doubly important role: first, to identify geographical areas affected by the global fire activity, establishing spatio-temporal fire risks and frequencies (fire activity seasonality) that will allow to spatially decompose this phenomenon, this paper deals with these aspects; and, second, to estimate atmospheric CO2 – CO emissions from burned surfaces and their inter-relationships.

Remote sensing appears as a unique opportunity to study and characterize the spatio-temporal dynamics of this phenomenon at global scale (Malingreau et al., 1995). So far, little is known about

biomass burning from remote sensing at global or continental scale and only some few works deal with this thematic at this level (Moreno-Ruiz et al., 1999; Dwyer et al., 2000; Barbosa et al., 1999). In this way, Dwyer et al. (2000) listed global inventories of the active fires on the basis of a limited number of NOAA-AVHRR remote sensing data (from April 1992 to March 1993) with 1.1 by 1.1 $km^2$ of resolution. In terms of global change, these data have considerable constraints for characterizing standard biomass burning behaviours: first and main reason, the analysis covers a too much short period of time (13 months); second, the period considered corresponds to an anomaly of the global fire activity (see Fig. 1); and, third, active fire maps issued from an EO instrument with a one day pass represent a limited way to characterize spatio-temporal behaviour of the global fire activity because of the intrinsic characteristic of such data acquisition system and the phenomenon.

This paper deals with the characterisation of the global fire activity seasonality (average seasonal cycle and the inter-annual variability) from a long time series of global burned surfaces detected from NOAA-AVHRR-8km data at low resolution (from January 1982 to December 1993).

## 2. MATERIALS AND METHODS

A new weekly satellite Earth Observation product called Global Burned Surface Map (GBS) (Moreno-Ruiz et al., 1999) to produce time series (from 1982 to 1993) provide us with an opportunity to better understand the global fire activity phenomenon.

The burned surface detection algorithm implemented for obtaining burned surface maps uses NOAA-AVHRR remote sensing data based on a weekly composite data set. The algorithm is a global extension of the multi-temporal multi-threshold algorithm developed for the Africa continent by (Barbosa et al., 1999). The Global Burned Surfaces (GBS) maps obtained by the application of the algorithm have been decomposed in two time series, one per hemisphere: Southern Burned Surfaces (SBS) and Northern Burned Surfaces (NBS).

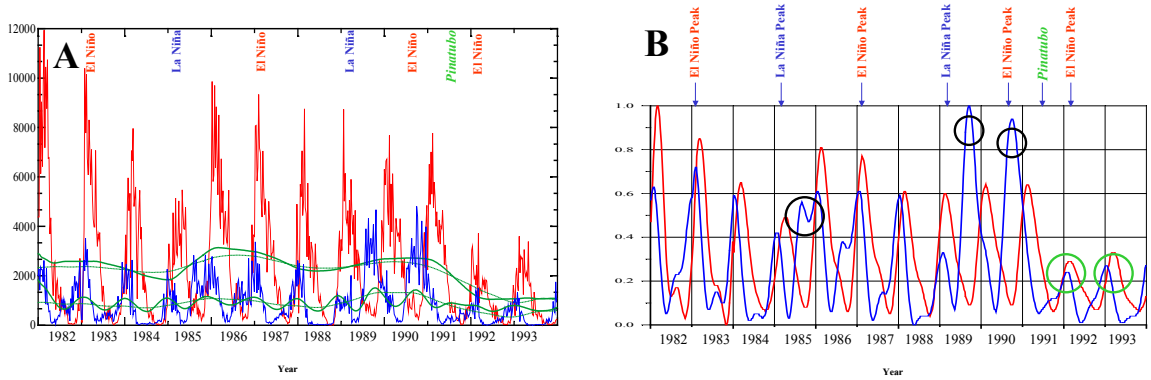


Figure 1. GBS time series decomposed in NH (red line) and SH (blue line) components (NBS and SBS, respectively). (**A**) Green lines represent the trends on different time basis (solid lines correspond with 1 year and dashed lines with two years). (**B**) represents the normalized and smoothed quantity of burned surface for each hemisphere. Black circles show the time period in which the usual SH annual local maximum (Fig. 2A) becomes an unusual annual absolute maximum. These anomalies are probably connected with exceptional climatic episodes. The green circles show the years affected by the Mount Pinatubo eruption occurred in June 12-16, 1991 at 15°08'N lat, 120°21'E long.

The study presented in (Moreno-Ruiz et al., 1999) concluded that the main spatial and temporal patterns of fire activity at global scale are clearly depicted by the data set used in this paper. GBS time series has been developed for global fire activity behaviour analysis and research purposes, but caution should be exercised when interpreting the GBS time series on a quantitative basis because of the coarse spatial resolution of the EO data used (NOAA-AVHRR 8km).

From the analysis of these data, we deduce the inter-annual variability and the average seasonal cycle of the fire activity for each hemisphere (Fig. 1, A and B). The trends (see green lines in Fig.1A)

were obtained by decomposition of the original GBS time series reconstructed from 5 principal components using the multidimensional unfolding method (Buchstaber, 1994) for both hemispheres. The green solid lines correspond with the reconstruction base equal to 52 weeks (1 year) and the green dashed lines correspond with the reconstruction base equal to 104 weeks (2 years).

The NH and SH Fire Activity average seasonal cycles were obtained by the Tukey's method (Buchstaber, 1994) based on median filter (one year step) with a 9 degree smoothing polynomial function. In order to obtain a representative standard seasonal cycle, years with evident anomalous behaviours (1985, 1989, 1990) were removed from this analysis. Both curves (Fig. 2A) present clear absolute peaks/maxima located (green circles) in December-January-February and in February-March (SH and NH, respectively) with two small local peaks/maxima located (black circles) in July-August-September and May-June-July (SH and NH, respectively).

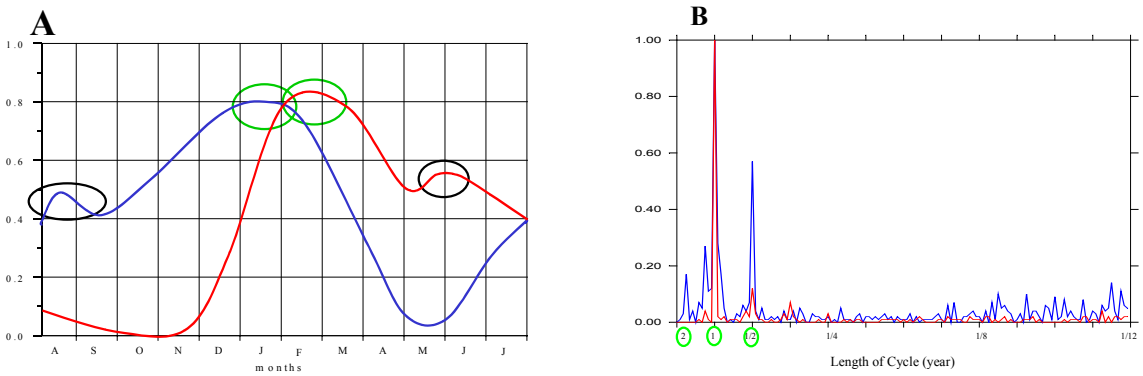


Figure 2. Normalized Fire Activity average seasonal cycle for the period 1982-1993 and Periodgram. (A) The red curve represents the NH Fire Activity average seasonal cycle and the blue curve the SH Fire Activity average seasonal cycle. (B) The frequencies were computed using the Fourier Transform of the GBS time series. The curve in red represents the frequencies obtained for the NBS time series and the curve in blue those for the SBS.

## 3. RESULTS AND CONCLUSIONS

The Northern fire activity presents a stable behaviour (low frequencies are predominant) of the seasonal cycle in contrast with the Southern fire activity which is characterised by important high frequencies, as we see in the periodgram of the Fig 2B. In this figure, we also observe an important 1 year-seasonal component (Fig. 2B) for both hemispheres with a small 0.5 year periodicity component.

In Fig 2A, we see a clear peak around January-February-March in the Northern hemisphere produced by a major contribution of the fire activity in the northern tropical areas (Fig. 3). This hemisphere is also characterized by a local maximum occurring during the early summer period (May-June-July) at medium Northern latitudes (Fig. 2A and 3). Although the Southern fire activity presents a much more complex behaviour with high frequency effects (Fig. 2B), we can also clearly identify the absolute maximum usually occurring in December-January-February at the low Southern latitudes and the local maximum occurring during July-August-September at the medium-low Southern latitudes. These elements would allow the scientist to further spatially decompose the phenomena.

For this hemisphere, a quasi-biennial component is clearly identified in Fig 2B. This quasi-biennial component of the SBS periodgram (Fig. 2B) would reinforce the hypothesis of correlation between the also quasi-biennial occurrences of the ENSO phenomena (Ropelewski et al., 1992) during the considered period (Fig. 1). These results would highlight the sensitivity of the coupled ocean-atmosphere phenomena in the forming of fire activity in the SH. Further analyses are needed to confirm this hypothesis.

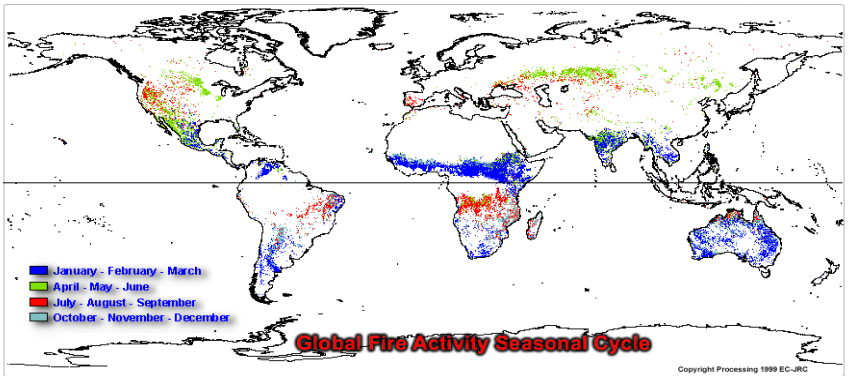


Figure 3. Global Fire Activity Seasonal Cycle. This figure represents the seasonal distribution of the fire activity obtained from the averaged spatio-temporal distribution of the Global Burned Surface (GBS) products for the period 1982-1993.

## 4. REFERENCES


Andreae M.O., Biomass burning: Its history, use, and distribution and its impact on environmental quality and global climate, in Global Biomass Burning, Atmospheric, Climatic and Biosphere Implication, (MIT Press, edited by J.S. Levine, Cambridge, pp.3-21, Mass., 1991).

Barbosa, P.M., Stroppiana, D. and Gregoire, J.M., An assessment of vegetation fire in Africa (1981-1991). Burned areas, burned biomass and atmospheric emissions. International Journal of Global Biogeochemical Cycles 13, N4, pages 933-950, (1999).

Buchstaber, V.M., Time series analysis and grassmanians, Transactions of the American Mathematical Society (2) Vol. 162. 1-17 (1994).

Crutzen, P.J. & Carmichael. G.R. in Fire in the Environment: Its Ecological, Climatic and Atmospheric Chemical Importance, edited by Goldammer, J.G. Publisher Wiley, John & Sons, Incorporated, NY, July (1993)

Dwyer, E., Pinnok, S, and Gregoire, J.-M., Global spatial and temporal distribution of vegetation fire as determined from satellite observations. International Journal of Remote Sensing. 21, No6&7,1289-1302 (2000).

Malingreau, J.P. , Zhuang, Y.H., Biomass burning: an ecosystem process of global significance in Proc. IGBP-SAC Conference Asian Change in the context of Global Change. Beijing, October (1995).

Moreno-Ruiz, J.A., Barbosa, P.M., Carmona-Moreno, C., Gregoire, J.M., Belward,A.S., "GLINTS-BS – Global Burn Scar Detection System". European Union Technical Note I.99.167. May (1999).

Ropelewski C. F., Halpert M. S. & Wang X., Observed Tropospheric Biennial Variability and Its Relationship to the Southern Oscillation. Journal of Climate, vol. 5, 594-614 (1992).

# Assessment of the potential of the SAC-C/multispectral medium resolution scanner (MMRS) imagery for mapping burned areas

M. García and E. Chuvieco,
*Department of Geography, University of Alcalá, Madrid, Spain*
mariano.garcia@uah.es

Keywords: burned areas mapping, SAC-C/MMRS, spectral indices

## 1. INTRODUCTION

Forest fires constitute a critical hazard in Mediterranean countries, since they cause important ecosystem and social damages. The number of fires has increased considerably in the last decades, thus the average number of fires as well as the burned areas is nearly twice as many as during the 1970s (Alexandrian et al., 1999). Despite the high incidence of fires in the Mediterranean basin, there is a lack of homogeneity of both, the burned area statistics, as a consequence of the different methodologies employed by each country (Barbosa et al., 2001; Vélez, 1991), and an adequate cartography of burned areas, which hampers an accurate estimation of the affected areas.

Remote sensing constitutes a valuable tool for burned areas mapping, providing spatial and timely assessment. Methods previously used depend upon the temporal, spatial and spectral resolution of the images being used. Most of the attempts have relied on low resolution sensors such as NOAA/ AVHRR (Pereira, 1999; Martín and Chuvieco, 1995), SPOT-VEGETATION (Stroppiana et al., 2002; Fraser et al., 2000), or ATSR data (Eva and Lambin,1998). Within high resolution sensors Landsat TM data have been the most widely used (Koutsias et al., 2000). Medium spatial resolution sensors have seldom been used (Vázquez et al., 2001), although IRS-WiFS images are being operatically used for mapping burned areas in Europe by the Joint Research Center (http://natural-hazards.jrc.it/fires/).

## 2. THE SAC-C-MMRS SENSOR

The SAC-C satellite is the first Argentinean Earth Observation satellite. It is part of the so-called “morning constellation”, comprising Landsat 7, EO-1, TERRA and SAC-C platforms. The four satellites have the same orbital parameters but with descending equatorial crossing times at 10:00 a.m., 10:01 a.m., 10:30 a.m. and 10:15 a.m. (GMT) respectively. The MMRS (Multispectral Medium Resolution Scanner) sensor is a push- broom scanner with a spatial resolution of 175m and a swath of 360Km. It has 5 bands:

Band 1: 480-500 nm (Blue)
Band 2: 540-560 nm (Green)
Band 3: 630-690 nm (Red)
Band 4: 795-835 nm (NIR)
Band 5: 1550-1700 nm (SWIR)

Considering the medium spatial resolution and good spectral coverage, this sensor may be a good alternative to validate burned land maps generated from MODIS or AVHRR images, as well as

to improve the spatial coverage of higher resolution sensors, such as Landsat-ETM or SPOT-HVR. It provides better spectral resolution than IRS-WiFS, although lower temporal frequency (one image every 7-9 days).

## 3. OBJECTIVES

The main objective of this study is to assess the potential of the new sensor SAC-C/MMRS for burned areas mapping. The specific goals of this study are:

- To identify which MMRS bands and vegetation indices generated from them provide better sensitivity to discriminate burned areas.
- To estimate, as accurate as possible, the area affected.
- To achieve these objectives two windows were extracted from the images, where several fires had occurred in the summer of 2002. The first area is located at the south-east of Spain, where a shrub fire occurred at the beginning of June, and the second one is at the centre of Spain, where two fires occurred in August affecting shrub-land and woodland.

## 4. METHODS

### *4.1 Pre-processing*

The SAC-C/MMRS images were recorded on board and downloaded by the Argentinean receiving station in Cordoba. The following images were available for this study: 2/06/2002 and 27/06/2002 for the first study area, and 18/07/2002 and 21/08/2002 for the second one. In both cases, the most cloud-free pre-fire and post-fire images were selected.

All images were geometrically corrected using orbital models, and the multitemporal matching improved by using ground control points with second-degree polynomial equations. Pre-fire images were corrected against a vector layer containing hydrological information, post-fire images were corrected against the pre-fire ones. In all cases the RMS error obtained was less than 0.5 pixels. Subsequently subsets of the images were extracted to isolate the study area.

After performing the geometric correction the raw data were converted to reflectance values. Since the calibration parameters required to correct the images were not available, a "cross calibration" method was used, using a Landsat ETM image and a SAC-C image acquired at the same date and time (9$^{th}$ June, 2002). The calibration parameters to convert from digital counts to radiance were obtained from linear regression analysis. Well identifiable areas, in both the MMRS and ETM images were selected to compute the regression coefficients. Sun angles were derived from latitude and ephemeris data. Atmospheric correction was based on Chavez's dark object approach (Chavez, 1996).

### *4.2 Spectral Indices*

The use of vegetation indices for burned area mapping is widely used due to the important spectral changes caused by fire on vegetation cover. Traditional vegetation indices (such as the NDVI) show a severe decrease after fire, as a result of deterioration of pigments and leaf structure. However, since those vegetation indices were derived for vigorous vegetation, they may not be appropriate for burned land discrimination, since the spectral ranges of burned areas are quite different from photosynthetic vegetation. Accordingly, some authors have proposed index specifically designed for burned area discrimination (Martín, 1998; Pereira, 1999).

For this study the following indices were generated to test their sensitivity for burned land discrimination:

NDVI, defined as: $(\rho_{NIR}-\rho_{RED})/(\rho_{NIR}+\rho_{RED})$

NDII, defined as: $(\rho_{NIR}-\rho_{SWIR}\ /\rho_{NIR}+\rho_{SWIR})$ by (Hunt, 1989) and applied by Fraser et al. (2000) to SPOT-VEGETATION data.

GEMI, defined as: $\eta(1-0.25\eta)-(\rho_{RED}-0.125)/(1-\rho_{RED})$

$\eta=(2(\rho_{NIR}^2-\rho_{RED}^2)+1.5\rho_{NIR}+0.5\rho_{RED})/(\rho_{NIR}+\rho_{RED}+0.5)$ (Pinty and Verstraete,1992)

BAI, defined as: $1/(pc_{RED}-\rho_{RED})^2+(pc_{NIR}-\rho_{NIR})^2$ (Martín,1998); where $pc_{RED}$ and $pc_{NIR}$ are the converge points of the red and near infrared bands respectively.

*4.3 Discrimination ability of burned areas of the SAC-C bands and spectral indices created*

In order to identify the most suitable bands and index for our purpose, their discrimination ability for burned areas mapping was tested. Representative samples of points, corresponding to burned and unburned areas, over the post-fire images were collected and a simple statistic measurement of the separability was carried out. The index used is defined as:

$$M=|\mu_u-\mu_b|/(\sigma_u+\sigma_b) \qquad \text{(Kaufman and Remer, 1994)}$$

where $\mu_u$ is the mean value of the unburned areas, $\mu_b$: is the mean value of the burned areas, $\sigma_u$ is the standard deviation of the unburned areas and $\sigma_b$: is the standard deviation of the burned areas.

After identify the band and index presenting the highest separability, the simple difference between the post-fire and the pre-fire images was calculated. Subsequently the image was segmented into two classes (burned/unburned) by a multithreshold approach.

## 5. RESULTS

*5.1 Calibration Parameters*

Table 1 presents the calibration parameters obtained from the regression analysis to convert SAC-C/MMRS raw data to radiance values ($L= a_0 + a_1*DN$).

Table 1. Raw to radiance calibration coefficients for the SAC-C/MMRS bands

| BAND | $a_1$ | $a_0$ |
|---|---|---|
| Blue | 0.5864 | 0.166 |
| Green | 1.4559 | -22.68 |
| Red | 0.9665 | -12.239 |
| NIR | 1.0631 | -20.768 |
| SWIR | 0.1483 | -4.6114 |

*5.2 Discrimination ability of burned areas of the SAC-C bands and spectral indices created*

The results of the sensitivity analysis are presented in tables 2 and 3. Differences found between the two study sites may be caused by the different characteristics of burned areas, both related to the date occurring (late spring the former, and middle of the summer the latter). Considering the post-fire image, the NIR band and the BAI index presented the highest separability in the first study area, while Blue and Red bands presented the best discrimination capability in the second site. As for the multitemporal differences, BAI and NIR showed the highest values in the first area, whereas NIR and GEMI presented the best separability for the second one.

Table 2. M values for South-east of Spain

| Post-fire | M | Pre-Post fire | M |
|---|---|---|---|
| BLUE | 2.216 | BLUE | 1.010 |
| GREEN | 1.893 | GREEN | 1.015 |
| RED | 2.218 | RED | 1.101 |
| NIR | 3.169 | NIR | 1.991 |
| SWIR | 2.014 | SWIR | 1.274 |
| NDVI | 2.172 | NDVI | 1.509 |
| NDII | 2.495 | NDII | 0.902 |
| GEMI | 1.962 | GEMI | 1.706 |
| BAI | 2.658 | BAI | 1.993 |

Table 3. M values for Central Spain

| Post-fire | M | Pre-Post fire | M |
|---|---|---|---|
| BLUE | 3.097 | BLUE | 1.166 |
| GREEN | 2.278 | GREEN | 1.405 |
| RED | 2.789 | RED | 1.438 |
| NIR | 2.271 | NIR | 2.103 |
| SWIR | 1.907 | SWIR | 1.033 |
| NDVI | 1.242 | NDVI | 0.817 |
| NDII | 1.901 | NDII | 0.851 |
| GEMI | 1.400 | GEMI | 1.791 |
| BAI | 1.301 | BAI | 1.297 |

Should be considered here that the unburned category included very different covers, and therefore, the M values can hinder specific discrimination problems such as cloud shadows, that could be solved by SWIR data, as reported by other authors (Koutsias et al., 2000). The unexpected high value of the blue band in the second study area was a consequence of the presence of clouds, with a very high M value for the blue band. Thus if clouds are not included in the separability analysis NIR (M=3.249) and BAI (M=2.551) showed the best discrimination capability.

After analysing problems with specific land covers, the final step of this project was the cartography of burned areas using multiple thresholds. The multitemporal difference in BAI values and the post-fire NDII index were used for discrimination purposes. The first index solved most confusion of burned areas with vegetation and bare soil covers, while the latter reduces problems with water and cloud shadows. Once the discrimination of core burned pixels was achieved a better delimitation of burned areas was generated from a region growing algorithm, where the burned pixels were used as seed pixels (figure 1).

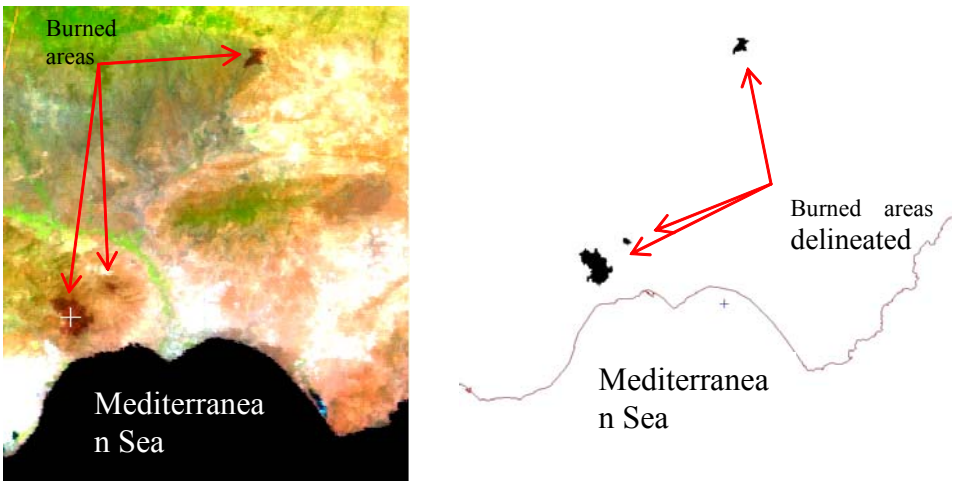


Figure 1: Burned areas discriminated using seeded region growing algorithm in the first study area (R: SWIR, G: NIR, B: Red).

For the second study area, despite the higher separability of the GEMI index, difference of the BAI index was also used in order to test the suitability of the method used for the first site. Thresholding of the BAI difference yielded confusion with cloud shadows and water bodies. Thresholding of the post-fire NDII gave a satisfactory solution to the commission error found, due to the high separability of burned areas with cloud shadows and burned areas with water in the SWIR

band. Next the burned areas were delineated applying a seed region growing algorithm, as for the first site. Comparison with fire perimeters derived from Landsat-ETM data showed a good agreement.

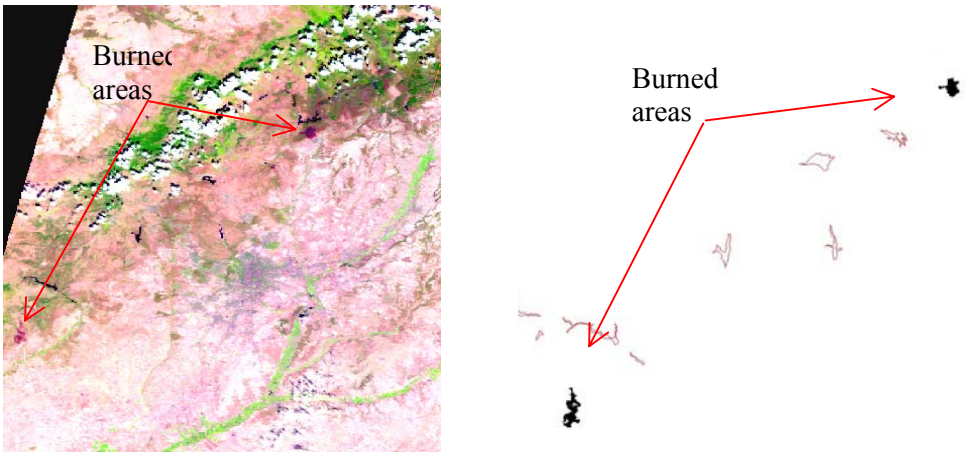


Figure 2: Burned areas discriminated using seeded region growing algorithm in the second study area (R: SWIR, G: NIR, B: Red).

## 6. CONCLUSIONS

SAC-C/MMRS data may be a good alternative to low-resolution sensors (such as AVHRR or Vegetation) for burned land mapping at regional scale. The spectral characteristics of this sensor and the medium resolution make it very promising for this task. The main problem found in this study was the low temporal coverage of this sensor, which difficult obtaining a cloud-free coverage of large territories.

## 7. REFERENCES


Alexandrian, D., Esnault, F. and Calabri, 1999, Forest fires in the Mediterranean area, [on line] last accessed on 3-06-2002 at URL: http://www.fao.org/docrep/x1880e/x1880e07.htm

Barbosa, P.M., San-Miguel-Ayanz, J. And Schmuck, G, 2001, Remote sensing of forest fires in Southern Europe using IRS-WiFS and MODIS data, [on line] last accessed on 2-06-2002 at URL: http://natural-hazards.aris.sai.jrc.it/documents/fires/2001-publications/SPIE2001.pdf

Chavez, P. S. ,1996, Image-based atmospheric corrections. Revisited and improved. *Photogrammetric Engineering and Remote Sensing* 62(9): 1025-1036.

Eva, H. And Lambin, E.F. 1998, Burned area mapping in Central Africa using ATSR data, *International Journal of Remote Sensing, 19(18):3473-3497.*

Frasser, R.H., Li, A., and Landry, R., 2000, SPOT VEGETATION for characterizing boreal forest fires, *International Journal of Remote Sensing, 21(18): 3525-3532.*

Hunt, E. R. and B. N. Rock ,1989.Detection of changes in leaf water content using near and middle-infrared reflectances. *Remote Sensing of Environment* 30: 43-54.

Kaufman , Y.J. and Remer, L.A., Detection of forests using Mid-IR reflectance: an application for aerosol studies, *IEEE transactions on geoscience and remote sensing, 32(3):672-683.*

Koutsias, N., Karteris, M. And Chuvieco, E., 2000, The use of Intensity-Hue-Saturation transformation of Landsat-5 Thematic Mapper data for burned land mapping, *Photogrammetric Engineering and Remote Sensing, 66(7): 829-839.*

Martín, P. And Chuvieco, E., 1995, Cartografía y evaluación superficial de grandes incendios forestales a partir de imágenes de satélite. *Ecología 9:9-21.*

Martín, P., 1998, Cartografía e inventario de incendios forestales en la Península Ibérica a partir de imágenes NOAA/AVHRR, PHd thesis, Department of Geography University of Alcalá.

Pereira, J.M.C., 1999, A comparative evaluation of NOAA/AVHRR vegetation indexes for burned surface detection and mapping, *IEEE transactions on geoscience and remote sensing, 37(1): 217-226.*

Pinty, B. and Verstraete, M., 1992, GEMI: a non-linear index to monitor global vegetation from satellites, *Vegetatio 101:15-20*.

Stroppiana, D., Pinnock, S., Pereira, J.M.C., Grégoire, J.M., 2002, Radiometric analysis o SPOT-VEGETATION images for burned area detection in Northern Australia. *Remote Sensing of Environment 82:21-37*.

Vázquez, A., Cuevas, J.M. and González-Alonso, F., 2001, Comparison of the use of WiFS and LISS images to estimate the area burned in a large forest fire, *International Journal of Remote Sensing, 22(5): 901-907*.

Vélez, R., 1991, Los incendios forestales en el Mediterráneo: Perspectiva regional, [on line] last accessed on 4-06-2002 at URL: http://www.fao.org/docrep/t9500S/t9500s02.htm

# Identifying burnt areas in the Siberian boreal forests between 1990 and 2000 using SPOT VEGETATION

France Gerard, Charles George and Heiko Balzter
*Centre for Ecology and Hydrology Monks Wood, Abbots Ripton, United Kingdom*
ffg@ceh.ac.uk

Keywords: Fire scars, Siberia, boreal, forest, carbon, segmentation, SPOT Vegetation

ABSTRACT: The boreal forest contains almost half the total carbon pool of world forest ecosystems, and so has a very significant role in global biogeochemical cycles. The flux of greenhouse gases in and out of these forests is influenced strongly by disturbances such as diseases, logging and predominantly fire. It is important to quantify these disturbances to enable the modelling of major greenhouse gases. However, because of the remoteness and vastness of the boreal forest, little data is available on the type, extent, frequency and severity of these disturbances in Siberia. For fire scars of between one year and up to ten years of age, one of the more responsive wavelengths is the short wave infra-red (1.6 – 1.7μm) which is sensitive to canopy moisture content, and therefore canopy structure. The area of this study covers approximately three million $km^2$ running from Lake Baikal in the south to above the Arctic Circle. A vegetation index, based on the short wave infrared and near infrared band, was calculated for each in a set of multi-temporal SPOT-VGT images from the summer of 2000. These were segmented, before being combined into a fire scar probability map. Monthly 1km hotspot data were used to verify and date the presence of fire. Landsat ETM and ENVISAT ASAR images were used to check the shape of the fire scars and will be used in the future to improve the fire scar area estimates from the SPOT-VGT images. The results show a good agreement between the fire scar probability map, the hotspots and the higher resolution imagery, any discrepancies being accounted for by the differing dates of imagery and low resolution of SPOT-VGT.

## 1. INTRODUCTION

Fire disturbances in the boreal forests play a major part in many ecosystem processes. About 16,000 forest fires occur in Russia every year, with an average annual area burned of 0.9 million hectares (Odintsov 1996). Future climate change may alter the frequency and size of these fire events and consequently the forest cover, carbon storage and biogeochemical cycles, which in their turn may accelerate climate change. In order to improve our understanding of boreal forest fires and its impact on the global biogeochemical cycles, we need spatial data describing fire dynamics in terms of frequency and size stretching for a period of 100+ years. Dendrochronology can provide point sample based information of fire damage extending back centuries (Swetnam and Lynch 1993), and fire statistics for the past 20 years are available for most northern hemisphere countries, but there is little information for the Siberian Boreal forest. Earth observation has the appropriate spatial and within-year temporal resolution for fire and fire scar mapping. The longest global record extends from 1981 to the present, in the form of AVHRR-NOAA imagery. The thermal data of the AVHRR sensors have been used for locating fires in real time, i.e. fire hot spots (Li et al. 2000); the optical data for estimating burned area one month to one year after the fire has occurred, i.e. recent fire scars (e.g. Kasischke et al. 1993, Barbosa et al. 1999, Fraser et al. 2000) and a combination of both for monitoring wildfire evolution (Al-Rawi et al. 2001). Similarly, the thermal data and optical data of more recent coarse scale sensors are being used for hot spot detection (ATSR series and MODIS) and recent fire scar mapping (ATSR series: Eva and Lambin 1998, Piccolini 2000, and SPOT

VEGETATION (SPOT-VGT): Fraser et al. 2000) respectively. At higher spatial resolution (30m) the optical sensor, Landsat TM, and the active microwave sensor, ERS-1 SAR, have been used to map burned areas (Pereira and Setzer 1993, Bourgeau Chavez et al. 1997). With respect to the large area monitoring of older fire scars (i.e. areas burned up more than one year prior to image acquisition) and their regeneration patterns, Eastwood et al. (1998) and Fraser and Li (2002) have shown that the shortwave-infrared band (SWIR: 1.6 – 1.7μm) is critical to the detection of older forest fire scars. Gerard et al. (2002) and Fraser and Li (2002), also revealed a close association of a vegetation index, $NDSWIR = (R_{nir} - R_{swir})/(R_{nir} + R_{swir})$, with fire scars of varying age but found that fire scars created more than 10 years before image acquisition could not be reliably detected. Canopy moisture content, to which SWIR is sensitive, may be linked to canopy structure which may explain why in the SWIR older regenerating fire scars are detectable.

The following sections concern the detection of older fire scars in the boreal forest of Siberia. The results are an extension of previous work that developed a system using time series of segmented NDSWIR SPOT-VGT images, acquired during a single year, to map up to 10 year old forest fire scars in Canada (Gerard et al 2002).

## 2. STUDY AREA AND DATA ACQUISITION

The full Siberian study area is 3 million km² between 52°-72° Northern latitude and 88°-110° Eastern longitude (Fig. 1). It includes steppe, tundra and typical fir and larch taiga forests. We have access to daily 1km SPOT-VGT surface reflectance composites (S1-product) for the year 2000. Current results are based on seven composites acquired between June 2000 and September 2000 and focus on three 150km x 150km test sites (Fig. 1). Water and cloud masks are provided by the supplier. Landsat TM quicklooks and 1 km hotspot data (IGBP-DIS Global Fire Product and World Fire Atlas) were used for a preliminary assessment of the proposed method.

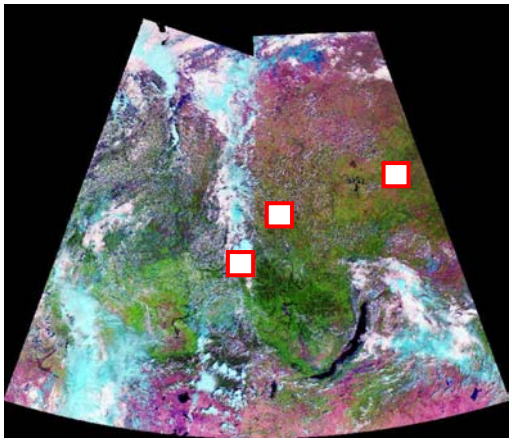

Figure 1. False colour composite of SPOT VGT S1 (17 June 2002) showing the three test sites located in the Siberian study area.

## 3. METHOD

The method is based on the principle that although segmentation results from individual images vary with image quality and season, a consistency in segments is expected across images for constant features which are distinct in the NDSWIR (e.g. fire scars). The 'probability' that a pixel is a fire scar pixel is based on the cumulative co-location of such individual image segments. The key steps involved in the creation of a fire 'probability' map are (Fig. 2):

- Segmentations are applied to multi-temporal images from one acquisition year.
- The original NDSWIR imagery is subdivided into fire scar pixels and non-fire scar pixels by applying localised NDSWIR threshold values. These local threshold values are found by optimising the "t" statistic for 200km x 200km windows.
- The percentage of segment pixels identified as a fire scar pixel is calculated for each segment and assigned to all pixels belonging to that segment.

- A per-pixel fire scar probability $P_f$ is computed: $P_f = \sum_n X_i / (n - c)$ where, $X_i$ = per-pixel percent value for image i ; n = total number of NDSWIR image layers used; c = number of images for which the pixel is tagged as contaminated by cloud, water, or no-data.

The use of the "t" statistic allows for an automated and image specific threshold optimisation which is not dependent on the shape of the NDSWIR histogram. For this approach to work it is important to exclude all image pixels outside the forested area from the histogram, for example, arable land, grasslands and water.

Figure 2. Flowchart showing key steps of method

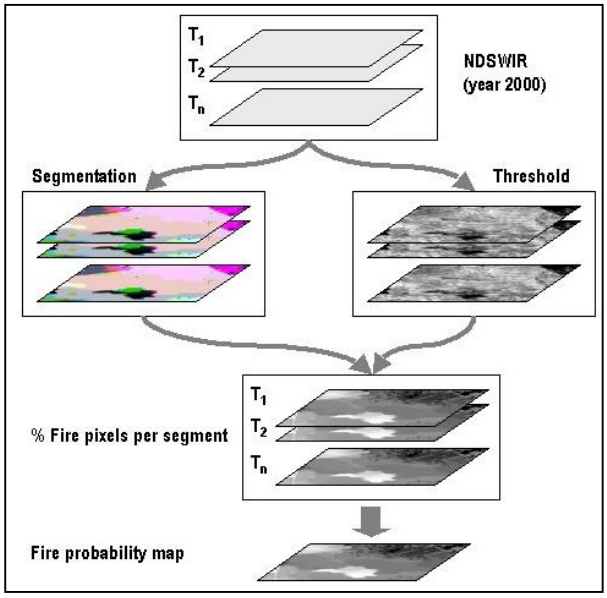


## 4. RESULTS

Fig. 3 shows the results for three test areas. The first column of images shows the NDSWIR calculated for one of the seven selected S1 composites. The false colour composites of three NDSWIR segmentations in column two illustrate the principle of cumulative co-location of segments representing constant features (i.e. fire scars) in the landscape. The third column gives the resulting fire scar 'probability' map which when visually compared against Landsat TM quicklooks (fourth column) shows a good match with areas of disturbance or regeneration. Column five shows the probability map overlaid with hot spot information for 1992, '93, '96 and '97. All main hotspot clusters correspond with high probability values on the fire scar map. No high probability values are found for very small hotspot clusters or single hotspots. There may be several reasons for this: the spatial extent of the resulting scars may have been too small to be detectable at a 1 $km^2$; the damage caused may have been limited and consequently vegetation regeneration quicker; an inadequate cloud and haze mask may be affecting image segmentation and the resulting probability values. Because the hotspot data is not complete (hotspots products for 1994, 1995 are currently not available and data for more recent years have not yet been incorporated in our GIS) it is difficult to establish whether the areas of high fire scar probability which show no hotspot match are errors of commission or not.

## 5. CONCLUSIONS

The method presented aims at providing the location and estimates of the annual area burned in the boreal forests for as far back in time as possible by means of multi temporal imagery acquired in one single year. The criteria for the required satellite data are (i) acquisition in the NIR (~0.7-0.8 μm) and SWIR (~1.6-1.8 μm) spectrum and (ii) high temporal resolution to allow for cloud free multi temporal coverage. ATSR-2, SPOT-VGT and MODIS fulfil these requirements and came into operation in 1995, 1998 and 2001 respectively allowing for a potential backdating to the early 80'ies. However, cloud cover is a major problem in Siberia and although the proposed method can cope with some degree of cloud it still relies on a minimum number of cloud free coverages within one season. Further work will involve thorough validation of the method and fire scar products, improved identification of cloud and haze and reliable dating of fire scars.

## 6. ACKNOWLEDGEMENTS

The work is partly funded by the European Commission through the ongoing FPV project SIBERIA II.

## 7. REFERENCES

Al-Rawi, K. R., J. L. Casanova, and A. Romo. 2001. IFEMS: a new approach for monitoring wildfire evolution with NOAA-AVHRR imagery. International Journal of Remote Sensing 22:2033-2042.

Barbosa, P. M., J. M. Gregoire, and J. M. C. Pereira. 1999. An algorithm for extracting burned areas from time series of AVHRR GAC data applied at a continental scale. Remote Sensing of Environment 69:253-263.

Bourgeau Chavez, L. L., P. A. Harrell, E. S. Kasischke, and N. H. F. French. 1997. The detection and mapping of Alaskan wildfires using a spaceborne imaging radar system. International Journal of Remote Sensing 18:355-373.

Eastwood, J. A., S. E. Plummer, B. K. Wyatt, and B. J. Stocks. 1998. The potential of SPOT-Vegetation data for fire scar detection in boreal forests. International Journal of Remote Sensing 19:3681-3687.

Eva, H., and E. F. Lambin. 1998. Burnt Area Mapping in Central Africa using ATSR data. International Journal of Remote Sensing 19:pp. 3473-3497.

Fraser, R. H., and Z. Li. 2002. Estimating fire-related parameters in boreal forest using SPOT VEGETATION. Remote Sensing of Environment 82:95-110.

Fraser, R. H., Z. Li, and J. Cihlar. 2000. Hotspot and NDVI differencing synergy (HANDS): A new technique for burned area mapping over boreal forest. Remote Sensing of Environment 74:362-376.

Gerard, F. F., H. Balzter, A. Ferreruela, R. Wadsworth, and S. E. Plummer. 2002. Detecting and mapping forest disturbances in the boreal forests of Canada and Siberia. in ForestSAT Symposium, Edingburgh.

Kasischke, E. S., N. H. F. French, P. Harrell, N. L. Christensen, S. L. Ustin, and D. Barry. 1993. Monitoring of Wildfires in Boreal Forests Using Large-Area AVHRR NDVI Composite Image Data. Remote Sensing of Environment 45:61-71.

Li, Z., S. Nadon, J. Cihlar, and B. Stocks. 2000. Satellite-based mapping of Canadian boreal forest fires: evaluation and comparison of algorithms. International Journal of Remote Sensing 21:3071-3082.

Odintsov, D. 1996. Fire prevention. Forest Management 3:2-4.

Pereira, M. C., and A. W. Setzer. 1993. Spectral characteristics of fire scars in Landsat-5 TM images of Amazonia. International Journal of Remote Sensing 14:2061-2078.

Piccolini, I. 2000. Adaptive algorithm for global automatic burnt surfaces estimation with ATSR-2 data, Algorithm Technical Background Document. European Space Agency.

Swetnam, T. W., and A. M. Lynch. 1993. Multicentury, regional-scale patterns of western spruce budworm outbreaks. Ecological Monographs 63:399-424.

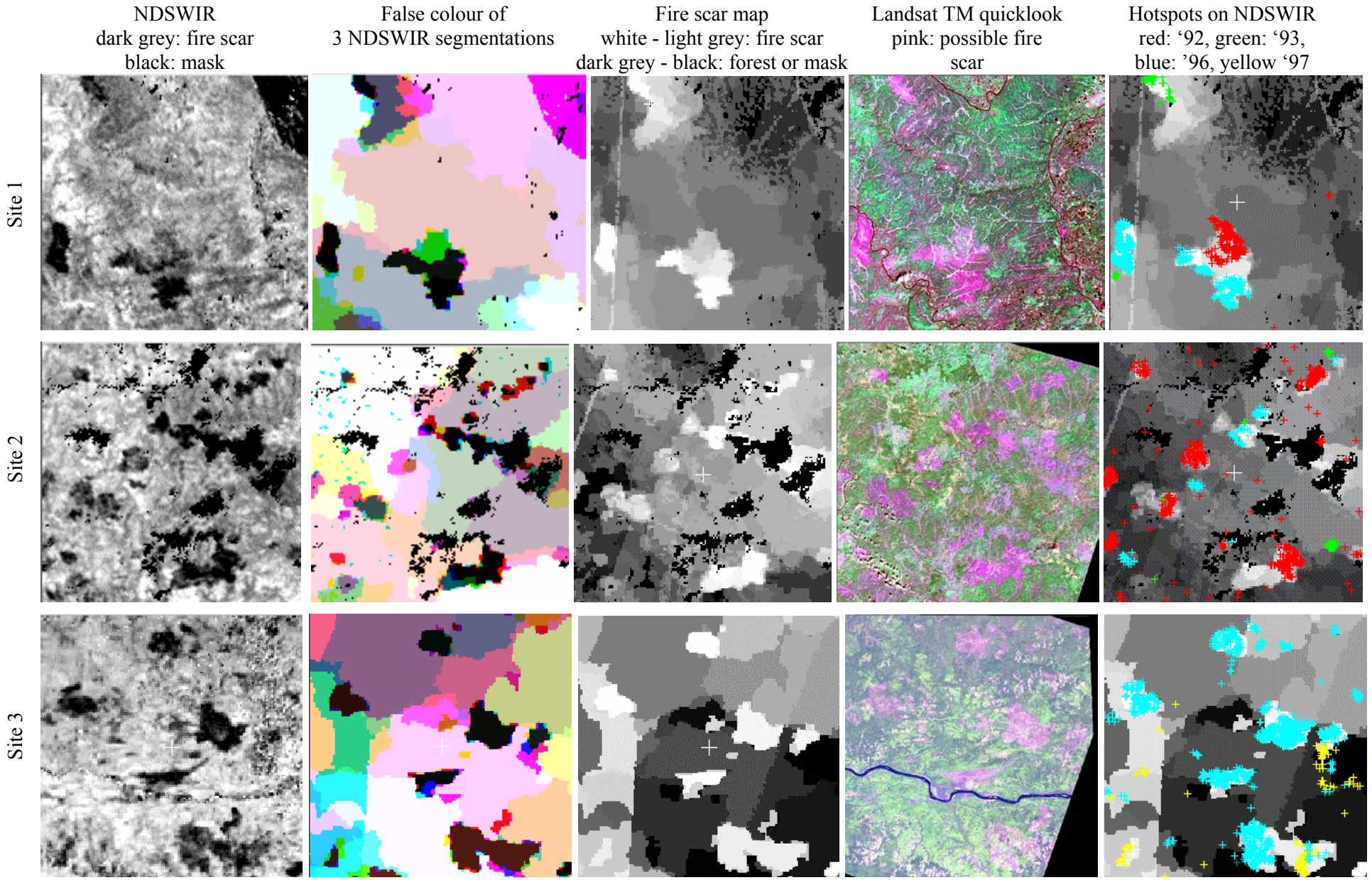


Figure 3. The NDSWIR, segmented NDSWIR, resulting fire scar probability map compared against Landsat TM quicklooks and hotspot data.

# Evaluation of RADARSAT-1 data for identification of burnt areas in Southern Europe

Meritxell Gimeno, Jesús San-Miguel Ayanz
*European Commission, Directorate General Joint Research Centre, Institute for Environment and Sustainability, Land Management Unit, INFOREST*
meritxell.gimeno@jrc.it

Keywords: SAR image interpretation, RADARSAT-1, geometric and radiometric correction, forest fires, burnt area mapping, change detection, neural network.

ABSTRACT: This study presents the combined analysis of RADARSAT products of different spatial resolutions acquired under different incidence angles for mapping burnt areas on a forested region of Central Portugal. Prior to the SAR data analysis, a number of pre-processing procedures were carried out. Noise was eliminated by adaptive texture preserving filtering. A specific algorithm for the geocoding of SAR images, based on a range-doppler approach, enabled precise geocoding of the SAR data by means of a single very accurate ground control point. A novel incidence-angle-normalization for SAR imagery was applied to normalize the backscatter coefficient to a given incidence of 30 degrees. This angle was selected as a compromise among the original settings of image acquisitions. Further, a model-based slope correction was applied to reduce the topographic effect applying a cosinus function. The images were classified using a back-propagation neural network classifier, after a qualitative and quantitative investigation of the backscattering as related to the slope angle and time changes. The best results obtained when maximizing the discrimination of burnt areas, were selected as the input for the neural network classification. From these preliminary results it can be concluded that SAR data can play a significant role for burnt area mapping in Europe, in those areas were optical data cannot be used due to persistent cloud cover.

## 1. INTRODUCTION

Forest fires constitute a recurrent phenomenon in the Mediterranean region. The mapping of the burnt areas is one of the logic steps to perform after the fire events in order to estimate fire impact. Burnt area mapping allows determining the measures necessary to protect the environment from fire-related effects such as erosion and soil loss. Although optical satellite data have traditionally been used for mapping burnt areas, there is still a limited success of this application, since clouds and smoke can prevent the acquisition of optical data. On the contrary, microwave remote sensing imagery from synthetic aperture radar (SAR) instruments has the potential to overcome this limitation, since SAR systems are able to acquire images under nearly all meteorological conditions. However, the use of SAR imagery for mapping burnt areas has been restricted so far mainly to boreal (Kasischke *et al.* 1994, Bourgeau-Chavez *et al.* 1997, Dwyer *et al.* 2002) and tropical (Kuntz and Siegert 1999, Siegert *et al.* 1995) forests. Very few publications exist on the applicability of SAR data for mapping burnt areas in Mediterranean landscapes. In particular, no publications exist on the use of RADARSAT data for burnt area mapping. In all cases in which SAR imagery was used to map burnt scars, only one type of SAR data was utilized. The combined analysis of different SAR products or the analysis of same SAR product with different incidence angles has not yet been investigated. The possibility of using SAR data of different spatial resolutions and incidence angles permits increasing significantly the frequency in data acquisition over a given region and may be critical in the monitoring of environmental processes such as fire propagation or flood extent mapping. A novel incidence-angle-normalization for SAR data is presented. This is a required process previous to the inter-comparison of SAR imagery acquired by different sensors. Although this additional step increases the pre-processing

of SAR imagery, it allows the synergistic use of the different SAR products, and the direct comparison of different types of SAR imagery. This article presents the combined analysis of RADARSAT products of different spatial resolutions acquired under different incidence angles for mapping burnt areas in Mediterranean forests.

## 2. DATA SET AND STUDY AREA

The Canadian satellite RADARSAT-1 launched in November 1995 acquires C-band HH polarisation SAR data in a wide range of beam modes and incidence angles and, consequently, in various spatial resolutions. In this study, the Wide Beam W1 data with 24.1º-30.2º incidence angle, the ScanSar Narrow SCNA data with 19.3º-38.9º incidence angle and the ScanSar Narrow SCNB data with 30.1º-46.5º incidence angle were used to investigate the suitability of RADARSAT data for burnt area mapping. Descending mode scenes acquire on three different dates (passing time 06:30h) were used to study the temporal backscatter characteristics of this Mediterranean forest environment with regard to the fires occurred in summer 2000. The descending orbit was selected for all scenes because backscatter increases when dew is present on the canopy, and early morning dew is often observed on the canopy at the time of the satellite overpass (Wood *et al*., 2001). Two scenes corresponding to post-fire conditions (dry and wet season) and one scene corresponding to pre-fire conditions (dry season) were analysed.

Hilly terrain dominates the south-eastern and north-western parts of the scenes over the study area. Altitude ranges from 600 m to 1200 m with slopes up to 30°. On the scenes, the slopes facing the sensor (face-slope) will appear brighter than surfaces sloping away from it (back-slopes), and the steep back- slopes may be completely shadowed (no data recorded). A mixed look-up table, which suitable for the pre-processing SAR data on areas of high relief (RADARSAT Illuminated, 1995), was chosen for the RADARSAT-1 imagery.

The study site was located in Central Portugal between the districts of Coimbra and Castelo Branco, which are separated by the Zêzere river, tributary of the river Tagus. Several fires took place in this area between July 15$^{th}$ and August 15$^{th}$ in the year 2000. The study site covers an area of 50 x 50 km$^2$ where the main vegetation consists of 80% woodland and 20% agriculture. The woodland categories are mainly Atlantic pine (*Pinus pinaster*, 80%), *Eucalyptus sp.* (16%), and in some areas oak (*Quercus robur*), cork oak (*Quercus suber*) and chestnut trees (*Castanea sativa*, 4%). The understory is composed of degraded forest and shrubs. The agricultural areas are covered by vineyards, olive groves, and fruit trees. Moreover, given the favourable climatic conditions for timber production in Portugal, large areas of new plantations of both coniferous and deciduous species, particularly eucalyptus, have recently been established (Wilkinson *et al.* 1995).

## 3. METHODOLOGY

The processing of RADARSAT-1 was performed using SARscape® software (Sarmap, 2002). Prior to the SAR data analysis, a number of pre-processing procedures were carried out. Noise was eliminated by the Frost filter with a 5x5 pixel window (Frost, 1982). A specific algorithm for the geocoding of SAR images, based on a range-doppler approach, enabled precise geocoding of the SAR data by means of a single very accurate ground control point. The nominal incidence angles of the original scenes varied between 25 and 38 degrees. Given the topographic dependence and the effects of local incidence angle variation on SAR backscatter, an angular normalisation was applied to allow the application of change detection techniques between scenes. A novel incidence-angle-normalization for SAR imagery was applied to normalize the backscatter coefficient to a given incidence of 30 degrees. This angle was selected as a compromise among the original settings of image acquisitions. Further, a model-based slope correction was applied to reduce the topographic effect applying a cosinus function. This correction can be tuned through the variation of the radiometric normalisation value which represents the cosinus power n (Teillet *et al*., 1985).

The images were classified using a back-propagation neural network (BPNN) classifier. Since the BPNN is non-parametric classifier, no assumption on the distribution statistics of the scenes is needed. BPNN is reported to be better suited for classification of SAR data than the widely used Maximum Likelihood classifier (Chakraborty *et al.*, 1997; Gimeno *et al*., 2002 a, b). The classification accuracy was evaluated using the Kappa coefficient and the confusion matrix.

## 4. RESULTS

A number of widely distributed sample plots were chosen to characterize homogeneous forests and burnt areas. Different backscatter intensities were observed on forests and fire-disturbed areas over the time under different slope angles. Forests can be recognized by backscatter intensities in the range of -11 dB to -6 dB. As seen on Figure 1a, the backscatter intensity is higher on the face-slope than on the back-slopes. Both scenes present a similar hyperbolic decreasing trend. However, the scene acquired during the wet season shows a marked higher backscatter coefficient than the other scenes. On the burnt areas, the backscatter changed from -8 dB (before the fire event) to 2 dB (after the fire event) depending on the slope. Face-slopes appeared bright with backscatter intensities around -2 dB to 1 dB. Figure 1b shows consistent lower backscatter values on the scene acquired before the fire event. Within the post-fire scenes, the wet-season scene presents higher backscatter values than the dry-season scene. Moreover, both scenes present a parabolic increasing trend in backscatter with increasing slope.

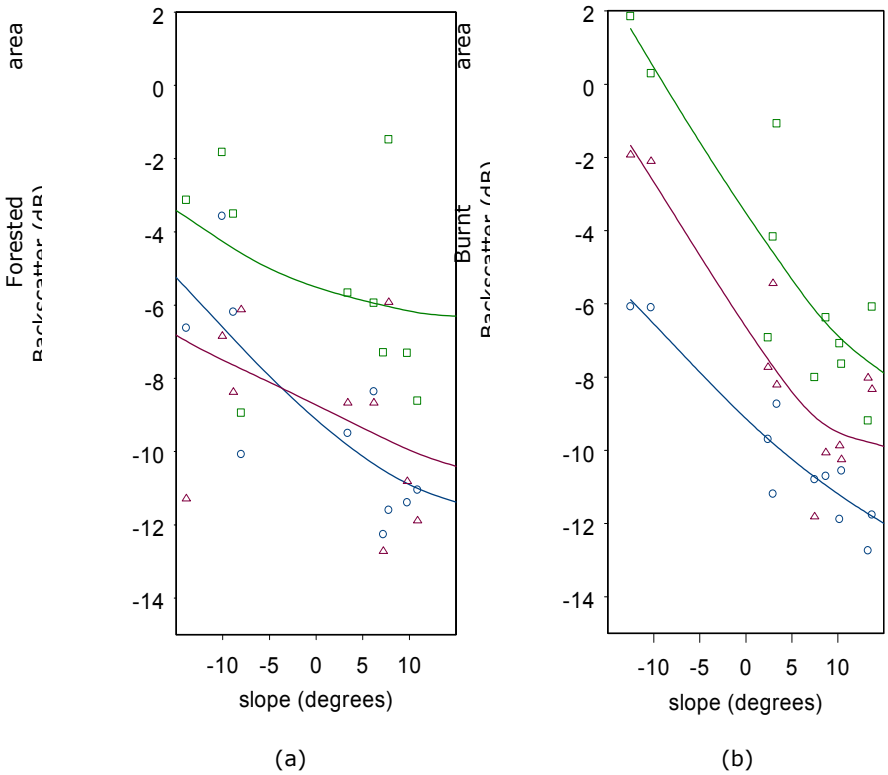


Figure 1. Changes in backscatter behavior of forest (a) and fire-disturbed (b) areas with time and slope angle (blue: 12/aug/1998, red: 11/sep/00, green: 06/feb/2001).

The inputs for classification in the BPNN were the image before the fire, the post-fire image (wet-season), and the maximum ratio image between them. The classification accuracy of the burnt areas on the images acquired on August 1998 (dry season) and February 2001 (wet season) was 80% (seen Figure 2).

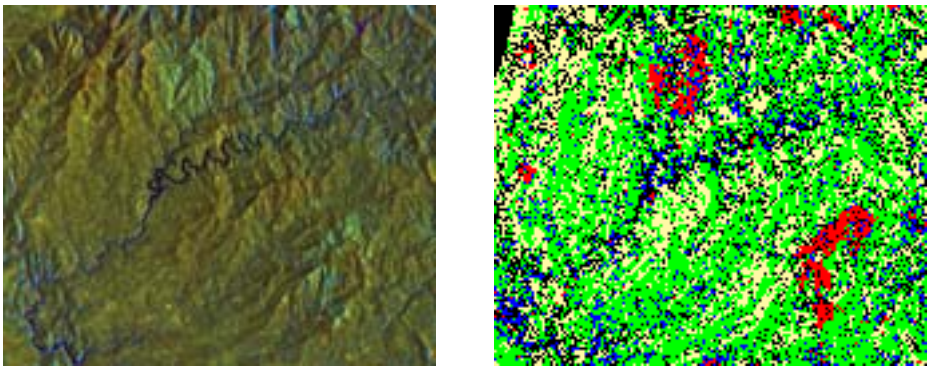

Figure 2. Color composite image (R: 12/aug/1998, G: 06/sep/2001, B: maximum ratio) and classified image (Red: burnt areas; green and yellow: forest areas; blue: water bodies).

## 5. DISCUSSION AND CONCLUSIONS

This multi-temporal analysis of SAR imagery allowed discriminating the burnt areas from the forested areas and, consequently, mapping the burnt scars. Burnt areas showed a characteristic temporal behaviour, which is similar to that observed in case of ERS-2 SAR data (Gimeno *et al.*, 2002 a, b). This equal response can be associated to the volumetric scattering which often occurs in vegetation. This is the main kind of scattering mechanism of these types of landcover and the cause of the incoming signal depolarization. Consequently, this scattering mechanism produces a similar response for both instruments. However, the expected return from forested areas is slightly greater at vertical polarization than that at horizontal polarization.

From these preliminary results it can be concluded that SAR data can play a significant role for burnt area mapping in Europe, in those areas were optical data cannot be used due to persistent cloud cover.

## 6. REFERENCES


Bourgeau-Chavez, L. L., Harrell, P. A., Kasischke, E. S., and French, N. H. F., 1997, The detection and mapping of Alaskan wildfires using a space borne imaging radar system. *International Journal of Remote Sensing, 18, 355-373.*

Bourgeau-Chavez, L. L. and Kasischke, E. S., 2002, Mapping fire scars in global boreal forest using imaging radar data. *International Journal of Remote Sensing, 23, 4211-4234.*

Chakraborty, M., Panigrahy, S., and Sharma, S.A., 1997, Discrimination of rice crop grown under different cultural practices using temporal ERS-1 SAR data. *ISPRS J. Photogrametry Remote Sensing, 52, 183-191.*

Dwyer, E., Stocks, B. J., and Arino, O., 2002, Burn Scar Mapping in Canada using ERS time series data. *Earth Observation Quarterly, n.70 January 2002, ESA, Nordwijk, Netherlands, pp. 10-11.*

French, N. H. F. and Bourgeau-Chavez, L. L., 1999, Initial observations of RADARSAT imagery at fire-disturbed sires in interior Alaska. *Remote sensing of Environment, 68, 89-94.*

Frost, V.S., Stiles, J.A., Shanmugan, K.S. and Holtzman, J.C., 1982, A model for radar images and its application to adaptive digital filtering of multiplicative noise. *IEEE Transactions on Pattern analysis and machine intelligence, Vol. PAMI-4, No. 2, pp. 157-165.*

Gimeno, M., San-Miguel-Ayanz, J., Barbosa, P.M., and Schmuck, G., 2002, Using ERS-SAR images for burnt area mapping in Mediterranean landscapes. *Forest Fire Research & Wildland Fire Safety, Viegas (ed.) © 2002 Millpress, Rotterdam, ISBN 90-77017-72-0. Proceedings of IV International Conference on Forest Fire Research, Luso-Coimbra.*

Gimeno, M., San-Miguel-Ayanz, J., Barbosa, P.M., and Schmuck, G., 2002. Burnt area mapping from ERS-SAR time series using the principal components transformation. *SPIE 9th International Symposium on Remote Sensing, 22-27 September 2002 Capsis Beach Hotel and Conference Center, Aghia Pelagia, Crete, Greece*.

Kasischke, E. S., Bourgeau-Chavez, L L., and French, N. H. F., 1994, Observations of variations in ERS-1 SAR image intensity associated with forest fires in Alaska. *IEEE Transactions on Geoscience and Remote Sensing, 32, 1*.

Kuntz, S., and Siegert, F., 1999, Monitoring of deforestation and land use in Indonesia with multitemporal ERS data. *International Journal of Remote Sensing, 20, 2835-2853.*

RADARSAT Illuminated 1995. RADARSAT International, version 07/95.

Sarmap, 2002, SARscape® 1.2, system for optical and SAR image analysis. Cascine di Barico, Purasca, Switzerland.

Siegert, F., Kuntz, S., Streck, C.,and Bergbauer, B., 1995, Land use planning and monitoring in Indonesia using ERS-1 RADAR data. *Proceeding of International Conference on Remote Sensing and GIS for Environmental Resources Management –The Indonesian – European Experience, Jakarta, Indonesia, 6-8 June.*

Teillet, P.M., Guindon B., Meunier J.-F., and Goodenough, D.G., 1985, Slope-aspect effects in synthetic aperture radar imagery, *Canadian Journal of Remote Sensing, 11, n.1.*

Wang, Y., Kasischke, E.S., Bourgeau-Chavez, L. L., O'Neill, K. P., and French, N. H. F., 2000, Assessing the influence of vegetation cover on soil-moisture signatures in fire-disturbed boreal forests in interior Alaska: modeled results. *International Journal of Remote Sensing, 21, 689-708.*

Wilkinson, G.G., 1995, Forest mapping from multi-source satellite data using neural network classifiers-An experiment in Portugal. *Remote Sensing Reviews, 12, 83-106.*

Wood, D., McNairn, H., Brown, R.J., and Dixon R., 2001, The effect of dew on the use of RADARSAT-1 for crop monitoring choosing between ascending and descending orbits. *Remote Sensing of Environment, 80, 241-247.*

# Object-oriented image analysis for burned area mapping using NOAA-AVHRR imagery in Creus Cape, Spain

I. Z. Gitas & G. H. Mitri
*Dept. of Environmental Management, Mediterranean Agronomic Institute of Chania*
I.Z.Gitas.93@cantab.net

E. Chuvieco & G. Ventura
*Dept. of Geography, University of Alcalá, Madrid, Spain*

Keywords: NOAA-AVHRR, object-oriented image analysis, burned area mapping

ABSTRACT: Due to the wide coverage and high frequency offered by NOAA-AVHRR sensors, it is possible to quickly obtain a general overview of the situation over large areas of terrain and to assess the damage of recent large forest fires by mapping the extent of the burned areas. The aim of this study was to develop an object-oriented model for mapping a recently burned area in the Mediterranean on a regional scale. The classification methodology included segmentation of the NOAA-AVHRR image into two different levels before its final classification, using different spectral as well as contextual object features. The burned area map resulting from the image classification was compared with the fire perimeter produced by the Forest Service in terms of spatial overlap in order to distinguish the extent of agreement between them. The results of the comparison indicated a high degree (≈ 80%) of spatial agreement. It was concluded that the object-oriented approach can accurately map large recently burned areas on a regional scale using the low spatial resolution data of NOAA-AVHRR.

## 1. INTRODUCTION

Forest fires represent a major environmental problem in Mediterranean regions, with large areas being affected each summer. The fundamental cause of forest fires is linked to changes in traditional land uses, the consequence of which is higher fuel accumulation; and to global climatic warming which reduces fuel humidity and increases fire risk and fire spread (Pausas and Vallejo 1999).

An assessment of the environmental impacts requires the collection of information concerning the location and the spatial extent of fire (Caetano et al. 1994, Pereira et al. 1997). Reliable monitoring and effective analysis techniques need to be implemented in order to estimate the ecological impact of fire on the Mediterranean ecosystems (Gitas 1999). The wide area coverage and high frequency offered by satellite sensors, as well as their ability to provide information about non-visible spectral regions, makes them a very valuable tool for the prevention, detection and mapping of wildland fires. Indeed, remotely sensed data can contribute to a better, cost effective, objective and time-saving method to quantify the location, aerial extent and intensity of fire events (Chuvieco et al. 1999).

Remote sensing, particularly low spatial resolution data such as NOAA is a powerful tool for the study of large forest fires at a regional scale. The thermal channels of AVHRR can contribute significantly to separate burned area from other land covers (Martin et al. 2002).

Object-oriented image classification allows the integration of a broad spectrum of different object features, such as spectral values, shape and texture. Classification techniques, incorporating

contextual and semantic information, can be performed for burned area mapping by utilizing not only image object attributes but also the relationship between networked image objects (Mitri and Gitas 2002).

The aim of this work is to develop an object-oriented model for large burned area mapping at a regional scale using NOAA-AVHRR imagery.

## 2. STUDY AREA

The study area is situated at the Eastern extremity of the Pyrenees, in Spain (Figure 1). The surface area of the cape is almost 9 000 ha, the majority of which is included within a plan of basic environmental protection. From a climatic point of the view, the conditions are typically Mediterranean. The most unusual feature is the predominant "tramuntana" wind. This is a cold, dry wind coming from the north, which can reach speeds of more than 120 km/h and blow for many days at a stretch. Human activity over the centuries subjected the zone to recurrent fires, exploitation and breaking up of the forests and pasturing of animals. This has resulted in the substitution of the old forests by *cistus* scrub and dry grasses and encouraged the progressive abandonment of the vineyards and olive groves. In the middle of this relatively bare landscape there are patches of oaks or deciduous trees and river-bank forests in some hollows and beside watercourses.

Figure 1. Location of the study area


Map o f Europe | Map of Catalonia | Burned area (LANDSAT 7 Quicklook, Creus Cape)

We centered our work in a large fire occurred (almost 6000 ha, 2500 ha from the Natural Park called Cap de Creus) on the 6$^{th}$ of August, 2000 in the area previously described. The fire began at 11:00 in the morning in a town called Garriguella, and stopped the following day. It was mainly provoked by cleaning works, and then the strong wind supported it. In this study, one NOAA-14 AVHRR image (10$^{th}$ August 2000), which was acquired immediately after a large fire in Spain, was used.

## 3. METHODOLOGY

The methodology of the object-oriented approach (using the software eCognition) consisted of three main steps (Figure 2). A prerequisite to classification was image segmentation which is the subdivision of an image into separated regions. Image objects resulting from a segmentation procedure are intended to be rather image object primitives, serving as information carriers and building blocks for further classification or other segmentation processes (Baatz and Schäpe 1999). In this sense, the best segmentation result is the one that provides optimal information for further processing. The two levels of segmentation were generated one after the other, using different scale parameters. Level one was segmented at a smaller scale while level two was segmented at a larger scale. The thermal band at the two levels was assigned to a bigger weight than the other bands, to take advantage of the thermal channel in order to detect easily higher temperatures on the pixels image. Throughout the

segmentation procedure, the whole image was segmented and image objects were generated based upon several adjustable criteria of homogeneity in colour and shape. Each image object has a large number of characteristic properties, the so-called object features or attributes. The segmentation in object-oriented image analysis was used to construct a hierarchical network of image objects, which represents the image information in different scales simultaneously. The hierarchical network allowed an evaluating context – the relations of the local neighbourhood of image objects at one level – and dependencies among the two levels. Each image object 'knew' its context (neighbourhood), its super-object and its sub-objects. Thus, it was possible to define relations between objects. All of these numerous object features provided the input for a subsequent classification. One of the most important tasks was to find the best discriminating features for a given task.

In the classification process, each class of a classification scheme contains a class description that consists of a set of fuzzy expressions allowing the evaluation of specific features and their logical operation. A fuzzy rule consisted of a combination of several conditions which have to be fulfilled for an object to be assigned to a class. The fuzzy sets were defined by membership functions that identify those values of a feature that are regarded as typical, less typical, or not typical for a class, in that they have a high, low, or zero membership to the fuzzy set, respectively. Three different classes were created at level 1 representing “non-burned”, “burned” areas smaller than 3900 ha, and “burned” areas bigger than 3900 ha. For the classification, features such as “ratio of” band three and four, “mean” of band three and “area” of objects were used. The second step was to apply to the image a classification based-fusion. In this way, a number of image objects forming a “burned” areas smaller than 3900 ha and attached to the objects of “burned” areas bigger than 3900 ha, could be merged into one image object representing an entire “burned” area. A structure is defined by organizing all classes which semantically form this structure in a structure group. At level two, classes for “burned” and “non-burned” areas were also defined using class-related features. Contextual features that determine the relationship among the networked image objects were used in the classification. With this procedure, the large fire under examination was finally mapped (Figure 3).

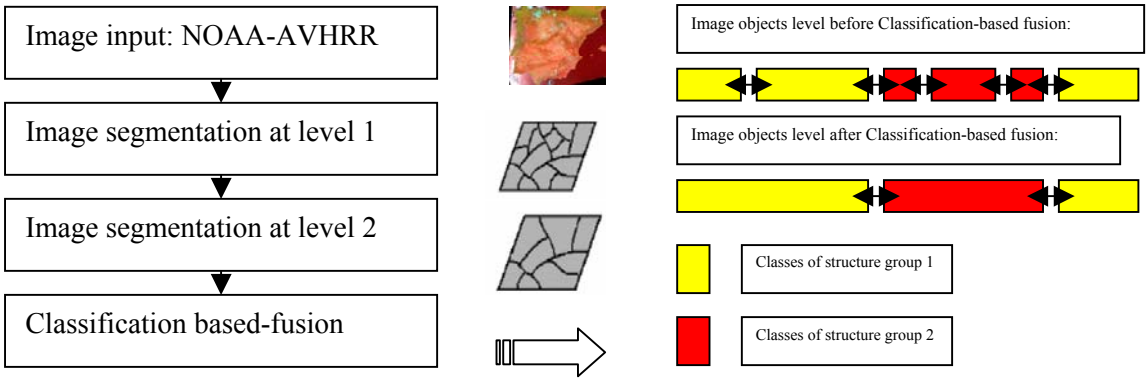


Figure 2. Flowchart of the methodology

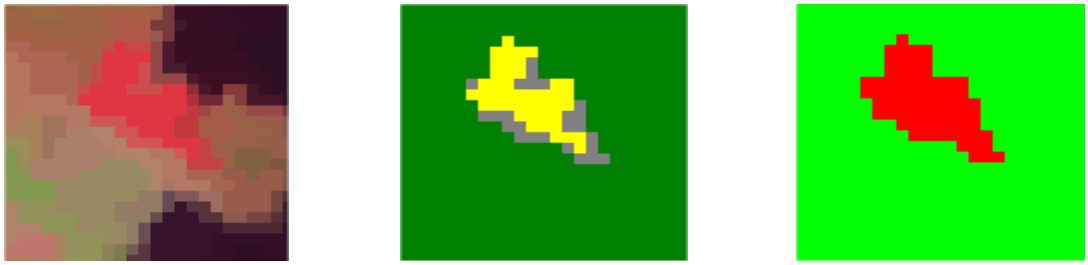

Original image (subset) Level 1 Level 2

Figure 3. Burned area classification at the different levels. The figure at level 1 shows in yellow a "burned" object bigger than 3900 ha and in grey "burned" objects smaller than 3900 ha.

## 4. RESULTS

The object-oriented classification accuracy assessment was based on a comparison in terms of area and shape of the resulting burned area map with the fire perimeter produced by the Catalan Service of Forestry Prevention (Figure 4).

The spatial comparison (overlay) between the burned area map obtained from the object-oriented classification of the image and the Forest Service fire perimeter indicated a high degree (≈ 80%) of spatial agreement. The total burned area classified was 6900 ha and the fire perimeter statistics showed a burned area of 6000 ha. This difference was due to the fact that NOAA-AVHRR image has a low spatial resolution of 1.1 km. Nevertheless, the results appear to be promising.

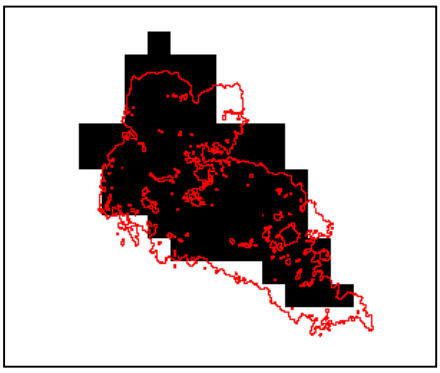

Figure 4. Classification result (black) vs. fire perimeter (red)

## 5. CONCLUSIONS

In this study, object-oriented image analysis employing a NOAA-AVHRR image for use in the mapping of a large recently burned area was investigated. The main conclusion drawn from this study was that object-oriented classification showed very promising results in burned area mapping on a regional scale using low spatial resolution data. The segmentation into two levels and the classification based-fusion of the image prior to its classification allowed us to considerably avoid confusion between burned and non-burned areas. This study also demonstrated the potential use of the object-oriented approach as a tool for fast and effective mapping of large recently burned areas.

## 6. REFERENCES


Baatz, M. and Schäpe, A., 1999b. Object-Oriented and Multi-Scale Image Analysis in Semantic Networks. In: Proc. Of the 2nd Int. Symposium on Operationalization of Remote Sensing, Enshede, ITC: 16-20

Caetano, M.S., Mertes, L.A.K. and Pereira, J.M.C., 1994. Using Spectral Mixture Analysis for Fire Severity Mapping, 2nd Int. Conf. Forest Fire Research, Coimbra, pp. 667-677.

Chuvieco, E., Deshayes, M., Stach, N., Cocero, D. and Riaño, D., 1999. Short-term fire risk: foliage moisture content estimation from satellite data. In: E. Chuvieco (Editor), Remote Sensing of Large Wildfires in the European Mediterranean Basin. Springer-Verlag, Berlin, pp. 17-38.

Gitas, I.Z., 1999. Geographical information systems and remote sensing in mapping and monitoring fire-altered forest landscapes. PhD Dissertation, University of Cambridge, 237 pp.

Martin, P.M., Diaz Delgado, R., Chuvieco, E. and Ventura, G., 2002. Burned land Mapping using NOAA-AVHRR and TERRA-MODIS. In: Domingos Xavier Viegas (Editor), ADAI, Portugal, Forest Fire research and Wildland Fire Safety. Millpress, Luso, Coimbra, Portugal, pp. 227-244.

Mitri, G. and Gitas, I., 2002. The development of an object-oriented classification model for operational burned area mapping on the Mediterranean island of Thasos using LANDSAT TM images. In: Domingos Xavier Viegas (Editor), ADAI, Portugal, Forest Fire research and Wildland Fire Safety. Millpress, Luso, Coimbra, Portugal, pp. 227-244.

Pausas, J.G. and Ramón Vallejo, V., 1999. The role of fire in European Mediterranean ecosystems. In: E. Chuvieco (Editor), Remote Sensing of Large Wildfires in the European Mediterranean Basin. Springer, Berlin, pp. 3-15.

Pereira, J.M.C., Chuvieco, E., Beaudoin, A. and Desbois, N., 1997. Remote sensing of burned areas. A review of remote sensing methods for the study of large wildland fires. Universidad de Alcalá, Alcalá de Henares, 127-183 pp.

# Creating a Forest Fire Database for the Far East of Asia using NOAA/AVHRR observation

J. Kučera & Y. Yasuoka
*Institute of Industrial Science, The University of Tokyo, Meguro-ku, Tokyo, Japan*
kucera@iis.u-tokyo.ac.jp

D.G. Dye
*Ecosystem Change Research Program, Frontier Research System for Global Change, Yokohama, Japan*

Keywords: forest fire, burn scar mapping, NDVI, AVHRR

## 1. INTRODUCTION

The main low-resolution sensor used for fire detection and mapping of burned areas in the boreal forest in last 20 years has been the Advanced Very High Resolution Radiometer (AVHRR) onboard on NOAA satellite series (Kasischke et al. 1999, Pereira 1999, Fraser et al. 2000, Li et al. 2001, 2000a, 2000b). Recently, the AVHRR burned scar products are being replaced by up-to-date Moderate Resolution Imaging Spectroradiometer (MODIS) (Kaufman et al. 1998). However, because of its extensive data archive, the NOAA/AVHRR sensor remains the major data source for establishment of burned area time series datasets, study of forest fire historical patterns and post fire vegetation succession (Kasischke and French 1997, Kučera and Yasuoka 2001).

There are three major methodologies for mapping burned areas using NOAA/AVHRR summarized by Fraser et al (2000). The first one is based on detection of active fire using multi-channel threshold algorithms (Li et al. 2000a, 2000b) or contextual algorithms (Kaufman et al. 1998, Giglio et al. 1999). The second methodology detects post-fire vegetation degradation using subtraction operation of pre-fire and post-fire NDVI composites (Kasischke and French 1997, Li et al. 2000a). The final third approach is a hybrid technique, which employs both previously described methods in synergic manner and exhibits the best performance (Fraser et al. 2000, Li 2001).

This study introduces a technique for generating yearly burned scar maps based upon synergic approach. Since the long time (18 years) AVHRR data were available, the whole time series were fully utilized for detection of abrupt change in NDVI and active fire detection. The developed algorithm is employed for burned scar mapping in part of the boreal region of Far East Asia for the years 1984-2001.

## 2. METHODOLOGY

The burned scar mapping algorithm consists of two parts. The first part is a purely multi-channel threshold algorithm developed for boreal environments (Li et al 2000a). It detects hotpots during biomass burning, provided the view is cloud-free. Its advantages and limitations are described in Frazer et al (2000). The second part of the algorithm is based on detection of abrupt lowering of NDVI in monthly 18 years the time series and uses the procedure described in Bohm et al (1990). If there is an NDVI decrease (NDVId), that place is suspect for land cover change. The spots detected by this part of the algorithm are not only burned places but also clear cuts and areas with vegetation stress during drought. The two previously described parts are merged; if the pixel is marked as fire by multiple channel threshold hotspot algorithm and the NDVI has appropriate decrease at the same time, the pixel is marked as real burned pixel (RBP). RBP are pixels, which were “seen” during a fire event.

In order to involve pixels which surround RBP and were marked as NDVId but not as RBP (e.g. these pixels were covered by clouds but were actually burned and experienced NDVI decrease), the RBP are used as a base for extrapolating among NDVId pixels surrounding RBP in order to delineate all trully burned pixels. Those are then summed and their total area on yearly bases is calculated.

## 3. RESULTS AND DISCUSSIONS

The burned area for each year and administrative region can be found in Kučera et al. (2002). The total sum of burned area available for Russian part for fires in 1998 and for Heilongjiang province for 1987 was used for validation. Spatial agreement was evaluated using Landsat-5 TM.

The sum of burned forest for year 1998 in Khabarovsk region was obtained from Russian Aerial Forest Fire Protection Agency (Aviolesookrana, Kondrashev, personal communication) and was estimated to be 20,000 $km^2$; the estimate obtained from this study is 17,821 $km^2$. Another estimate (little over 20,000 $km^2$) of burned area is provided by Kasischke et al. (1999) for regions Amur, Khabarovsk and Sakhalin and is consistent with the result obtained from this study e.g. 20,544 $km^2$.

In 1987, the total damaged area in Heilongjiang province was estimated to be 8.900 $km^2$ (Lifu and Xiaorui 2001). Our study shows the value of 6,703 $km^2$.

Spatial agreement was examined using the data from Landsat-5 Thematic Mapper acquired on 5.7.1999 (path 111, row 25 and 26). The total burned area detected using Landsat-5 TM data was computed to be 4,600 $km^2$. The area estimated from NOAA data was equal to 4,550 $km^2$ in the same spatial coverage. Minor spatial disagreement was caused by almost one-year time gap between fire event and acquisition of Landsat data and by residual errors in NDVI compositing and active fire detection algorithm.

The described methodology for creation of forest fire time series database could be extended to continental and global scale and can be used for assessing of yearly burned areas and their time trends, description of post-fire vegetation patterns (Kučera and Yasuoka 2001), for estimation of greenhouse gases from forest fires as well as for connection to global terrestrial ecosystems models.

## 4. REFERENCES


Bohm, J., Radouch, V., and Hampacher, M., 1990, Teorie chyb a vyrovnávací počet. (in Czech) *Geodetický a kartografický podnik, Praha, 1990.*

Giglio, L., Kendall, J.D., and Justice, C.O., 1999, Evaluation of global fire detection algorithms using simulated AVHRR data. *Int. J. Remote Sens.* 20(10):1947-1985.

Fraser, R.H., Li, Z., and Cihlar, J., 2000, Hotspot and NDVI differencing synergy (HANDS): a new technique for burned area mapping over boreal forest. *Remote Sens. Environ.* 74:362-376.

Kasischke, E.S., Bergen, K., Fennimore, R., Sotelo, F., Stephens, G., Janetos, A., and Shugard, H.H., 1999, Satellite imagery gives clear picture of Russia's boreal forest fires. *EOS.* 80(13):141, 147.

Kasischke, E.S., and French, N.H.F., 1997, Constraints on using AVHRR composite index imagery to study patterns of vegetation cover in boreal forests. *Int. J. Remote Sens.* 18(11):2403-2426.

Kaufman, Y.J., Justice, C., Flynn, L., Kendall J., Prins E., Giglio, L., Ward, D.E, Menzel, P., and Setzer, A. 1998, Potential global fire monitoring from EOS-MODIS. *J. Geophys. Res.* 103:32215-32238.

Kučera, J., Yasuoka, Y., and Ito, A., 2002, Monitoring of forest fires and description of post-fire succession using terrestrial ecosystem model. *Proceedeing of the ISPRS commission VII symposium: Resource and Environmental Monitoring, Hyderabad, 2002.*

Kučera, J., and Yasuoka, Y., 2001, Regional monitoring fo froest disturbances and their potential effects to carbon cycling. *Proceeding of the 22nd Asian Conference on Remote Sensing, 5-9.11. 2001, Singapore.* 510-514.

Li, Z., Kaufman, Y.J., Ichku, Ch., Fraser, R., Trishchenko A., Giglio, L., Jin, J., and Yu, X., 2001, A review of AVHRR-based active fire detection algorithms: principles, limitations, and recommendations. In: *F. J. Ahern, J. G.Goldammer and C. O. Justice, (Editors): Global and Regional Vegetation Fire Monitoring from Space, Planning a Coordinated International Effort, , SPB Academic Publishing bv, The Hague, The Netherlands.* pp. 199-226.

Li, Z., Nadon, S., and Cihlar, J., 2000a, Satellite-based detection of Canadian boreal forest fires: development and application of the algorithm. *Int. J. Remote. Sens.* 21(16):3057-3069.

Li, Z., Nadon, S., Cihlar, J., and Stocks, B., 2000b, Satellite-based mapping of Canadian boreal forest fires: evaluation and comparison of algorithms. *Int. J. Remote Sens.* 21(16):3071-3082.

Lifu, S., and Xiaorui, T., 2001, Fire Situation in China. *FAO Global Forest Fire Assesment1990-2000., http://www.fao.org*

Pereira, M.C., 1999, A comparative evaluation of NOAA/AVHRR vegetation indexes for burned surface detection and mapping. *IEEE Trans. Geosci. Remote Sens.* 37(1):217-226.

# A performance evaluation of a burned area object-oriented classification model when applied to topographically and non-topographically corrected TM imagery

G.H. Mitri & I.Z. Gitas
*Dept. of Environmental Management, Mediterranean Agronomic Institute of Chania*
gmitri@maich.gr

Keywords: object-oriented classification, burned area mapping, topographic correction, LANDSAT TM

ABSTRACT: Operational use of remote sensing as a tool for post-fire Mediterranean forest management has been limited by problems of classification accuracy arising from confusion of burned and non-burned areas especially shaded areas. Object-oriented image analysis has been developed to overcome the limitations and weaknesses of traditional image processing methods for feature extraction from high resolution images. The aim of this work was to evaluate the performance of an object-oriented classification model developed for burned area mapping, when applied to topographically and non-topographically corrected LANDSAT TM imagery for a site on the Greek island of Thasos. The image was atmospherically and geometrically corrected before its object-oriented classification. The results were compared with the forest perimeter map generated by the Forest Service. The accuracy assessment using error matrix as well as fuzzy concept indicated that the removal of the topographic effect from the image before applying the object-oriented classification model resulted in only a slightly more accurate mapping (1.16%) of the burned area. It was concluded that topographic correction is not essential prior to object-oriented classification of a burned Mediterranean landscape using TM data.

## 1. INTRODUCTION

According to the literature, the spectral signature of recently burned areas can be confused with the signature of shaded areas (Chuvieco and Congalton 1988). Frequently, this occurs as a result of slope illumination and shadowing effects caused by the complex topography encountered in many forested areas. Moreover, it can result in a less accurate estimation of the burned area when multispectral classification, one of the most traditional used methods used to extract information from satellite data, is applied to satellite images (Gitas 2002).

The basic difference, especially when compared with pixel-based procedures is that image object analysis does not classify single pixels but rather image objects that have been extracted in a previous image segmentation step (Baatz 1999). Object-oriented classification, incorporating contextual and semantic information, is performed by utilizing not only image object attributes but also the relationship between networked image objects.

The combination of the new approach of object-oriented image analysis and the multispectral high resolution data of LANDSAT TM showed very promising results in burned area mapping and in discriminating among the different classes of confusions with the recently burned areas (Mitri and Gitas 2002). As it is reported in the literature (Gitas 2002), the removal of the topographic effect from

LANDSAT TM before its multispectral classification significantly improved (40%) the accuracy of the burned area mapping.

The aim of this work was to evaluate the performance of an object-oriented model developed for burned area mapping, when applied to topographically and non-topographically corrected LANDSAT TM data.

## 2. STUDY AREA AND DATA PRE-PROCESSING

The study area is Thasos, Greece's most northerly island, mountainous (the mean elevation is approximately 305 m, while the slopes range from 0 to 80 degrees) with Mediterranean climate. A satellite image that was acquired immediately after a large fire had burned out (15$^{th}$ August 1985) was obtained. In addition to the satellite image, a 30 m Digital Elevation Model (DEM) was also used. Other data retrieved included the official fire perimeter published by the Greek Forest Service and a topographic map of the island.

The LANDSAT TM image was atmospherically corrected. The Spatially-Adaptive Fast Atmospheric Correction Algorithm (ATCOR2), developed by Richter (1997) and compiled using the MODTRAN-2 and the SENSAT-5 codes, was used in this study. The model calculates a ground reflectance image in each spectral band: the first step assumes an isotropic (Lambert) reflectance law neglecting the neighbourhood of each pixel. The second step accounts for the influence of the neighbouring background (adjacency effect). The LANDSAT model was used to geometrically correct the LANDSAT TM image. The LANDSAT model allowed an ortho-rectification of LANDSAT data. A 10-metre grid size Digital Terrain Model (DTM) and a 1:50 000 planimetric map were used in the process. The geometric correction proceeded by identifying GCPs in the LANDSAT images and on the planimetric map.

Then, a Digital Elevation Model (DEM) was used to obtain information about surface elevation, slope, and orientation (Richter 1997). A model based topographic normalisation was performed by estimating the value Ls (the radiance that left the surface in the direction of the sensor), then using a reflectance behaviour model such as the Minnaert model to convert the Ls, which was reflected in the direction of the sensor under the particular incidence and exitance angles of each pixel, into normalised radiance (Ln) (Gitas 2002). The De-Relief programme that was developed by Costa-Posada (1997) was used in order to topographically normalize the LANDSAT TM image. The De-relief algorithm corrects radiometrically remote sensed data for the topographic effect using the Minnaert model (1941) with a single k coefficient for every different band of the image. Using it for each band separately makes it possible to correct each band with a different k coefficient (Gitas 1999). The first step was to calculate the cosine intercept. Slope and aspect images were derived from the DEM of Thasos, while sun elevation and sun azimuth were obtained from the metadata file. After the cosine incidence had been calculated, it was used in the second step of the model, together with the slope raster map, the atmospherically corrected single TM bands, and the k constant. The k value was used for each band individually, and the best value which produced the best result was chosen empirically (Figure 1, Figure 3a and 3c).

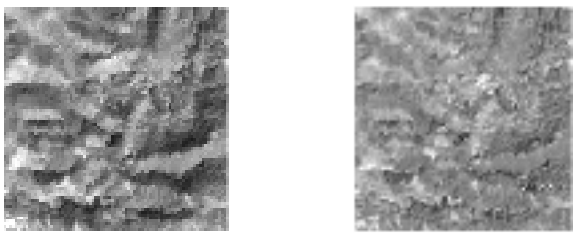

Figure 1. An image extract (NIR) before (left) and after (right) the topographic correction. Notice the absence of shadows in the latter image.

## 3. METHODOLOGY

The pre-processed image was used to build an object-oriented model (using eCognition) for burned area mapping. The same model was applied to the non-topographically corrected LANDSAT TM image of 1985. The model was tested to see whether it was robust enough to discriminate shaded areas from burned areas and whether it was effective for burned area mapping using non-topographically corrected LANDSAT images. By applying the object-oriented classification model using simultaneously the LANDSAT TM image with and without the topographic correction, the four levels were generated one after the other, using different scale parameters (5, 10, 23 and 30). The six TM bands were weighted differently at every level. Throughout the segmentation procedure, the whole image was segmented and image objects were generated based upon several adjustable criteria of homogeneity in colour and shape (Figure 2).

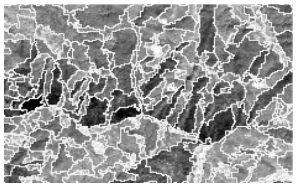

Figure 2. An image extract in NIR band showing the segmentation results in shaded areas (dark colour)

In the classification at level one the basic six classes "water", "unburned vegetation", "burned area", "slightly burned", "shaded areas" and "urban/bare ground" were distinguished. All the classes were classified based on membership functions for different spectral and shape features. At level three, a classification of only three classes took place before the classification of level 2. Few sources were used for the classification of "water", "not burned" and "possibly burned". Features were based on spectral information and contextual information. After classifying level 3, a classification based fusion took place. The principle of classification-based fusion is that all adjacent image objects that represent identical structures or are parts of identical structures are merged into one new image object. In this way, a number of image objects forming a "burned area", a "slightly burned area" and "shaded areas" could be merged into one image object representing an entire "possibly burned area". A structure is defined by organizing all classes which semantically form this structure in a structure group. At level two, the main classification level of burned area took place. Several sources were used for the classification. The two classifications of the sub-objects and the super-objects were used at level 2 to determine the percentage of burned area in every single object. Six sub-classes that represent the percentage of burned area were assigned to the parent class "burned area". Level four was created for the classification refinement based on initial classification. Class features such as "relative area of sub-objects" and "existence of sub-object" were used for this purpose.

## 4. RESULTS AND DISCUSSION

The accuracy of the two classified images was assessed by comparing the results with the fire service perimeter and by producing an error matrix. Apart from the classical methods of accuracy assessment, special methods based upon fuzzy concepts were used.

The overall classification accuracy of the topographically corrected classified image was estimated to be 98.85%. Users' accuracy and producers' accuracy for burned area mapping were estimated at, respectively, 94.59% and 97.22%. The burned area mapping using the non-topographically corrected image resulted in an overall accuracy of 97,69%. Burned area classification producer's accuracy was high (96.88%), while user's accuracy was estimated to be 93.94%. The objects "burned area" could strongly be separated from the other classes at the same level of classification (mean = 0.989 ± 0.093 of standard deviation).

The removal of the topographic effect from the satellite image before its classification improved only slightly (1.16%) the accuracy of the burned area mapping. The hierarchical network of image objects in different scales created by the patented segmentation represented the image information in different spatial resolutions. The resulting objects had as attributes not only spectral statistics but also shape information, contextual and texture. Thus, confusion between burned and shaded areas could be easily avoided allowing high classification accuracy in the non-topographically corrected image (Figure 3).

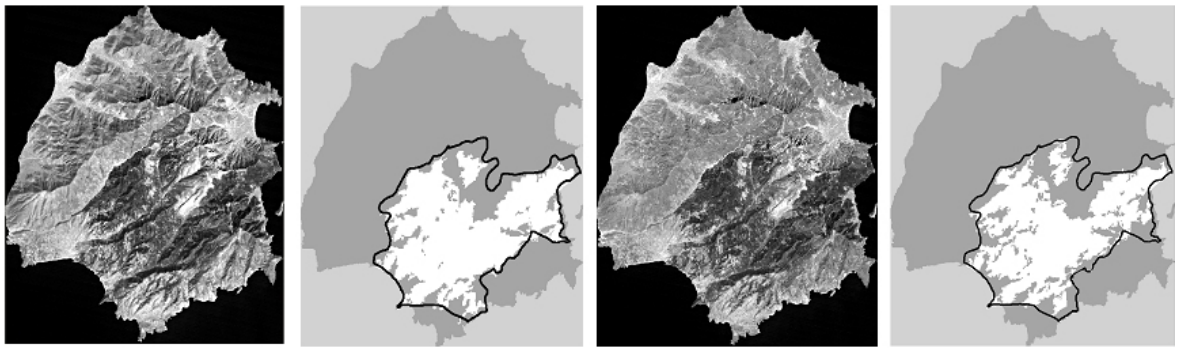

a b c d

Figure 3. LANDSAT TM in NIR before topographic correction (a), after topographic correction (c) and the classification results of image a (b) and of image c (d). The white colour in b and d represents the burned area and the black line represents the fire perimeter from the Greek Forest Service.

## 5. CONCLUSIONS

In this work the performance of a burned area object-oriented classification model when applied to topographically and non-topographically corrected LANDSAT TM imagery was evaluated. The general conclusion drawn from the study was that the topographic correction of the TM image prior to the object-oriented classification improved only marginally (1.16%) the accuracy of the burned area mapping. Thus, object-oriented classification can be successfully employed to map a burned area with very high accuracy (≈ 97%) independently of whether the LANDSAT TM image is topographically or non-topographically corrected. Finally, the findings underline how successfully object-oriented classification can be used as a tool for rapid operational burned area mapping of the Mediterranean forest fires using LANDSAT TM images without the need to employ complex and time-consuming topographic correction techniques.

## 6. ACKNOWLEDGEMENTS

This work was carried out as part of the SPREAD project (EVG1-2001-00043), supported by the European Commission, within the Fifth Framework Programme (Energy, Environment and Sustainable Development). The authors are grateful to Dr. Bernard Devereux and Dr. Carlos Costa-Posada, Unit for Landscape Modelling, University of Cambridge for their kind permission to use the DE_RELIEF software. Definiens Imaging GmbH's development of the eCognition software was greatly appreciated.

## 7. REFERENCES

Baatz, M. and Schäpe, A., 1999b. Object-Oriented and Multi-Scale Image Analysis in Semantic Networks. In: Proc. Of the 2nd Int. Symposium on Operationalization of Remote Sensing, Enshede, ITC: 16-20

Chuvieco, E. and Congalton, R.G., 1988. Using cluster analysis to improve the selection of training statistics in classifying remotely sensed data. Photogram. Eng. & Remote Sensing, 54: 1275-1281.

Costa-Posada, C., 1997. The Topographic Effect in Visible and Near Infrared Satellite Imagery. PhD Thesis, University of Cambridge, Cambridge, UK, 199 pp.

Gitas, I.Z., 1999. Geographical Information Systems and Remote Sensing in mapping and monitoring fire-altered forest landscapes. PhD Dissertation, University of Cambridge, 237 pp.

Gitas, 2002. An investigation into the usefulness of applying topographic correction prior to the mapping of recently burned areas from LANDSAT TM images. In: Domingos Xavier Viegas, ADAI, Portugal (Editor), Forest Fire research and Wildland Fire Safety. Millpress, Luso, Coimbra, Portugal, pp. 227-244.

Minnaert, M., 1941. The reciprocity principle in Lunar photometry. Astrophysical, 93(2): 403-410.

Mitri, G. and Gitas, I., 2002. The development of an object-oriented classification model for operational burned area mapping on the Mediterranean island of Thasos using LANDSAT TM images. In: Domingos Xavier Viegas, ADAI, Portugal (Editor), Forest Fire research and Wildland Fire Safety. Millpress, Luso, Coimbra, Portugal, pp. 227-244.

Richter, R. 1997. Correction of Atmospheric and Topographic Effects for High Spatial Resolution Satellite Imagery. In: International Journal of Remote Sensing 18(5), 1099-1111.

# Active fire recognition by the small satellite on Bi-spectral Infrared Detection (BIRD)

D. Oertel, K. Briess, E. Lorenz, W. Skrbek, & B. Zhukov
*Institute of Space Sensor Technology and Planetary Exploration, German Aerospace Center (DLR)*
dieter.oertel@dlr.de

Keywords: fire detection, small satellite, bush fires, fire characteristics retrieval

ABSTRACT: BIRD is a new experimental small satellite dedicated to recognition and quantitative characterisation of hight temperature events on the Earth surface like vegetation-, peat- and coal seam fires and volcanic activity. BIRD successfully demonstrates innovative fire recognition technology for small satellites that permits to retrieve quantitative fire characteristics, such as the effective fire temperature, fire area, radiative energy release, fire front length and fire front strength. As an example, BIRD observations of bush fires in the area of Canberra, Australia are analysed and compared with MODIS.

## 1. BIRD SMALL SATELLITE MISSION

The DLR satellite on Bi-spectral InfraRed Detection (BIRD) is a technology demonstrator of new infrared push-broom sensors dedicated to recognition and quantitative characterisation of thermal processes on the Earth surface (Briess et al., 1996). BIRD was piggy back launched with the Indian Polar Satellite Launch Vehicle in a 570 km circular sun-synchronous orbit on 22 October 2001 and is successfully operated by DLR since that time.

BIRD primary mission objectives are:

- test of a new generation of infrared array sensors with an adaptive radiometric dynamic range,
- detection and scientific investigation of high temperature events such as forest fires, volcanic activities, and coal seam fires,
- test of small satellite technologies, such as an attitude control system using new star sensors and new actuators, an on-board navigation system based on a new orbit predictor and others.
- The BIRD main sensor payload consists of:
- a two-channel infrared Hot Spot Recognition Sensor system (HSRS),
- a Wide-Angle Optoelectronic Stereo Scanner (WAOSS-B).

Their characteristics are given in Table 1.

A unique feature of the BIRD Hot Spot Recognition System mid infrared (MIR) and thermal infrared (TIR) channels is the real-time control of their dynamic range (Skrbek & Lorenz, 1998). That allows the observation of hot events without sensor saturation, preserving at the same time a good radiometric resolution of 0.2 K at ambient temperatures of about 300 K. Due to its higher spatial resolution, BIRD can detect fires with the area a factor of seven smaller than operational polar orbiting systems such as the Advanced Very High Resolution Radiometer (AVHRR) or the Moderate Resolution Imaging Spectro-radiometer (MODIS). However, one has also keep in mind that AVHRR

and MODIS can provide daily global coverage while BIRD is a demo mission providing only episodical data sets.

Table 1: Characteristics of the BIRD main sensor payload

| | WAOSS-B | HSRS |
|---|---|---|
| Spectral bands | VIS: 600-670nm<br>NIR: 840-900nm | MIR: 3.4-4.2µm<br>TIR: 8.5-9.3µm |
| Focal length | 21.65mm | 46.39mm |
| Field of view | 50° | 19° |
| f-number | 2.8 | 2.0 |
| Detector | CCD lines | CdHgTe Arrays |
| Detector cooling | Passive, 20°C | Stirling, 80-100 K |
| Detector element size | 7µmx7µm | 30µmx30µm |
| Detector element number | 2880 | 2x512 staggered |
| Quantisation | 11bit | 14bit (for each exposure) |
| Ground pixel size | 185m | 370m |
| Sampling step | 185m | 185m |
| Swath width | Max. 533km | 190km |

## 2. DETECTION AND ANALYSIS OF AUSTRALIAN BUSH FIRES BY BIRD AND COMPARISON WITH MODIS

The BIRD hotspot detection algorithm (Zhukov et al., 2002) comprises the following thresholding tests:

- adaptive MIR thresholding to detect potential hot pixels,
- NIR thresholding to reject strong sun glints,
- adaptive MIR/NIR radiance ratio thresholding to reject weaker sun glints, clouds and other high-reflective objects,
- adaptive MIR/TIR radiance ratio thresholding to reject warm surfaces,
- consolidation of the adjacent hot pixels in hot clusters (hotspots) and estimation of hotspot characteristics: the effective fire temperature and area, radiative fire energy release (FRE).
- the effective fire temperature and area are retrieved with the Bi-spectral technique (Dozier, 1981) using the MIR and TIR cluster radiance fluxes and background radiance estimation from the neighbouring pixels. In contast to the usual application of the Bi-spectral technique, we apply it not to separate hot pixels but to entire hot clusters. The advantages of the cluster-level approach are:
- the effective fire area does not depend on the point spread function (PSF) of the MIR and TIR channels, and
- the estimations of effective fire temperature and area are low-sensitive to sub-pixel inter-channel MIR/TIR geometric co-registration errors and MIR/TIR PSF difference.

The FRE characterizes the intensity of burning. However, it accounts only for the radiated part of the energy released by a fire, while a significant portion of fire energy is consumed by convection, evaporation and heat transfer in the ground. The FRE is estimated using the effective fire temperature and area or alternatively the MIR radiance method (Wooster et al., 2003) that is applicable for fires with a temperature of ≥600 K.

As an example of the recent BIRD data, let us consider a fragment of the BIRD image of bush fires observed ~100 km south-west of Canberra, Australia that was acquired on 26 January 2003 and compare it with the MODIS image acquired ~40 min earlier (Fig.1). For this purpose, the MODIS image was co-registered with the BIRD image and re-sampled to the BIRD sampling step.

While only larger fires are resolved in the MODIS MIR image (Fig. 1a), the BIRD MIR image reveals a much more detailed picture of the burning (Fig. 1b). A lot of small fires that can be recognized in the BIRD image do not show up in the MODIS image or can not be reliably separated there from warm soils.

An application of the BIRD hotspot detection algorithm to both data sets resulted in detection of 11 hot clusters in the MODIS image and of 56 hot clusters in the BIRD image – see Fig. 1c and 1d. Some of the MODIS hotspots turn out to be composed of a few separate fires in the higher-resolution BIRD data. Many of the small hotspots detected in the BIRD data do not have counterparts in the MODIS data. Hot clusters in Fig. 1c and 1d are color-coded using their FRE values. For this purpose, the MIR radiance method was used that provides stable results even for small fires.

Estimations of the effective fire temperature and area for the hot clusters detected in the MODIS data were generally low stable and did not allow a reliable differentiation of the burning regimes. This is due to a relatively low fire proportion in the MODIS hot pixels and to a strong thermal non-homogeneity of the background composed of unburned vegetation and warm fire scars.

BIRD provided a higher accuracy of the Bi-spectral retrievals due to its smaller pixel size and consequently a higher fire proportion in the hot pixels. The temperature retrieval error for larger hot clusters was typically in the range of 100-200 K. Table 2 gives the values of the effective fire temperature and area and of FRE for some of the larger clusters in Fig. 1. In two cases, only the lower bound for the effective fire temperature could be estimated. The effective fire temperature of most of the hot clusters is typical for active flaming burning. Only the hot clusters 8 and 10 can be interpreted as smouldering fires.

Table 2. Characteristics of some hot clusters estimated from the BIRD data in Fig. 1

| No | Effective fire temperature, K | Effective. fire area, Ha | Fire radiative energy release, GW |
|---|---|---|---|
| 1 | 910 | 1.7 | 0.69 |
| 2 | >1000 | <3.0 | 3.6 |
| 3 | 900 | 2.9 | 1.1 |
| 4 | 780 | 5.7 | 1.1 |
| 5 | >800 | <0.7 | 0.84 |
| 6 | 820 | 4.8 | 1.2 |
| 7 | 830 | 10.5 | 2.8 |
| 8 | 660 | 7.9 | 0.65 |
| 9 | 910 | 2.6 | 1.0 |
| 10 | 640 | 2.7 | 0.19 |

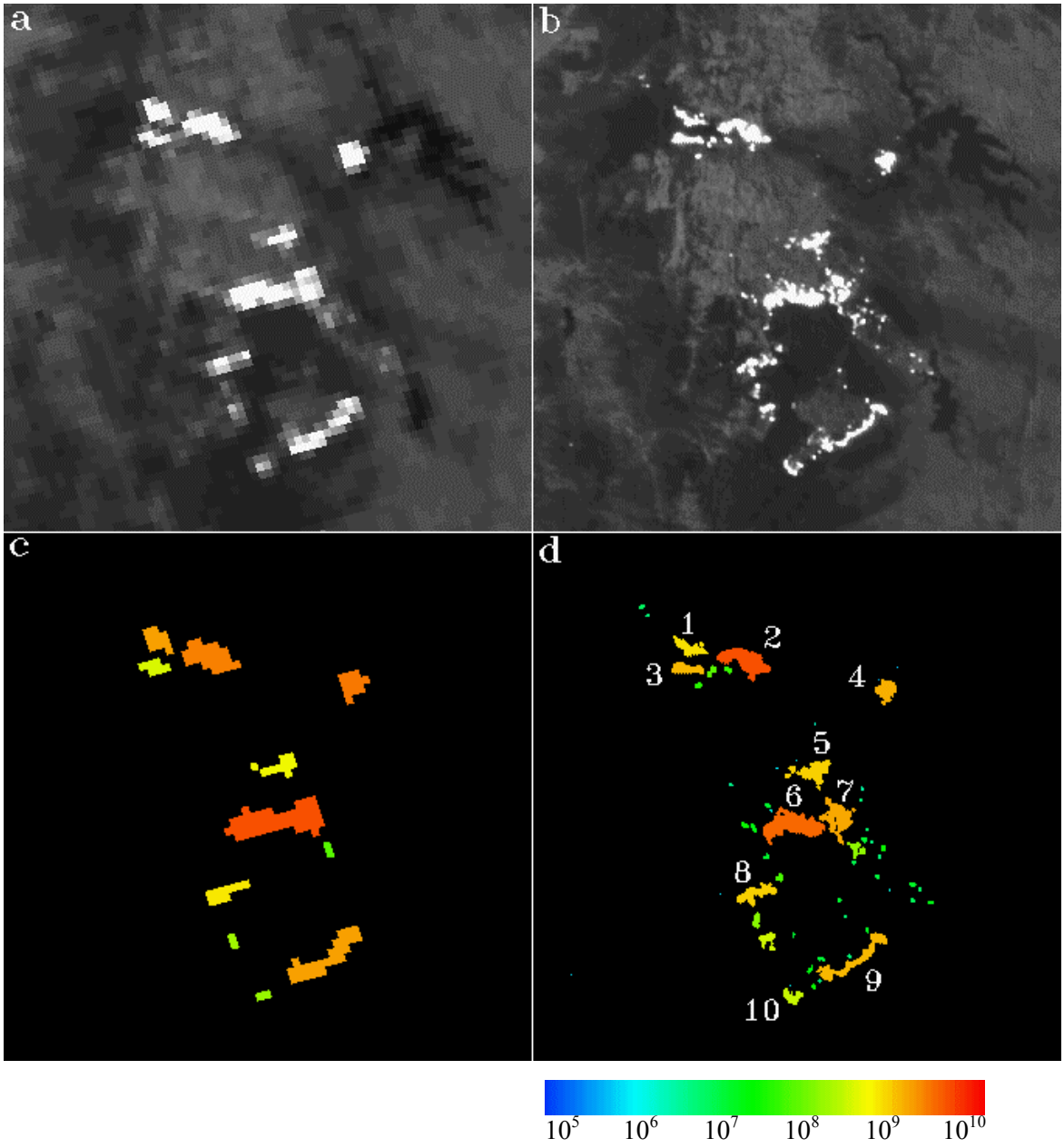


Figure 1. MODIS and BIRD images of bush fires in the area of Canberra, Australia obtained on 26 January 2003: a – MODIS MIR channel 21; b – BIRD MIR channel; c – detected hotspots in the MODIS image; d - detected hotspots in the BIRD image; the hotspots are color-coded using their radiative fire energy release (FRE) W

The total FRE in the scene in Fig. 1 is estimated from the MODIS and BIRD data as 12.8 and 14.1 GW, respectively. Some FRE underestimation by the MODIS may be due to missing the small fires. FRE values for separate clusters in the MODIS and BIRD data also show a reasonable agreement. However, a direct comparison in some cases is difficult due to different shape and extent of the hot clusters (compare Fig. 1c and 1d).

## 3. CONCLUSIONS

The data provided by the BIRD Hot Spot Recognition System permit the application of the Bi-spectral method to retrieve:

1- the effective temperature,
2- the effective area, and
3- the fire radiative energy release
4- of high temperature events such as forest fires, coal seam fires or volcanic activities.

The BIRD Hot Spot Recognition System can be considered as a innovative remote sensing tool and a prototype sensor for new Earth observation missions targeting on quantitative analysis of high temperature events.

## 4. REFERENCES


Briess, K., Jahn, H. & Roeser, H.-P. 1996. A DLR Small Satellite Mission for the Investigation of Hot Spots, Vegetation and Clouds. *Acta Astronautica* Vol. 39: 899-908.

Dozier, J. 1981. A method for satellite identification of surface temperature fields of Sub-pixel Resolution. *Remote Sensing of Environment* Vol. 11: 221–229.

Skrbek, W., & Lorenz, E. 1998. HSRS – An infrared sensor for hot spot detection. *Proceedings of SPIE, Infrared Spaceborne Remote Sensing VI* Vol. 3437, 167 – 176.

Wooster, M. J., Zhukov, B & Oertel, D. 2003. Fire radiative energy for quantitative study of biomass burning: Derivation from the BIRDexperimental satellite and comparison to MODIS fire products. *Remote Sensing of Environment.* In press.

Zhukov, B., Briess, K., Lorenz, E., Oertel, D. & Skrbek, W. 2002. BIRD Detection and Analysis of High-temperature Events: First Results. *Proc. SPIE* Vol. 4886.

# Analysis of plant community regeneration in burnt areas by multitemporal Landsat TM and field data

Fernando Pérez-Cabello & Juan de la Riva
*Department of Geography, University of Zaragoza, Spain*
lavasier@posta.unizar.es

Keywords: NDVI, Forest fire, vegetation cover, floristic and physiognomic changes

ABSTRACT: In this paper plant community regeneration using satellite imagery (Landsat TM) and field data is analysed. Several burnt communities of *Pinus sylvestris* and scrub affected by fire in 1990 through multi-temporal NDVI (1990-1997) and vegetation inventories are checked to determine the explicative capacity of NDVI previous and the physiognomic-floristic component of regeneration process. The NDVI previous value has a great importance in the determination of the space discontinuities of vegetation covering after fire (63%). Nevertheless the information support obtained from field data shows important floristic and physiognomic changes. In this way, the necessity to complete the results of the NDVI with field data is suggested.

## 1. INTRODUCTION AND OBJECTIVES

NDVI presents high correlation with some of the biotic properties of the vegetation -green biomass, vegetation cover or leaf area index (LAI) (Elmore *et al.*, 2000)-. A great number of studies uses NDVI as an indicator of plant cover changes after fire (e.g., Milne, 1986; Díaz-Delgado *et al.*, 1998; Miller & Yool, 2002; Riaño *et al.*, 2002).

Nevertheless, the analysis of the vegetation cover through NDVI only explores re-geration in terms of the biotic properties with which it is correlated, as it is not operative in the analysis of the physiognomic or floristic component of the regeneration process. This subject -equally necessary to suitably diagnose the regeneration process- can be analyzed through multi-temporal classification or with the incorporation of data of floristic inventories, in spite of the complexity to correlate information of field with satellite registries (Salvador, 1999).

This paper analyses the vegetation response of several burnt communities in a wildfire, occurred 21st August 1990 through both NDVI and floristic-physiognomic data taken from fieldwork. Two goals are stated: to determine the explicative capacity of the previous vegetation so that the recovery degree of the communities of substitution can be predicted; to analyse vegetation re-establishment levels in terms of recovery, physiognomic and floristic response through field data.

The 400 ha fire, which is analysed, is located in the upper part of the *Bco. de Nofuentes*, Spanish Pre-Pyrenees (Figure 1). Although its extension, the vegetation typology of the a-ffected communities is quite wide as a consequence of the peculiar and diverse environment of the area, located between the Mediterranean and Eurosiberian biogeographic regions. Different facies of *Pinus sylvestris* are analysed, both in pure communities and in a mixture with *Quercus rotunfoliae, Q.* gr. *cerrioides* and *Fagus sylvatica*, and shrubs of *Buxus sempervirens*, *Echinospartum horridum* and *Genista scorpius.*


Figure 1. Location of the study area.

## 2. METHODS

The methodology related to the use of remote sensing images has been developed in a framework of detection of change techniques. This implies a robust radiometric and geometric consistence in the images used. Six summer Landsat TM images have been selected from technical and methodological criteria: 12th July 1990, 24th August 1991, 12th July 1993, 29th June 1994, 18th July 1995 and 7th July 1997. A second-order polynomial equation and a nearest-neighbour interpolation method have been used for the geometric correction. Conversion to spectral reflectance has been applied for the radiometric correction by normalizing the topographic and atmospheric effects (Pons & Solé, 1994).

Subsequently, the burnt area perimeter has been delimited (Pérez-Cabello, 2002). In order to remove pixels showing very different combustion levels, a PCA of the NDVI va-lues has been performed as well as a supervised classification of a RGB composition from the 4th, 5th and 7th principal components.

Both the *Forest Map of Aragón 1:50.000* and the cartography derived from the digital classification have been used to determine types of affected communities. From each community 95 pixels (5'9 ha) have been selected eliminating the ones having the lowest probability of being correctly classified ($\chi^2 < 3$) or showing a different level of severity. Later the NDVI of the different images have been generated. Some of these are shown in Figure 2.

Representative plot areas of the burnt communities have also been selected for the fieldwork. Each of them includes a *burnt* area and a *control* area which is non-burnt but with similar characteristics. The vegetation analysis has been done using floristic inventories and estimating the percentage of recovery for each species according to both the total inventory surface and the stratum where it is located.

## 3. RESULTS AND DISCUSSION

According to the type of vegetation, the Figure 3 shows the evolution of recovery after fire interpreted from annual mean NDVI values. The highest values, in 1990, correspond to the tree communities. The values decrease just one year after the wildfire and increase progressively until they reach the highest levels in 1997. The similarity of the NDVI values of each community one year after the fire fades progressively till 1997 when they reach a distribution per communities quite similar to the one in 1990.

Statistically significant differences have been detected between NDVI values of diffe-rent years in tree-communities (*p-value* < 0.001); not being thus in the case of the scrubs for the extreme years (before and 7 years after the fire). This might be related to resilience and the smaller demand of resources for re-establishment after fire from scrubland communities in relation to the tree-communities.

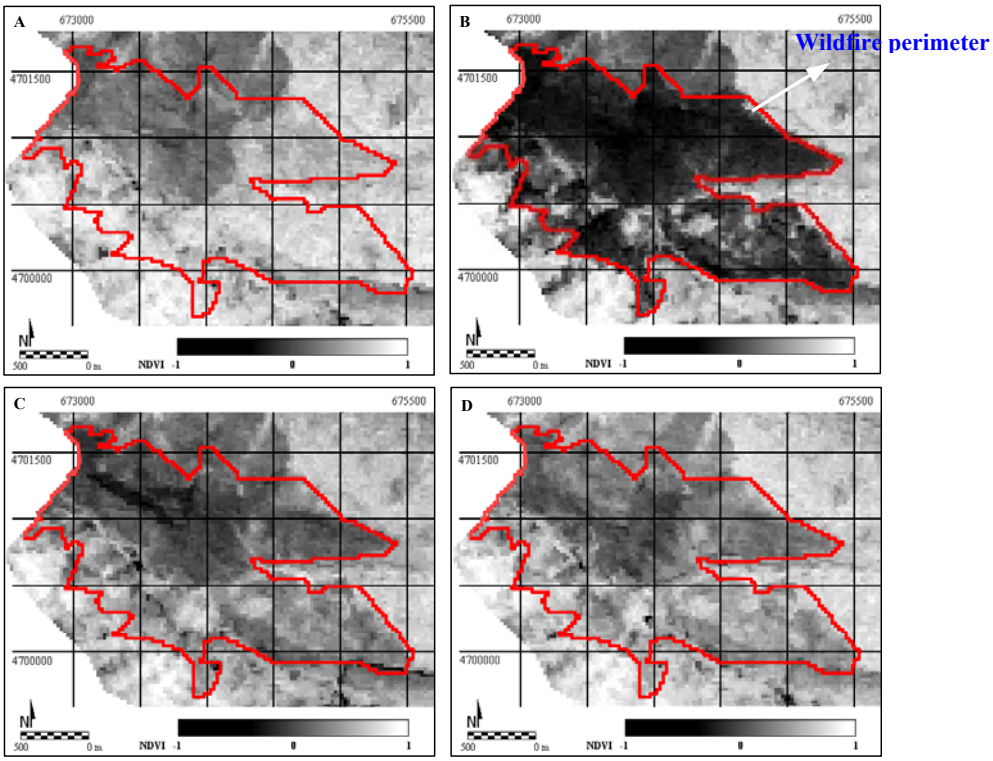


Figure 2. A: NDVI 1990. B: NDVI 1991. C: NDVI 1994. D: NDVI 1997.

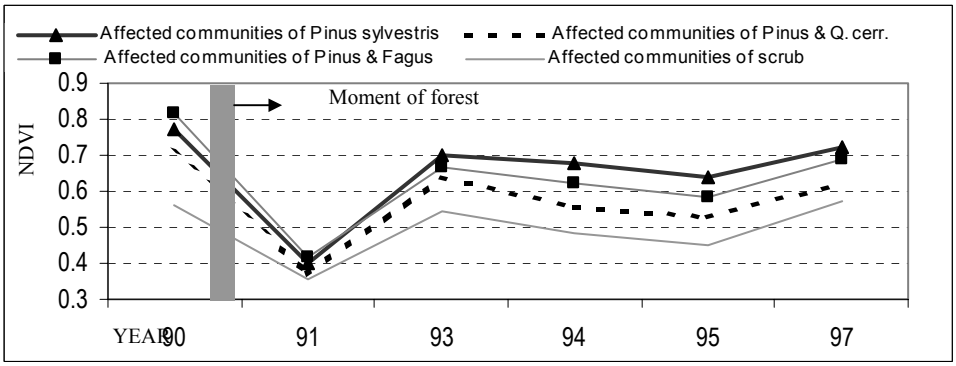


Figure 3. Evolution of recovery after fire interpreted from NDVI annual mean.

Detected values of NDVI after fire seem to indicate the structural character of the post-fire vegetation recovery process, that is to say, the existence of positive relations between the amounts of burnt and regenerated biomass, measured through the NDVI (Figure 4). The explicative capacity of the previous vegetation -NDVI 1990- to predict the reco-very degree of the substitutes communities is 63% ($r$ = 0'791, *p-value* < 0.001) according to the 1997 image. The relation between the 1990 and 1991 NDVI has also a positive character but does not present the same intensity; in this case, the explained variance is 21%.

Similar results are obtained analyzing regular intervals of NDVI (Table 1). While that pixels with values between 0.5 and 0.6 -before the wildfire- present the lower average value in 1997 (mean of 0.567), in the rest of the intervals mean values smaller to those of before the fire are computed, although these being always superior to those of the lowest interval (0.5 a 0.6).

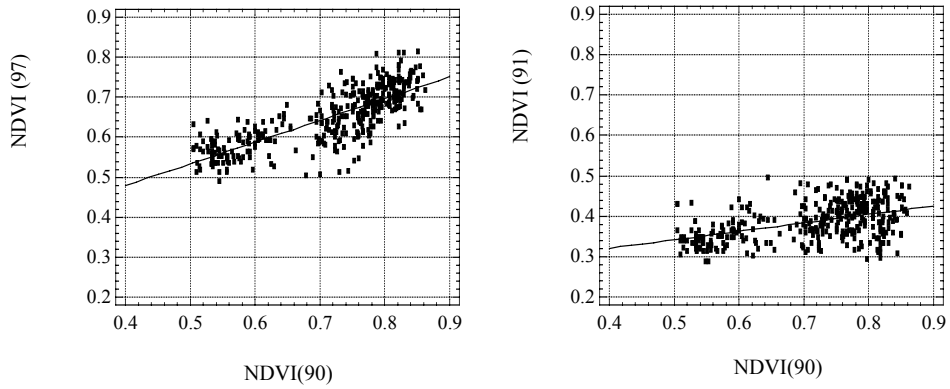


Figure 4. Correlation between 1991 and 1997 NDVI in relation to the 1990 values before the fire.

Table 1. Mean values and standard deviation of the NDVI by regular intervals.

| | | NDVI 1990 | | NDVI 1997 | |
|---|---|---|---|---|---|
| *Intervals NDVI* | *Nº pixels* | *mean* | *stand. dev.* | *mean* | *stand. dev.* |
| 0.5-0.6 | 78 | 0.551 | 0.026 | 0.567 | 0.033 |
| 0.6-0.7 | 42 | 0.642 | 0.036 | 0.605 | 0.039 |
| 0.7-0.8 | 171 | 0.757 | 0.028 | 0.665 | 0.054 |
| 0.8-0.9 | 89 | 0.825 | 0.015 | 0.722 | 0.038 |

Plant communities considerations are extracted from fieldwork complete the results obtained by the NDVI values. In terms of recovery surface -accumulated percentage of the recovery stratum- the mean of the values obtained in the control areas double the average of the values obtained in the burnt areas (141 and 72% respectively); with NDVI values differences are smaller (0'717 and 0'652). Such a dysfunction between real values and NDVI values for the year 1997 might be related to the problems of saturation presented by NDVI with recovery levels above 100%, but also to the fact that the sensor only collects data from the vegetation canopy.

The analysis per vegetation communities shows important physiognomic (inversion of stratum organisation) and floristic (replacement by different communities) variations registered in burnt forest-tree areas (Figure 5). It is much less accusing in the case of the scrubs. Mainly the replaced arboreal facies are formed by herbaceous vegetation and scrublands dominated by *Genista scorpius*, *Buxus sempervirens* and several species from *Rosaceae* genus. Structure and composition are very similar to the control and burnt plot of scrubland.

Related to NDVI, the communities that registered the highest NDVI values are precisely the ones that have been replaced by communities completely different to the original ones, although it is also where a greater amount of green biomass has been generated.

The NDVI is elevated like good indicator of the rate of vegetation recovery in covering terms, but a good re-establishment of the NDVI is not synonym of good post-fire vegetation regeneration; although it can be good for the recovery, it is not in terms of vegetation succession.

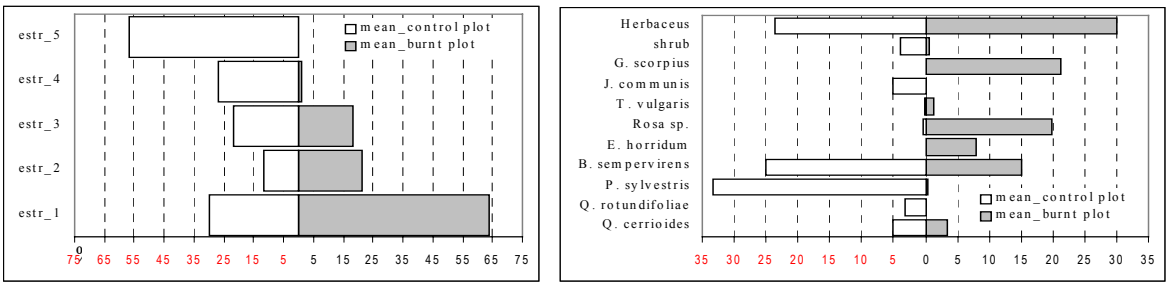


Figure 5. Physiognomic (*percentage of covering by stratum*) and floristic differences (*percentage of covering by main species*) between burnt and control sectors computed in the arboreal facies.

## 4. CONCLUSIONS

Independent of the type of forest community, the density of the previous vegetation has a great importance in the determination of the space discontinuities of the processes of vegetation covering and geomorphology reactivation after fire. In this way, positive relations have been detected between the values of NDVI before the fire and seven years after it. The explicative capacity of the previous vegetation -calculated with the NDVI- in order to predict the degree of covering of the formation substitutes is considered in 62,56%. Nevertheless, the use of the NDVI to make a precise diagnosis of the characteristics of the process of vegetation regeneration after fire requires complementary information of field data. An identification of the NDVI with the regeneration process after fire can be erroneous since the diagnosis of the degree of vegetation recovery demands a reading of the component of covering like the referred one to the floristic-physiognomic characteristics of the secondary communities.

## 5. ACKNOWLEDGEMENTS

This reach was supported by the *Spanish Ministry of Science and Techonology* (contracts AGL2000-0842 & Ren2002-00133). Special thanks go to *Servicio de Investigaciones Agrarias* (*DGA*) for the cession of four Landsat TM images.

## 6. REFERENCES

DÍAZ-DELGADO, R., SALVADOR, R. & PONS, X. 1998. Monitoring of plant community regeneration after fire by remote sensing. In Trabaud, L. (Ed.): *Fire Management and Landscape Ecology*.. Montpellier: Centre d'Ecologie Fonctionnelle et Evolutive, CNRS. 315-326.

GAMON, J.A., FIELD, C.B., GOULDEN, M.L., GRIFFIN, K.L., HARTLEY, A.E., JOEL, G., PEÑUELAS, J. & VALENTÍN, R. 1995. Relationships between NDVI, canopy, structure and photosynthesis in three Californian vegetation types. *Ecological Applications*, 5: 28-41.

MILNE, A. K. 1986. The use of remote sensing in mapping and monitoring vegetational change associated with bushfire events. *Geocarto International* 1: 25-32.

MILLER, J.D. & YOOL, S.R. 2002. Mapping forest post-fire canopy consumption in several overstory types using multi-temporal Landsat TM and ETM data. *Remote Sensing of Environment*, 82: 481-496.

PÉREZ CABELLO, F. 2002. *Paisajes forestales y fuego en el Prepirineo occidental oscense. Un modelo regional de reconstrucción ambiental*. Serie Investigación, 33. Zaragoza: Publicaciones del Consejo de Protección de la Naturaleza de Aragón.

PONS, X. & SOLÉ, L. 1994. A simple radiometric correction model to improve automatic mapping of vegetation from multispectral satellite data. *Remote Sensing of Environment*, 48: 191-204.

RIAÑO, D., CHUVIECO, E., USTIN, S., ZOMER, R., DENNISON, P., ROBERTS, D. & SALAS, J. 2002. Assessment of vegetation regeneration after fire through mulititemporal analysis of AVIRIS images in the Santa Monica Mountains. *Remote Sensing of Environment*, 79: 60-71.

# Map of burnt zones in Asturias in the period 1991-2001 created from Landsat-TM Images

C. Recondo, E. Wozniak & C. S. Pérez-Morandeira
*Institute of Natural Resources and Land Distribuition (INDUROT).University of Oviedo, Spain*
crecibdi@relay.etsimo.uniovi.es

Keywords: forest fire, burned zones mapping, Landsat-TM

## 1. INTRODUCTION

Forest fires, due to their extension, frequency and intensity reached in recent years, are one of the main ecological problems under consideration in the Principality of Asturias (Álvarez *et al*., 2001). These fires have considerable repercussions upon ecosystems, biodiversity, lasting management of forest resources and on local and national economies. Traditionally, the inventory of these fires has been carried out in this Community by CEISPA (Extinction of Fires, Rescue and Salvage and Civil Protection Consortium for the Principality of Asturias), but CEISPA only deals with the location where the fire has occurred and with the estimated damaged area indicated by forest guards who are in charge of inspecting the land; this data has been available since 1988. More recently, this organisation created a unique map by means of GPS during flight between summer and autumn in 2000, which adhered solely to the burnt zones of greatest extension.

For a more thorough study on the effects of these continuos fires in our region, one needs to rely on a precise map which serves to recognise the exact location of burnt zones, their size and the surface vegetation affected in each case. One of the ways to obtain this information on past fires (in the case of this article, for the past decade), is by resorting to old satellite images. The use of satellite images for the map of burnt areas, even though it is novel in our Community, has long been assiduously and successfully applied in other Spanish regions, especially in Catalunya (Díaz-Delgado & Pons, 2001), even though its images proceed from various sensors and the work method is different to that applied by us.

## 2. INICIAL DATA

The series of selected images for this study are derived from Landsat-TM (nº 5 and 7) and cover the period 1991-2001, at the rate of approximately one image per year. The selection has been extremely conditioned by the existence of cloudiness affecting the image, a prevailing problem in our region, which makes it difficult to find more than two valid images in an entire year. Nevertheless, when it has been possible to select, it has been preferable to use images from the end of spring and the beginning of autumn, as the monthly distribution of fires obtained from CEISPA data present two important peaks, one in March and another in August (Álvarez *et al.*, 2001). Images taken in winter have been rejected because, even though some were free from clouds, the level of the Sun over the horizon was very low (<35°), which produced several shadows and rendered the image useless for the detection of burnt zones. The images finally selected are ten from Landsat-5 (dates: 07-10-91, 19-06-92, 08-07-93, 09-06-94, 28-06-95, 14-06-96, 14-04-97, 07-08-98, 09-07-99 and 25-06-00) and two from Landsat-7 (dates: 07-10-00 and 20-06-01). With regard to the latter, only the 7 bands in common with Landsat-5 have been used.

For the geo-reference and topographic correction of images, (necessary for areas in relief), we have relied upon a Digital Elevations Model (DEM) of the whole of the Principality of Asturias. The DEM was carried out on the basis of manual digitalisation of topographic maps of the IGN (National Geographic Institute) scaled at 1:25,000, taking level curves equidistant at 50*m* as well as singular points and lines. The final result of the process produced a DEM raster, pixel size 50*m*, which was later resampled at 30*m* in order to coincide with the Landsat-TM image resolution.

Other data used were various vectorial maps with different information covering the whole of Asturias: rivers, municipalities and coastline limits, the three of which are derived from the 1:25,000 of the IGN, the vegetation from the Thematic Cartography of the Principality and the maps created by INDUROT for the '*Natural Risks in the Principality of Asturias - forest fires*' project (Marquínez *et al.*, 2001): soil erosion risk, natural value loss, economical exploitation losses, and the forest fires dangers and risks maps. The rivers and coastline were used to geo-reference the TM images. The municipalities, vegetation and thematic maps from INDUROT were used to create statistics of the damages produced.

The sole support field map has been carried out by CEISPA by means of perimetering by GPS by helicopter in the summer of 2000, which we will use to validate our method.

## 3. METHOD USED AND ITS VALIDATION

### *3.1 Correction of images*

The application of whatever algorithm for the detection of changes requires an adequate correction, both geometric and radiometric, of the satellite images. Therefore, and in this order, our images have been atmospherically corrected, geo-referenced and topographically corrected.

The correction for atmospheric excess in the DN of each band was based on two hypotheses: that this excess might be measured in approximation in areas of very low reflectivity, for example, water surfaces, for which the sensor would detect a low and constant radiance in absence of atmospherics (generally accepted hypothesis). The second hypothesis was to consider that all areas of deep, clear water have a similar radiance, taking as reference the values obtained by Bukata *et al.* (1983) for the selected areas of water on our images (Arbón, Doiras and Rioseco reservoirs). These values, as well as their conversion to DN using coefficients of TM-5 and ETM-7 sensor calibrations, are shown in Table 1. In band 6, radiometric homogenisation was also carried out upon water zones by means of a low arbitrary value, but in this case the purpose of homogenisation was not that of an atmospheric correction.

Table 1: Radiance for water (Bukata *et al*., 1983) and its corresponding ND for the TM-5 & ETM-7 sensors.

| Band | Radiance=L ($mW/cm^2\ sr\ \mu m$) | DN TM5 | DN ETM7 | Band | Radiance=L ($mW/cm^2\ sr\ \mu m$) | DN TM5 | DN ETM7 |
|---|---|---|---|---|---|---|---|
| 1 | 1.23 | 23 | 24 | 4 | 0 | 2 | 8 |
| 2 | 0.72 | 9 | 17 | 5 | 0 | 3 | 8 |
| 3 | 0.12 | 3 | 10 | 7 | 0 | 3 | 8 |

The geometric correction and geo-referencing were carried out by using some 60 control points distributed throughout the Principality of Asturias. The vast relief of the region makes it is necessary to include the altitude (via DEM), in the polynomials of adjustment implied in this process, that is to say, the images must be orthorectified (using the method by Palá & Pons, 1995). The *r.m.s. mean* finally obtained for all the images is between *0.6* and *1*.

The topographic correction is carried out in relief zones in order to improve the later classifications which are carried out on the images. Our correction uses the DEM and the Minnaert model to calculate the radiance of a non-lambertian surface (Recondo *et al.*, 2000; 2001a).

The comparison between the image taken in June (from the TM-5 sensor) and that of October 2000 (from the ETM-7), requires a radiometric homogenisation not only for the low values, but in all values as well, as the calibration parameters are different for each sensor. Therefore, the conversion of

$DN_{band}$(ETM) a $DN_{band}$(TM) is carried out by selecting the aforementioned water zones (of low and constant radiance) and others of high radiance, which are supposed constant as well (bare ground, asphalt, etc; in our case, we have selected the airstrip at Ranón airport, which is flat) and obtaining a linear fit between both values.

*3.2 Map of burnt areas and its validity*

Burnt areas are obtained by applying a detection of changes method to every two images and, later, by carrying out a supervised classification on the image of changes. The selection of the best method and classifier for the detection of these zones in Asturias was obtained in an earlier work (Recondo *et al.*, 2001b), where it was concluded that the best detection method for burnt areas was the simple difference of images (before and after the fire) and that the best classifier was that of maximum probability highlighting its immediate surroundings in a 5x5 filter. This selection is confirmed to be the most appropriate for the series of images used in this study. Nevertheless, in this case, the best visualisation of burnt zones was obtained by a composition of RGB=b4-b5-b7 difference images, where these zones clearly stand out from the others due to the intense orange colour that they create (Figure 1a). Thus, training polygons for the class of burnt zones are introduced into the orange zones, although other polygons are also necessary to separate the diverse colours that appear in the difference image into classes and which represent other changes (the maximum number of classes are between 11 and 25). Once the supervised classification has been carried out, we retain only the class of burnt areas in order to obtain the map of it.

The validation of the method used in this study to obtain a burnt zone map between every two dates, has only been able to be carried out with the aforementioned map from CEISPA obtained by GPS in the summer-autumn 2000. This validation refers to the major fires (>10 ha), given that the field map only adhered to these fires. The statistics for the comparison between the image difference map June 2000-October 2000 and the GPS map are shown in Table 2. Although the obtained results by both methods coincide quite well in general (20 out of 31 fires show a consistency of $\geq$ 80%) discrepancies were found due to the following effects: the GPS map smoothes the contour and doesn't distinguish unburned areas within the affected zone (cases 4, 5, 6, 7, 11, 13, 18, 19, 21, 22, 27 and 31 in Table 2). Some zones have achieved a rapid recuperation of vegetation and they don't appear burned in the post-image (case 3). Burnt zones have been detected at a later date to those of the GPS flight in connection to earlier fires (cases 2 and 5). Specific remote sensing problems are the clouds and the topographic occultation (cases 1, 15, 26 and 28). For some cases the difference is unknown (cases 11, 23 and 29). Finally, as an example of the consistency between both maps, one of the 31 zones (case 13), mapped by CEISPA, is given in detail in Figure 1.

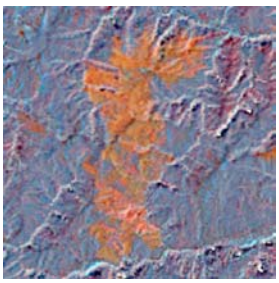

Figure 1. Detail of a burnt zone in the Cangas de Narcea municipality between June and October 2000.
**Left:** image difference (before image - after image); RGB =457; and
**Right:** classified image (grey area) and GPS cartography (red line).

Table 2: Comparison between the difference image June 2000-October 2000 map and the GPS map.

| Nº fire | GPS (ha) | Landsat (ha) | % in common | Nº fire | GPS (ha) | Landsat (ha) | % in common | Nº fire | GPS (ha) | Landsat (ha) | % in com. |
|---|---|---|---|---|---|---|---|---|---|---|---|
| 1 | 2052 | 1963 | 88 | 12 | 120 | 138 | 94 | 23 | 93 | 66 | 67 |
| 2 | 1353 | 1396 | 86 | 13 | 930 | 834 | 86 | 24 | 18 | 17 | 85 |
| 3 | 260 | 149 | 57 | 14 | 107 | 112 | 93 | 25 | 136 | 142 | 94 |
| 4 | 391 | 221 | 55 | 15 | 305 | 210 | 67 | 26 | 81 | 17 | 17 |
| 5 | 321 | 383 | 89 | 16 | 278 | 250 | 84 | 27 | 95 | 82 | 80 |
| 6 | 331 | 221 | 57 | 17 | 76 | 76 | 92 | 28 | 114 | 101 | 72 |
| 7 | 159 | 148 | 90 | 18 | 179 | 167 | 87 | 29 | 25 | 16 | 64 |
| 8 | 193 | 202 | 96 | 19 | 193 | 169 | 80 | 30 | 13 | 14 | 85 |
| 9 | 169 | 174 | 94 | 20 | 272 | 249 | 80 | 31 | 184 | 149 | 78 |
| 10 | 316 | 297 | 90 | 21 | 533 | 415 | 75 | | | | |
| 11 | 191 | 154 | 78 | 22 | 106 | 103 | 90 | | | | |

*3.3 Integration in a GIS: total statistics of damages produced*

According to data obtained from Landsat images, 85,727 fires occurred in Asturias in the decade 1991-2001 which affected to a 1,061,057 *ha* surface. The statistics of fires per municipalities has also been carried out, revealing the gravity of the problem in some of them, where the surface burnt is more than 25% of its total surface (Ibias, Degaña, Allande and Cangas de Narcea). Furthermore, many of the fires in these zones are repeated, probably intentionally provoked.

Combining the **vegetation** map of the Principality with the map of burnt zones the statistics of affected vegetation has been obtained: 73% of the burns have been produced in areas covered by thickets; 9% by mature forests; 7% by fields and pastures and the rest in other units. Besides, various GIS analyses between the cartography of burnt areas obtained by remote sensing and by maps created by INDUROT (Marquínez *et al.*, 2001) have allowed for the estimation of the environmental and economical incidence of forest fires in Asturias.

## 4. CONCLUSIONS

- The method allows for the localisation and delimitation of burnt areas in Asturias with a high level of precision, although confusions may occur in zones where vegetation has been destroyed by other means, for example, reaped or felled. The minimum surface reliable has been estimated at *10 ha*.
- The reliability of the method depends upon the temporal intervals between images because, when the time is excessive, the vegetation may have regenerated by then. Other limitations of the method are the topographical occultation and the presence of clouds. Besides, the zones twice burned will appear without change in the difference image of the two consecutive images.

## 5. REFERENCES


Álvarez, M.Á. *et al.*, 2001. *INDUROT.*

Bukata, R.P., J.E. Bruton, and J.H. Jerome, 1983. *RSE,* 13: 161-177.

Consejería de medio rural y pesca del principado de Asturias, 1999. *Producto Neto de la Agricultura Asturiana 1999.*

Díaz-Delgado, R., Pons, X., 2001: IX National Conference of Remote Sensing. pag. 248-252.

MARQUÍNEZ, J. *et al.*, 2001. *INDUROT.*

Palá, V., Pons, X., 1995. Photogram.Engineering & Remote Sensing, nº 61 (7), pag. 935-944.

Recondo González, C. *et al.,* 2000. Revista de Teledetección, nº 14, pag. 49-59.

Recondo González, C., *et al.,* 2001a. Mapping, nº 67, pag. 24-33.

Recondo González, C., *et al.,* 2001b: Mapping, nº71, pag. 6-16.

# Validation of two MODIS single-scene fire products for mapping burned area: hot spots and NIR spectral test burn scars

J.M. Salmon, W.M. Hao, M.E. Miller & B. Nordgren
*USDA Forest Service, Rocky Mountain Research Station, Fire Sciences Laboratory, Missoula, Montana, USA*
jmsalmon@fs.fed.us

Y. Kaufman & R. Li
*Affiliation NASA Goddard Space Flight Center, Greenbelt, Maryland, USA*

Keywords: MODIS, burn area mapping, burn scar mapping, validation, active fire, hot spots

ABSTRACT: Two MODIS fire products were validated for use for mapping burned areas: hot spots (MOD14) and burn scar (preliminary algorithm in development). Forest Service (US and Canadian) and Bureau of Land Management fire perimeters from several major fires in 2001 and 2002 were used as the ground truth data set. Strong correlations were found between each of these fire products and the series of perimeters. The results show that both of these products are highly effective at monitoring burned area in real time, but the burn scar detection is restrained to certain conditions (daytime with no smoke or clouds).

## 1. INTRODUCTION

In the United States, wildland forest fires burned six million acres in 2000 and 2002, the worst fire seasons since 1910. When not under control, fires pose a serious threat to personal property in the urban-wildland interface. Fires also reduce air quality via smoke production and possibly contribute to global climate change. Monitoring forest and grassland fires is important for predicting their impacts on local communities, quantifying their impact on air quality and global climate, and effectively mitigating their damages. Recently, satellite remote sensing has become an important alternative for detecting the presence of fire in remote areas as well as monitoring its progression and effects. The advantages to monitoring fire in this way include a synoptic view, information from areas inaccessible on the ground, and increased freedom from human error and subjectivity.

The MODerate resolution Imaging Spectrometer (MODIS) covers the visible and infrared regions with 36 spectral bands. Two of these bands (red and near infrared) have 250m resolution at nadir. Five more bands in the visible range have 500m resolution, and the rest (covering 405 nm – 14.4 μm) are 1km resolution. This instrument is aboard two NASA EOS (Earth Observing System) satellites: Terra and Aqua. Each of these satellites collects data over the entire globe twice daily, meaning that each location on the earth is "photographed" by a MODIS instrument four times daily. As the MODIS instrument collects data, it is constantly transmitting this information back to Earth. The data can then be collected with an X-band satellite receiver. Our laboratory has installed a DB (Direct Broadcast) station and has been receiving this data from the Terra and Aqua satellites as they pass overhead since April 2002. NASA provides algorithms for processing the MODIS data collected by our DB station and others' into more meaningful products.

One of these products is the "MOD14" active fire detection / thermal anomalies algorithm. This algorithm responds to "hot spots" or pixels where the energy emitted in the 4 μm region is much

higher than the average in the surrounding pixels. This product has a great deal of potential value to the Forest Service's Geographic Area Coordination Centers (GACC's) for tracking fire growth as well as the global change community. There is also currently a strong desire within the US Forest Service to track fire emissions in real time. Doing this effectively requires reliable, real-time data on area burned in the last 24 hours. The MOD14 product has potential for providing this information (Li et al 2000a, Li et al 2000b). However, before it can be reliably used operationally, it must be validated for these purposes. Another MODIS product with potential for meeting these needs is currently in development. It is a spectral test for locating burn scars using two NIR channels with 500m resolution. We conducted a validation of the operational hot spots algorithm and the preliminary burn scar algorithm, both for use in mapping area burned in real time (since last overpass).

## 2. METHODOLOGY

Validation of the active fire product consisted of combining the MODIS active fire data with Forest Service and Bureau of Land Management fire perimeter data, some contributed by the Canadian Forest Service. This was done for several major western U. S. and Canada fires from 2001 and 2002. The perimeters were generated approximately once per day, mostly collected between midnight and early morning via a processed IR scan image, though sometimes in the early evening, via airborne GPS. Although the methods of collection are not standardized, the perimeters are always much higher spatial resolution than the MODIS data (~2-10m). MODIS data (from Terra only) was available usually twice per day, the times varying with the location of the fire and the day. The pre-processing stream is described below for aligning these data sets for a single fire.

First, each data set (perimeters and MODIS hot spots) was collected in full. Whenever a hole existed in the MODIS data archived at the Fire Sciences Lab, MOD02 level 1B products were downloaded from the Data Acquisition and Archive Center (DAAC) and processed with the MOD14 algorithm used for the DB data here. This was chosen over downloading the DAACs' MOD14 product to preserve consistency within the datasets. This was also done for the entire time range of any active fire in 2001 that we studied, since the DB station was not collecting data until the 2002 fire season. Once the data sets were complete, they were sorted and matched. Next, the hot spots were combined for all MODIS scenes preceding the collection of each perimeter. Each set of hot spots was then converted into an ArcGIS point coverage and reprojected into the local coordinates (zone 10 to 13 UTM (Universal Transverse Mercator) NAD83 or NAD27 (North American Datum, 1983 or 1927, respectively)) to match with the perimeters. At this stage, the hot spots and perimeters could be visually compared, but further steps are required for a statistical comparison.

There are several obstacles to comparing the hot spots to the perimeters. A major one is that the perimeters are usually not collected at the time of a MODIS overpass. What was burned at the exact time of the MODIS overpass is not known. Data are usually taken several hours before or after. In some cases, it may be possible to interpolate using the diurnal fire activity cycle. The requirements for this case are: daily perimeters available and nearly constant slope, winds and fuels. These requirements are unlikely to all be met throughout a real fire. A fire behavior model, such as Farsite, could account for variations in fuels, weather, and topography. However, these models are not well validated enough to be used here without introducing uncertainties.

Another major obstacle to statistically comparing the hot spots to the perimeters at this stage is that the subpixel area burned is not known. An active fire detection in a pixel does not necessarily mean that the entire pixel is on fire. Most often, only a fraction of the pixel is burning. Dozier (1981) developed a strategy for calculating the subpixel burning area and fire temperature. However, Giglio and Kendall (2001) found the error of this method to be +/- 50% for retrieving area within one standard deviation. This suggests that the benefits of this technique do not justify the added computation time, and thus it was not used here. It was observed that for major fires, hot spot pixels generally occur in clusters, suggesting that fire is active over large spatial extents at a time. Therefore, it was assumed that hot spot detection generally indicates a square kilometer of area burned. Although

this assumption may lead to overestimation, this is countered by a similar overestimation in the ground truth data sets, where all area inside the fire perimeter is assumed to be burned, omitting unburned islands within the perimeter (Li et al 2000a).

In the current GIS coverage, hot spots are represented as points (the location of the center of the hot spot pixel). Ideally, to convert the hot spots into areas, one could recreate the original pixel to which the hot spot refers. However, this is computationally intensive due to the variation of pixel size and shape within a scene and the variation of pixel orientation between scenes. Two methods were explored: drawing a 1 $km^2$ box around each point, and creating a 546 m (the radius of a $1km^2$ circle) buffer around the point. These methods yielded similar results, and the circular buffer was chosen for its consistency. The square approximation would be more accurate in some cases and less so in others, depending on the pixel's distance from nadir and the orientation of the scene. Merging the resultant circles into a single area facilitates a statistical comparison between the hot spot's area burned and the fire perimeters. Finally, to quantify the validity of the hot spot detection algorithm for mapping burned area, we formed a regression between the area of the combined, buffered hot spot modeled pixels and the area inside of the perimeters at each time that perimeter data was available (see figure 2).

Validation of the burn scar algorithm followed a similar path. The first task was to apply the burn scar algorithm to the MOD02s collected for the hot spot validation described above. These scenes were 1km resolution, aggregated from 500m in the bands of interest for the burn scar algorithm. The higher resolution (500m) data was collected for a couple of cloud-free scenes to determine the improvement with utilizing the highest possible resolution. Then, the binary classification outputs (burned / not burned) were geo-registered in ENVI and saved as ARC rasters. Next, an AML (ARC Macro Language) script was written and used to reproject the burn classifications into the local (zone 10 to 13) UTM NAD83 or NAD27 projection of the perimeters. Another AML then converted the rasters into polygon coverages, selected the polygon(s) in the immediate vicinity of the fire of interest, and calculated the total areas of (1) the MODIS burn scar classification, (2) the Forest Service fire perimeter, and (3) the overlap between these two. Finally, regressions were formed between the MODIS-derived burned area and the FS perimeter area. These regressions excluded data from any scene indicating a decrease from a previously reported burned area, as a simple, automated, and consistent way to reduce the effects from cloud and smoke obscuration.

In some cases, Landsat imagery will be used as well for validation. To do this, a standard burn scar algorithm will be applied to the Landsat scene. The resulting classification is then compared to the MODIS burn scar classification closest in collection time to the Landsat scene.

## 3. RESULTS

The figures below illustrate the results from the major steps of the methodology described above. First, Fig. 1 shows two selections from a time series of the fire progression as tracked by both the MODIS hot spot algorithm and the Forest Service perimeters, as well as the most recent burn scar classification at the time of perimeter collection. Fig. 2 shows two regressions from this same fire, from June 10 to June 21, 2002. Fig. 2a shows the relationship of cumulative hot spot area to perimeter area, and fig. 2b shows the relationship of the most recent cloud- and smoke-free burn scar classification area (around the fire of interest) to each perimeter. Similar data was generated for the Moose fire in NW Montana, the Biscuit fire in Oregon, the Rodeo fire in Arizona, and the House River and Dogrib fires in Alberta, Canada.

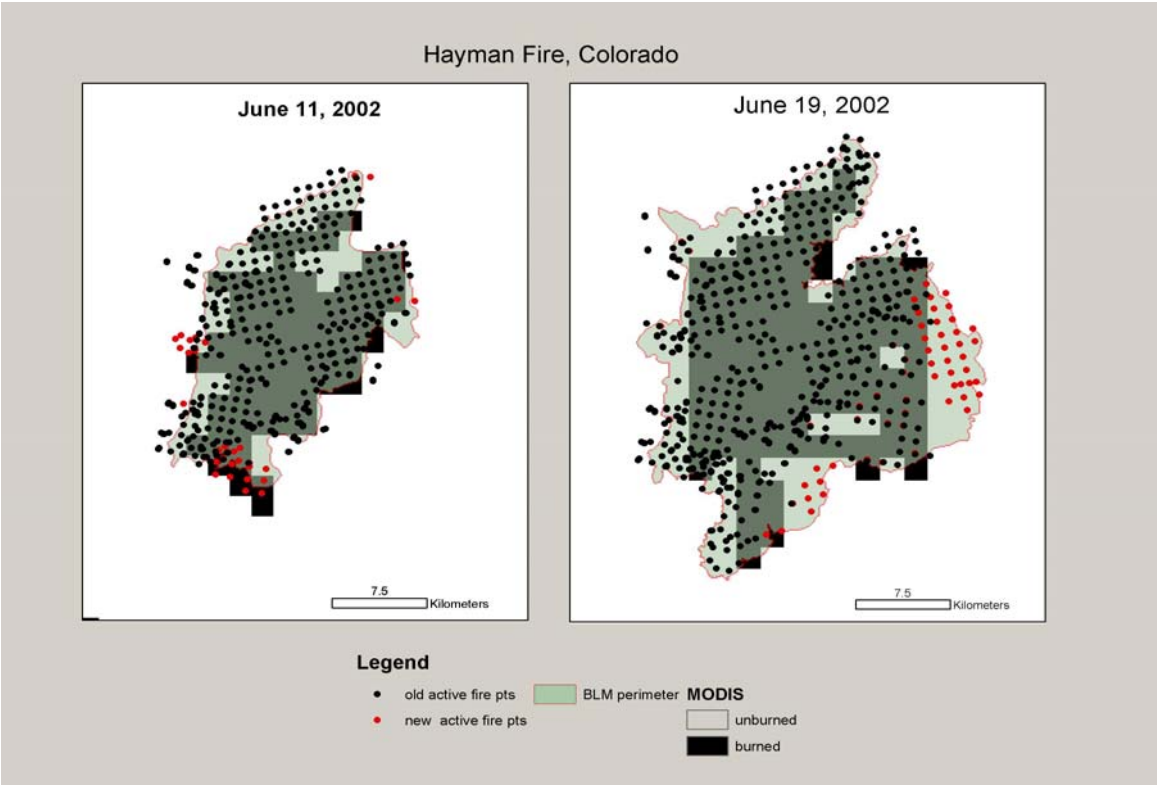


Figure 1. Two examples of fire progression as tracked by MODIS hot spots (black and red points), burned area (black pixels), and the Forest Service (red perimeters with FS green filling) for the Hayman fire in SW Colorado

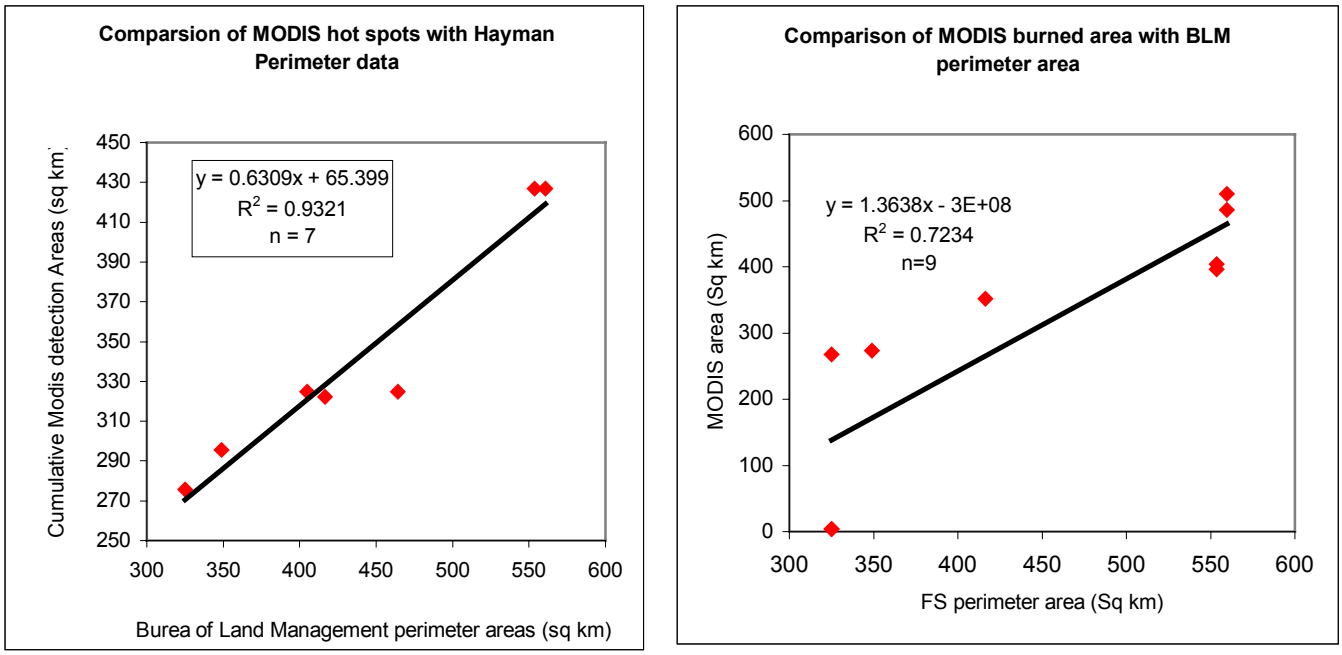


Figure 2. A regression of the MODIS-derived cumulative hot spot area (a) and MODIS-derived burned area from the spectral test (b) with respect to the Forest Service's perimeter area for nine days of the Hayman fire

## 4. DISCUSSION AND CONCLUSIONS

The MODIS-derived hot spot areas were consistent with the Forest Service's ground truth dataset for the major fires in the U.S. in 2001 and 2002, as well as some in Canada, and are therefore effective at monitoring fires. This is an impressive degree of accuracy considering the temporal resolution of the data (twice per day using the Terra satellite only). Inclusion of data from the MODIS instrument aboard Aqua, where possible, would improve this relationship. It is important to note however, that the slope of the regression in fig. 2a is not constant, but rather varies with the temporal resolution of the data used (satellite return interval) and fire's rate of spread (Li et al 200c).

The burn scar algorithm has proved to be less effective at daily monitoring of fire growth areas, because it relies upon bands that do not penetrate through cloud and smoke. However, when MODIS has an unobstructed view of the area, this algorithm does provide information about previously burned areas that may have been missed by the hot spots. These two fire products have strong potential to form a comprehensive fire monitoring system, with the consistent 2/4 times daily availability of the hot spots and 1/2 times daily availability of burn scar under cloud-free conditions.

## 5. REFERENCES


Dozier, J. 1981. A method for satellite identification of surface temperature fields of subpixel resolution. Remote Sensing of Environment. 11:221-229, 1981.

Giglio, Louis and Jacqueline D. Kendall. 2001. Application of the Dozier retieval to wildfire characterization: A sensitivity analysis. Remote Sensing of Environment. 77:34-49, 2001.

Li, Zhanqing, Serge Nadon, and Josef Cihlar. 2000a. Satellite Detection of Canadian Boreal Forest Fires: Development and Application of the Algorithm. International Journal of Remote Sensing.

Li, Z., S. Nadon, J. Chilar, and B. Stocks. 2000. Satellite-based mapping of Canadian boreal forest fires: evaluation and comparison of algorithms. International Journal of Remote Sensing. Vol. 21, No. 16, 3071-3082, 2000.

Li, Z., Y. J. Kaufman, C. Ichoku, R. Fraser, A. Trishchenko, L. Giglio, J. Jin, and X. Yu. 2000b. A Review of AVHRR-based Active Fire Detection Algorithms: Principles, Limitations, and Recommendations.

# Assessing the accuracy of burned area maps made with moderate to coarse spatial resolution data: improving reliability and intercomparability.

S. Trigg
*University of Maryland, College Park, Maryland, USA*
trigg@umd.edu

S. Flasse
*Flasse Consulting Ltd, Maidstone, UK*

J. Le Roux
*Etosha Ecological Institute, Okaukuejo, Namibia*

Keywords: accuracy assessment, reference data, validation period, TM, MIRBI, Caprivi, Namibia

ABSTRACT: Our study presents concepts and methods designed to improve the reliability of accuracy assessments performed on burned area maps made from moderate to low spatial resolution data. It demonstrates how confidence in accuracy assessments can be improved using quality-control measures designed to ensure that requisite image reference data accurately delimits burned areas over a known, representative portion of the burning season. Such reference data is developed for a case study area in East Caprivi, Namibia over two main steps: First, we analyse *in situ* spectral-temporal data to explore the suitability of different candidate sources of image reference data (air photos, SPOT HRVIR, Landsat TM); this results in the choice of Landsat TM. Next, the *in situ* data is incorporated with other quality control measures to create and test a method to make TM-based reference data suitable for use in quantitative accuracy assessments. The concepts and general approach we present are generic and can be used to improve the reliability and intercomparability of accuracy assessments performed by different burned area mapping initiatives.

## 1. INTRODUCTION

Scientists working on the remote sensing of burned areas at regional to global scales have repeatedly stressed the need to deliver burned area maps to a quantified level of accuracy (e.g. Eva and Lambin 1998, GOFC-Fire 2001). This ability to attach accuracy figures to burned area maps is considered essential for two main reasons: First, it tells users how well the map describes real burned areas on the ground - and hence how useful the maps really are - for instance, when making fire management decisions. Second, it enables algorithm developers to assess and compare algorithms in their ability to detect burned areas across different ecosystems and conditions. In short, both users and producers of burned area maps have a vested interest in understanding the accuracy of burned area maps.

Any attempt to quantify map accuracy primarily depends on the availability of suitable *reference data* (Congalton and Green 1999). For regional to global studies, this reference data is usually image-based and needs to sample both the 'true' extent of burned and unburned areas and their seasonal variability. Reference data is compared digitally with the map and the resulting instances of agreement and disagreement are used to calculate map accuracy figures.

However, although accuracy figures for burned area maps should be attainable using appropriate reference data and analysis, the methods used typically invoke large uncertainties in accuracy figures

delivered. For example, for African savannah ecosystems, Trigg (2002) identified two major weaknesses common to accuracy assessments of burned area maps:

- Problems encountered with matching the time period of image reference data to that of the map.
- Problems with guaranteeing the temporal representativity of image reference data.

Both problems relate to the quality of image (e.g. Landsat TM) reference data used to assess the accuracy of maps made from lower spatial resolution image data (e.g. AVHRR, ATSR, VGT). In particular, they both encompass limitations with reference data in the temporal domain; these problems have undermined confidence in reported accuracy figures, since it is not always clear the extent to which errors reported in the map are artefacts arising from use of erroneous or inappropriate reference data (Trigg 2002).

To help address these problems, we focus on improving methods to make image reference data suitable for assessing the accuracy of burned area maps made using moderate to low spatial resolution data. This is done using a case study area centred on East Caprivi, North East Namibia, composed of woodland savannah. We argue that both temporal domain problems can be solved if we first understand the time period that burned areas remain spectrally apparent on the image source used to make the reference data. Our proposed solution therefore draws on *in situ* spectral-temporal data collected on burned areas within the study area; this data is analysed to understand the temporal variation in the magnitude of burned area signals apparent to different candidate sources of image reference data. Having gained this spectral-temporal knowledge we apply it to create a reference data method.

## 2. METHODS

As the departure point for tackling the two temporal domain problems, and hence to develop appropriate reference data for the East Caprivi study area, we propose the formal concept of the 'validation period'. The validation period is defined as the number of days prior to the date of a single reference image that this reference image detects burned areas (figure 1).

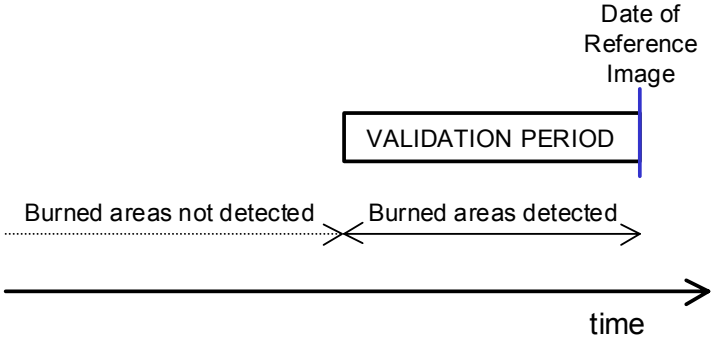


Figure 1. Definition of the validation period

We argue that solving problem 1 requires research to establish the validation period of the reference data. Then, a temporal subset can be extracted from the remote monitoring data to include only burned areas that were detected during the same validation period (assuming sufficiently regular imagery are available).

This matching of the times of the reference and monitoring data removes the possibility that differences in burned area extents between data sets are merely due to them each inventorying burned areas that occurred over different time periods. This solves problem 1.

However, addressing problem 2 requires that the validation period meets a further criterion, namely that it is long enough to ensure that the reference data includes a representative sample of both

early and late-season burns (which, in our savannah case study, tend to be relatively small and large respectively).

To address the both temporal-domain problems, we first investigate the temporal sensitivity to burned area signals of three candidate sources of image reference data for the East Caprivi study area: panchromatic air photos, Landsat TM and SPOT HRVIR. We do this first by applying a Jeffries-Matusita separability analysis to spectral-temporal data collected on burned areas *in situ* (by Trigg and Flasse 2000). This analysis enables us to choose a reference data source that offers spectral bands capable of reliably mapping burned areas over a validation period sufficiently long to include both early and late season burns. The results are then used to derive a new method to make reference data from the chosen data source. Finally, the *in situ* predictions and reference data method are tested by applying the new reference data method to remotely acquired imagery.

## 3. RESULTS

The spectral-temporal investigations suggest that, of the candidate reference data (air photos, Spot HRVIR and Landsat TM), the best adapted to solving problems 1 and 2 is Landsat TM. In particular, TM bands 5 and 7 are shown to remain highly sensitive to spectral signals from burned areas with time after burning; this makes TM 57 suitable for making reference data to inventory burned areas over temporally representative validation periods.

The TM 57 method we therefore develop creates reference data by applying a numerical threshold to a TM-57-generated Mid-Infrared Burn Index (MIRBI) image. To improve confidence in choosing the MIRBI threshold used, we employ ancillary data, including an image interpretation color key (made by displaying the *in situ* data taken on burned and unburned areas as TM 57 color composite and MIRBI images); local knowledge and vegetation maps of the area. The use of the MIRBI image in conjunction with ancillary data gives high confidence in the threshold chosen to make the TM reference data.

The resulting TM reference data is shown to have addressed problems 1 and 2, through its comparison with an indicative date-of-burn map developed from a temporally comprehensive AVHRR dataset. Through use of this indicative date-of burn map, we show that this reference data spans a validation period of 127 days: suitable to include both early and late-season burns. This solves problems 1 and 2; in doing so, the new reference data enables the quantitative accuracy assessment of burned area maps from low spatial, high temporal resolution sensors.

Even though we anticipate the need to adapt our reference data method to optimize it for new locations, our theoretical concept of the validation period and the general approach to determine it are generic and could be applied to enable quantitative accuracy assessments anywhere.

## 4. CONCLUSION

At the GOFC - Fire Satellite Product Validation conference in Portugal in 2001, scientists producing the first global burned area maps highlighted the urgent need to deliver burned area maps to a robustly quantified level of accuracy. By working to reduce uncertainties with the requisite reference data, this study helps to deliver these needs. In particular, it provides an integrated solution to match the TM and map data to the same temporally representative validation period, thus enabling quantitative accuracy assessments.

Even though we expect that the validation period of reference data will vary with ecosystem, our general approach to establishing it is generic; it can therefore help to realize quantitative accuracy assessments in ecosystems elsewhere.

Furthermore, we recommend that future research to assess the accuracy of burned area products adopts the formal concept of the validation period, through determining it accurately, stating it explicitly, and indicating how well it matches the period covered by the map under assessment. This

will help to standardise accuracy assessments and improve confidence and intercomparability of accuracy figures stated by different groups.

This work has again highlighted the urgent need to move towards a standard approach to the accuracy assessment of burned area maps from remote sensing and provides important practical recommendations to that effect.

## 5. REFERENCES


Congalton, R. G. and Green, K., 1999, Assessing the accuracy of remotely sensed data. Florida. CRC Press.

Eva, H. and Lambin, E. F., 1988, Remote sensing of biomass burning in the tropical regions: sampling issues and multisensor approach. Remote Sensing of Environment, 64: 292-318.

GOFC – Fire, 2001, Executive Summary, GOFC – Fire Satellite Product Validation Workshop, 9-11 July 2001, Lisbon, Portugal.
http:// gofc-fire.umd.edu/products/pdfs/ events/Lisbon_7_01_ExecSum.pdf

Trigg, S. and Flasse, S., 2000, characterizing the spectral-temporal response of burned savannah using *in situ* spectroradiometry and infrared thermometry. International journal of remote sensing, 21, 3161-3168.

Trigg, S. N., 2002, Towards improving the use of remote sensing for monitoring burnt vegetation in African savannah. PhD Thesis. University of Greenwich, Chatham.

# Multitemporal compositing techniques for burned land mapping

G. Ventura , E. Chuvieco
*Departament of Geography, University of Alcalá, Madrid, Spain*
gemma.ventura@uah.es

P. Martín
*Institute of Economy and Geography (C.S.I.C.), Madrid, Spain*

Keywords: AVHRR, Composites, Burned land mapping

## 1. INTRODUCTION

Spatial analysis of burned areas is critical to improve ecological fire effects assessment and fire management at different scales (from local to regional and global). Field sketches drawn after the fire were used traditionally by forest fire managers to map fire effects, although in many cases only a general estimation of fire location was available. The use of GPS surveys and remote sensing techniques makes this spatial evaluation more accessible. Several studies have shown the potentials of different remote sensing systems for burned land mapping (Ahern et al., 2001), which range from aerial sensors (Ambrosia and Brass, 1988) to satellite acquisitions. In the last years, the extended use of NOAA-AVHRR (Chuvieco and Martín, 1994) and Landsat-TM images (Koutsias et al., 1999) have been broadened with new satellite missions, mainly at medium and coarse resolutions: Terra-Modis (Justice et al., 2002), Spot-Vegetation (Eastwood et al., 2000), and IRS-WIFS.

The use of coarse resolution images for burned land mapping is most commonly performed on multitemporal composites, since daily images for large territories frequently present observation artifacts, clouds and other atmospheric disturbances. We hypothesized that common multitemporal compositing criteria may be not appropriate to discriminate burned areas from surrounded unaffected regions, since they were defined to emphasize the vegetation signal, which is quite different from burned signal. In fact, the most used technique, the maximum value composite (MVC; Holben, 1986), selects the maximum NDVI value of the time series that form the temporal series. Therefore, this criterion may select a non-burned pixel within a burned area when there is at least one day with a pre-fire pixel, or even one affected by clouds or a cloud shadows, since the NDVI of a burned area is very low (Pereira et al., 1999b). Additionally, other authors have shown that the MVC does not solve atmospheric disturbances and may not choose the most vertical observations (Cihlar et al., 1997; Qi et al., 1993; Van Leeuwen et al., 1999). Consequently, some authors have proposed to use different compositing techniques for burned land mapping studies, which should optimize discrimination of burned signal (Pereira et al., 1999a). A previous study on this topic proposed the use of minimum albedo or minimum reflectance of channel 2 in AVHRR-GAC images over the African continent (Barbosa et al., 1998).This choice may be adequate for GAC data (5x5 km), but is not very convenient for HRPT images (1.1x1.1 km), since cloud shadows may be retained instead of good pixels. A similar approach was followed recently by Stroppiana et al. (2002) with SPOT-Vegetation data, although in this case instead of the minimum values, the third minimum was selected to avoid cloud shadow contamination.

## 2. METHODOLOGY

The analysis of multitemporal compositing techniques was undertaken in the framework of global mapping of burned land areas for the Iberian Peninsula for the years of 2001 and 2002. The specific time period used for assessment of compositing techniques is the second half of August 2001 (7-day composites). Daily AVHRR HRPT images were acquired by the Department of Geography's receiving station. Pre-processing of the images included navigation to a standard UTM projection and multitemporal matching using automatic window correlation, as well as generation of reflectance and brightness temperature calibrated data. In addition to the 5 calibrated bands, 5 additional bands were derived for each image: zenith and azimuth sun angles, sensor zenith angle, NDVI and surface temperature**.**

For each multitemporal compositing criterion, a new image was generated with the values of all those bands for the day selected by the criterion. The following proceedings were used:

- The standard Maximum Value Composite (MVC), selecting the maximum NDVI of all the images included in the serial time (MaxNDVI).
- Minimum reflectance of channel 1 (MinR1).
- Minimum reflectance of channel 2 (MinR2).
- Minimum Sun Zenith Angle (MinSZA)
- Maximum Brightness Temperature of channel 4 (MaxTb4).
- Minimum sensor zenith angle from the 3 maximum brightness temperatures of channel 4 (MinSZMaxTb4)
- Minimum reflectance of channel 2 from the 3 maximum brightness temperatures of channel 4 (MinR2MaxTb4).
- Maximum brightness temperature of channel 4 from the 3 minimum reflectance of channel 2 (MaxTb4MinR2)

The performance of each criterion was evaluated using 4 tests:

Test 1. *Discriminability between burned and unburned areas*. A total set of 2007 points from burned zones (125), and different land covers were extracted from each composite to evaluate which provided the highest separability from other land covers. The CORINE Land Cover map of Europe was used to select the homogeneous categories for the selection, while pixels representative of burned areas were selected by visual analysis of Landsat-ETM images acquired in the same period.

The discrimination ability was measured using normalised distances:

$$D = \frac{\left|\bar{x}_1 - \bar{x}_2\right|}{s_1 + s_2} \qquad (1)$$

where $x_1$ and $x_2$ are the sampled means of burned (1) and unburned (2) categories and $s_1$ and $s_2$ are the standard deviations of the same classes. This distance was computed for the 3 reflectance channels of AVHRR (1, 2 and 3b) and the brightness temperature of channel 4. According to this test, the most optimal composite would be the one having the maximum D.

Test 2. *Presence of artifacts*. For each image to be included in the composite, various artifacts were flagged: clouds, cloud shadows, reception problems, no data, etc. to be tackled afterwards in the composite. Since no previous filtering was applied to the daily images, the composites could eventually retain a pixel with some sort of artifact (for instance a cloud or a cloud shadow). The most adequate composite would be in this case the one that retained fewer artifacts.

Test 3. *Distribution of sensor zenith angles*. According to several authors, the closer to nadir is an acquisition, the lower the observation of atmospheric disturbances (Van Leeuwen et al., 1999). Therefore, the composite retaining the lowest sensor zenith angles would be the most optimal.

Test 4. *Spatial coherency*. One of the problems found in any compositing criteria is the mosaic effect produced by retaining neighbour pixels that may be acquired at different dates and observation

geometries. Consequently, the most appropriate technique should render a similar spatial variability as that found in a single image. In this case, we measure spatial variability computing images of the standard deviation of a 3 x 3 pixels moving window for channel 2 of all the composites and a single image of the time series with low cloud coverage. Afterwards, 10 x 10 pixels plots were selected randomly and the average mean of the standard deviation images was computed. The most convenient composite would be in this case the one having the more similar standard deviation to that computed for the single image.

Considering the final goal of this experimental study, the best composite for burned land mapping would be the best rated in the first test. However, the other 3 tests would assure the global radiometrical (and to some extent geometrical) quality of the final product. In addition, the spatial coherence test would facilitate the selection of the best composite to improve cartographic accuracy in drawing fire perimeters.

## 3. RESULTS

Results from the discrimination test provided the best results for MaxTb4 and MinSZMaxTb4 composites. The most discriminant band found was the near infrared ratio.

Table 1 summarizes the results obtained for the four tests with the 8 composites. To simplify the presentation, we have only included the normalized values of each test. Since the range of values is different from one test to the other, a common scale of 0 to 100 was created, by normalizing each value with the reference to the maximum and minimum value found for all the composites. Because some tests have a "positive" nature (the higher the values, the most convenient the composite), they were normalized from the maximum value, while the "negative" test (the higher the value, the less convenient), were normalized from the minimum. The positive tests are the separability and artifacts, while sensor zenith angle tests and texture are within the latter group. Since separability and texture were computed for four bands (R1, R2, R3 and Tb4), only average values for all bands are included in the table, to simplify the results. For the same reason, the artifacts have been reduced to clouds and cloud shadows. Each test was given an arbitrary weight according to the relative importance for burned land mapping, being higher for separability.

Table 1. Normalized values of the different test for the 8 compositing criteria

| | **Average Separability** | **Clouds** | **Cloud shadows** | **Average texture** | **Average sensor zenith angle** | **Total** |
|---|---|---|---|---|---|---|
| MinB1 | 31.25 | 100.00 | 83.64 | 71.59 | 25.87 | 251.78 |
| MinR2 | 35.33 | 100.00 | 80.00 | 34.94 | 40.87 | 236.47 |
| MaxTb4 | 76.61 | 100.00 | 100.00 | 51.28 | 81.37 | 385.87 |
| MinSZA | 60.12 | 96.36 | 100.00 | 61.69 | 0.00 | 280.12 |
| MaxNDVI | 24.61 | 98.18 | 100.00 | 18.67 | 32.40 | 199.39 |
| MinSZMaxTb4 | 79.66 | 98.18 | 100.00 | 24.36 | 100.00 | 382.77 |
| MinR2MaxTb4 | 58.28 | 100.00 | 98.18 | 45.66 | 66.70 | 328.01 |
| MaxTb4MinR2 | 35.58 | 100.00 | 96.36 | 58.13 | 42.03 | 269.50 |
| ***Weight*** | ***2.00*** | ***0.50*** | ***0.50*** | ***1.00*** | ***1.00*** | |

Results of the tests show a poor performance of the MaxNDVI, the most extended criterion for multitemporal compositing of AVHRR images. This finding agrees with results from other authors (Barbosa et al., 1998). MaxNDVI performs the lowest in average separability, which also agrees with other authors (Pereira, 1999), and retains more clouds than other composites and selects pixel with off-nadir angles.

Among the alternative compositing criteria, minimum reflectance of channels 1 and 2 do not offer good separability in vertical observations and retained cloud shadows, although they present good spatial coherency. Those results differ from other authors (Stroppiana et al., 2002), who found that the minNIR (channel 3 in SPOT Vegetation and channel 2 in our case) is the most appropriate criterion for burnt area mapping. They concluded that minNIR composites are least affected by artifacts, and our results show that it does not retain clouds, but clouds' shadows are presented in the final composites.

Maximizing Sun zenith angle offers good separability and texture, but retains clouds and the most off-nadir pixels among the tested composites. The best results by far are obtained when maximum brightness temperature is considered, either as a sole criterion (MaxTb4) or combined with minimum sensor zenith angle (MinSZMaxTb4). Both composites offer the highest average separabilities and the most vertical observations. Although MaxTb4 selects less vertical observations than MinSZMaxTb4, it provides better spatial coherency and selects more cloud-free pixels. Consequently, it obtains the highest ranks among the tested criteria. The combinations of maximum temperature and minimum reflectance provide intermediate values, with good texture and separability, and average in regards off-nadir observations.

## 4. ACKNOWLEDGEMENTS

This research was funded by the SPREAD project (EVG1-CT-2001-0043), under the V Research Framework Program of the European Commission, as well as by the DGCN (Spanish Ministry of the Environment).

## 5. REFERENCES

Ahern, F.J., Goldammer, J.G. and Justice, C.O. (Eds.) (2001). Global and Regional Vegetation Fire Monitoring from Space: Planning a coordinated international effort. SPB Academic Publishing, The Haghe, The Netherlands.

Ambrosia, V.G. and Brass, J.A. (1988), Thermal analysis of wildfires and effects on global ecosystem cycling, *Geocarto International*. 1: 29-39.

Barbosa, P.M., Pereira, J.M.C. and Grégoire, J.M. (1998), Compositing criteria for burned area assessment using multitemporal low resolution satellite data, *Remote Sensing of Environment*. 65: 38-49.

Chuvieco, E. and Martín, M.P. (1994), Global fire mapping and fire danger estimation using AVHRR images, *Photogrammetric Engineering and Remote Sensing*. 60(5): 563-570.

Cihlar, J., Ly, H., Li, Z., Chen, J., Pokrant, H. and Huang, F. (1997), Multitemporal multichannel AVHRR data sets for land biosphere studies artifacts and corrections, *Remote Sensing of Environment*. 60: 35-57.

Eastwood, J.A., Plummer, B.K. and Wyatt, B.K. (2000), The potential of SPOT-Vegetation data for fire scar detection in boreal forests, *International Journal of Remote Sensing*. 19(18): 3681-3687.

Holben, B.N. (1986), Characteristics of maximum-value composite images from temporal AVHRR data, *International Journal of Remote Sensing*. 7: 1417-1434.

Justice, C.O. et al. (2002), The MODIS fire products, *Remote Sensing of Environment*. 83: 244–262.

Koutsias, N., Karteris, M., Fernández, A., Navarro, C., Jurado, J., Navarro, R. and Lobo, A. (1999), Burnt land mapping at local scale. In: *Remote Sensing of Large Wildfires in the European Mediterranean Basin* (E. Chuvieco, Ed.) Springer-Verlag, Berlin, pp. 123-138.

Pereira, J.M., Sa, A.C.L., Sousa, A.M.O., Martín, M.P. and Chuvieco, E. (1999a), Regional-scale burnt area mapping in Southern Europe using NOAA-AVHRR 1 km data. In: *Remote Sensing of Large Wildfires in the European Mediterranean Basin* (E. Chuvieco, Ed.) Springer-Verlag, Berlin, pp. 139-155.

Pereira, J.M., Sa, A.C.L., Sousa, A.M.O., Silva, J.M.N., Santos, T.N. and Carreiras, J.M.B. (1999b), Spectral characterisation and discrimination of burnt areas. In: *Remote Sensing of Large Wildfires in the European Mediterranean Basin* (E. Chuvieco, Ed.) Springer-Verlag, Berlin, pp. 123-138.

Pereira, J.M.C. (1999), A comparative evaluation of NOAA-AVHRR vegetation indices for burned surface detection and mapping, *IEEE Transactions on Geoscience and Remote Sensing*. 37: 217-226.

Qi, J., Huete, A.R., Hood, J. and Kerr, Y., (1993). Compositing multi-temporal remote sensing data sets, Pecora 12. *American Society of Photogrammetry and Remote Sensing*, Sioux Falls, pp. 206-213.

Stroppiana, D., Pinnock, S., Pereira, J. M. C and Grégoire, J. M. (2002). Radiometric analysis of SPOT-VEGETATION images for burnt area detection in Northern Australia. *Remote Sensing of Environment* 82: 21-37.

Van Leeuwen, W.J.D., Huete, A.R. and Laing, T.W. (1999), MODIS Vegetation Index Compositing approach: a prototype with AVHRR data, *Remote Sensing of Environment*. 69: 264-280.

# Monthly burned area and forest fire carbon emission estimates for the russian federation from SPOT Vegetation burned area mapping

M.J.Wooster & Y-H. Zhang
*Department of Geography, King's College London, United Kingdom*
martin.wooster@kcl.ac.uk

Keywords: Burned area, Russian boreal forest, SPOT VGT, Carbon Emission

ABSTRACT: Russian boreal forests play a key role in global carbon cycling, but there is a lack of good quality quantitative data on the extent of fire activity in Russian forests. This study provides the first comprehensive monthly satellite-based surveillance of fires occurring across entire Russian Federation in 2001.Using data from SPOT VGT, We map a total burned area of 41,782 km² with underestimation by around 20% in comparison to Landsat ETM+ measurement. Using these data we estimate direct carbon emissions from these Russia forest fires to be 39.3 - 55.4 Mt.

## 1. INTRODUCTION

Boreal forests cover 9 to 12 million km², representing around one third of Earth's forested area, and their vegetation and soils represent around 37% of the total terrestrial carbon pool. Approximately two thirds of Earth's closed boreal forest lies within the Russian Federation (Kasisichke, 2000) where forest fires regularly occur, particularly in parts of Siberia and the Russian Far East. These fires release terrestrially stored carbon into the atmosphere (Van Cleve *et al.*, 1983; Kasisichke, 2000) and, given the size of the boreal carbon pool, this means that changes in boreal forest fire activity can have potentially significant effects on global atmospheric $CO_2$. Thus it is vital to know the annual area burnt in the boreal zone if current $CO_2$ flux levels are to be quantified and the effects of potential climate changes examined. This latter point is pertinent since it is predicted that any atmospheric warming related to increasing greenhouse gas concentrations will be most severe at higher latitudes, and that this could result in significant increases in boreal zone fire activity (Flannigan and Van Wagner, 1991).

Good quality data on burnt area in the entire North American boreal region are available for at least the last 50 years and show an interannual variability of an order of magnitude (Kasischke and French, 1995). However, for Russian forests there is a lack of comparable data even for recent years, which may well be the largest source of error in providing estimates of direct carbon release from the boreal region (Kasischke et al., 2000). Published estimates themselves vary enormously, with many of the smallest values being the official figures produced by Russian Government agencies. Satellite remote sensing appears the only feasible method to collect systematic, quality controlled data on fire activity over areas as large and as remote as those in Russia. Here for the first time we map monthly burnt area over the entire Russian Federation using a single, standardised method applied to remote sensing data obtained from SPOT VGT (Saint, 1996). Mapping on a monthly basis, rather than annually, substantially increases our ability to compare these data to other fire activity indices, such as measures of atmospheric pollution.

## 2. MAPPING BURNT AREA WITH SPOT VGT

The pushbroom VGT sensor onboard SPOT-4 provides visible-infrared imagery over a 2250 km swath. VGT has a similar temporal resolution and spatial resolution as AVHRR but it shows significantly better performance with regard to geometric fidelity, radiometric calibration, multi-spectral registration, multi-temporal registration and absolute geolocation (Saint, 1996). VGT's excellent geometric and radiometric characteristics make it attractive for mapping burnt area (Eastwood et al. 1998). Fraser *et al.* (2001) have investigated VGT as a partial replacement for AVHRR in the burnt area mapping methodology used in Canadian forests and here we apply a multispectral, multi-temporal differencing strategy to map monthly burned area from VGT over the Russian Federation.

## 3. VALIDATION

Following Fraser *et al.* (2001) and Smith *et al.* (2002) the ability of our algorithm to accurately map burned area was tested by comparison to burned area maps derived from multi-spectral supervised maximum likelihood classification of Landsat-7 ETM+ imagery. In all cases VGT underestimates the size of the burnt area, on average by around 20%, because our rule-based method used for mapping fires tends not to select all pixels on the perimeter of burned areas since many of these pixels will be dominated by unburnt vegetation. The spectral reflectance characteristics of these very mixed perimeter pixels prevent them being classified as burnt by our statistical criteria. This is a markedly different result to that of Fraser et al. (2001) who found SPOT VGT to overestimate the size of burnt areas in Canadian forests by on average of 71% when compared to ETM+, most likely due to differences in the type of mapping algorithm employed.

## 4. RESULTS

Figure 1 shows the map of burnt area for 2001. We have used these data within the emissions modelling framework of Conard and Ivanova (1997) and Conard *et al.* (2002) to estimate monthly emissions directly from the burning itself (Figure 2) – this does not include the emissions due to post-fire activity (e.g. increased soil decomposition). See Conard and Ivanova (1997) for details on the modelling procedure, which assumes a range of burning conditions to provide both maximum and minimum emission estimates.


Figure 1. Burned area across the Russian Federation in 2001, mapped from VGT in a Lambert azimuthal equal area projection down to a fire size of 2 km² (though such small fires cannot be seen in this rendition). Boxes indicate some large fires >1000 km²

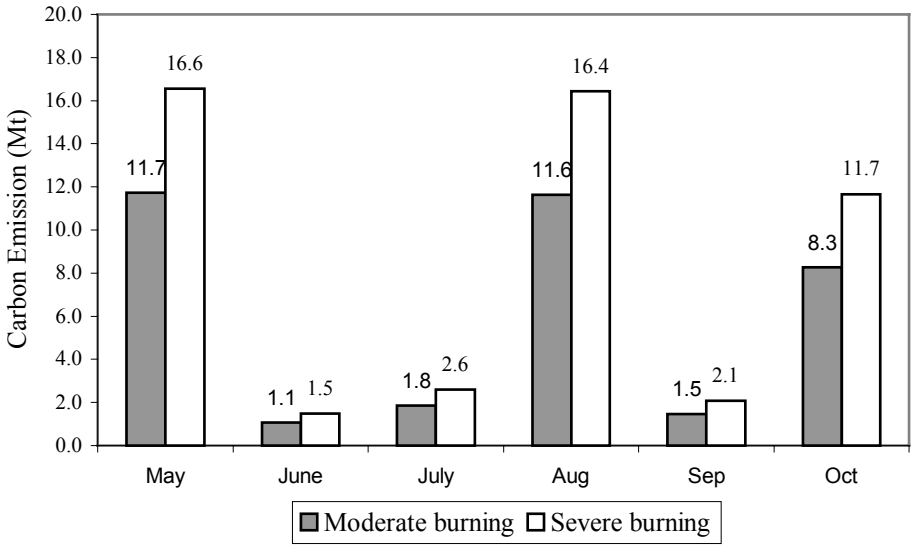


Figure 2. Monthly direct carbon emissions (tonnes x $10^6$) due to forest fires occurring in Russia for 2001, estimated from VGT-derived burnt area and the modelling strategy of Conard and Ivanova (1997). A range of moderate to severe fire conditions (controlling carbon volatized per unit area burnt) is used to provide the range of emission estimates

## 5. CONCLUSIONS

Using SPOT VGT data this study provides the first comprehensive satellite surveillance of monthly burnt areas occurring in forests and other landuse classes across entire the Russian Federation. In 2001 we detect 2764 separate burnt areas covering a total of 41782 km², with 31217 km² in forest land-cover classes. The largest fire burnt 4063 km², whilst the longest-lived fire burned for three months. May, August and October are the peak fire months and the majority of fires occur in

Eastern Siberia and the Russian Far East. Comparison to Landsat ETM+ suggests our methodology successfully detects burned areas larger than 2 km² but underestimates their size by around 20 %. We estimate that in 2001 Russia forest fires released 5 to 8 times more carbon than fires in Canadian and Alaskan forests, due primarily to the much larger area affected. The 39 – 55 Mt of carbon we estimate to have been directly released in the 2001 Russian forest fires represents between 11 and 17% of that year's fossil fuel carbon emissions for the Russian Federation.

## 6. ACKNOWLEDGEMENTS

*This work is supported by the Leverhulme Trust and the UK Royal Society. SPOT VGT data are CNES copyright distributed by SpotImage and produced by VITO.*

## 7. REFERENCES

Conard S.G., and Ivanova G.A. (1997) Wildfire in Russian Boreal forests-potential impacts of fire regime characteristics on emissions and global carbon balance estimates. *Environmental Pollution*, 98, 305-313

Conard, S., *et al.* (2002) Determining effects of area burned and fire severity on carbon cycling and emissions in Siberia, *Climatic Change*, 55, 197-211.

Eastwood, J. A., Plummer, S. E., Wyatt, B. K., Stocks, B. J. (1998) The potential of SPOT-Vegetation data for fire scar detection in boreal forests, *Int.J. Remote Sens.*, 19, 3681-3678.

Flannigan, M. and Van Wagner, C.( 1991) Climate change and wildfire in Canada*, Canadian J. Forest Res.*, 21, 61-72.

Fraser, R. H., Hall, R. J. and Landry, R. (2001) Burnt area mapping across Canada's boreal forest zone using SPOT VEGETATION calibrated with Landsat TM imagery, *3rd International workshop on remote sensing and GIS applications to Forest fire management*, EARSEL, Paris, pp.133-137.

Kasischke, E.S., Bourgeau-Chavez, L. L., O'Neill, K.P., and French, N.H. (2000) Indirect and long-term effects of fire on the boreal forest carbon budget, in J. Innes, M. Beniston, and M. Verstraete (eds.), *Biomass Burning and its Inter-relations with the Climate System*, pp. 263-280, Kluwer, Dordrecht.

Kasischke, E. and French, N. (1995), Locating and estimating the areal extent of wildfires in Alaskan boreal forests using multi-season AVHRR NDVI composite data, *Remote Sens. Environ.,* 51, 263-275.

Saint, G. (1996). The VEGETATION Programme, *The Earth Observer*, 8(4).

Smith, A., Wooster, M., Powell, A. and Usher, D. (2002) Texture based feature extraction: application to burn scar detection in Earth Observation Imagery, *Int.J. Remote Sens.*, 23, 1733-1739.

Van Cleve, K., Oliver, R., Schlentner, L., Viereck, L. A. and Dyrness, C. T. (1983) Productivity and nutrient cycling in taiga forest ecosystems*. Canadian J. Forest Res.*, 13, 747-766.

# Improving satellite-derived fire products with Airborne Thermal Imaging Systems: detection, calibration and rapid data collection and delivery systems

V.G. Ambrosia
*California State University – Monterey Bay, NASA-Ames Research Center, Moffett Field, CA., USA*
vambrosia@mail.arc.nasa.gov

C.A. Hlavka, J.A. Brass & S.S. Wegener
*NASA-Ames Research Center, Moffett Field, CA., USA*

S.W. Buechel
*Buechel Consulting*

Keywords: Fire detection, AIRDAS, MODIS.

Fire imaging from sensing platforms can be divided into two distinct categories: **strategic** and **tactical**. **Strategic** observations are those that provide a regional view of fire occurrences (satellite systems such as AVHRR, MODIS and others) (Matson and Dozier, 1981; Matson *et al*., 1984; Justice *et al*., 2002; Roy *et al*., 2002; and others). Currently, the MODIS Rapid Response fire product provides a strategic overview of fire activity on a national scale. The US Forest Service - Remote Sensing Applications Center in Salt Lake City, Utah has adopted this technology and is evaluating the operational use of such to assess daily fire activity. **Tactical** observations are those that are provided on airborne platforms and have improved spatial and temporal resolution (Ambrosia and Brass, 1988). Tactical imaging allows continuous coverage and data accessibility over individual fire events (Brass, et al., 1987; Ambrosia, 1990). This paper focuses on improving the estimation of satellite-derived hot-spot detection using tactical airborne remote sensing systems.

The authors focus on improving the estimation of satellite-derived strategic fire locations by employing coincident aircraft under-flights with a highly calibrated thermal scanning system and real-time data telemetry (Ambrosia, et al., 1998; Ambrosia, et al., 2003). This paper discusses the initial findings and planned experiments designed to assist the US Forest Service in validating the MODIS Fire Rapid Response Product being generated for the continental US. The MODIS RR system has been employed at the USFS Remote Sensing Applications Center (RSAC) in Salt Lake City, and is undergoing evaluation by the staff for use in fire response by the agency (Sohlberg, Descloitres, and Bobbe, 2001). The algorithm for determining fire thresholds from the daily MODIS thermal imagery was developed by Goddard and the University of Maryland (Justice, et al., 2002; Justice and Korontzi, 2001; Kaufman, et al., 1998; Roy, et al., 2002; Giglio, et al., 1999, Justice, et al., 1996; Kaufman, et al., 1990) and relies on brightness temperatures derived from the MODIS 4 and 11 um channels (channels 21/22 and 31). The algorithm is derived from determining temperature thresholds for "hot" pixels, corrected by surrounding background pixel values. The algorithm is dependant on defining "fire" as being any pixel of a value greater than a predetermined threshold. The MODIS algorithm identifies "hot" pixels by applying three tests: The primary test is the application of predetermined thresholds (for nighttime or daylight detection). A secondary, lower threshold test detects "hot pixels" in areas with high TIR attenuation due to water vapor, as determined by differences in apparent temperature at 4 and 11 Um. Additional "hot" pixels associated with small, isolated fires are identified as those that are significantly hotter than surrounding pixels. A fire detection confidence estimate (low, nominal confidence, high confidence) is provided to the USFS in order to evaluate the

product for day-to-day operational use. To assist the USFS in evaluating this regional fire estimation product, we propose to validate fire products using a highly calibrated thermal airborne scanning system, relaying the information, via satellite telemetry in near-real-time to the USFS. By overflying either wildfires or prescribed burns during the coincident MODIS overpass, an estimate of both the MODIS sensitivity and detection confidence can be ascertained. It is important to justify the use of the AIRDAS scanner for evaluating the MODIS fire product; airborne systems more reliably detect fire due to finer spatial resolution (thus able to detect "thin" flame fronts or small patches of ground fire between trees that comprise a larger spatial domain on airborne imaging systems than on MODIS or AVHRR), higher temporal resolution (repeat coverage, allowing for observation of flare-ups in smoldering fires), and lower altitude of the sensing platform (resulting in relatively small TIR attenuation due to atmospheric water vapor and less obscuration by clouds).

A series of controlled ignitions in Southern California chaparral ecosystem and Northern California grass / woodland ecosystems are planned with simultaneous (and continuous) over-flight by a manned aircraft (or UAV) platform collecting thermal data from the AIRDAS scanning system (Brass, et al., 2001; Buechel, et al., 2001). The AIRDAS is a high emissive temperature, laboratory-calibrated, thermal imaging system that employs four channels of imaging capabilities (visible: 0.64 - 0.71 μm; near IR: 1.57 - 1.70 μm; short-wave thermal: 3.75 - 4.05 μm; and long-wave thermal: 5.50 - 13.0 μm). The instrument employs a 2-step pre-amplifier in the thermal channels to ensure low and high temperature calibration without sensor saturation up to ~700˚C (Ambrosia, et al., 1994). Although the AIRDAS is designed to provide discrete temperature estimations at high temperatures (commonly associated with fire events), modifications to the system are required to ensure precise calibrations at critical "lower" temperatures that are employed to define the temperature "threshold" of MODIS-derived fire products. The MODIS threshold temperatures are in the range of 315 – 360˚ K (42 – 87˚ C). In order to derive these lower temperature "thresholds" from the AIRDAS system, further low-temperature calibrations of the instrument are required to remove system "drift" and provide consistent, precise estimations of temperatures in that range. By using a unique two-step preamplifier in the AIRDAS instrument, and a high temperature laboratory calibration source, accurate thermal properties of imaged regions are derived. The authors discuss their laboratory calibration procedures required to ensure inter-comparison with the MODIS data.

This paper also discusses the information telemetry capabilities and improved geo-rectification procedures that allow improved flexibility in ingesting and sharing fire behavior information in near-real-time. The ability to telemeter data from the acquiring platform in near-real-time is essential to supporting tactical fire operations within the fire fighting community. The enabling technologies of air-to-ground or air-satellite-ground communications allow a near-real-time assessment of fire detection confidence with fire products derived from the MODIS system. By integrating a real-time data geo-rectification procedure, the tactical fire product can be integrated into the fire manager's decision support system for overlay with other critical data or integration with satellite-derived fire information. This allows rapid assessment of MODIS fire detection confidence.

The tactical fire observations mentioned above and future experiments, designed to increase the confidence of satellite-derived fire estimations, will be discussed. Initial findings from missions occurring in summer 2002 and early spring 2003 are presented.

## REFERENCES


Ambrosia, V.G., S.S. Wegener, D.V. Sullivan, S.W. Buechel, J.A. Brass, S.E. Dunagan, R.G. Higgins, E.A. Hildum and S.M. Schoenung. *Demonstrating UAV-Acquired Real-Time Thermal Data Over Fires*, Photogrammetric Engineering and Remote Sensing, (In Print), 2003.

Ambrosia, V.G and J.A. Brass, 1988. Thermal Analysis of Wildfires and Effects on Global Ecosystem Cycling, *Geocarto International*, 3(1): 29-39.

Ambrosia, V.G., 1990. High Altitude Aircraft Remote Sensing During The 1988 Yellowstone National Park Wildfires, *Geocarto International*, 5(3): 43-47.

Ambrosia, V.G., J.A. Brass, J.B. Allen, E.A. Hildum and R.G. Higgins, 1994. AIRDAS, Development Of A Unique Four Channel Scanner For Natural Disaster Assessment, *Proceedings of the First International Airborne Remote Sensing Conference*, 11-15 September, Strasbourg, France, Vol. II, pp 129-141.

Ambrosia, V.G., S.W. Buechel, J.A. Brass, J.R. Peterson, R.H. Davies, R.J. Kane and S. Spain, 1998. An Integration of Remote Sensing, GIS, and Information Distribution for Wildfire Detection and Management, *Photogrammetric Engineering and Remote Sensing*, 64(10): 977-985.

Brass, J.A., V.G. Ambrosia, R.S. Dann, R.G. Higgins, E. Hildum, J. McIntire, P.J. Riggan, S. Schoenung, R. Slye, D.V. Sullivan, S. Tolley, R. Vogler, S. Wegener, 2001. First Response Experiment (FiRE) Using An Uninhabited Aerial Vehicle (UAV), *Proceedings of 5th International Airborne Remote Sensing Conference*, 17-20 September, San Francisco, California, CD-ROM paper no. 56, pp 1-9.

Brass, J.A., V.G. Ambrosia, P.J. Riggan, J.S. Myers and J.C. Arvesen, 1987. Aircraft and Satellite Thermographic Systems for Wildfire Mapping and Assessment, *Proceedings, 25th Aerospace Sciences Meeting, American Institute of Aeronautics and Astronautics*, Reno, Nevada, 12-15 January, Paper. No. 87-0887, pp. 1-7.

Buechel, S., L. Pious, J. Brass, 2001. Near Real-Time Mapping For Wildland Fire Characterization and Model Calibration, *Proceedings of 5th International Airborne Remote Sensing Conference*, 17-20 September, San Francisco, California, CD-ROM paper no. 101, pp. 1-8.

Giglio, L. J.D. Kendall, and C.O. Justice, 1999. Evaluation of Global Fire Detection Algorithms Using Simulated AVHRR Infrared Data, *International Journal of Remote Sensing*, 20: 1947-1985.

Justice, C.O., L. Giglio, S. Korontzi, J. Owens, J.T. Morisette, D. Roy, J. Descloitres, S. Alleaume, F. Petitcolin, and Y. Kaufman, 2002. The MODIS Fire Products, *Remote Sensing of Environment*, 83: 244-262.

Justice, C.O. and Korotzi, 2001. A Review of the Status of Satellite Fire Monitoring and the Requirements for Global Environmental Change Research, in *Global and Regional Wildland Fire Monitoring From Space: Planning a Coordinated International Effort*, eds: Ahern, Goldammer and Justice, The Hague: SPB Academic Publishing, pp. 1-18.

Justice, C.O., J.D. Kendall, P.R. Dowty and R.J. Scholes, 1996. Satellite Remote Sensing of Fires During the SAFARI Campaign Using NOAA AVHRR Data, *Journal of Geophysical Research*, 101: 23851-23863.

Kaufman, Y.J., C.O. Justice, L. Flynn, J.D. Kendall, E.M. Prins, L. Giglio, D.E. Ward, W.P Menzel and A.W. Stezer, 1998. Potential Global Fire Monitoring From EOS-MODIS, *Journal of Geophysical Research*, 103: 32215-32238.

Kaufman, Y.J., A.W. Setzer, C.O. Justice, C.J. Tucker, M.C. Pereira and I. Fung, 1990. Remote Sensing of Biomass Burning In The Tropics, In J.G. Goldammer (Ed.), *Fire and the Tropical Biota: Ecosystem Processes and Global Challenges*, Berlin: Springer-Verlag, pp. 371-399.

Matson, M. and J. Dozier, 1981. Identification of Subresolution High Temperature Sources Using a Thermal IR Sensor, *Photogrammetric Engineering and Remote Sensing*, 47(9): 1311-1318.

Matson, M., S.R. Schneider, B. Aldridge and B. Satchwell, 1984. Fire Detection Using the NOAA-Series Satellites, NOAA Technical Report NESDIS 7, U.S. Department of Commerce; NOAA; National Environmental Satellite, Data and Information Service. Washington, D.C., 34 p.

Roy, D.P., P.E. Lewis and C.O. Justice, 2002. Burned Area Mapping Using Multi-Temporal Moderate Spatial Resolution Data – A Bi-Directional Reflectance Model-Based Expectation Approach, *Remote Sensing of Environment*, 83: 263-286.

Sohlberg, R., J. Descloitres and T. Bobbe, 2001. MODIS Land Rapid Response: Operational Use of TERRA Data for USFS Wildfire Management, *The Earth Observer*, 13: 8-14.

# Burn severity detection enhancement using AVIRIS hyperspectral data

Ralph R. Root
*USGS Rocky Mountain Mapping Center, Denver, Colorado, USA*

Carl H. Key
*USGS Northern Rocky Mountain Science Center, West Glacier, Montana, USA*

Jan W. van Wagtendonk
*USGS Western Ecological Research Center, El Portal, California, USA*
Jan_van_wagtendonk@usgs.gov

Keywords: burn severity assessment, multi-temporal images, AVIRIS, Yosemite National Park, USA

ABSTRACT: Our study presents data on burn severity collected from multi-temporal AVIRIS images using the Normalized Difference Burn Ratio (*dNBR*). Two AVIRIS data acquisitions recorded surface conditions immediately before and one year after the 26 July, 2001 Hoover fire at Yosemite National Park. Data were validated with 63 field plots using the Composite Burn Index (*CBI*). The relationship between spectral channels and burn severity was examined by comparing pre- and post-fire datasets. Based on the high burn severity comparison, AVIRIS channels 47 and 60 at wavelengths of 788 and 913 nm showed the greatest *negative* response to fire. Post-fire reflectance values decreased the most on average at those wavelengths, while channel 210 at 2370 nm showed the greatest *positive* response on average. Fire increased reflectance the most at that wavelength over the entire measured spectral range. Furthermore, channel 210 at 2370 nm exhibited the greatest variation in spectral response over the sample, suggesting potentially high information content for fire effects. Results seem to verify the foundational band-response relationships to burn severity as seen with TM/ETM+, and they confirmed this independently by way of a distinctly different sensor system.

## 1. INTRODUCTION

Information about burned areas is essential for land managers to assess the impacts of fires on landscapes. Required levels of information are often difficult to obtain, however, especially where fire size, remoteness and rugged terrain impede direct observation of burned areas. Thus, managers increasingly must turn to remote sensing technologies to extend knowledge and to quantify the extent and severity of fires. The remote sensing of severity has been captured by a Landsat TM radiometric index called the Normalized Burn Ratio, or *NBR* (Key and Benson 1999, Key and Benson 2002a, Key *et al*. 2000, White *et al.* 1996). Multi-temporal differencing was employed to enhance contrast and detection of changes from before to after fire. Coupled with a standard field measure of burn severity called the Composite Burn Index (*CBI*) developed by Key and Benson (2002b), the *NBR* provides an accurate, repeatable detection of burn severity. Additional work using TM and ETM+ imagery to look at vegetation mortality, vegetation depletion, and canopy consumption has been done by Patterson and Yool (1998), Rogan and Yool (2001), and Miller and Yool (2002). Similar techniques were used by Koutsias *et al*. (1999) to map burned areas in the fragmented landscape of the European Mediterranean basin. While these techniques have proven useful, it is possible that higher spatial and spectral resolution might provide more insight into the impact of severity on vegetation resources.

The Airborne Visible and Infrared Imaging Spectrometer (AVIRIS) is such a sensor. AVIRIS data have been used to map fuels (Roberts *et al.* 2000) and a similar sensor, Hymap, (HyVista Corporation, 2003) is being used to assess burned area extent (Morath *et al.* 2002), but no attempts have been made to assess severity using imaging spectroscopy for calculating the NBR before and after fire imagery. The opportunity to use multiple AVIRIS scenes arose in Yosemite National Park, USA, when imagery was reflown in consecutive years while a large lightning-caused fire was being allowed to burn under prescribed conditions.

## 2. METHODS

Two AVIRIS data acquisitions recorded surface conditions immediately before and one year after the 26 July, 2001 Hoover fire at Yosemite National Park. The relationship between spectral channels and burn severity was examined by comparing pre- and post-fire datasets. Temporal response in apparent reflectance was measured from before fire to after fire, for areas of high moderately high, low burn severity, and unburned.

## 3. RESULTS

Based on the high burn severity comparison (Figure 1), AVIRIS channels 47 and 60 at wavelengths of 788 and 913 nm showed the greatest *negative* response to fire (figure 1). Post-fire reflectance values decreased the most on average at those wavelengths, while channel 210 at 2370 nm showed the greatest *positive* response on average. Fire increased reflectance the most at that wavelength over the entire measured spectral range. Furthermore, channel 210 at 2370 nm exhibited the greatest variation in spectral response over the sample, suggesting potentially high information content for fire effects.

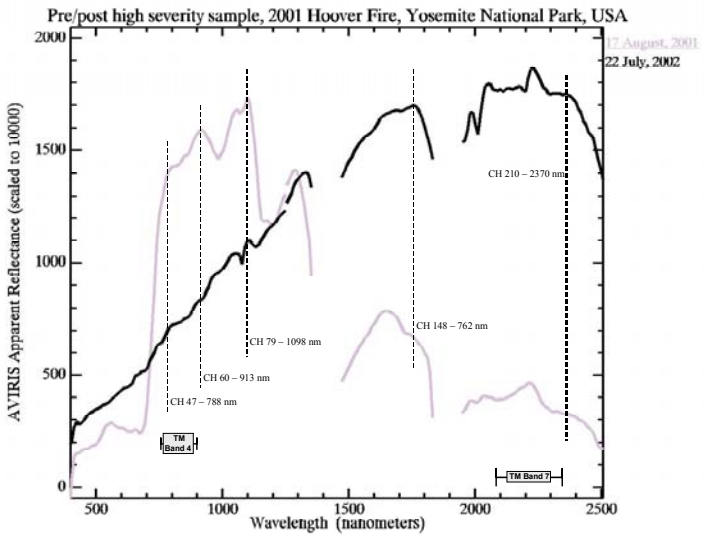


Figure 1. Pre and post fire high severity sample, 2001 Hoover Fire, Yosemite National Park, USA.

Channel 148 at 1762 nm also had fairly high positive change due to fire; however, the variation in that channel throughout the burn was considerably less than channel 210 at 2370 nm. Channel 79 at 1098 nm also had high negative response to fire, but was a little less than the change within channels 47 and 60 at 788 and 913 nm. The implication was that dynamic association of spectral responses at 788 or

913 nm and 2370 nm should provide significant statistical leverage for distinguishing degrees of burn severity on the ground.

The moderately high burn severity sample (Figure 2), shows close to the same separation of reflectance values in the short wavelength infrared (1500 to 2500 nanometers), but presence of a small amount of green vegetation is indicated by a slight "red-edge" response at 700 nanometers.

The low burn severity sample (Figure 3) shows very similar reflective response in the infrared portions of the spectrum (750 to 2500 nanometers), but a subtle decrease in chlorophyll absorption is visible in the 550 to 700 nanometer range.

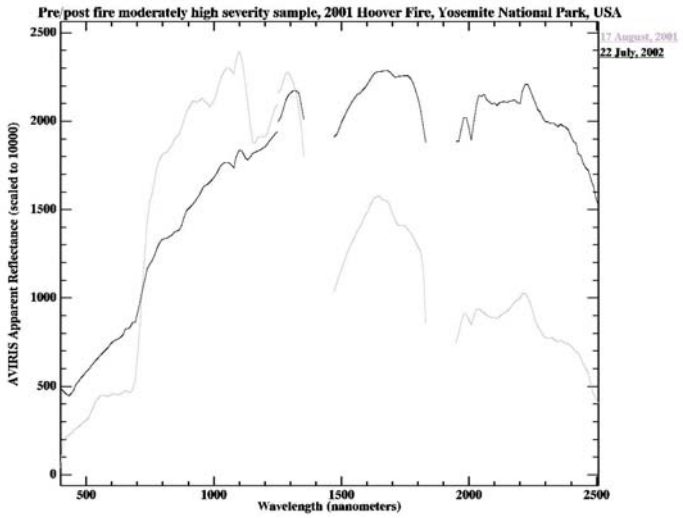


Figure 2. Pre and post moderately high severity sample, 2002 Hoover Fire, Yosemite National Park, USA.

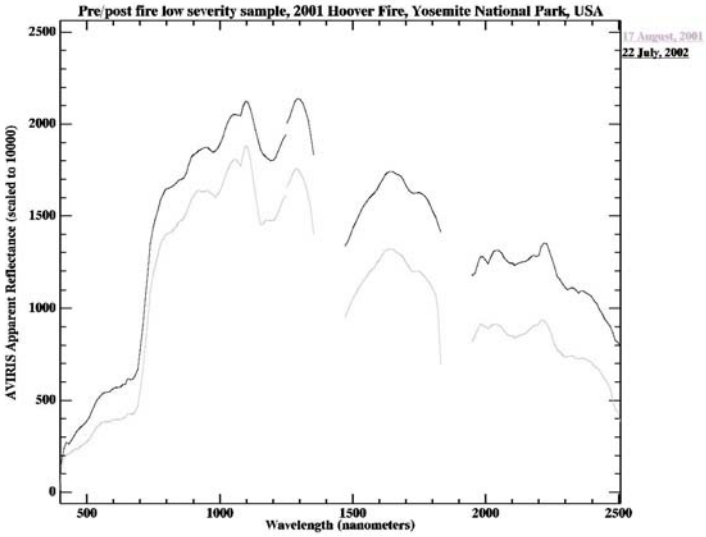


Figure 3. Pre and post low severity sample, 2001 Hoover Fire, Yosemite National Park, USA.

The unburned sample (Figure 4), as expected, looks nearly the same in both years. A slight difference in chlorophyll absorption and a tapering of the red edge on the 2001 image indicates that vegetation was slightly drier or less vigorous in 2001 as opposed to 2002. As can be seen by comparing all four figures, burn severity levels can be separated based on the response of the AVIRIS bands.

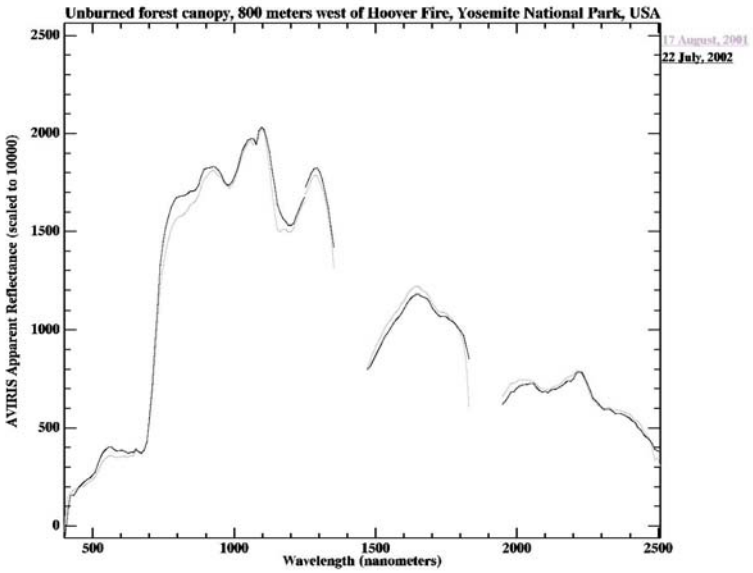


Figure 4. Pre and post fire unburned sample, 2001 Hoover Fire, Yosemite National Park, USA.

These results fit well with results reported for fire-effects detection using Landsat TM and ETM+ sensors. AVIRIS channels 47 and 60 occur within and adjacent to Landsat TM bandwidth 4 (750-900 nm) and AVIRIS channel 210 at 2370 nm occurs at the long wavelength edge of Landsat TM bandwidth 7 (2090-2350 nm). The latter band reflectances *($R_b$)* have been shown to respond most dramatically to burning among Landsat bandwidths, and have been associated in a radiometric index called the Normalized Burn Ratio [$NBR = (R_4 - R_7) / (R_4 + R_7)$]. The NBR is now widely used by land managers in the United States to assess landscape-level fire effects. Temporal difference of NBR, pre-fire to post-fire ($dNBR = NBR_{pre} - NBR_{post}$), is hypothesized 1) to represent optimal separation of burned area from unburned surroundings; and 2) to provide a scaled index of the magnitude of change caused by fire, hence the burn severity. Similar reasoning should be applicable to the 913 and 2370 nm AVIRIS channels, regarding their effectiveness for discriminating burn severity.

We validated the severity analysis by comparing Composite Burn Indices (*CBI*) from 63 field plots with *dNBR* values for both the ETM+ and AVIRIS imagery (Key and Benson 2002b). These plots were established in unburned, low severity, moderate severity, and high severity areas. For ETM+ data, the regression of *CBI* as a function of *dNBR* was:

$$CBI_{ETM+} = 0.281 + 0.007(dNBR_{ETM+}) - 5e^{-6(dNBR_{ETM+})},$$

with an $R^2$ of 0.884 ($p$=0.000). When applied to the AVIRIS data, the equation was:

$$CBI_{AVIRIS} = 1.207 + 0.005(dNBR_{AVIRIS}) - 4e^{-6(dNBR_{AVIRIS})},$$

with an $R^2$ of 0.924 ($p$=0.000), a 0.040 reduction in the unexplained variance over the ETM+ regression.

The fact that the two AVIRIS channels with greatest combined response fell within or very close to the TM/ETM+ sensor bandwidths having the most sensitivity to fire effects is encouraging. Results seem to verify the foundational band-response relationships to burn severity as seen with TM/ETM+, and they confirmed this independently by way of a distinctly different sensor system. Initially there was some question whether AVIRIS channels not sampled within TM/ETM+

bandwidths were more useful for sensing fire effects. That now, at least, does not appear to be the case.

There still remains, however, distinct potential for the 913 and 2370 nm AVIRIS channels to radiometrically enhance the burn signal over TM/ETM+. That may occur as only the key, peak AVIRIS channels are selected within TM/ETM+ bandwidths, where detected response typically exceeds that of the bandwidths overall. In fact, our results show that $dNBR_{TM}$ was less in magnitude, and had less variation within the burn than $dNBR_{AVIRIS}$. In addition, an obvious benefit to burn assessment from AVIRIS is improved spatial resolution, depending on aircraft altitude. Even in our case, AVIRIS nominal resolution of 17 meters represents a 3.1 times improvement over Landsat 30-meter resolution. That provides finer detail for sub stand-level measurements, and more precise geo-location of ground sample points within the image matrix.

## 4. CONCLUSION

Unfortunately, use of AVIRIS in multi-temporal differencing may chiefly be limited to unique opportunities, as in this case, due to complexity of mission planning and the high cost of data acquisition. Moreover, AVIRIS is not continuously flown and coverage is not geographically contiguous. On the other hand, most AVIRIS data acquisitions are eventually archived for access by users other than initial principal investigators. There are also issues of complexity in the geo-rectification necessary for temporal differencing, especially with multiple flight lines, and terrain exhibiting high topographic relief. Some large, socio-economically important burns may continue to attract AVIRIS overflights, but of those a smaller number still is likely to have comparable pre-fire data available to represent appropriate timing for the post-fire data. Thus, it is doubtful such data are currently practical for making burn assessments, until orbital imaging spectrometers with the capability of capturing data at regular intervals are in routine use.

Nonetheless, such opportunities should be explored with past AVIRIS datasets, and new pre- and post-fire hyperspectral datasets should be considered when research or management objectives justify. That may be the case, for example, when developing mechanistic models ultimately intended for more routine applications, or when needing to learn from relatively large prescribed burns. Such approaches apply knowledge gained in great detail about cause and effect to algorithms implemented at coarser resolutions

## 5. REFERENCES


HyVista Corporation, 2003. Sensors, HyMap™ Hyperspectral Scanner. http://www.hyvista.com/main.html.

Key, C. H., and Benson, N. C. 1999. Measuring and remote sensing of burn severity. In Proceedings Joint Fire Science Conference and Workshop, Vol. II. Edited by L. F. Neuenschwander and K. C. Ryan (Univ. Idaho and Int. Assoc. Wildland Fire), p. 284.

Key, C. H, and Benson. 2002a. Remote Sensing Measure of Severity, The Normalized Burn Ratio. In: Fire effects monitoring and inventory protocol, Landscape Assessment. Retrieved March 30, 2003 from Systems for Environmental Management and USDA Fire Sciences Laboratory, Rocky Mountain Research Station Web site: http://www.fire.org/firemon/lc.htm.

Key, C. H, and N. Benson. 2002b. Ground Measure of Severity, The Composite Burn Index. In: Fire effects monitoring and inventory protocol, Landscape Assessment. Retrieved March 30, 2003 from Systems for Environmental Management and USDA Fire Sciences Laboratory, Rocky Mountain Research Station Web site: http://www.fire.org/firemon/lc.htm.

Key, C. H, N. Benson, B. Sorbel, Z. Zhu, D. Ohlen, S. M. Howard, and B. Clement. 2002. National Park Service - U.S. Geological Survey National Burn Severity Mapping Project. Retrieved September 30, 2002 from USGS EROS Data Center archive and web site: http://edc2.usgs.gov/fsp/severity/fire_main.asp.

Morath, L., Kokaly., R. F., Rockwell, B., Root., R., and Goodman., S. 2002. "Post-fire Characterization of the Land Surface and Vegetation using Imaging Spectroscopy Data for Cerro Grande NM and Left Hand Creek, WY. Geological Society Abstracts with Programs Vol. 34, No. 6, p. 552.

Koutsias, N., M. Karteris, A. Fenandez, C. Navarro, J. Jurado, R. Navarro, and A. Lobo. 1999. Burnt land mapping at local scale. P. 123-138 *in:* Chuvieco, E. (Ed.). Remote sensing of large wildfires in the European Mediterranean basin. Springer-Verlag, Berlin.

Miller, H. J., and S. R. Yool. 2002. Mapping forest post-fire canopy consumption in several overstory types using multi-temporal Landsat TM and ETM+ data. Remote Sensing of Environment 82: 481-496.

Patterson, M. V., and S. R. Yool. 1998. Mapping fire-induced vegetation mortality using Landsat Thematic Mapper data: a comparison of linear transformation techniques. Remote Sensing of Environment 65: 132-142.

Roberts, D. A., Dennison, P. E., Morais, M. E., Gardner, M. E., Regelbrugge, J., and Ustin, S. L. 2000. Mapping wildfire fuels using imaging spectrometry along the wildland-urban interface. In Proceedings Joint Fire Science Conference and Workshop, Vol. I. Edited by L. F. Neuenschwander and K. C. Ryan (Univ. Idaho and Int. Assoc. Wildland Fire), pp. 212-223.

Rogan, J., and S. R. Yool. 2001. Mapping fire-induced vegetation depletion in the Peloncillo Mountains, Arizona and New Mexico. International Journal of Remote Sensing 22(16): 3101-3121.

White, J. D., Ryan, K. C., Key, C. H., and Running, S. W. 1996. Remote sensing of forest fire severity and vegetation recovery. International Journal of Wildland Fire 6(3): 125-136.

# Infrared signal processing for early warning of forest fires

L.Vergara, I. Bosch, P. Bernabeu & N. Cardona
*Dpto. Comunicaciones, Universidad Politécnica de Valencia, Spain*
lvergara@dcom.upv.es

Keywords: forest fire, infrared, signal processing, automatic detection

ABSTRACT: This paper presents an automatic detection scheme for infrared signals, for early detection of forest fires. The detector exploits different aspects of both the background noise and the signal, to reduce the false and undesired alarms, while keeping a high detection capability. The basic ideas of the algorithms are presented. Also, a description is included of a real pilot system, which uses the foregoing algorithms.

## 1. INTRODUCTION

Infrared signal processing has shown practical importance in environment monitoring both in satellite (Carlotto 1997, Li 2001) and terrestrial (Vergara 2000) systems. In this paper we are interested in automatic detection for early warning of forest fires using infrared sensors or cameras. To be more specific, our main problem is to detect "uncontrolled fire", we mean, that kind of fire which causes a continuous increase of temperature in a period of time. This type of fire should produce true alarms, whereas occasional effects (for example, a chimney, a cloud apparition, a car crossing the area under analysis) could produce undesired alarms, and the background infrared noise could produce conventional false alarms. It is important in this context to note the different between undesired and false alarms. Accordingly to this, we are interested in a system that, for a certain probability of false alarm (PFA), can maximize the probability of detection (PD) of an uncontrolled fire, while minimizing the probability of detecting undesired alarms (PDU).

We assume that the area under surveillance is divided into different cells of spatial resolution (ranges – azimuths). In a given instant, our sensor or camera will collect an infrared level (sample) to be associated to every given cell. To decide automatically if there is an alarm in a cell we should establish a procedure. A simple possibility could be to compare the sample level with a predetermined threshold. Thus, if we are able to characterize the background noise distribution, the threshold may be adjusted to satisfy a determined PFA, and once this is fixed, the obtained PD (desirably the maximum) will depend on the signal to noise ratio (*SNR*).

But, if we consider an isolated sample, we will not have a good way to distinguish between true alarms and undesired alarms: the PD could be similar and even less than PDU. Considering that there must be distinctive characteristics on the fire time evolution in a given cell, when compared with the evolution of occasional effects, we can think about the possibility of making the detections by means of analysing the fire "signatures", formed by various samples related to the same cell in instants of consecutive scans.

Another question to be considered is the possible non-gaussianity of the noise data, this complicates the detector design. In fact, the first analysis of real infrared data showed that the

hypothesis of Gaussianity is not always met. Despite the approach of considering detection schemes "ad hoc" to every type of noise, we face the noise problems using prediction schemes. In one hand, as we will observe, the prediction let us reduce the noise level, due to the large time correlation exhibited by the infrared environment. In the other hand we will show how the prediction "makes more Gaussian" the noise, thus adjusting itself to the conditions assumed by the conventional matched filter (Scharf 1991). Additionally, considering the possible non-gaussianity, the predictor should include some kind of nonlinearity to approximate the predictions to the conditional mean: optimum prediction under the least-mean-square error criteria (Scharf 1991). In any case, we will reduce the noise level, thus increasing the PD to every PFA.

## 2. BASIC DETECTION SCHEME

Following the ideas provided in the introduction, we propose a general scheme, shown in Figure 1. Two main parts compose this scheme: the prediction step and the detection step. In that figure, we have defined the following vectors: the noise vector $\boldsymbol{w} = [w_n\ w_{n-1} \ldots w_{n-N+1}]^{\mathrm{T}}$, noise samples collected from the $(n-N+1)$-*th* scan to the *n-th* scan in the same cell, i.e., we are assuming no signal present, the vector $\boldsymbol{x} = [x_{n+1}\ x_{n+2} \ldots x_{n+D}]^{\mathrm{T}}$, samples taken from the $(n+1)$-*th* scan to the $(n+D)$-*th* scan in the same cell. This vector will always have a noise contribution, and when a true or undesired alarm is present, a signal contribution, in general, $\boldsymbol{x} = \boldsymbol{s} + \boldsymbol{w_D}$, $\boldsymbol{w}_D = [w_{n+1}\ w_{n+2} \ldots w_{n+D}]^{\mathrm{T}}$.

In principle, we should decide if an alarm is present on the basis of the information provided by vector $\boldsymbol{x}$. Nevertheless, we may try to improve the *SNR* by predicting the vector $\boldsymbol{w_D}$ from the vector $\boldsymbol{w}$, assuming that the noise may be predicted up to a given degree. This is a realistic hypothesis, given the strong correlation that in general will exist between the background noise measurements taken in the same cell in successive scans. Let us call $\boldsymbol{w}_{NLP}$ the (in general nonlinear) prediction of $\boldsymbol{w_D}$ from $\boldsymbol{w}$.

The second part of the general scheme is the detector, which we apply on the prediction error vector $\boldsymbol{e} = \boldsymbol{x} - \boldsymbol{w}_{NLP}$, which in presence of signal will be given by $\boldsymbol{e}=\boldsymbol{s}+\boldsymbol{z}$, (with $\boldsymbol{z}$ residual noise). Two different detectors are proposed. The first one (downwards in figure 1) implements a subspace matched filter [4], where the signal is estimated ($\boldsymbol{s}_e$) by projecting the prewhitened error vector $\boldsymbol{u}$ into a subspace having a projection matrix $\boldsymbol{P}$. This projection will be useful, not only to estimate the possible signal $\boldsymbol{s}$ due the existence of an uncontrolled fire, but also to reject those possible signals due to occasional effects, whose signatures are outside the subspace $\boldsymbol{P}$. The second one (upwards) is call increase detector. Basically it tries to detect the presence of increasing trends in the prediction error vector $\boldsymbol{e}$. To this end, the vector $\boldsymbol{e}$ is transformed by the difference matrix $\boldsymbol{Q}^{(n)}$ which implements a *n*-difference operation, then a conventional matched filter follows. This later is matched to a DC component $\boldsymbol{s}_e$ having *D-n* elements. Prewhitening by the autocorrelation matrix $\boldsymbol{R}_{z'z'}^{-\frac{1}{2}}$ is necessary for a correct implementation of the matched filter. The vector $\boldsymbol{z}'$ is the residual noise $\boldsymbol{z}$ transformed by the *n*-difference matrix.

## 3. A PILOT SYSTEM

The above detection scheme is the core of e a pilot system. It is an advanced surveillance system for early automatic detection and warning of forest fires. It is based on several automatic lookout posts linked with an Alarm Central Station (ACS) through a communication system.

The lookout posts parts are: thermal sensors, detection, surveillance and communication units. The sensors are based on motorized infrared cameras, which are capable to detect the minimum rise of temperature. The lookout posts are strategically set up in order to watch over wide areas. The detection unit is the system kernel and it basically consists on a thermal image processor subsystem, which

processes every pixel of the infrared image using the foregoing algorithms. This allows reducing the false and undesired alarms while keeping a high detection capability. The surveillance unit has a remote control visual support system, which permits us to observe the scene under study in the visible and infrared ranges from the ACS. This unit allows verifying each alarm generated by the lookout post from the remote alarm station. The communication unit manages the information bear among the lookout posts and the ACS. These units are adapted to the telecommunication infrastructure for each geographic area via cable or radio frequency systems. Finally, the ACS receives alarms from the lookout posts, then it geocodes the alarms in a Geographic Information System (GIS), allowing the

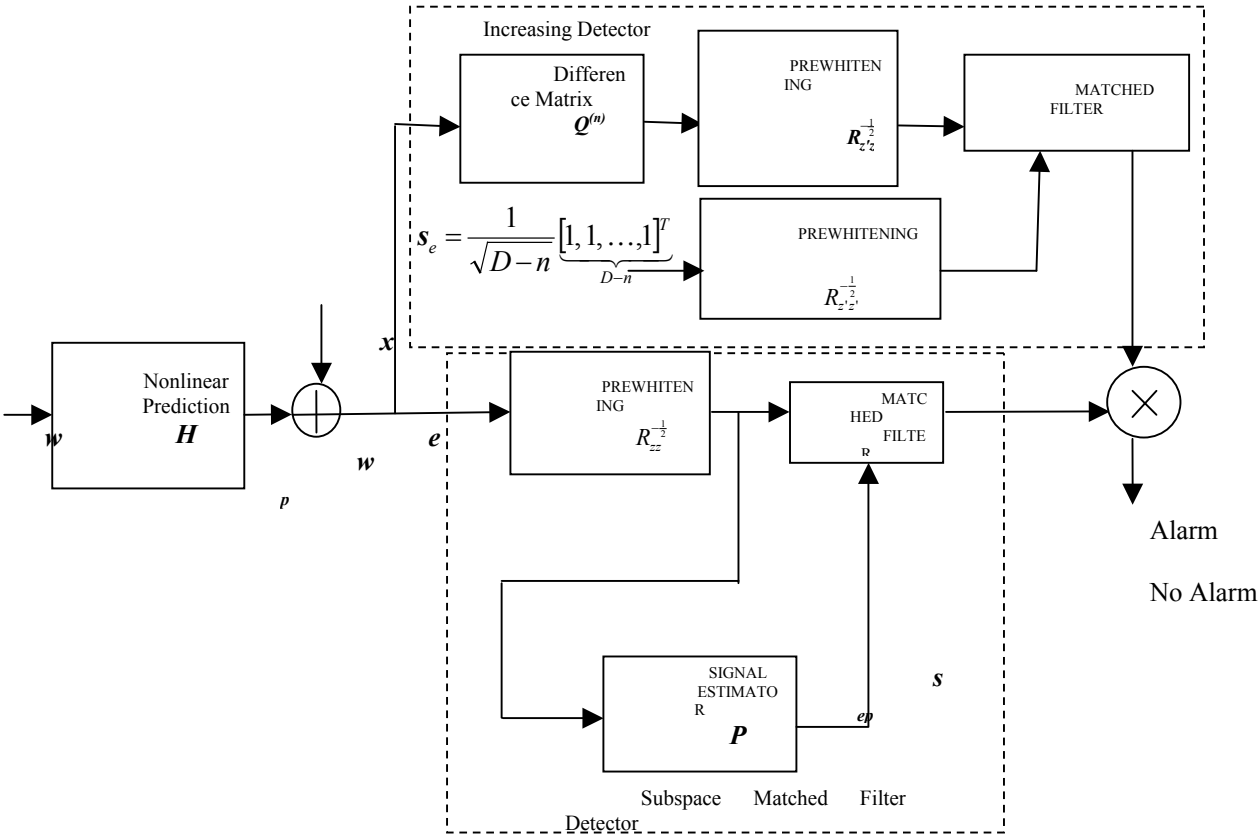


operator to watch alarms on a map. Alarm information comprises both the alarm type and the geographic coordinates. Additionally the operator may watch the alarm scenario on a screen, using the remote surveillance unit like in a closed circuit TV. Furthermore, the operator may control and monitor the lookout posts. Two systems are now working in the area of Valencia (Spain).

## 4. ACKNOWLEDGMENT

This work has been supported by the Spanish Science and Technology Ministry under grant TIC2002-04643.

## 5. REFERENCES

Carlotto, M. J. 1997. Detection and analysis of change in remotely sensed imagery with application to wide area surveillance. *IEEE Transactions on Image Processing,* Vol. 6 (No 1):189-202.

Li , Z. & al. 2001. A review of AVHRR-based active fire detection algorithms: principles, limitations and recommendations. In *Global and Regional Vegetation Fire Monitoring from Space, Planning and Coordinated International Effort* (Eds. F. Ahern, J.G. Goldammer, C. Justice):199-225.

Scharf, L. L. 1991. *Statistical signal processing: Detection, estimation, and times series analysis*. 1991 Reading, MA: Addison-Wesley.

Vergara, L. & Bernabeu, P. 2000. Automatic signal detection applied to fire control by infrared digital signal processing. *Signal Processing*, Vol. 80 (No 4):659-669.

Vergara, L. & Bernabeu, P. 2001. Simple approach to nonlinear prediction. *Electron. Lett*. Vol. 37 (No 14): 926-928.

# Abstracts presented in parallel
**(For timing reasons, they were not evaluated by the Scientific Committee)**

# Estimating stand structural attributes of ponderosa pine forests with discrete return lidar – Input layers for fire behaviour models

Hall, S.A. & Burke, I.C.
*Graduate Degree Program in Ecology, Dept. Forest, Range and Watershed Stewardship, Colorado State University, Fort Collins, CO, USA*

Box, D.O.
*Engineering and Technology Dept., 3Di Technology Inc., Eagle Scan Remote Sensing, Boulder, CO, USA.*
*Rocky Mountain Research Station, USDA Forest Service, Fort Collins, CO, USA.*

Kaufmann, M.R. & Stoker, J.M.
*EROS Data Center, U.S. Geologic Survey, Sioux Falls, SD, USA.*

Since the late 1990s, extensive crown fires have burned in ponderosa pine forests growing at low elevation in the Rocky Mountains, USA. Fire behaviour models can be used to gain insight into the fuel conditions that favour the occurrence of large crown fires (Scott and Reinhart, 2001), but there is a lack of spatially explicit data to be used as inputs for these models. Given the cost of detailed inventorying of forest structure, our objective was to develop simple regression models to estimate stand structural variables that are key inputs to fire behaviour models (mean stand height, canopy base height and canopy bulk density) using discrete return lidar.

Both profiling and discrete return lidar have been used successfully to estimate stand structural attributes in different forest types (Lefsky et al 2002). The main structural variables estimated using lidar metrics are height, basal area, total aboveground biomass and volume (Lefsky et al 1999a, 1999b, Means et al 1999, 2000, Naesset and Bjerknes 2001, Naesset 2002, Naesset and Okland 2002, Drake et al 2002). We collected data from 14 sites in ponderosa pine forests in Colorado, USA. Discrete, multiple return lidar data were collected in September 2001. We calculated 46 metrics from the lidar data, and used combinations of these metrics to generate simple linear and non-linear regression models to predict each of the three structural variables of interest. We used information theoretic approaches (Burnham and Anderson 2002) to select the best model/s and to determine model selection uncertainty (i.e. the probability that other models might be selected as the best if we had a new dataset). We were able to explain 86%, 54% and 82% of the variability of mean stand height, canopy base height and foliage bulk density, respectively (Fig.1). There was substantial model selection uncertainty associated with the estimates of canopy base height and somewhat less for the estimates of stand height. The information theoretic approach we used provides an objective way to incorporate this uncertainty, allowing us to provide estimates based on weighted averages of more than one model. Validation of these regression models with new data, especially for canopy base height and high values of foliage bulk density, will strengthen our confidence in the accuracy of estimates of these variables.

Our results support the use of lidar overflights as an efficient way to generate spatially explicit maps of overstory fuel characteristics in ponderosa pine forests, which can then be used as inputs to fire behaviour models.

REFERENCES

Burnham, K.P., Anderson, D.R. 2002. Model selection and multimodel inference – A practical information theoretic approach. 2nd Edition. Springer-Verlag, New York, USA.

Drake, J.B. et al. 2002. Estimation of tropical forest characteristics using large-footprint lidar. Rem. Sens. Environ. 79, 305-319.

Lefsky, M.A. et al. 1999a. Surface lidar remote sensing of basal area and biomass in deciduous forests of eastern Maryland, USA. Rem. Sens. Environ. 67, 83-98.
Lefsky, M.A. et al. 1999b. Lidar remote sensing of the canopy structure and biophysical properties of Douglas-fir western hemlock forests. Rem. Sens. Environ. 70, 339-361.
Lefsky, M.A et al. 2002. Lidar remote sensing for ecosystem studies. BioSci. 52, 19-30.
Means, J.E. et al. 2000. Predicting forest stand characteristics with airborne scanning lidar. PE&RS 66, 1367-1371.
Means, J.E. et al. 1999. Use of large-footprint scanning airborne lidar to estimate forest stand characteristics in the Western Cascades of Oregon. Rem. Sens. Environ. 67, 298-308.
Naesset, E. 2002. Predicting forest stand characteristics with airborne scanning laser using a practical two-stage procedureand field data. Rem. Sens. Environ. 80, 88-99.
Naesset, E., Bjerknes, K.-O. 2001. Estimating tree heights and number of stems in young forest stands using airborne laser scanner data. Rem. Sens. Environ. 78, 328-340.
Naesset. E., Okland, T. 2002. Estimating tree height and tree crown properties using airborne scanning laser in a boreal nature reserve. Rem. Sens. Environ. 79, 105-115.
Scott, J.H., Reinhardt, E.D. 2001. Assessing crown fire potential by linking models of surface and crown fire behavior. U.S. Forest Service, RMRS-RP-29.

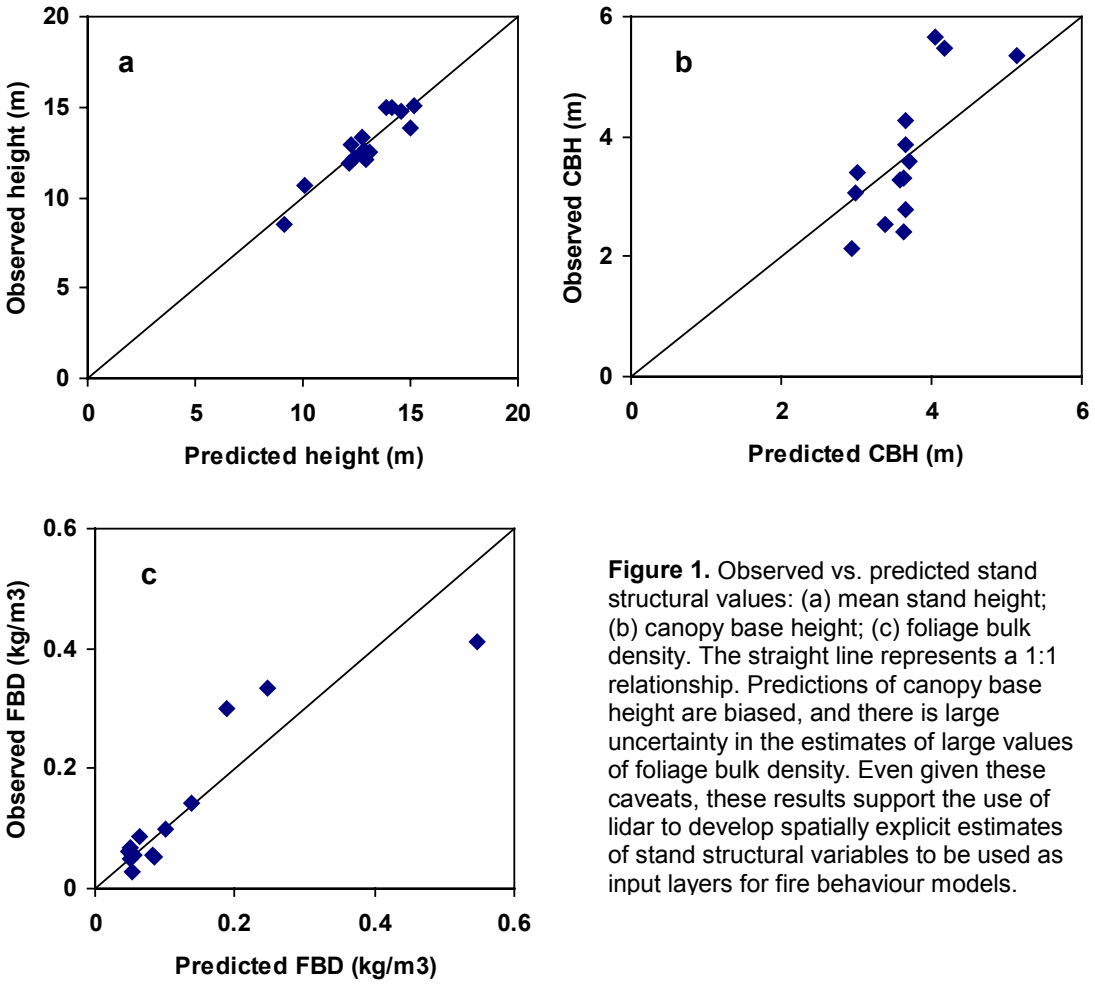


**Figure 1.** Observed vs. predicted stand structural values: (a) mean stand height; (b) canopy base height; (c) foliage bulk density. The straight line represents a 1:1 relationship. Predictions of canopy base height are biased, and there is large uncertainty in the estimates of large values of foliage bulk density. Even given these caveats, these results support the use of lidar to develop spatially explicit estimates of stand structural variables to be used as input layers for fire behaviour models.

# Remote Sensing of Forest Fire: Initiatives in India

Subhash Ashutosh
*Forest Survey of India, Dehradun, India*
Sashutosh30@yahoo.com

India has about 63.73 million ha of forest cover, which is 19.39% of the country's land area and it accounts for 1.66% of the world's total forest cover. India's forests are rich in biodiversity, making India to figure in the list of 12 mega-biodiversity countries in the world. The broad forest types include tropical evergreen, moist deciduous, dry deciduous, mangrove and temperate forests. Fire causes extensive destruction to forests in the country every year. According to a study based on remote sensing data, about 54.7% of India's forest is prone to fire. In the year 1995 about 2.31% of the total forest of India was found to be affected by fire. In another study of burnt area mapping, it was found that nearly 25 % of forest area of Uttaranchal (a province in the Himalayan region) was affected by forest fire in 1999.

Application of remote sensing with respect to forest fire in India has so far been limited to burnt area mapping only. Forest Survey of India (FSI) has done such mapping at the national scale using hard copy FCC in 1995 and digitally for one province in1999. Few other organizations have also undertaken similar studies for some regions or districts. The information generated through these efforts has helped in knowing the extent and severity of damage caused by forest fire. The great forest fire of Indonesia in 1997 has raised the global concern on the issue. The event has also led to wider application of modern tools like remote sensing and GIS in control and management of forest fires. With the increasing awareness, a plan has been chalked out by FSI to use remote sensing based systems for forest fire detection, monitoring, mapping of burnt area and early warning. An earth station to receive NOAA-AVHRR data is being established at the head quarters of Forest Survey of India at Dehradun for near real time detection of forest fire. Methodology for danger-rating system with inputs of weather data, terrain model and temporal series of satellite data derived vegetation indices is in the process of optimization.

The paper presents first hand account of initiatives in India in application of geo-informatics (remote sensing, GIS, GPS etc) for detection, monitoring, burnt area mapping and early warning for management of forest fires. The paper also discusses approach for developing National Forest Fire Danger Rating System and Forest Fire Risk Zonation using GIS.

# Postfire vegetation responses and soil erosion of burned surfaces time series (1983-2003) in the northeastern Patagonia, Argentina

H. F. del Valle & C. M. Rostagno
*Ecology of Arid Zones, Patagonian National Center (CENPAT), CONICET, Argentina*
delvalle@cenpat.edu.ar

G. E. Defossé
*Patagonian Andes Forest Research and Extension Center (CIEFAP), Argentina*

The northeastern region of Patagonia is a shrubby steppe dedicated to sheep ranching since the beginning of the century. This area is prone to wildfires during late spring and summer. These fires are in general small because they occur in heavily grazed paddocks in which fuel load lacks of horizontal continuity. In some areas, however, sheep ranching has been abandoned for different reasons, allowing the recovery of the vegetation, increasing then the fuel load and horizontal continuity. In this study, we evaluated the vegetation response and soil erosion to fire in 58 burned surfaces between January 1983 and February 2003 (99,497 hectares). A post-fire land cover map was developed based on classes derived principally from Landsat TM & ETM images (unsupervised and supervised classification). ERS/SAR and SIR-C images were considered to be sensitive to surface morphology at the scale of interest in soil erosion processes. Data fusion of selected scenes (Landsat & ERS) was also an interesting approach to combine different data set in order to receive better classification results and/or a better visual interpretation product. The organization of texture types was related to the distribution of structural elements within plant communities and soil erosion patterns. Such distributions are not randomly organized, since they are at least related to fire disturbances. Polarization signatures (Sir-C versus ERS) were used to support the visual and digital analysis of identifying the scattering mechanism that characterizes some burned surfaces test. Relationships between fire severity and slope azimuth, and slope magnitude + azimuth combinations were studied also using field observations and digital terrain models (obtained by interferometric techniques). There were stronger relationships between fire severity and slope azimuth classes than with slope magnitude and combinations, associated with grazing patterns in rolling plain landscapes.

# Collection of ancillary data for the monitoring of vegetation condition in the North Eastern part of South Africa

J. Verbesselt, K. Nackaerts & P. Coppin
*Geomatics and Forest Engineering Group, Department of Land Management, Katholieke Universiteit Leuven, Belgium*
Jan.verbesselt@agr.kuleuven.ac.be

Keywords: Field survey, Remote Sensing, GIS, Fire danger, Drought indices, Interpolation techniques

Current data collection strategy is developed to improve the monitoring of vegetation condition using coarse resolution earth observation (NOAA AVHRR) for integration in existing fire danger rating systems. This research fits in the framework of the GLOVEG project with the partnership of Vito – UCL – KUL, funded by the Belgian Government (OSTC; nr. VG/00/01), investigating global terrestrial ecosystem dynamics with the use of coarse resolution satellite imagery.

The North-Eastern region of South Africa is selected as a pilot site including Kruger National Park, the Mpumalanga and Northern Province. Grassland, savannah and plantation forestry represent the three main vegetation types. A dataset of pre-processed daily AVHRR images from 1995 till 2002 is available. No specific field measurements of for example fuel moisture content are carried out due to the high cost of a field survey at a regional scale and the fact that up-scaling of highly variable point measurements to a 1 km spatial resolution is a complex issue. Consequently, the interpolation of ancillary data stratified per vegetation type is essential for obtaining spatial data that can be used for current validation purposes.

First of all the available satellite imagery (AVHRR and LANDSAT ETM+) is stratified by combining classification methods and fuel models to delineate different fuel type units. These fuel type units are monitored by specific drought and fire danger indices derived from available interpolated climate data. This multi-temporal monitoring technique based on interpolation of ancillary data can be used to validate the results of the vegetation condition analysis by satellite imagery.